

University Library

Author/Filing Title Hoon, S.

.....

Class Mark T

Please note that fines are charged on ALL
overdue items.

--	--	--

**MODIFICATIONS OF POLYIMIDES
AND POLYIMIDE-INORGANIC OXIDE HYBRIDS
WITH PERFLUOROETHER OLIGOMERS FOR USE AS
MATRICES FOR CARBON FIBRE COMPOSITES**

by

SIM Seok Hoon

A Doctoral Thesis Submitted in Partial Fulfilment of the Requirements
for the Award of the Degree of

DOCTOR OF PHILOSOPHY
of
LOUGHBOROUGH UNIVERSITY

August 2004

Supervisor: Dr L. Mascia

Department of Institute of Polymer technology
and Materials Engineering

© S.H.SIM 2004

ACKNOWLEDGEMENTS

I would like to express my grateful appreciation to Dr L. Mascia for providing this opportunity for it to become a reality. I would also like to express my sincere gratitude to his immeasurable amount of patience and understandings throughout the whole of my PhD.

I am thankful to many other people within IPTME, my dearest friends and my family whose names do not appear here but who has assisted and supported me in many ways.

The whole process of this PhD owes a great deal to my husband. Thank you.

ABSTRACT

The performance of a polyimide derived from a low molecular weight polyamic acid (Skybond 703) and the corresponding polyimide-silica hybrids, used as matrices for carbon fibre composites, was evaluated. The study involved the incorporation of telechelically modified perfluoroether oligomers into the resin systems.

Telechelic modifications of the hydroxyl-terminated perfluoroether oligomer were carried out in order to achieve the required compatibility with the polyimide phase through grafting reactions with the polyamic acid precursor. In the case of hybrids, the compatibility requirements were extended also to the prehydrolysed alkoxysilane solution added to the polyamic acid mixtures. The latter was achieved with the incorporation of a silane coupling agent (γ -glycidyloxypropyltrimethoxysilane), which resulted in the formation of nano-scale silica domains in the polyimide.

Two levels of modifications were studied. The first step of the telechelic reaction involved heating the perfluoroether oligomer in bulk with chloroformic anhydride to convert the hydroxyl-terminal groups to carboxyl-terminal groups. The second step of the telechelic reaction involved an end-capping functionalisation reaction with a difunctional bisphenol-A epoxy resin in solution to produce an epoxy-terminated perfluoroether oligomer. Both the acid functionalised and epoxy functionalised perfluoroether oligomer were studied as modifiers for the polyimides and polyimide-silica hybrids. The effects of the modification were evaluated using modulated-temperature differential scanning calorimetry (MTDSC), infrared analysis, thermogravimetry (TGA), and electron microscopes.

The thermomechanical (DMTA) and mechanical properties were evaluated in a form of composites. Perfluoroether modification was found to enhance the efficiency of solvent removal in the composites, which resulted in an increase damping capacity and glass transition temperature in the cured composites.

TABLE OF CONTENTS

Page No

Acknowledgements		i
Abstract		ii
Table of Contents		iii
Chapter 1	Introduction	1
1.1	Historical Background of Polyimides	1
1.2	General Chemistry and Associated Properties of Polyimides	2
1.3	Toughening of Engineering Thermoplastics	3
1.3.1	Introduction	3
1.3.2	Historical Background	4
1.3.3	Methods of Manufacture of Toughened Polymers	5
1.3.4	Requirements of Toughening Agents	6
1.3.5	Frequently Toughened Polymers	7
1.4	Multiphase Polymers	8
1.5	Rubber Toughening of Polymer	8
1.5.1	Rubber Tear	8
1.5.2	Multiple Crazing	9
1.5.3	Shear Yielding	10
1.5.4	Cavitation-Shear Yielding	11
1.6	Aims and Objectives	11
Chapter 2	Literature Review	13
2.1	General Method of Preparation of Polyimides	13
2.2	Chemistry Involving of Polyamic Acid (PAA)	13
2.3	Thermal Conversion of Polyamic Acid to Polyimide	16
2.4	Reaction Kinetics Related to Imidisation	17
2.5	The Effects of Solvent on Imidisation	19
2.6	Structure-Properties Relationship in Polyimides	20
2.6.1	Chain-Interactions in Polyimides	20
2.6.2	Thermoxidative Resistance	20
2.6.3	Thermal Expansion Coefficient	21
2.6.4	Crystallisation of Polyimide	22
2.7	Flexible Polyimides	22
2.8	Rubber Toughening of Bismaleimides	23
2.9	Rubber Toughening of Norbornene-Terminated Oligomers	27
2.10	Rubber Toughening of Condensation Polyimides	29
2.11	Sol-Gel Chemistry	31
2.11.1	The Sol-Gel Process	31
2.11.2	Sol-Gel Process Involving Particulate Sol	32
2.11.3	Sol-Gel Process Involving Polymeric Sol	32

2.12	Silica Derived from Alkoxides	33
2.12.1	Organometallic Compounds Based on Silicon	33
2.12.2	Hydrolysis of Silicon Alkoxides	34
2.12.3	Condensation of Hydrolysed Silicon Alkoxides	35
2.12.4	Effects of Using Different Catalysts for Hydrolysis	36
2.12.5	Effect of Water and Solvents on the Hydrolysis and Condensation Reactions	37
2.12.6	Aggregation, Growth and Gelation	38
2.12.7	The Effect of pH on Gelation	38
2.13	Organic-Inorganic Hybrid Materials	41
2.14	Polyimide-Inorganic Oxide Hybrids	43
2.15	Material Preparations Involving Perfluoroether Oligomer	45
2.15.1	Perfluoroether Oligomer (Fomblins)	45
2.15.2	Toughening of Epoxy Resins	47
2.15.3	Preparation of Perfluoroether-Silica Hybrids	49
2.15.4	Preparation of Epoxy-Perfluoroether-Silica Hybrids	49
Chapter 3	Experimental	51
3.1	Materials	51
3.1.1	Polyimide Precursor	51
3.1.2	Modifiers	51
3.1.3	Precursor for Silica (Silicon Dioxide)	53
3.1.4	Coupling Agent	53
3.1.5	Catalysts	54
3.1.6	Solvents	54
3.1.7	Carbon Fibres	54
3.2	Methodology for the Modification and use of Perfluoroether Oligomers to Modify the Mechanical Performances of Polyimide and Polyimide-Silica Hybrids as Matrices for Carbon-Fibre Composite	55
3.3	Visual Appearance as a Basis for Preliminary Assessment of Compatibilisation and Miscibility in Reaction Mixtures	56
3.4	Telechelic Modification of the Perfluoroether Oligomer Using Chlorendic Anhydride	56
3.5	Epoxy Functionalisation of the Acid Terminated Perfluoroether Oligomer (Oligomer TX-CA)	58
3.6	Characterisations of Oligomer TX, Oligomer TX-CA and Oligomer TX-CA-E8	60
3.7	Preparation of Modified Polyimides with Acid-Functionalised Perfluoroether Oligomer (Oligomer TX-CA)	60
3.7.1	Effect of Solvent	62
3.7.2	Effect of Pre-Reaction Temperature	62

	3.7.3 Visual Examinations	62
	3.7.4 Morphological Studies	62
3.8	Preparation of Modified Perfluoroether Polyimides with Epoxy Functionalised Oligomer (Oligomer TX-CA-E8)	63
	3.8.1 Effect of Omitting Toluene Dilution in the Modification of the Polyamic Acid	64
	3.8.2 Effect of Pre-Reaction Conditions Prior to Curing	64
3.9	Preparation of a Prehydrolysed Alkoxysilane Solution	65
3.10	Hybridisation of Polyimides Modified with Perfluoroether Oligomer	66
3.11	Production of Composites	66
3.12	Properties Evaluation of Carbon Fibre Composites	72
	3.12.1 Cutting Composites to Size for Various Analyses	72
	3.12.2 Thermomechanical Characterisation	73
	3.12.3 Mechanical Testing	73
	3.12.4 Morphological Examinations	74
	3.12.5 Thermogravimetric Analysis	75
Chapter 4	Results	76
4.1	Telechelic Modification of Hydroxyl-Terminated Perfluoroether Oligomer	76
	4.1.1 Acid Functionalisation Using Chlorendic Anhydride	76
	4.1.2 Epoxy Functionalisation Using Epoxy Resin	76
4.2	Fourier Transform Infrared Spectroscopy	77
	4.2.1 Qualitative Analysis	77
	4.2.2 Quantitative Analysis	79
4.3	Miscibility of Mixtures	79
	4.3.1 Mixtures of Acid Functionalised Perfluoroether Oligomer and Polyamic Acid	79
	4.3.2 Mixtures of Epoxy Functionalised Perfluoroether Oligomer and Polyamic Acid	82
	4.3.3 Mixtures of Epoxy-Functionalised Perfluoroether Oligomer, Polyamic Acid and Prehydrolysed Alkoxysilane Solution	85
4.4	Morphology of Imidised Films	86
	4.4.1 Scanning Electron Microscopy of Non-Hybridised Films	86
	4.4.2 Transmission Electron Microscopy of Hybridised Films	86
4.5	Thermal Analysis Using Modulated Temperature Differential Scanning Calorimetry	94

	4.5.1	Characterisation of Epoxy Functionalised Perfluoroether Oligomer	94
	4.5.2	Thermal Evaluation of Uncured Mixtures of Polyamic Acid and Epoxy Functionalised Perfluoroether Oligomer	100
	4.5.3	Thermal Evaluation of Uncured Mixtures of Polyamic Acid, Hybridising Silica and Epoxy Functionalised Perfluoroether Oligomer	108
	4.5.4	Thermal Evaluation of Fully Imidised Films of Polyimides and Polyimide-Silica Hybrids Modified with Epoxy Functionalised Perfluoroether Oligomer	116
4.6		Thermal Analysis of Carbon Fibre Composites Using Thermogravimetry	128
	4.6.1	Weight-Loss Characteristics of Resins	128
	4.6.2	Weight-Loss Characteristics of Carbon Fibre Composites of Perfluoroether Modified Polyimide and Polyimide-Silica Hybrids Prepared Using Different Methods	128
	4.6.3	Effects of Acid Catalyst	136
4.7		Mechanical and Thermomechanical Properties of the Composites	146
4.8		Scanning Electron Microscopy of the Composites	167
Chapter 5		Discussion	186
	5.1	Perfluoroether Oligomer	186
	5.2	Acid Functionalisation of Perfluoroether Oligomer	187
	5.3	Epoxy Functionalisation of Perfluoroether Oligomer	189
	5.4	Effects of Epoxy Functionalised Perfluoroether Oligomer on Polyamic Acid and Polyamic Acid / Prehydrolysed Alkoxysilane Mixtures	189
	5.4.1	Characteristics of Curing Mixtures	189
	5.4.2	Characteristics of Cured Mixtures	191
	5.5	Thermogravimetric Weight-Loss Characteristics of Polyimide Composites	195
	5.6	Thermomechanical and Mechanical Properties of Composites	201
	5.7	Scanning Electron Microscopy of the Composites	206
Chapter 6		Conclusions	207
Chapter 7		Recommendation for Further Works	208
Chapter 8		References	209

1 INTRODUCTION

The ever-increasing use of polymeric materials in the form of composites in the aerospace and automotive industries can generally be attributed to their many desirable properties [1, 2], which compare favourably with traditional materials such as titanium and aluminium. Probably the most compelling advantage in using these materials in structure applications is the possibility of reducing weight substantially and still retaining high strength and rigidity.

One of the major limitations of structural polymers and their composites lies in their inadequate thermal stability. Hence, there has been an increasing search for high-temperature polymers (i.e. capable of withstanding temperature in excess of 200°C), for both of structural adhesives and as composites matrices [2]. Traditionally, polyimides are used commercially for both applications. They are known to have continuous service temperature up to 300°C in air and higher temperature for shorter period of time [3] and are considered to be at the "top-end" of temperature performance for organic polymers. In general, the grade used for composites is relatively low molecular weight systems and are, therefore, quite brittle.

1.1 Historical Background of Polyimides

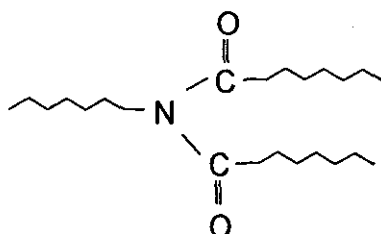
Bogert and Renshaw [3, 4] first reported the production of a polymeric imide in the beginning of the last century through the dehydration of 4-aminophthalic anhydride.

Du Pont introduced the first commercial material much later in the early 1960s [1]. They marketed a series of products obtained by condensing pyromellitic dianhydride with aromatic amines, particularly di (4-aminophenyl) ether. These include a range of soluble polyimide precursors (Pyralin) intended for wire coating applications, a coating resin (Pyre ML), film (originally H-film, later named Kapton) and in machinable block form (Vespel). In spite of their high prices, these materials have found established uses. Examples of expanded availability that followed include Monsanto's Skybond series, Rhone-Poulenc's Kerimid and Nolimid polyimides, Hitachi's PIQ range and Gulf Chemicals' Thermid system. By the mid 1970s, there

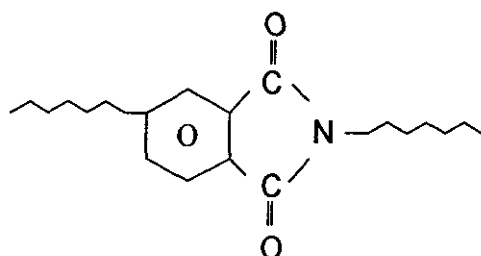
were over twenty suppliers in the United State and Western Europe alone, although some companies have withdrawn their products from the market.

1.2 General Chemistry and Associated Properties of Polyimides

The characteristic functional group of polyimide is shown below [1].



The branched nature of the functional group facilitates the production of polymers with ring structures within their backbone and not surprisingly, the most prominent characteristic of aromatic polyimide is the presence of phthalimide structure [1] as shown below.



Virtually all the backbone structures of most traditional polyimide are thermally stable. These include phenylene, carbonyl, imide and ether linkages. In addition, the rigid structure also allowed the material to retain their strength and rigidity extremely well at elevated temperature. These properties are responsible for making polyimides unique materials for high temperature applications [1].

Unfortunately, polyimides, by their very nature, cannot be moulded by conventional melt-processing techniques [2]. The molecular mobility of these materials is so restricted that thermal degradation occurs before the material acquires sufficient fluidity. This drawback is counteracted, to a certain extent, by preparing the materials from a soluble precursor [1, 2], in the form of polyamic acid (PAA) dissolved in polar aprotic solvent such as N-methyl 2-pyrrolidone (NMP), N, N-dimethyl acetamide (DMAc) and N, N-dimethyl formamide (DMF). These precursors are capable of undergoing internal condensation reactions (i.e. imidisation) to form the polyimide by the combined action of heating and solvent removal through evaporation, which are normally carried out during the final processing stage. For example, in adhesive applications, this conversion is conducted within the adhesive layer during bonding. In the case of a composite, imidisation is performed in the final fabrication stage under high pressure. The volatilisation of water from the condensation reaction and the original solvent, however, present a serious fabrication problem, as they will give rise to porous products with impaired mechanical properties [2].

1.3 Toughening of Engineering Thermoplastics

1.3.1 Introduction

Most plastics designed for engineering applications are multiphase materials that contain elastomeric impact modifiers and often other polymers. The addition of toughening agents usually increases the overall ductility of the polymer over a wide temperature range but also improves resistance to notch sensitivity and toughness of thick sections and reduces water absorption. As more knowledge of miscibility, compatibility and interaction of polymers has become available in recent years, more varied approaches to improved polymer blends have become apparent. Simultaneous with this, there has been an explosion of activity in the field of toughened engineering plastics. Many new toughened polymer blends based on polyamides, poly(phenylene oxide) (PPO), polyesters and polycarbonates (PCs) have been introduced in large volume applications, particularly in the automotive industry [5].

The manufacture of engineering polymer blends grew tremendously in the 1980s. Before 1980, blend technology leading to engineering polymers was essentially

unknown on a commercial basis [6-9], except, of course, for blends of PPO with high impact polystyrene that were introduced in the late 1960s by General Electric Company under the trademark Noryl. Recently, a number of multicomponent engineering polymers containing impact modifiers have been introduced. The world-wide patent activity of compositions useful for such applications has been explosive. Hundreds of patents on the modification of polyamides alone have been issued during the 1980s. It is clear that the growth of rubber toughened engineering plastics will continue at a very high rate involving many combinations of polymers.

Alloys and blends involving combinations of various engineering polymers designed for improved heat deformation characteristics, rigidity, solvent resistance and toughness will be the main area for significant growth.

1.3.2 Historical Background

Acrylonitrile, butadiene, styrene, or ABS materials, developed in the 1950s, were the first family of rubber toughened polymers that were useful for engineering applications. ABS polymers have an excellent balance of strength, rigidity and toughness, but they are deficient in some critical properties such as heat deformation temperature and resistance to solvent attack. These deficiencies have limited their use in many applications. Styrene-acrylonitrile grafted rubbers such as those that give ductility to the SAN matrix in ABS are widely used as components to enhance toughness in a number of modern engineering polymer systems.

Blends of poly(phenylene oxide) and high impact polystyrene (HIPS) were introduced in the late 1960s by the General Electric Company under the Noryl trademark. These products were useful in many applications that required high heat deformation temperature, mechanical strength and toughness. It is because of the thermodynamic miscibility of PPO and polystyrene (PS), a large number of tailor-made products with varying impact strength and heat distortion temperature were possible by adjusting the ratio of PPO to polystyrene in the matrix [10]. Addition of flame retardants, fiber reinforcement and so on, opened additional applications for these plastics.

Polycarbonate was introduced in the late 1950s and found rapid commercial acceptance of its transparency, high strength and high heat deformation temperature. However, its high melt viscosity, poor impact strength of thick sections, and high cost motivated development of improved compositions with better-balanced properties. ABS-PC blends were found to give a desirable combination of properties useful for many applications. These blends have steadily grown and today they are one of the principal engineering polymer alloys.

All three of these first engineering polymer blends were based on rubber modified styrenic polymers. This technology provided an excellent basis for the synthesis of starting materials for blends of engineering polymers.

1.3.3 Methods of Manufacture of Toughened Polymers

(a) Melt blending

The first commercially significant polymer blends in the late 1940s were prepared by extrusion blending. PVC modifications serves as an excellent example of this approach. Melt blending technology continues to be used for producing specialty formulations of HIPS, but most often those of ABS. With the advent of block copolymers and thermoplastic elastomers, more formulations were developed by melt blending with styrenic polymers. The development of PPO-HIPS blends by GE was entirely based on the melt blending approach. At the present time many of the multiphase engineering polymers are manufactured continuously by melt blending often in twin-screw extruders.

(b) In situ polymerisation

The polymerisation of styrene in the presence of dissolved butadiene based rubber with shearing agitation is used for the manufacture of high impact polystyrene [11, 12]. It is also used for the synthesis of some varieties of ABS like those that are used in blends with PC. However, emulsion polymerisation of SAN copolymers in the presence of rubber seed latex is the basis of a major portion of commercial ABS polymers. In this process the grafted rubber particle size is controlled by the size of

the seed rubber particle. The small (0.05 to 0.2 μm) graft rubber particles from the emulsion process are desirable for the modification of many engineering polymers. In situ polymerisation is also practiced in the rubber toughening of epoxy resins using low molecular weight carboxy-terminated nitrile rubbers (CTBN).

1.3.4 Requirements of Toughening Agents

The various toughening agents or impact modifiers described in the literature are manufactured by many synthetic approaches and involve numerous chemical compositions. There are several important criteria, however, that must be kept in mind to obtain tough engineering polymers successfully, regardless of the type of elastomer used. These requirements are important for obtaining commercially viable blends useful for demanding engineering applications.

It is recognised that the toughened engineering compositions are all multiphase systems that may contain several separate polymer domains in addition to the discrete elastomer particles that enhance blend toughness [13-15]. Rubber particles need to adhere to the matrix for satisfactory stress transfer in most instances. An exception, however, is observed in blends of PC with polyethylene, where the non-adhering polyethylene domains cause a change in the mechanisms of deformation of the blends that gives rise to improved impact strength of thick sections and specimens with sharp notches. Satisfactory adhesion is often obtained by the formation of chemical bonds between the matrix and the rubber phase. Physical interactions may also be used to provide adequate adhesion. In the modern view of polymer-polymer interfaces, interpenetration of the two polymers occurs to an extent related to their thermodynamic interaction that provides a mechanism for interfacial adhesion [14]. The adhering rubber particles often need to be quite small, typically less than 0.1 to 0.2 μm , and uniformly distributed. Wu has suggested that in modified nylon 6,6 there is a critical interparticle distance below which ductile compositions are observed [15-17]. Later Borggreve, Gaymans and co-workers [18-22] reached similar conclusions in studying the toughening of nylon 6. However, particles can be also too small for effective toughening [23, 24] and, in general, some optimum range of sizes is needed. Of course, there is often a critical concentration of toughening agent that must be exceeded. Another requirement for rubber toughened polymers is that the rubber

phase morphology must not change during melt fabrication processes, i.e. rubber particle size and distribution should remain unaltered. This is usually assured by crosslinking the rubber phase, such as in the core-shell impact modifiers. The use of chemically modified gum rubber involves more variables for achieving a stable, controlled morphology. To achieve improved impact strength at low temperatures the glass temperature of the elastomer must be well below the desired use temperature.

In addition to the requirements summarised above, it is desirable that commercial toughening agents be thermally stable, easily dispersible and stable to oxidation and UV light.

1.3.5 Frequently Toughened Polymers

Engineering polymers that are most frequently rubber toughened include polyamides (PA), polyesters (PET and PBT), epoxy resins, poly(phenylene oxide) [10], polycarbonates and polyacetals [25, 26]. Toughening of polyimides and polysulfones and polyarylether ketones are also common. Combinations of engineering polymers have been found to be useful in applications requiring high strength, high heat deformation temperatures, solvent resistance and toughness. Rubber modified PA-PPO [27, 28], PBT-PC, PA-PC, PET-PBT and PET-PC blends serve as examples of this fast-growing segment of engineering plastics.

Recent patent literature reveals that numerous elastomers, particularly those that contain some acid or polar functionality, are effective in toughening a variety of engineering polymers. The voluminous patent by Epstein [29] on rubber modification of polyamides serves as an excellent example. His claimed invention requires elastomer particles to be from 0.01 to 1 μm in diameter, and to adhere to the polyamide matrix, and to have a tensile modulus in the range from 0.007 to 130 MPa. Within this broad range of requirements for the rubber toughening component, a very large variety of elastomers is described in 168 examples and 55 claims [29].

1.4 Multiphase Polymers

When two or more polymers or oligomers are mixed physically, to form products with desirable properties, the mixtures are referred to as polymer blends [30]. This technology can be utilised to 'tailor-make' polymer compositions with versatile properties for specific applications without the need to synthesise new polymers.

The miscibility of a polymer mixture depends on its thermodynamic conditions of mixing [30]. In partially miscible blends, the miscibility within the systems can sometimes be adjusted to better suit the property requirements of the final products. The degree of miscibility and its associated morphology can be characterised by measuring the changes in the glass transition temperature of each component and by using microscopic techniques.

1.5 Rubber Toughening of Polymer

Toughening can be described as the process of improving fracture resistance, which is related to the amount of mechanical energy that a polymer can absorb. Toughening is an important feature of semi-miscible polymer blends. A small amount of a toughening phase is usually introduced into a polymer system to achieve a substantial increase in fracture toughness and very frequently with little or no loss in strength and rigidity [2, 30]. Many different mechanisms have been proposed over more than three decades to explain this enhancement in toughness.

1.5.1 Rubber Tear

As early as 1956, Mertz, Claver and Baer [31] have proposed that toughening is solely due to deformation and tearing of rubber particles, which will otherwise hold opposite faces of propagating cracks together and delay rupture. They observed an increase in volume and stress whitening in HIPS as a result of dilatational stress in the material and explained that this is associated with the formation of microcracks.

Much later, in 1980, Kunz-Douglas et al. [32] developed a quantitative model for such toughening mechanism and produced the following expression for the fracture toughness of a rubber toughened polymer.

$$G_{IC} = G_{ICC} [1 - v_p] + [1 - 6/(\lambda^2 + \lambda + 4)] 4 \gamma_t v_p$$

- Where:
- a) G_{IC} is the energy absorbed during rupture for polymer blend,
 - b) G_{ICC} is fracture energy of the epoxy matrix,
 - c) V_p is the volume fraction of the rubber particles,
 - d) γ_t is the particle tear energy and,
 - e) λ is the rubber particle extension ratio at failure.

The main limitation of these proposed theories is that they are concerned primarily with the rubber rather than with the matrix. It has been estimated [33] that the total amount of energy associated with the deformation of the rubbery phase accounts for no more than a small fraction of the observed enhanced impact energies.

Consequently, this mechanism plays a minor role in the toughening of multiphase polymers.

1.5.2 Multiple Crazing

Bucknall and Smith in 1965 [34] proposed that toughening of glassy polymers, by the inclusion of rubbery particles, results from the initiation of crazes and the control of their growth. Under a tensile stress, crazes are formed at the points where the maximum principal strain reaches a critical value, i.e. near the equator of the rubber particles. The outwards growth of crazes stops as a result of stress relaxation when they meet energy absorbing obstacles, such as smaller particles, which prevent them from developing into large cracks. A high level of adhesion between the matrix and the rubber particles is necessary for the craze arresting mechanism to operate. A weakly adhering rubber particle would be pulled away from the matrix, leaving a hole, which would only serve to intensify the stresses locally. The positive result of a strong bond between particles and matrix is a large number of small crazes, in contrast to a small number of large crazes formed in the same polymer in the absence of such rubber particles. The high level of crazing that occurs throughout a

comparatively large volume of the multiphase material accounts for the extensive stress whitening, which accompanies deformation and failure and is the main cause for the high energy-absorption observed in tensile and impact tests. Microscopy studies have confirmed that crazes frequently initiate from the rubber particles, and have provided considerable information concerning the constituents of a craze and the detailed mechanisms of craze initiation, growth and breakdown around rubber particles [35, 36].

Although to the naked eye, a craze appears to be similar to a crack in its shape, it actually contains fibrils of oriented polymer in the direction of the maximum tensile stress, bridging the two surfaces. This makes it load bearing and consequently, very different from a crack. Cracks can form, however, by the breakdown of craze fibrils and can grow to a critical size causing catastrophic fracture [37-40].

1.5.3 Shear Yielding

Newman and Strella [41] proposed a shear yielding theory in 1965, following their work on the fracture behaviour of ABS (acrylonitrile-butadiene-styrene terpolymer). Mechanical and optical experiments showed that necking, drawing and strain hardening takes place together with localised plastic deformation of the matrix around the rubber particles. Therefore, it was proposed that the function of the rubber particles was to produce enough triaxial tension in the matrix. This increases the local free volume and given to the extensive shear deformation in the interfacial regions, which take the form of shear bands or simply a diffuse shear yielding zone. Not only does this phenomenon act as energy absorbing process, but the shear band slowed down the propagation of crazes and the formation of cracks growth, which effectively delays the failure of the material.

However, this mechanism cannot account for stress whitening, which is a characteristic of rubber toughening and does not explain why triaxial tension promotes shear yielding rather than the formation of crazes.

1.5.4 Cavitation-Shear Yielding

This mechanism was independently proposed and developed by Kinloch, Shaw and Hunston [42], and also by Pearson and Yee [43].

The primarily source of energy absorption in epoxies is believed to be due to shear yielding. This applies to both unmodified and rubber-toughened epoxies. Hence, the presence of the two-phase morphology and the modulus differential between the matrix and the toughening phase must account for the considerable enhancement for the plastic deformation process [42-46].

The role of rubber particles can be considered two-folds. Firstly, the particles act as stress concentrators under axial loads and encourage yielding of the matrix by the development of shear stresses. Secondly, the development of the stress concentration in the matrix due to the rubber particles, and the inherent state of triaxial stress within the particles due to differential contraction during curing, would combine to provide a favourable condition and initiate cavitation of the rubber [42-46].

Cavitation in itself does not appear to constitute a major energy absorption process. However, this phenomenon could increase the dilation of the matrix in the interparticle region, thereby, creating a more favourable condition for yielding within the matrix [42-46].

1.6 Aims and Objectives

This project aimed in combining two research themes based in IPTME at Loughborough:

1. The first technology involved the use of thermally stable perfluoroether oligomers to enhance the mechanical performances of high temperature polymers, such as epoxy resins, through the generation of rubbery perfluoroether inclusions in the polymer matrices [47-50].

2. The second technology involved the production of organic-inorganic hybrids through the hydrolytic sol-gel route. In this case, this referred to polyimide-silica hybrids. In IPTME, the effective use of coupling agents and solvents for compatibilisation, combined with the established approach of producing prehydrolysed alkoxysilanes, has allowed hybridisation to be achieved with the end polymers, without the contemplation of involving its polymerisation process [51-53].

In combining these two technologies, this project attempted to explore the possibilities of minimising the effects of plasticization involving perfluoroether modifiers through the generation of hybrids. In vice versa, it also attempted to explore the possibilities of minimising the embrittlement effects of hybridisation through perfluoroether modifications.

The specific objectives are as follows:

1. Compatibilisation of the perfluoroether with the polyimide and silica precursor solutions through telechelic modifications and grafting reactions.
2. To understand the effects of solvent removal in polyimide-carbon fibre composites using an inert modifier.
3. To establish the correlation between the damping capacity of the composites and the presence of a rubbery inclusion.

2 LITERATURE REVIEW

2.1 General Method of Preparation of Polyimides

The general reaction scheme for the synthesis of polyimides is outlined in Figure 2.1. A dianhydride is first allowed to react with a diamine at room temperature in solution using a suitable polar aprotic solvent such as DMF, NMP and DMAc [54, 55]. The result is a high molecular weight polymer known as polyamic acid (PAA), which is soluble in the original solvent. Upon heating, the solvent is removed and PAA will undergo an imidisation reaction, liberating water as a by-product, to form the corresponding polyimide [1, 4].

In principle, the vast majority of dianhydride and diamine combinations can be used to produce polyimides. However, the products of commercial interests are usually highly aromatic in nature [1]. These include phenylene diamine (PDM), diamino diphenylmethane (DDM), diaminobenzophenone (DABP) and diaminophenylether (DAPE); and pyromellitic dianhydride (PMDA), biphenyl tetracarboxylic acid dianhydride (BTDA) and oxydiphthalic anhydride (ODPA).

2.2 Chemistry Involving of Polyamic Acid (PAA)

The stepwise polymerisation of dianhydride and diamine is sensitive to the stoichiometric quantities of the two reactants [56]. Deviations from equimolar ratio are known to cause considerable reduction in the overall yield and hence, the final molecular weight of the PAA formed. This delicate balance can often be upset by the presence of water. Dianhydrides are hydrophilic species and they will undergo hydrolysis readily to form acids that are considerably less reactive with diamine. This, therefore, would hinder further conversion.

This form of polymerisation is also known to be highly reversible [57, 58]. The initial reduction in the viscosity of the PAA solution during storage at room temperature has been shown to be due to depolymerisation [59, 60] and was thought to be thermodynamically driven toward monodispersity [61]. This is confirmed by studies

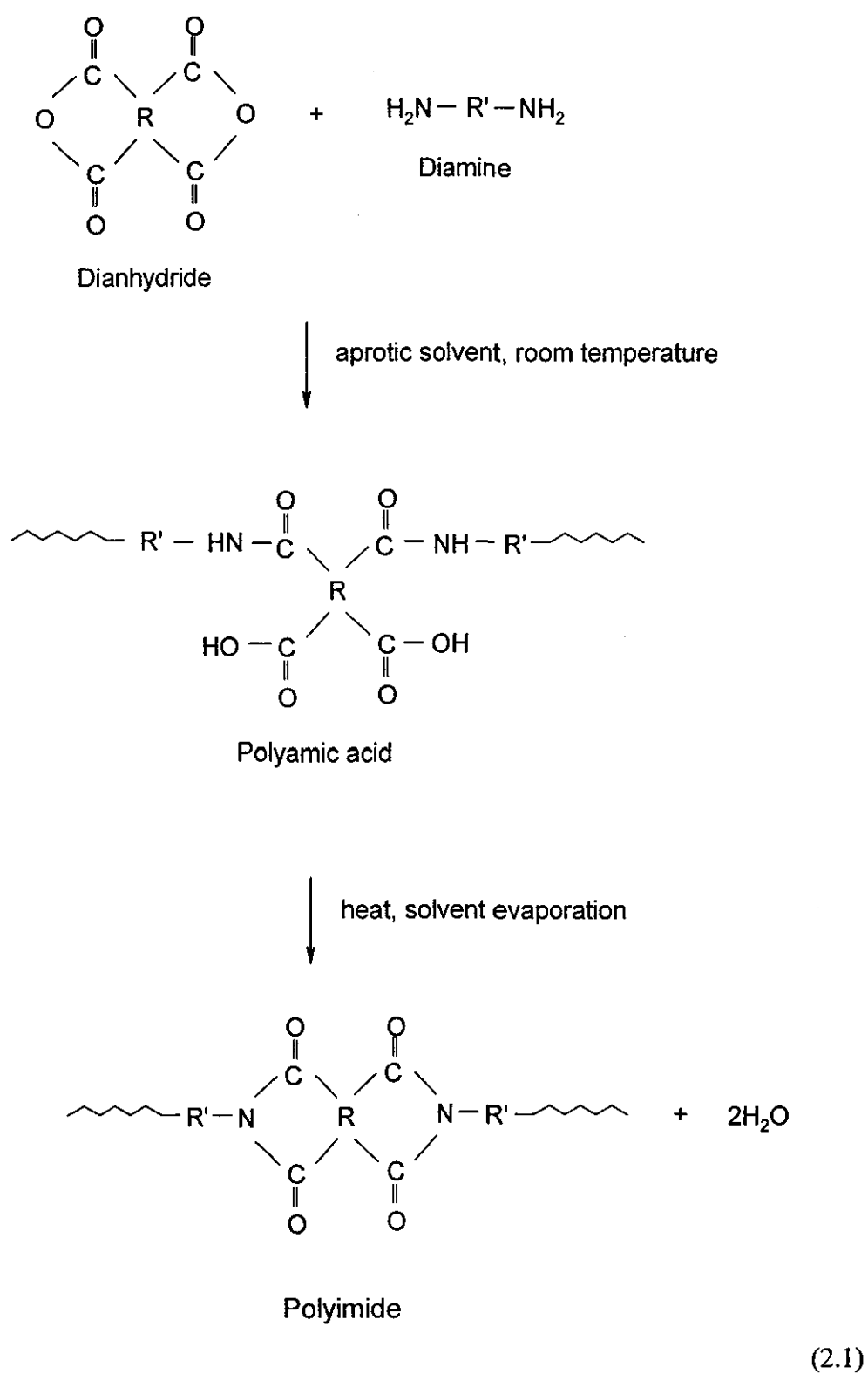


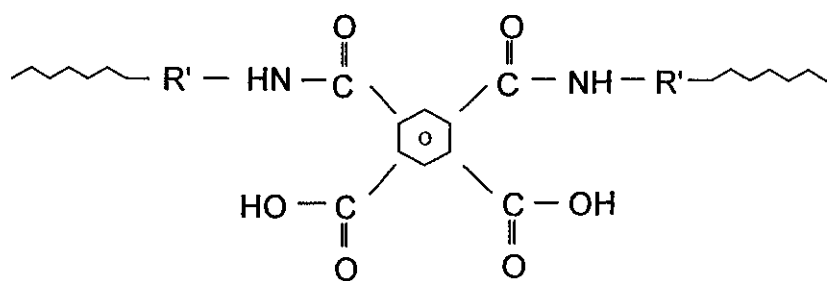
Figure 2.1: The general reaction scheme for the synthesis of polyimides.

using GPC [57, 58], which have indicated that the weight average molecular weight, M_w , decreased while the number average molecular weight, M_n , remained relatively constant. This narrowing of molecular weight distribution (MWD) arises from the fact that only the larger molecular weight species are significantly affected by chain scission. Miwa and Numata [62] studied the stability of these materials at elevated temperature. Using light scattering technique, they concluded that the viscosity reduction is associated directly with the decrease in M_w .

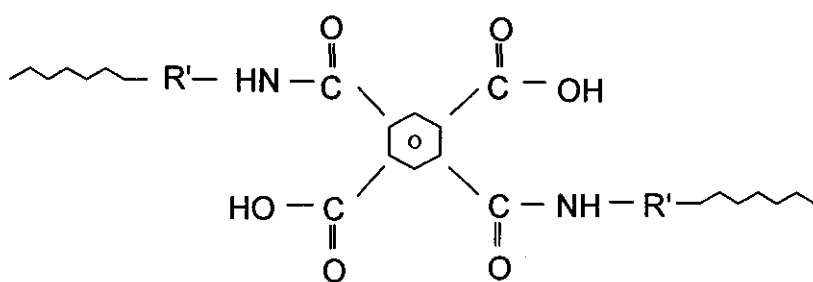
This degradation process was reported to occur to a lesser extent by the following expedienices:

- a. Increase the solid content of PAA in solution [63] in order to minimise the extents of depolymerisation through hydrolysis. Assuming that the ratio of water to solvent is the same in all concentration, dilute solutions would be less stable due to the higher amount of water present, thereby explaining the faster reduction in viscosity. It should be noted that these are intramolecular reactions in which the stability of the polymer is not related to chain mobility.
- b. Neutralise the carboxylic group of PAA with a basic compound such as a tertiary amine [64] or by introducing an electron-donating linkage such as carbonyl group, in the polymer structure near to the amic acid units [60]. This assumes that the mechanism of the reverse reaction is associated with the intramolecular protonation of the carboxylic acid of the polyamic acid. By reducing the extent of ionisation of the acid, these processes reduce the availability of the proton, causing the process of degradation to take place at a lower rate.
- c. By storing the PAA solution at very low temperature [65].

In the synthesis process, the diamine can attack either one of the two carboxylic groups of the dianhydride [66]. This resulted in the generation of isomeric repeat units consisting of meta or para configuration as shown below:



meta



para

Meta configuration has been reported to interfere with subsequent chain packing in polyimide by disturbing its regularity, which results in lowering T_g (this will be discussed in detail later).

2.3 Thermal Conversion of Polyamic Acid to Polyimide

The essence of producing PAA is to provide the capability of utilising polyimides for manufacturing [1]. Imidisation can be carried out later in a manufacturing process by heating. The physical and chemical events that occur during heating can be summarised as follows:

1. In the initial heating stage between room temperature and 150°C , the prominent process is solvent volatilisation, with very little imidisation taking place [4].
2. Between 150°C to 250°C , most of the imidisation takes place in conjunction with further solvent removal. Some depolymerisation also takes place in a

fashion similar to that described earlier [66-68]. The reverse reaction can be evident by the formation of amine and anhydride groups in the process. The generation of anhydride can be followed using IR spectroscopy [69-71], by monitoring the carbonyl group absorption around 1860cm^{-1} . This absorption was reported to peak at reaction temperatures between 200°C and 250°C , but decrease progressively to zero with increasing temperature to around 300°C , possibly due to further polymerisation taking place subsequently. This degradation process follows a similar explanation used in the observation of viscosity reduction during storage. Evidently, amine salts of PAA and polyamic esters do not generate anhydrides during imidisation and, therefore, will increase the storage stability of the precursor solution [67, 72, 73].

3. The maximum level of imidisation is achieved at temperature between 250° to 300°C . Although the step at this temperature range only contributes a small increase in imidisation, it has been reported to be essential for completing the reaction and to totally expel the solvent [69-71].
4. Heating above 300°C is reported to initiate intermolecular reaction leading to crosslinking [74-78].

2.4 Reaction Kinetics Related to Imidisation

A reaction rate can generally be expressed as a derivative of conversion [79-90]. In a chemical reaction, conversion may generally be defined as a ratio of the actual weight of the reacted material to the initial weight of the unreacted material:

$$\alpha = \frac{M_0 - M}{M_0} = 1 - \frac{M}{M_0}$$

where α is conversion, M is the actual weight of the reactants and M_0 is the initial weight before reaction.

The rate of conversion (i.e. reaction rate) can in turn, generally be expressed as followed:

$$\frac{d\alpha}{dt} = k(T) f(\alpha)$$

where $k(T)$ is the rate constant, which is dependent on temperature and $f(\alpha)$ is a function of the degree of conversion.

For polymer reactions showing decelerating rate behaviour under isothermal condition, it may be assumed that conversion is proportional to the concentration of the unreacted materials and is a function of the reaction order, n [79-90]:

$$\text{i.e. } f(\alpha) = (1 - \alpha)^n = \frac{M}{M_0}^n$$

Hence, the rate of conversion under isothermal conditions can be defined as followed:

$$\frac{d\alpha}{dt} = k(1 - \alpha)^n = k \frac{M}{M_0}^n$$

Imidisation of polyamic acids is an intramolecular reaction involving two different functional groups. Despite this, it is reported to be treated as first order (i.e. $n=1$) [74].

Laius *et al* [91] and Kreuz *et al* [92] studied imidisation made under isothermal conditions and found that at temperature greater than 150°C, imidisation proceeded rapidly initially, but changes subsequently to a much slower reaction rate. Assuming a first order reaction throughout, the rate constant was found to decrease with time in the second stage from the initial constant value of the first stage. It was proposed [93] that the reaction rate may be governed by two non-equivalent-kinetic states, associated respectively with two different planar conformations of the PAA. The difference in activation energy barriers between the two conformations toward imidisation was used to explain the disparate rate effect between the initial and the second stage of the reaction. Accordingly, molecular orientation and rotational transition from high-energy barrier conformation to lower energy barrier conformation may prolong the initial stage of the imidisation reaction.

There is also considerable evidence to indicate that this change in reaction rate is related to a physical transitional state [91]. Numerate *et al* [94] have found that the temperature at which the fast-to-slow change in reaction rate takes place in a dynamic condition is closely related to the glass transition temperature of the resulting polyimide. Based on these observations, the slowing down of the reaction rate was thought to be due to molecular restrictions as a result of the high T_g. This conclusion suggests that the fast reaction rate is associated with segmental motion. Although, cyclisation can continue even in the glassy state, it would proceed at a much slower rate.

It is worth noting that the kinetics of imidisation may also be affected by the molecular weight of the polyamic acid. Bessenov *et al* [95] have shown that the lower the molecular weight of PAA, the faster is the imidisation rate.

2.5 The Effects of Solvent on Imidisation

As it has been pointed earlier, a polyamic acid may be capable of undergoing conformational changes, which result in the transition of one kinetic state to another. Therefore, it is not difficult to imagine that in the presence of residual solvent, plasticisation action facilitates this transformation and increase the rate of imidisation [96-100]. However, there is considerable evidence to indicate that intramolecular imidisation does not occur until solvent decomplexation has taken place [97, 99].

For instance, NMP has been reported to complex strongly with PAA in solution. Using Fourier Transform Raman spectroscopy, NMP was shown by Johnson and Wunder [101] to interact with carboxylic group of PAA through hydrogen bonding. Hsu and Liu [102] studied the effect of different levels of residual solvent on films of PAA using DSC. At a molar ratio of 4 NMP to 1 repeat unit of PAA, a sharp endothermic peak associated with the decomplexation of solvent was observed between 140°C and 170°C. When this molar ratio was reduced to 0.81 by controlled heating, the decomplexation peak became broader and imidisation began to take place at a lower temperature. It is worth noting that like solvent decomplexation, the imidisation reaction is itself also an endothermic process.

Following the decomplexation step, the residual solvent in the PAA plays a vital role in the conversion process. From a physical point of view, the benefit of plasticisation has already been illustrated earlier. From a chemical point of view on the other hand, a solvent such as NMP can act as a proton acceptor for the carboxylic acid of PAA, thereby acting as a catalyst for the imidisation reaction [98]. This explanation is supported by the fact that amine salts of polyamic acid imidise up to ten times faster than the corresponding free acid [64]. Ginsberg *et al* [103] have reported that thicker films can achieve a higher degree of conversion, due to the higher retention of residual solvent. More advanced states of imidisation are also observed when a fast heating rate was used in a dynamic heating process [104]. At slow heating rate, solvent volatilisation was achieved more efficiently, resulting in lower retention of residual solvent.

2.6 Structure-Properties Relationship in Polyimides

The properties of polyimides are naturally very dependent on their molecular structure. Furthermore, the types of intermolecular interaction and chain configuration also play an important role [105, 106].

2.6.1 Chain-Interactions in Polyimides

Polyimides are known to form molecular aggregates through intermolecular charge transfer or electronic polarisation [105]. These forms of chain-chain interactions were thought to have an important effect on the final properties of the polyimides such as glass transition temperature, mechanical properties and thermal resistance. In these complexes, adjacent chains are held together in alignment, resulting in very close packing. This also causes a hindrance to molecular rotations. These states of aggregations can be described as ordered phases and are believed to act as pseudo crystals [106, 107].

2.6.2 Thermoxidative Resistance

Most aromatic dianhydrides commonly used in the synthesis of polyimide are thermally stable. As a consequence, the thermal oxidative stability of a polyimide is

strongly dependent on the type of diamine used. The order of stability for commonly used diamine is as follows: biphenyl, phenyl > benzophenone > para or meta-phenylene > diphenylether > diphenylmethane [1].

Bessonov *et al* [95] have observed that the most stable polyimides are those produced from aromatic diamine without hinge structures. Polyimide having diamine containing aliphatic group are the least stable.

In addition to the details of chemical structure, other factors such as residual moisture, method of preparation, molecular weight and the type of end groups will also influence thermal stability [108]. Degradation can be accelerated considerably, both in air and in an inert atmosphere, in the presence of residual water. Films cast from more viscous solutions were found to be more heat resistant than those prepared from low viscosity solution. Prolonged storage of PAA results in a less thermally stable polyimide. Chemically imidised films are more stable than those prepared by thermal imidisation. Polyimides, in the form of powders are more stable than those in the form of films are. High molecular weight polyimides are more stable than those with low molecular weight.

2.6.3 Thermal Expansion Coefficient

Dimensional stability and low thermal expansion at high temperature are very important properties of polyimide, particularly with respect to electronic applications. These characteristics of polyimide are thought to be associated with chain rigidity and molecular orientation [109]. To a certain extent, these two properties are related. Increasing chain rigidity generally increases tendency of orientation. Logically, thermal expansion is the lowest along the direction of orientation, and highest in the expense of the transverse direction [109-112]. In fact, polyamic acid undergoes plane orientation during solvent evaporation to form a film. Consequently, the thermal expansion coefficient is lowest in the direction normal to the thickness. If the film is stretched, thermal expansion coefficient becomes even lower.

2.6.4 Crystallisation of Polyimide

Most polyimides are crystallisable unless they are cross-linked or have long and bulky side groups. However, when films are cured in the commonly used conditions, they are generally amorphous or have very low level of crystallinity. This is because the rate of crystallisation of these materials is very slow [66].

The crystallisability of polyimides is dependent on the type of dianhydride and diamine used. Hergenrother *et al* [113] showed that the tendency toward significant level of crystallinity is in the following order, with reference to the type of dianhydride: benzophenone > biphenyl tetracarboxylic dianhydride \equiv oxydiphthalic dianhydride.

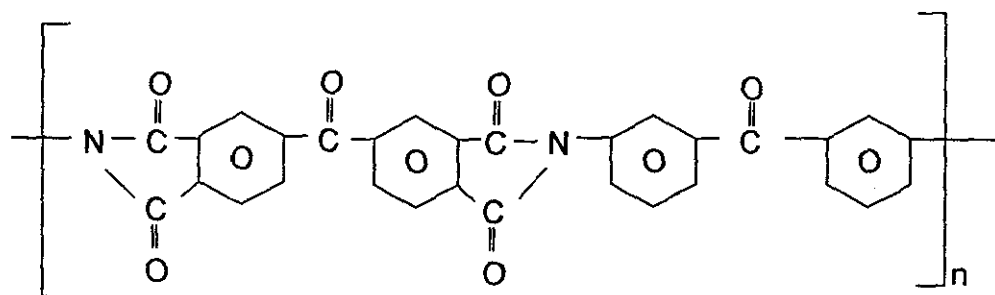
2.7 Flexible Polyimides

Polyimides may be made more flexible (i.e. decreasing T_g) by introducing "hinge linkages" in the backbone structure [66, 114]. These include carbonyl, ether, sulfonyl and methylene linkages. Altering the isomeric configuration of the diamine or dianhydride moieties may also reduce the T_g [115, 116].

The effect of isomeric configuration of diamines has been studied by Bell *et al* [115] and was reported that T_g decreased as polymer went from all para to all meta configuration. Gerber *et al* [116] studied the effect of using three different isomers of oxydiphthalic anhydride with different diamines and concluded that isomerism in the dianhydride has less effect on T_g than the isomerism in the diamine component.

The effect of introducing flexible hinge linkages on T_g is more pronounced when these are placed in the dianhydride than in the diamine [114]. The difference in T_g reduction is unlikely to be due chain rigidity as the degree of freedom being introduced is the same in both cases. Consequently, the possible cause must be associated with the difference in intermolecular interaction and chain orientation. In addition, highly polar linkages such as carbonyl or sulfonyl are less effective in decreasing T_g than the less polar linkages such as methylene or ether [66].

In considering the ways of exploiting all the above structure-property relationships, by introducing hinges and meta configurations to both diamine and dianhydride within one molecular structure, it has been possible to produce polyimides with sufficient molecular mobility to be melt-processed [117-120]. An example of such polyimides is LARC-TPI [117, 118] developed by the National Aeronautics and Space Administration in the USA, which has the following structure.



From an even wider prospective, polyetherimide is another such example [119, 120].

These materials can even eliminate the need of using solvent and performing imidisation during processing. As well as being processable, they are also substantially tougher than conventional polyimides of same molecular weight.

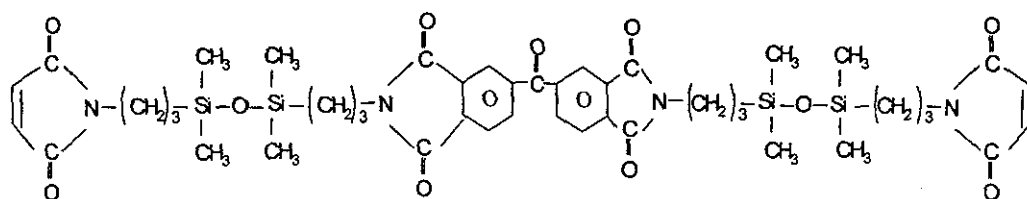
2.8 Rubber Toughening of Bismaleimides

In 1979, McGarry [121] attempted to toughen bismaleimides by using amine-terminated butadiene acrylonitrile (ATBN) rubber. The amine-termination used was intended to achieve chain extension with the unsaturation of bismaleimide through the Michael type addition reactions. However, only marginal improvements in toughness were achieved.

ATBN was also used by Varma *et al* [122] to improve the properties of two phosphorus containing bismaleimides. It was reported that impact strength improved using up to 7% rubber modification. However, toughness was not assessed by fracture mechanics and, therefore, there are, no indication of the effects on K_{IC} or G_{IC} values.

Maglio *et al* [123] studied the effect of ATBN modification on the thermal stability of bismaleimides and found that only marginal deterioration resulted for levels of incorporation up to 30% w/w. Microphase separation was observed, but no proper assessment of effects on toughness was made.

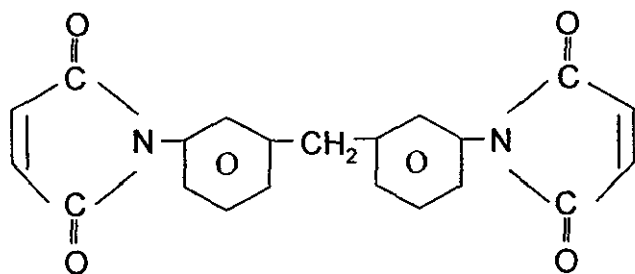
Maudgal and St.Clair [124] synthesised a polysiloxane-containing bismaleimide by using maleic anhydride, benzophenone tetracarboxylic dianhydride and bis(γ -aminopropyl) tetramethyldisiloxane as their starting materials. The structure of their bismaleimide oligomer is:



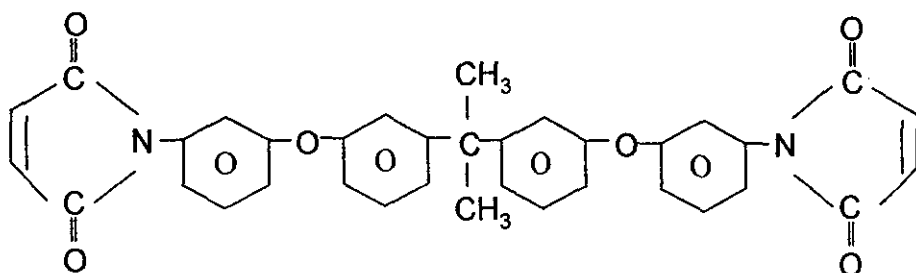
Substantial improvements in properties were found in terms of lap shear strength and processing properties, but at the expense of thermal oxidative stability, T_g and modulus.

The use of carboxylic acid-terminated butadiene acrylonitrile (CTBN) rubber as a toughening modifier for bismaleimides has also been investigated by a number of authors [125-135].

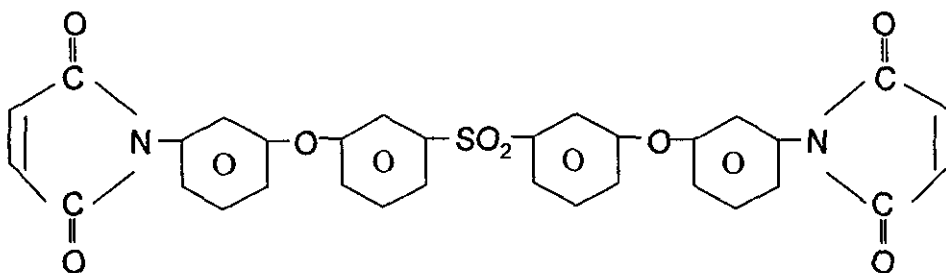
In the studies carried by Takeda *et al* [132] using CTBN as toughening agent, three types of bismaleimides were used, i.e.



4,4'-bismaleimidodiphenylmethane (BDM)



2,2-bis[4-(4-maleimidophenoxy)phenyl]propane (BPPP)



3,3'-bis[4-(3-maleimidophenoxy)phenyl]sulphone (BPPS)

Binary eutectic mixtures of the three species were also studied: 50% w/w BDM and 50% w/w BPPP; 50% w/w BDM and 50% BPPS. Systems such as these were further investigated by Shaw and Kinloch [126, 127] and were found to be appropriate for CTBN modifications, wherever long gel time and low melting temperatures are required. Incorporation of the CTBN was simply achieved by mixing the liquid elastomer into the molten bismaleimides. Both Shaw *et al* [125-127] and Takeda *et al* [132] indicated that pre-heating of the CTBN with the bismaleimides at a slightly lower temperature (as compared to curing) of around 120°C to 130°C for between 5

hours and 24 hours was crucial to achieve some enhancement in properties of the materials. Unlikely ATBN, carboxylic functionality has no reactivity with bismaleimides. Not surprisingly, therefore, the analysis of the reaction medium during the pre-heating stage did not showed any participation of the carboxylic group of CTBN in the curing chemistry of bismaleimides [132-134]. , However, both Takeda *et al* [132] and Stenzenberger *et al* [134] reported the occurrence of limited amount of reactions between the butadiene unsaturation and bismaleimides terminal groups.

With CTBN modification of up to 140 phr, Shaw *et al* [2] reported greater than five fold increases in K_{IC} and approximately fifty fold increase in the corresponding G_{IC} . Similar findings were reported by Segal *et al* [128], Stenzenberger *et al* [134] and Takeda *et al* [132].

Using SEM examinations, Stenzenberger showed that the fractographic morphology was similar to that obtained with epoxy/CTBN systems [130].

Both Shaw *et al* [2] and Takeda *et al* [132] have investigated the effect of acrylonitrile content on the properties of the products. Although Shaw *et al* indicated that the concentration of acrylonitrile in CTBN has little effect on K_{IC} , visual observation of casted sheet showed increase transparency with increasing concentration of acrylonitrile. On the other hand, Takeda *et al* indicated a decrease in G_{IC} with acrylonitrile content.

Shaw *et al* also reported a substantial reduction in modulus (in the region of 30% to 65% reductions) with 100 phr of CTBN. The degree of reduction was found to be dependent on acrylonitrile content. The higher the acrylonitrile level, the lower was the reduction in modulus. Again, Takeda *et al* reported a different observation, indicating that acrylonitrile level has no significant effect on modulus.

Shaw *et al* [125-127] using a variety of instrumental techniques such as TMA, DSC, and DMTA investigated the effect of CTBN on T_g . In TMA experiments [125], an unexpected increase in T_g was observed at 10 phr of CTBN modification. The reason

for this observation was not well understood. St. Clair [131] also claimed similar results.

Stenzenberger *et al* [129], Shaw *et al* [125-127], Segal *et al* [128] and Takeda *et al* [132] essentially reported that the incorporation of relatively large concentration of CTBN cause a substantial decrease in T_g .

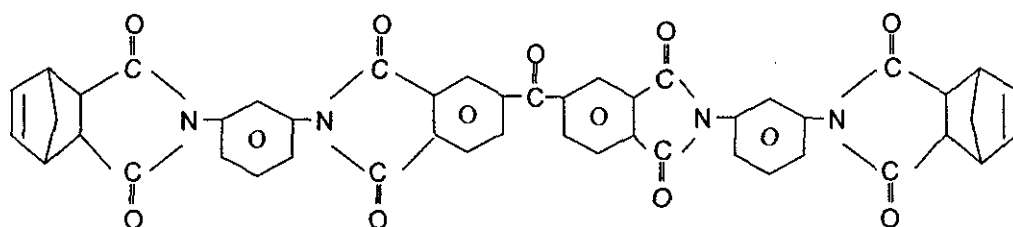
Using thermogravimetric analysis, Shaw and co-workers [125] established that the temperature for onset weight loss was reduced progressively from 450°C for unmodified system to 400°C for one containing 100 phr CTBN in a nitrogen atmosphere. In a more elaborate experiment [127], the effect of thermal ageing was evaluated by heating three samples containing 30, 50 and 100 phr CTBN at 170°C for up to 100 hours. While the 30 phr system showed a moderate reduction (30%) in K_{IC} after 1000 hours, the systems containing 50 phr and 100 phr CTBN showed a maximum in the K_{IC} values within the initial 100 hours of heating. A subsequent reduction in toughness after this maximum resulted in K_{IC} values similar to those of the unaged materials. While the modulus at 30 phr and 50 phr addition were not significantly affected by the ageing process, the 100 phr system showed a substantial increase in modulus over this period of time.

Tod and Shaw [135] studied the water absorption characteristics of CTBN systems and showed that water uptake decrease considerably with increasing CTBN concentration. They further explained that this was due to the reduction of microvoids formation in the toughened systems, which limited the uptake of water.

In addition to CTBN, Shaw *et al* [125] also studied vinyl-terminated butadiene acrylonitrile rubber. They concluded that this elastomer system does not give significantly different results from the CTBN systems.

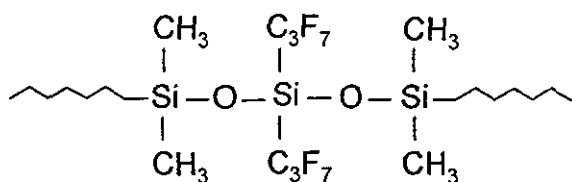
2.9 Rubber Toughening of Norbornene-Terminated Oligomers

St. Clair [117, 118, 131, 136] has conducted a series of investigations on a norbornene-terminated oligomer known as LARC-13 (see molecular structure below). A variety of elastomers and several approaches were used.

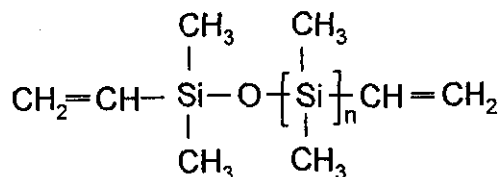


LARC-13

In the first approach [117], elastomeric modifiers were mixed physically with the oligomers in the solution form prior to imidisation. Examples of modifiers used are shown below:

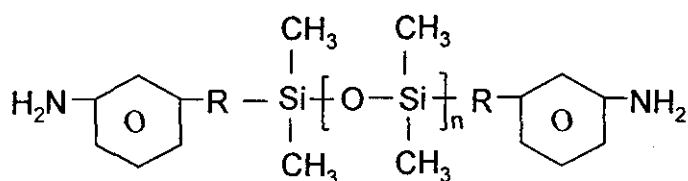


Fluorosilicone (FSE)



Vinylterminated Silicone (VTS)

In the second approach [117], amine terminated elastomeric modifiers were used to partially replace a calculated portion of the original diamine so that the elastomeric component becomes part of the backbone of the resulting oligomers. The amines used were respectively ATBN and ATS, which is an amine-terminated silicone with the following structure:



ATS

With the exception of the FSE based systems, substantial toughening was achieved in all cases, especially those using the second approach, which gave a fourfold increase in G_{IC} . In most cases, this improvement was achieved at the expense of lap shear strength, while the peel strength showed a significantly different trend, indicating substantial property improvements at both room temperature and 232°C.

Two T_g s were found for all the systems. The first transition lies between -65°C and -115°C, which correspond to the T_g of the modifier and the second transition lies between 227°C and 300°C, which correspond to the T_g of the polyimides. It should be noted that the incorporation of toughening modifiers has little effect on the T_g of the original polyimides. In addition, the thermal stability was also not significantly compromised.

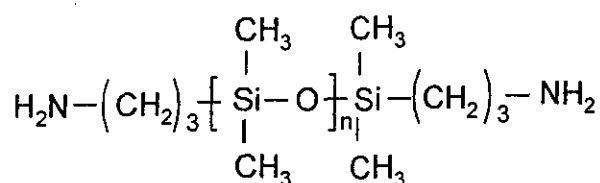
2.10 Rubber Toughening of Condensation Polyimides

Ezzell et al [137] studied the use of ATBN as a mean of improving tear resistance in polyimide films made from polyamic acid solutions. A typical two-phase morphology of rubber modified systems was reported. It was found that the tear energy reaches a maximum at 15% modification. T_g was found to decrease from 281°C to 264°C monotonically up to 20% w/w modification. No undesirable deterioration of thermal stability was observed in all the samples.

Spontak and Williams [138] studied the microstructure and properties of siloxane-imide block copolymers. A two-phase morphology was found for all systems. With one of the copolymer, a bimodal distributed domains in the region of 3 nm and 16 nm sizes were observed. Although these domain sizes are very small from the point of view of rubber toughening of polymers, the particle size distribution is very wide,

with some particles reaching a few microns. It is interesting to note that the energy-dispersive x-ray analysis showed that the dispersed domains were imide-rich while the matrix was siloxane-rich. T_g was found to decrease from 227°C to between 225°C and 215°C, which obviously indicated very little deterioration. A second T_g at approximate 61°C was found, which corresponds to the T_g of the siloxane-imide copolymer component.

Arnold *et al* [139] also studied the use of polysiloxane as a mean of improving solvents solubility in polyimides. A series of siloxane-imide copolymers were made with different dianhydrides and diamine. The siloxane oligomers used have the following structure:



The molecular weight of the polysiloxane was varied from 800 to 1000 g/mole and the level of modification ranged from 5%w/w to 70% w/w. At 40% w/w modification, the originally intractable polyimide was found to be soluble in tetrahydrofuran and dichloromethane. In this system, the T_g was found to decrease from 265°C to 218°C. It should be noted that by increasing the molecular weight of polysiloxane component, the reduction in T_g was considerably lesser. A second transition was also found at between -117°C and -123°C, which correspond to the T_g of the siloxane elastomer. Transmission electron microscopy revealed that the siloxane domains were in the region of 5 nm. A substantial reduction in water absorption was reported, which was assumed to result from the change in morphology. This drastic increase in moisture resistance ultimately led to a significant improvement in long-term durability of adhesive joints employing this material.

2.11 Sol-Gel Chemistry

2.11.1 The Sol-Gel Process

The sol-gel process can be defined as the chemical route to produce ceramic or related materials, which involve a sol-gel transition [140]. This transition allows the solidification of a precursor fluid through a physiochemical reaction.

The term sol refers to the original fluid precursor mixture, which can generally be subdivided into particulate sol and polymeric sol [141, 142]. Particulate sol is a colloidal dispersion of charged inorganic oxide particulates with no polymeric phases. Polymeric sol refers to the solution of hydrolysed metal alkoxides with domain size smaller than colloidal limit of 1nm.

Gelation can generally be achieved by the percolation of dispersed particles in the presence of the liquid medium or by polymeric crosslinking reactions and chain entanglement, forming a co-continuous morphology between the solid phase and the liquid medium.

According to Mackenzie [143], the advantages and disadvantages of sol-gel process relative to the conventional melting techniques for mineral oxides can be summarised as followed:

a) Advantages:

- Better homogeneity
- Better purity
- Lower processing temperature
- New non-crystalline solids outside the range of normal glass formation
- New crystalline phases from non-crystalline solids
- Better glass products from the special properties of gels
- Special products, e.g. films and fibres.

b) Disadvantages:

- High cost of raw materials
- Large shrinkage during processing
- Residual fine pores
- Residual hydroxyl groups
- Residual carbon
- Health hazards of organic solutions
- Long processing times
- Difficulty in producing large pieces.

2.11.2 Sol-Gel Process Involving Particulate Sol

By using this method [144], amorphous ceramics can be made which depend on the generation of stable dispersion of inorganic oxide particulates using stabilising ions. Gelation is achieved by adjusting the pH so as to destabilise the dispersion. This gel formation can be reversible if the coagulation of the particles does not result in chemical bonding.

2.11.3 Sol-Gel Process Involving Polymeric Sol

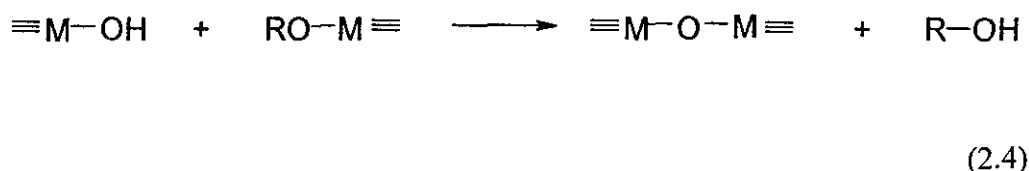
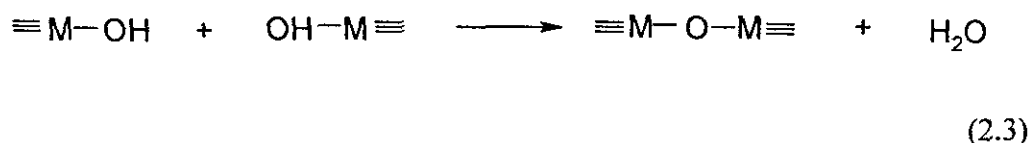
The first reaction step in preparing polymeric sol involved the hydrolysis of metal alkoxides in which hydroxyl group replaces the alkoxy ligand [140]:



M represents a metal.

(2.2)

To achieve gelation, molecular network formation must be encouraged through condensation reactions [140]:



These condensation reactions frequently occur simultaneously with hydrolysis reaction in which the nature of the reaction kinetics between the two will determine the structural characteristic of the oxides formed. Both reactions are also frequently incomplete [145, 146]. As such, unreacted alkoxy and hydroxyl functionalities can often be found in the final oxides. The concentrations of these unreacted groups depend on various factors such as water content, reaction condition, types of alkoxides, types of solvent and others [140].

2.12 Silica Derived from Alkoxides

2.12.1 Organometallic Compounds Based on Silicon

A vast number of alkoxysilanes and silicon-based materials can be used as starting materials in the sol-gel process of silica. These materials differ in terms of their organic groups that are attached to the silicon atom, which in turn determine their reactivity and the structural characteristics of the final oxides formed [140].

Tetraalkoxysilanes usually formed the basis of a polymeric sol. A large variety of these materials are available commercially, but the most important ones are silicon tetramethoxides (TMOS) and silicon tetraethoxide (TEOS) [147].

In addition to tetrafunctional alkoxides, alkyl substitutes alkoxysilanes are also frequently used to modify the chemistry of sol-gel reactions or to achieve compatibilisation as a coupling agent in multiphase system [140, 148-155].

2.12.2 Hydrolysis of Silicon Alkoxides

Under basic conditions [156, 157], the hydrolysis process involved hydroxide nucleophilic substitution of the alkoxy group by attacking the positively charged silicon atom of the alkoxides. It was thought that a five-co-ordinated complex was formed as an intermediate in the process, which will subsequently convert into a substituted silicic acid by expelling an alkoxide ion (see Figure 2.2).

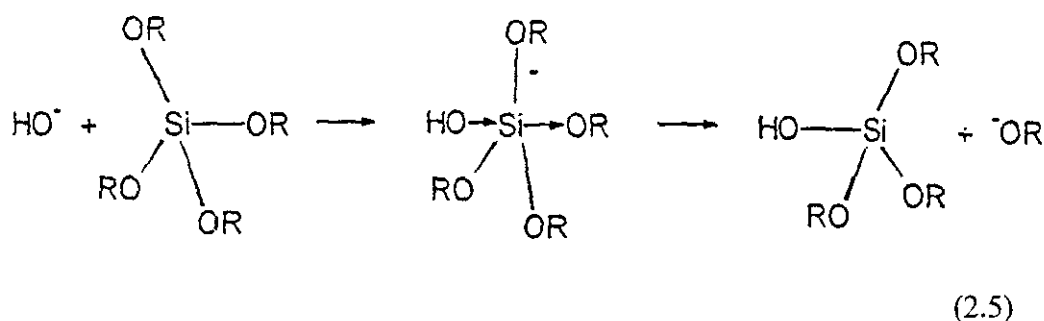


Figure 2.2: The mechanism of base-catalysed hydrolysis by nucleophilic substitution; R = H, Et or Si(OR)₃ [157].

Under acidic conditions [156, 157], the hydrolysis process involved electrophilic reaction of the hydronium ion by forming an activated complex with the tetraalkoxysilane. This subsequently results in the liberation an alcohol and the formation of a silanol functionality (see Figure 2.3).

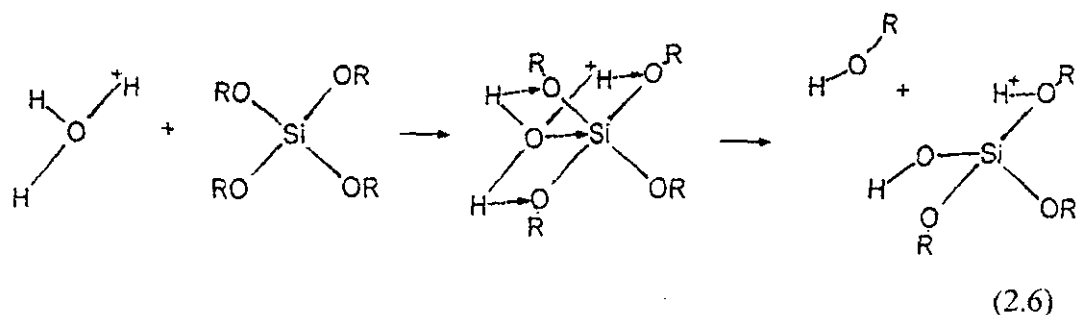


Figure 2.3: The mechanism of acid-catalysed hydrolysis by electrophilic reaction [157].

2.12.3 Condensation of Hydrolysed Silicon Alkoxides

The nature of the condensation reactions is very dependent on pH. According to Iler [144], at pH between 3 to 12, condensation occurs through nucleophilic substitution. A protonated silanol is attacked by a deprotonated silanol (the nucleophile) to form the Si-O-Si linkage (see Figure 2.4). Based on this mechanism, the most probable reacting species that will react are those of the highest polymer reacting with the smallest monomeric unit. This is because they have the largest difference in charges between them. As such, small reacting units are preferentially removed from the reacting media.

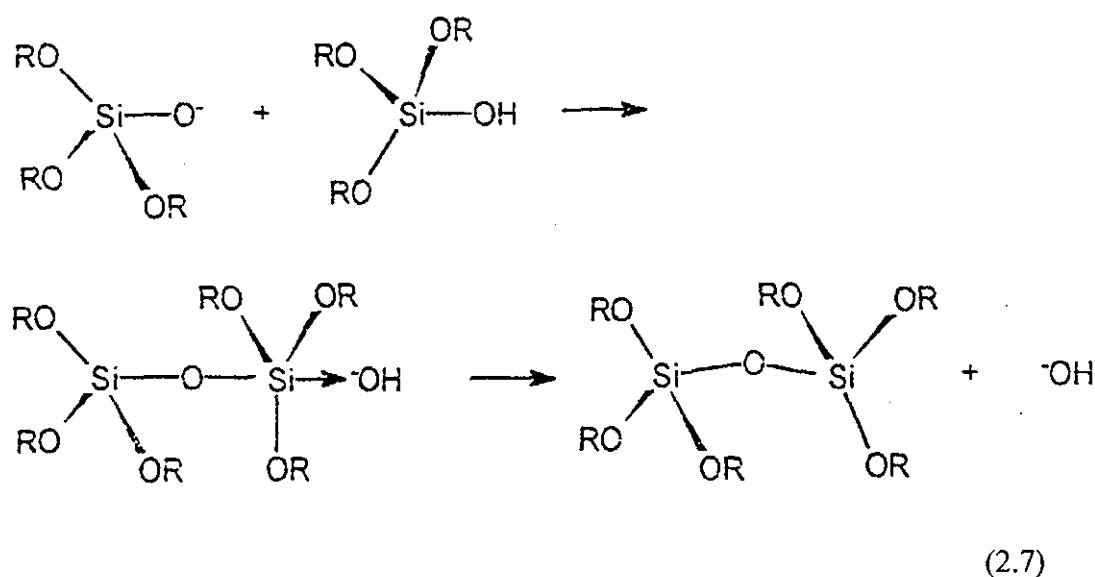


Figure 2.4: The mechanism of condensation by nucleophilic substitution; source [157].

At pH less than 3, the condensation mechanism is electrophilic [144, 157, 158] (see Figure 2.5). The smallest reacting units are the most prone to protonation and become an electrophile. These positively charged species will then attack the most condensed units (most acidic) in the media. Again, as with higher pH, smaller units are more preferentially removed from the reacting media.

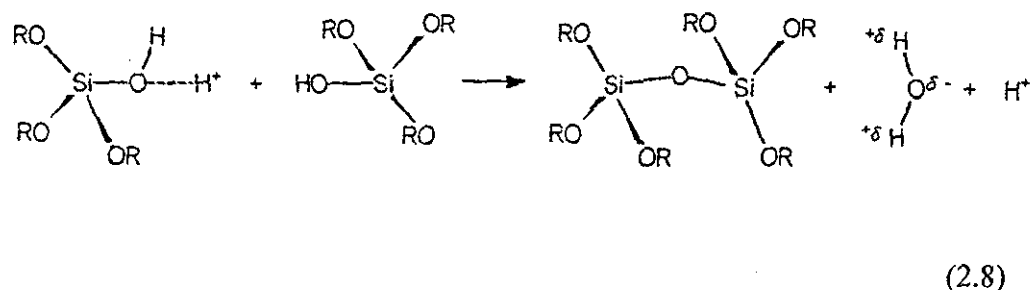


Figure 2.5: The mechanism of condensation by electrophilic substitution.

2.12.4 Effects of Using Different Catalysts for Hydrolysis

The rate of hydrolysis is dependent on the strength and concentration of the catalyst used [156, 159]. Strong acids and strong bases are considerably more efficient catalysis for the hydrolysis than their corresponding weak acids and weak bases. However, in certain cases, having longer reaction time and higher catalyst concentration can compensate the inefficiency of weaker catalysts.

In a base-catalysed hydrolysis, the reaction becomes progressively more favourable with each alkoxy group being reacted and removed from the alkoxysilane molecules [157, 158]. This is because the substituted silanol is more acidic than the displaced alkoxy group and hence becomes more prone to attack by negatively charged nucleophiles. As a result, higher degree of hydrolysis within each monomer can be attained, which will eventually lead to a higher degree of cross-linking during polymerisation. In basic conditions, the polysiloxanes formed are more soluble in the reacting medium and delay their precipitation as silicas.

In an acid-catalysed hydrolysis, the reaction becomes progressively more difficult due to the electrophiles being positively charged and are less likely in attacking the acidic silanol [157, 158]. As a result, the network formed is only lightly crosslinked or almost linear with a large number of sites unreacted [160]. Using NMR analysis [161], the heterogeneity of the hydrolysis reaction can be confirmed. Incompletely

hydrolysed species at different stages of hydrolysis can be detected at a given time of the reaction.

It is worth noting that the network structure of an acid hydrolysed system can be improved by maintaining the pH of the sol-gel reaction at around 2 [157]. In this condition, efficient hydrolysis is coupled with minimum condensation and hence, it provides the best environment to achieve a higher degree of cross-linking.

2.12.5 Effect of Water and Solvents on the Hydrolysis and Condensation Reactions

In considering the fact that hydrolysis and condensation reactions normally occurs simultaneously, the stoichiometric ratio of water to alkoxide for the complete formation of silica is equal to 2 [145]. However, in practical terms, excess water (i.e. more than the stoichiometric amount) will facilitate the hydrolysis reactions and allows crosslinking to occur more intensively [162]. This is particularly so in acid-catalysed reaction, in which higher crosslink density of the polymer network can be attained [157, 163-166].

Most alcohols form azeotropes with water [157]. In these systems, the least concentrated component evaporates first and leaves behind the other component in the sol-gel mixture. It is, therefore, important that the concentration of water must be higher than that of alcohol so that water remains in the reaction mixture to continue hydrolysis. This also reduced the possibility of depolymerisation as a result of the action of the alcohol.

The size of the alkyl group of an alcohol can also influence the rate of hydrolysis and condensation [146]. Smaller alcohol facilitates better diffusion of reactants and allows reactions to proceed to more advanced state [167].

Polar solvents are thought to be capable of solvating reacting species and decrease the rate of condensation [161, 168-173].

2.12.6 Aggregation, Growth and Gelation

The growth and gelation characteristics of silicic acid are shown in Figure 2.6.

Iler [144] described the polymerisation of silicic acid monomer as the formation of discrete polymeric particles, which then grow and join into a network. The particle size of the polymeric unit determines the radius of curvature of its surface, which controls its solubility.

At pH above 7, the rates of silica dissolution and redeposition rates are both high. The particles formed are capable of reaching colloidal dimensions. In moderately diluted systems, the negative charges on particles may be capable of producing enough mutual repulsion so that growth can occur without aggregation [144].

At low pH, particles formed are very small in size because under these conditions, there is a tendency of forming networks rather than growth of particles. This is due to the low ionic charges on the particle surfaces, which allow higher rates of interparticle collisions giving rise to aggregation [144].

Gelation is only possible below a certain pH, where the repulsive forces are low enough to promote aggregation and growth. The formation of three-dimensional networks, which occupy an increasing fraction of the sol, through progressive polymerisation, is known as microgel development [144]. For acid catalysed systems, there is a predominance of chain entanglement. For base catalysed systems, on the other hand, branched clusters of polymeric units impinge onto each other. These result in a sudden increase in viscosity to form a gel [141].

2.12.7 The Effect of pH on Gelation

The effect of pH on gel-time is shown in Figure 2.7 [144].

The observation of a peak in the gel time curve at around pH 2 corresponds to the isoelectric point [144] i.e. conditions where the surface charges are zero. This is also

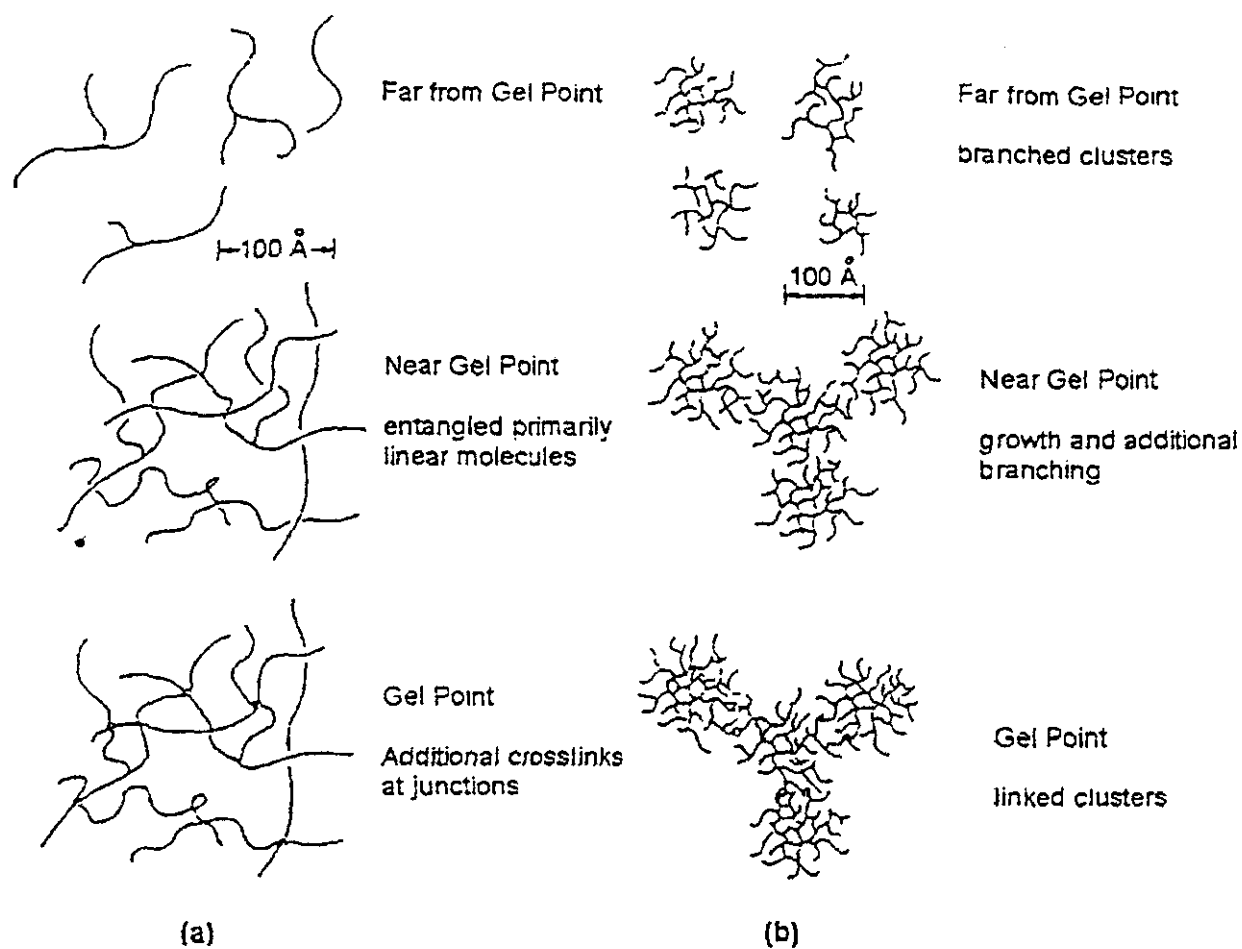


Figure 2.6: Polymer growth and gel formation in (a) acid- and (b) base-catalysed systems [141].

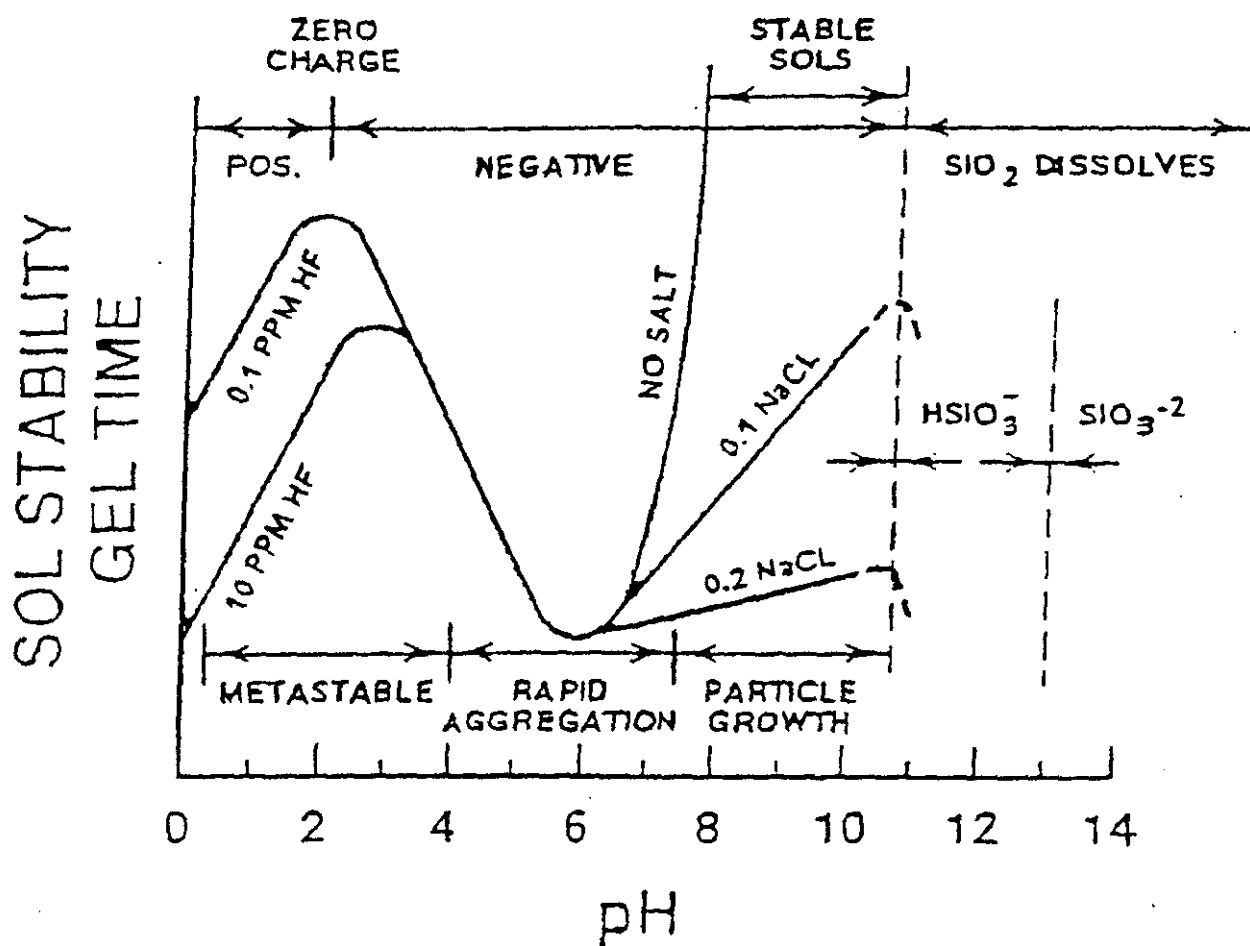


Figure 2.7: Hydrolysis-condensation behaviour of aqueous alkoxy silane solutions [144].

corresponds to conditions where the rate of condensation reaction is at its minimum so that extensive chain branching takes place.

At pH below 2, gelation becomes faster, due to the accumulation of surface charges, which promote surface attraction of particles. However, this acceleration in gelation is also catalysed inevitably by traces of hydrogen fluoride, which are present in silicas originated from most synthetic route [144]. Iler [144] explained that fluoride ion is smaller than hydroxide ion and can act in its place to raise the co-ordination number of the silicon atom from 4 to 5 or 6, so that the activated complex necessary from nucleophilic reaction can be formed [174]. Both hydrolysis and condensation reaction are accelerated by this process. This effect may be partially counteracted by the formation of complexes by metal impurities [144].

At pH above 7, silica becomes increasingly more soluble and nucleation of gel particles becomes more difficult [144].

2.13 Organic-Inorganic Hybrid Materials

The combination of materials with different characteristics in order to gain new properties in the final composites is a constant objective of researches concerns with materials developments. The tendency is to decrease the unit size of the components and eventually mechanical mixture at the nanometre scale becomes hardly possible. Two-dimensional layered hybrids [175], however, have been made by intercalation techniques and are a new generation of promising materials specialised technologies such as the electronics industry. Since the sol-gel process is not restricted to any particular shape, it has been widely investigated as the most suitable way to synthesise at low temperatures ceramic precursors for hybrid materials.

The degree of phase separation in organic-inorganic materials can vary, but domain sizes are typically on the nanometre scale. In such cases, the domain sizes are reduced to a level such that true 'molecular composites' are formed. As a result of this intimate mixing, these hybrids or creamers (ceramic-polymer materials) are often transparent, a property outside the scope of traditional composites. In the absence of

match in the refractive indexes for matrix and embedded particles, scattering losses are minimised only when the phase domains of the composites are smaller than the wavelength of the incident radiation. In the particular case of the human eye, the composite will be transparent when its domain sizes are smaller than approximately 380 nanometres.

It is important to define the approach under which the hybrid material is considered. If the consideration starts with examples of inorganic network or gel formers as inorganic, like SiO_2 or TiO_2 , the chemical, optical and mechanical properties should be related to those of the corresponding bulk glasses or ceramics. If the consideration starts from the organic polymeric side, the properties of the resulting hybrid should be related to high thermal expansion, low glass transition temperature values, softness and low densities. In addition to this, the influence of the interface organic polymer-inorganic network is a third parameter.

There are two obvious routes to the formation of organic-inorganic composite materials through the sol-gel process. The first method to produce hybrids is to fill the pores of the inorganic gel with a polymer produced in-situ or through impregnation techniques after gel stabilisation. Following the work of Pope and Mackenzie [176], Abramoff and Klein [177] impregnated a xerogel with methyl methacrylate, which was subsequently polymerised by UV light, and obtained large improvements in mechanical and optical properties. The excellent optical properties found in poly(methyl methacrylate)/silica hybrids [178], with the organic phase created in situ, were explained in terms of the hydrogen bonding between residual hydroxyl groups on the surface of silica particles and the carbonyl group in the polymer backbone, therefore, preventing phase separation.

The second route involves carrying out the hydrolysis/condensation reactions in the presence of a preformed organic polymer. If conditions can be identified under which the organic polymer will not phase separate during both the gel forming and drying processes, then optically transparent materials can be obtained. The issue of polymer solubility is paramount in the synthesis of these materials. The most important parameter in controlling polymer solubility is the co-solvent used, typically tetrahydrofuran, aliphatic alcohols or DMF. The ongoing hydrolysis processes can

change the solvent properties (from polar protic to polar aprotic). Only a limited number of polymers remain homogeneously embedded within a silica matrix at the end of the condensation and drying stages. Polymers with basic functional groups such as poly(2-vinylpyridine) or polyacrylonitrile are soluble in the acid catalysed tetraethoxysilane (TEOS) solution using organic acids as co-solvents [179]. Slow drying produced highly transparent glassy materials.

2.14 Polyimide-Inorganic Oxide Hybrids

In considering the physical approach for producing organic-inorganic hybrids based on polyimides, it is possible to use an intercalation technique [175]. Yano *et al* [180] achieved this by dispersing nanodimensional plates of montmorillonite clay in DMAc. The hybrid material was produced by mixing this dispersion with polyamic acid, also dissolved in DMAc, and subsequent curing (through imidisation) reactions the mixture to produce transparent film.

Alkoxides of silicon and titanium were originally used by Nadi *et al* [181], in an initial attempt to producing polyimide hybrids by generating the inorganic phase in-situ. Their approach involved the mixing of the respective alkoxide with different combination of dianhydrides and diamines for the polyimide synthesis. The carboxylic groups of the polyamic acid, derived from the polymerisation of diamines and dianhydride, were proposed to act as coupling sites of the polymer and the metal oxides. They also postulated that the water liberated from the subsequent imidisation reaction could be used for the hydrolysis reaction of the alkoxides, and could be accelerated by adding trace amounts of acid prior to curing. Transparent films were produced containing nano-sized particles of titania and silica as described or as mixed oxides products.

Morikawa *et al* [182] produced polyimide-silica hybrids by mixing the solution of TEOS in DMAc with a polyamic acid also in DMAc. Water was subsequently added to hydrolyse the alkoxide. At silica contents greater than 10%, the films produced were opaque due to the formation of coarse particles a few microns in size. At low silica content, the T_g of the films produced was lower than that of the unmodified polyimide. This suggest that the hydrolysis of the alkoxides were incomplete and that

the presence of uncrosslinked polysiloxane chains caused plasticisation of the polyimide matrix. The tensile strength and elongation at break were also considerably lower than the values for the unmodified polyimides.

This system was subsequently improved by producing polyimides containing different levels and types of pendent alkoxyisilane functionality [183]. The modulus was found to increase with increasing silica content, while the tensile strength remained unchanged and the elongation at break decreased considerably. Excessive compatibilisation with higher level of alkoxyisilane functionality was found to be undesirable as the polyimide obtained started to lose its characteristics, such as lower T_g .

In a further investigation [184], the same research group studied the use of amine salt of polyamic acid for the production of hybrids using either methanol or DMAc as solvents. The use of different proportions of methyltriethoxysilane and dimethyldiethoxysilane, as network modifiers, were also investigated. DMAc system produced films with a coarser morphology than those produced with methanol. The mechanical properties of the latter system were also better. In parallel work, where TMOS was instead of TEOS, it was pointed out that spinodal decomposition was responsible for the interconnected globular structure observed.

For the production of organic-inorganic hybrids compatibilisation can be achieved by using coupling agents that act as bonding sites between the organic-inorganic phases. This was achieved by Mascia *et al* [51] with the use of γ -glycidyloxypropyltrimethoxysilane (GOTMS) in their work. The morphology of the hybrid films was controlled by adjusting the reaction time at 80°C in a NMP solution of polyamic acid with the prehydrolysed TEOS/GOTMS mixture. Under the same reaction condition, coarser morphologies were obtained when a high molecular weight polyimide was used and compared with a low molecular weight polyimide. The compatibilisation mechanism was originally interpreted in terms of the epoxide ring opening of GOTMS and subsequently reacting with carboxylic group of polyamic acid. However, it was noted that this esterification reaction of GOTMS did not prevent full imidisation of the polyamic acid. The storage modulus and the T_g

values of the compatibilised systems were higher than those recorded for non-compatibilised systems. Based on the examination of the $\tan \delta$ data, it was suggested that polyimide chains were entrapped within the continuous silica network, which contributed to a reduction in viscoelastic losses to a much greater extent than it predicted from the law of mixtures [52]. The tensile strength was found to increase with silica concentration up to 25% in the compatibilised system. The elongation at break and the coefficient of thermal expansion decreased according to morphology changes. The addition of small amounts of dimethyldiethoxysilane (DMES) to compatibilised films can increase the elongation at break and improve toughness.

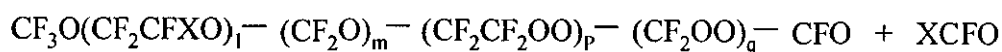
Wang *et al* [185] used aminophenyltrimethoxysilane (APTMOs) as a coupling agent, which were added either to the polyamic acid solution or the TMOS solution before the two mixtures were mixed together. The latter method gave better transparency and higher heat stability in films.

2.15 Material Preparations Involving Perfluoroether Oligomer

2.15.1 Perfluoroether Oligomer (Fomblins)

Perfluoroether Oligomers are produced commercially by a unique method developed by Ausimont. This method consists of a direct conversion of perfluorolefins to oligomeric products by photooxidation.

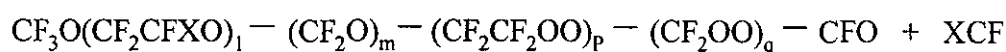
The first step is performed by simultaneously introducing a fluorolefin such as hexafluoropropylene (HFP), tetrafluoroethylene (TFE) or a mixture of the two and oxygen into a cold reactor (i.e. 45°C or less) equipped with an immersion light source with a frequency of 2600 Hz (wave number 8700 nm^{-1}). HFP acts as its own solvent while an external solvent has to be used with TFE. The fluoroligomers produced are terminated by trifluoromethyl and fluoroformate groups, while the major byproducts of the reaction (see below) are C_2F_4 or CF_3 .



(2.9)

where $X = \text{CF}_3$ or F

The relative value of the repeating units can be varied over a wide range by adjusting the conditions of the reaction. The final reaction consists of a peroxide deactivation step by fluorination and heat as follows:



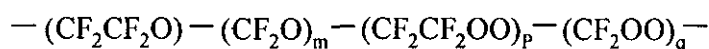
(2.10)

where m is usually very small.

The resulting neutral perfluoropolyethers consists of two products, known commercially as Fomblin Y and Fomblin Z according to whether $X = \text{CF}_3$ or $X = \text{F}$.

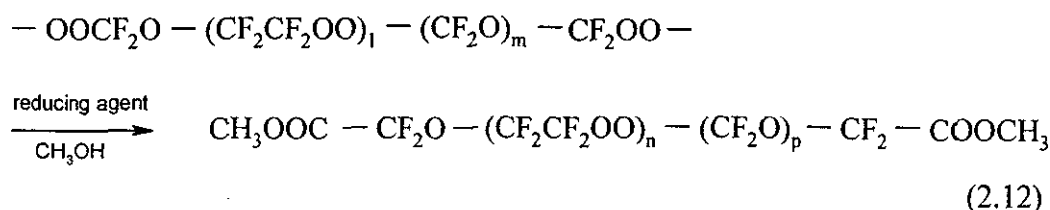
Furthermore, the neutral perfluoropolyethers, particularly the Fomblin Z types are converted to more versatile difunctional oligomers, according to the method described below.

In the Fomblin Z series, (i.e. when TFE is used as monomer), the photooxidation reactions lead to the foration of peroxidic perfluoropolyethers of the following formula:



(2.11)

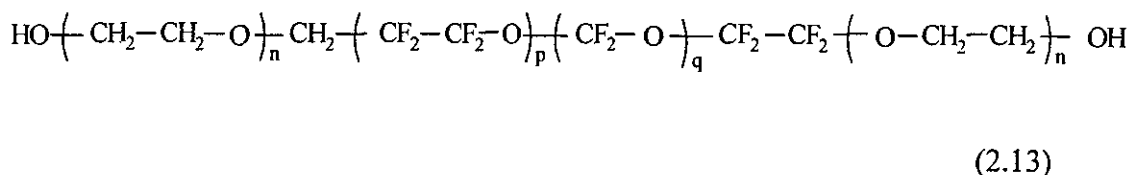
The peroxide groups are chemically reduced forming functional perfluoropolyethers and capped with methyl ester groups according to the following reaction:



The perfluoropolyether produced is called "Standard Fomblin ZDEAL", its molecular weight is around 2000 and has a viscosity at room temperature in the range 1 to 30 Pa.s.

Using the standard Fomblin ZDEAL, a number of derivatives can be obtained, through hydrolysis reactions, i.e. Fomblin ZDEAL is transferred to alcoholic Fomblin ZDOL derivatives, which in turn can be reacted with ethylene oxide to form ZDOL TX.

The chemical structure is as follows:



where $n = 1$ to 3

2.15.2 Toughening of Epoxy Resins

With an appropriate telechelic modification, Zdol-TX can be used as an impact modifier for epoxy resin [47, 48]. The chemical modification involved the consecutive reactions with chlorendic anhydride (CA) and caprolactone (CL), which result in full miscibilisation of the modified Zdol-TX with epoxy resin. Both difunctional system i.e. diglycidylether of bisphenol A (DEGBA) [47, 48] and tetrafunctional system i.e. tetraglycidyl diamino diphenyl methane (TGDDM) [49, 50] were investigated. Curing with anhydride based hardeners and benzyl dimethyl amine

catalyst produce transparent products exhibiting a finely phase-separated, but co-continuous morphology for both systems.

In the DEGA system, pre-reaction of the modified Zdol-TX (carboxylic terminated) with an excess epoxy resin in the presence of triphenyl phosphine (TPP) catalyst, resulted in products that were opaque and morphologically different. They displayed a dispersed particulate structure [47, 48]. Microhardness measurements revealed that the matrix has approximately the same hardness as that of the original epoxy resin. Energy disperse X-ray analysis by Scanning Electron Microscopy (SEM) clearly indicated that the precipitated particles are rich with the fluorinated modifier, while the measurements of volume fractions indicated that the particles also contained approximately 50% epoxy/hardener content. Substantial improvement in toughness and strength were achieved in these systems, but at a relatively small expense of their modulus. These effects can be clearly observed even at very low modification such as 5% w/w and are more pronounced in the particulate system [47, 48].

In the TGADDM system, no particulate system has been reported yet. With respect to its transparent products, similar improvement in toughness with moderate loss of modulus was also observed. However, the yield strength was found to decrease slightly, instead of gaining as compared to that of the DEGA system. A considerable increase in water diffusion coefficient and a reduction in the maximum amount of water absorbed were also reported [49, 50]. Using small angle x-ray scattering (SAXS) examination, the co-continuous morphology of the system revealed the presence of heterophase domains, in the order of 16 to 17 nm [49].

Interestingly, both the DEGA system and TGDDM system showed a slight increase in T_g at low level of modification, which peak at around 2.5 to 5% w/w [47, 49]. This observation is very similar to that reported by Shaw *et al* [125-127], and St. Clair [131] involving the rubber toughening of bismaleimides (see section 2.8). At higher level of modification, the T_g of the TGDDM system reduced gradually to a relatively constant level, which was around the same magnitude as the unmodified epoxy resin [49]. The reduction in T_g at higher level of modification of DEGA system was slightly more significant at around 10% modification, when the T_g was found to be about 15°C lower than for the unmodified resin. However, in considering the fact that

the T_g of the perfluoroether oligomer is around -70°C or lower, this reduction in T_g is notably marginal as compared to that predicted theoretically for miscible blend [47]. In the attempt to understand the reasons for the increase in T_g at low level of modification, the curing kinetics of TGDDM system was investigated by following the reaction using near infrared equipped with a heating environment chamber to carry out the reactions. A significant reduction in reaction rate was found to take place for the modified systems, while the degree of conversion remained essentially unaffected by the modification [50].

2.15.3 Preparation of Perfluoroether-Silica Hybrids

Mascia *et al* [53] achieved compatibilisation between the perfluoroether oligomer and silica by reacting the telechelically modified Zdol-TX (using CA and CL consecutively as described above) further with γ -glycidyloxypropyltrimethoxysilane (GOTMS) at 85°C for 1 hour in bulk. 85% conversion was estimated using NMR. A transparent mixture was obtained by mixing the alkoxysilane functionalised perfluoroether oligomer with a prehydrolysed TEOS solution in a large quantity of aprotic solvent such as DMF or THF, for 15 hours or more. The hybrids formed by casting are highly transparent.

Transparency of the final product may be affected if inadequate compatibilisation was carried out [53]:

- (i) having insufficient GOTMS functionalisation;
- (ii) having insufficient dilution with solvent;
- (iii) having excessive amount of silica.

2.15.4 Preparation of Epoxy-Perfluoroether-Silica Hybrids

In order to achieve compatibilisation with silica, 10% of the epoxy group of a difunctional epoxy resin is functionalised with bis (γ - trimethoxysilylpropyl) amine in bulk at 90°C for 2 hours [186, 187]. It was found that the level of compatibilisation

achievable, can be enhanced by increasing the magnitude of the following parameter [186]:

- (i) molecular weight of the epoxy resin;
- (ii) degree of functionalisation;
- (iii) polarity of the solvent;
- (iv) processing temperature.

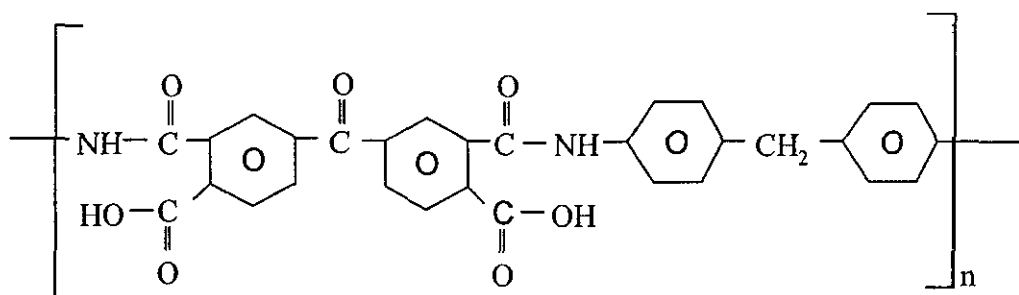
Hybrids were prepared by mixing this functionalised epoxy resin with the miscibilised Zdol-TX/TEOS solution as described above and curing the miscibilised mixture subsequently with methyl nadic anhydride or diamino diphenyl sulphone hardener. The films produced were transparent and has considerably lower surface energy as compared to the original epoxy ceramer even with only 1% modified TX. This was found to be due the fluoro-oligomer migrating to the product surface [187].

3 EXPERIMENTAL

3.1 Materials

3.1.1 Polyimide Precursor

This is a low molecular weight polyamic acid solution, Skybond 703 (S703), commercially available from Monsanto. It consists of approximately 65% solid in a mixture of NMP, ethanol and xylene. The molecular structure of the polymer is shown below:



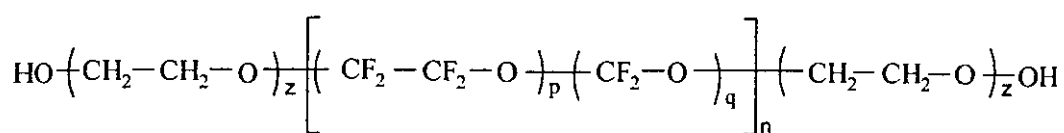
Skybond 703

3.1.2 Modifiers

The modifiers used are:

a. Hydroxyl-Terminated Perfluoroether Oligomer

This is the starting material for the production of the morphology modifiers of polyimide. It is commercially available as Fomblin Zdol TX from Solvay Solexis. The material is a clear liquid (25.08 Pas at 20°C) with number average molecular weight of 2150. Hydroxyl functionality constitutes the oligomer chain ends. The chemical structure is shown below:

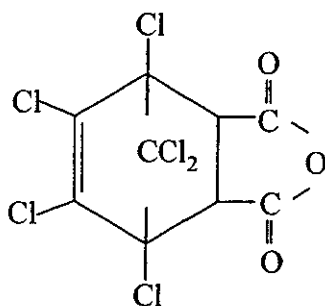


where: p/q molar ratio = approximately 0.67
 n = approximately 10
 z = approximately 1.5

This product will be referred as Oligomer TX.

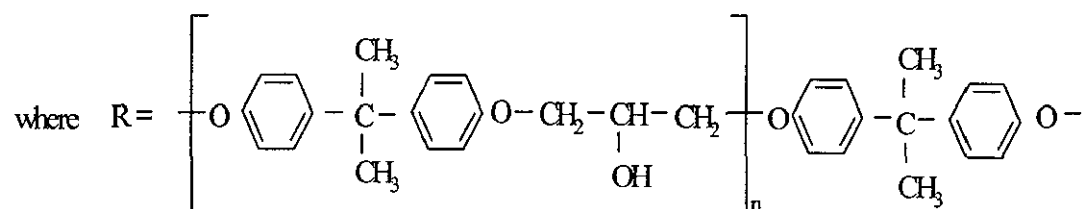
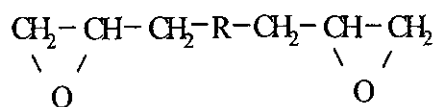
b. Chlorendic Anhydride

Chlorendic anhydride (CA) is an extremely reactive anhydride and is used as a telechelic modifier for Oligomer TX. It is a white powder with a melting point of 335°C and can be obtained from Aldrich Company. The chemical structure is as follow:



c. Difunctional Epoxy Resin

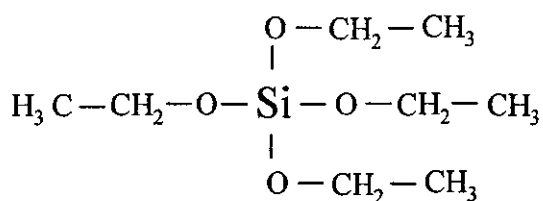
This is a diglycidylether of bisphenol A, Epikote 828 (E828), manufactured by Shell Chemical Company. The material is medium viscosity (approximately 125 Pas at 25°C) and has an epoxide equivalent of 182 to 192. The chemical structure is:



$n = \text{approximately } 0.13 \text{ to } 0.15$

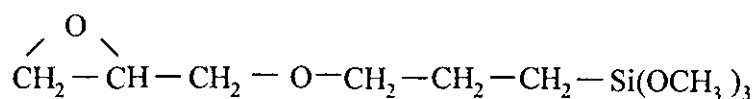
3.1.3 Precursor for Silica (Silicon Dioxide)

Tetraethoxysilane (TEOS) is used in the generation of silica during hybridisation of polyimides in this study. It was obtained from Aldrich Chemical Company and the chemical structure is:



3.1.4 Coupling Agent

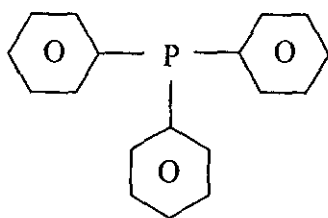
γ -glycidyloxypropyltrimethoxysilane (GOTMS) is an organofunctional alkoxy silane and was used to improve compatibility between the inorganic and organic components during the production of hybrids. The chemical structure is:



3.1.5 Catalysts

a. Triphenylphosphine

Triphenylphosphine (TPP) is used to catalyse the esterification reaction between an epoxide group and a carboxylic acid. It was obtained from Aldrich Chemical Company and the chemical structure is:



b. Hydrochloric Acid

Hydrochloric acid (HCl) is used to catalyse the hydrolysis of TEOS. It was obtained as a 35% concentration solution from Aldrich Chemical Company.

3.1.6 Solvents

The solvents used are distilled water, ethanol, NMP and toluene. The latter three were obtained as analytical grades material from Aldrich Chemical Company.

3.1.7 Carbon Fibres

These were used for the production of continuous composites. The tow used is an epoxy-sized system supplied by Tenax Fibres GmbH under the tradename Tenax HTA 5131. It is made up of 3000 filaments, 7 μm in diameter and possesses a density of about 1.8 gcm^{-3} . The tensile strength and modulus are 3.95 GPa and 2.38 GPa, respectively.

3.2 Methodology for the Modification and use of Perfluoroether Oligomers to Modify the Mechanical Performances of Polyimide and Polyimide-Silica Hybrids as Matrices for Carbon-Fibre Composite

The hydroxyl-terminated perfluoroether oligomer (Oligomer TX) available from Solvay Solexis is immiscible and non-reactive with polyamic acid based precursors of condensation polyimides (Skybond 703 from Monsanto, used in this project), even in the presence of polar aprotic solvents, such as dimethyl formamide (DMF), N-methyl 2-pyrrolidone (NMP) and butanol.

As a part of an on-going research programme, this project is concerned with the modification of the mechanical performances of polyimides and polyimide-silica hybrids, which are generally accepted as extremely brittle, especially after hybridisation. Based on previous experience with perfluoroether oligomers in IPTME [47-53, 186,187], it was clear right from the beginning that it is vitally important for the purpose of enhancing mechanical properties that appropriate and suitable compatibilisation must be attained between the polyamic acid and the perfluoroether oligomer. In the case of hybrids, the sol-gel reaction of silicon alkoxides should not result in any undesirable and/or uncontrollable phase separation of the perfluoroether or silica components from the reaction mixtures.

In this project, compatibilisation of the perfluoroether oligomer with polyamic acid and sol-gel precursors was exploited through the following approaches:

- (i) Appropriate telechelic modifications of the oligomer
- (ii) The suitable use of non-polar aprotic co-solvents
- (iii) Partial graftings (i.e. through the formation of primary bondings) of the perfluoroether oligomer with the polyamic acid
- (iv) The appropriate use of coupling agents

It is important to note (even though a rather idealistic aim), that compatibilisation should not result in excessive plasticisation from the rubbery oligomers.

Consequently, the compatibilised perfluoroether should only be fully miscibilised with the polyamic acid solution initially. It should then phase separate out in a

controlled fashion during the curing stage of the polyimides or during the gelation stage of the silica sol-gel process.

3.3 Visual Appearance as a Basis for Preliminary Assessment of Compatibilisation and Miscibility in Reaction Mixtures

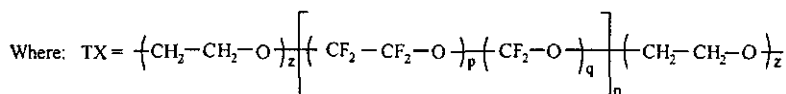
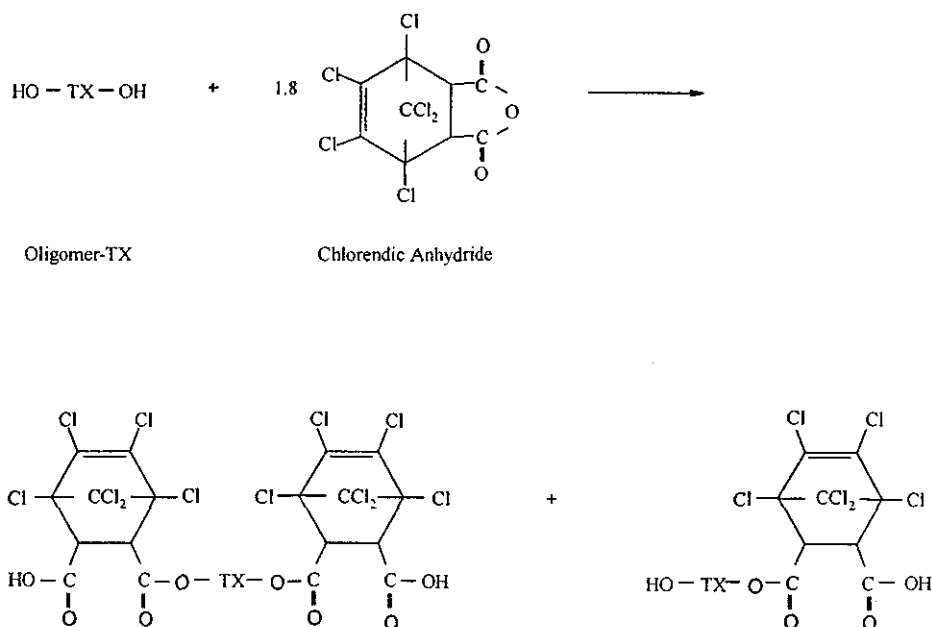
In this study, optical transparency of a mixture was used as an initial indication for miscibility. This form of assessment was adopted essentially throughout the whole project and was particularly important in the following circumstances:

- (i) Effectiveness of the various telechelic modification reactions. Modified perfluoroether oligomers that were not miscible (i.e. optical opaque) with the corresponding polyamic acid solutions were usually discarded without further evaluation.
- (ii) Suitable use of solvents for a specific physical or chemical reaction.
- (iii) Determination of premature and undesirable phase-separation during drying, curing, and gelation.

3.4 Telechelic Modification of the Perfluoroether Oligomer Using Chlorendic Anhydride

The hydroxyl-terminated perfluoroether oligomer (Oligomer TX) was allowed to react with chlorendic anhydride in a round bottom flask at a molar ratio of 1:1.8. The mixture was heated at about 150°C with vigorous stirring using a magnetic follower until all the chlorendic anhydride powder were no longer visible and a clear fluid was formed. This reaction took about 20 minutes. The heating was then continued for another 20 minutes to ensure completion. These reaction conditions have been established as being satisfactory to achieve complete conversion [47, 48]. This product is referred to Oligomer TX-CA.

The reaction that takes place is depicted below:



p/q molar ratio = approximately 0.67

n = approximately 10

z = approximately 1.5

(3.1)

Since the amount of CA used is 1.8 moles instead of 2 moles, it is to be expected that there will be some terminal hydroxyl group left in the resulting acid functionalised oligomer. The exact amount of the hydroxyl terminal groups present would depend on the extent of condensation reaction that had taken place to form higher molecular weight species.

Oligomer TX-CA was allowed to dissolve in NMP to form a 50 wt% solution and was used in a number of experimental stages later. This mixture is referred to as Oligomer TX-CA solution.

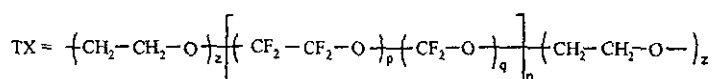
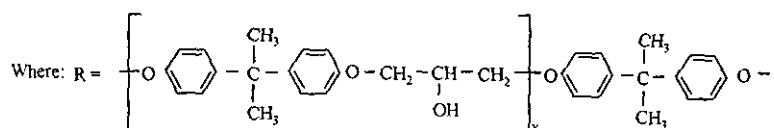
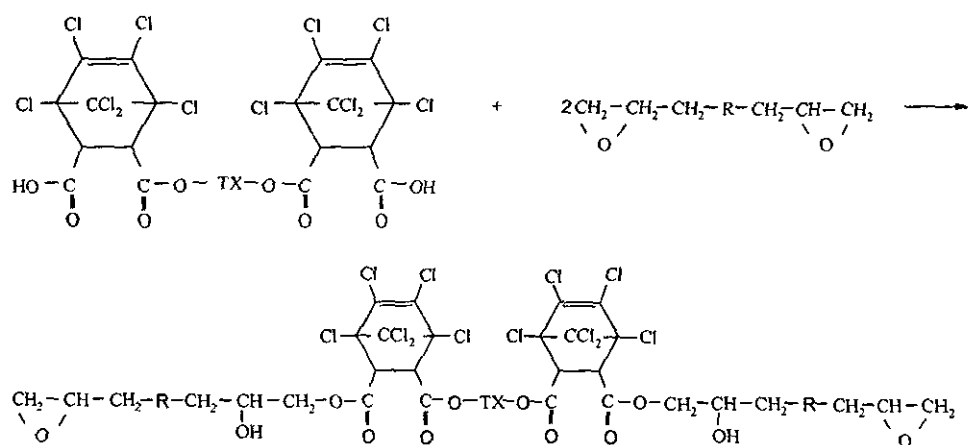
3.5 Epoxy Functionalisation of the Acid Terminated Perfluoroether Oligomer (Oligomer TX-CA)

The difunctional epoxy resin, E828, was first dissolved in toluene to form a 50% w/w solution. One part per hundred (1 phr) of TPP was then added. This solution was then mixed with Oligomer TX-CA solution in which the E828/Oligomer TX-CA molar ratio was equal to 2. Heating was then carried out at 80°C under reflux condition for up to 3 hours. The extent of the reaction was followed quantitatively by collecting samples at every half an hour interval for infrared analysis. These samples were prepared by smearing a small amount of the intermediate products on a sodium chloride disc and solvent removed by placing the casting under an infrared lamp for 30 minutes. The analysis was carried out using a transmission method with a single beam using a Fourier Transform Infrared (FTIR) spectrometer – Unicam Instrument (Mattson 3000). The absorption result of the spectrum was used for the quantitative study.

The Epoxy Index (EI) was used to estimate the minimum time required for the functionalisation reaction to be adequately carried. It is defined as the ratio of the optical density of the peak at 914 cm^{-1} , corresponding to the epoxide group of E828, to the optical density of the invariant at 1500 cm^{-1} , corresponding to the aromatic ring of E828, i.e.

$$\text{Epoxy Index (EI)} = \frac{\text{Area of absorbance peak at } 914 \text{ cm}^{-1}}{\text{Area of absorbance peak at } 1500 \text{ cm}^{-1}}$$

The expected reaction is depicted below:



p / q molar ratio = approximately 0.67

$x =$ approximately 0.13 to 0.15

 $z = 1.5$

$n = \text{approximately } 10$

(3.2)

The reacted mixture is referred to as Oligomer TX-CA-E8 solution.

3.6 Characterisations of Oligomer TX, Oligomer TX-CA and Oligomer TX-CA-E8

The nature of the telechelic reactions of Oligomer TX was also studied qualitatively by comparing the infrared (FTIR) spectrum of Oligomer TX, Oligomer TX-CA and Oligomer TX-CA-E8.

All samples were prepared by smearing them on sodium chloride discs. In addition, the solvent of Oligomer TX-CA-E8 was removed by exposing the casted sample to an infrared lamp for 30 minutes.

The thermal characteristics of the oligomers were evaluated using a modulated-temperature differential scanning calorimetry (MTDSC). Oligomer TX and Oligomer TX-CA were examined directly. Toluene was present in Oligomer TX-CA-E8 and was removed by casting the sample on a glass slide and placing in a vacuum oven at around 100°C for 1 day. All the analyses were carried out using a TA Instrument (DSC2920 modulated DSC) under the following conditions: oscillation amplitude of 1°C, oscillation period of 60 seconds, heating rate of 2°C/minute, and nitrogen gas testing environment. Data acquisition was made from -120°C to 30°C

3.7 Preparation of Modified Polyimides with Acid-Functionalised Perfluoroether Oligomer (Oligomer TX-CA)

The original polyamic acid solution (S703) was first diluted with NMP to 50% w/w in concentration.

Samples were prepared by mixing various weight fractions of Oligomer TX-CA solution with the diluted polyamic acid solution, varying from 5% to 30% w/w with respect to the amount of perfluoroether in the final mixtures. It was thought that reactions may take place between the acid functionality of the Oligomer TX-CA and the amide group of the polyamic acid, i.e. external imidisation. The molar ratios of the acid functionality of Oligomer TX-CA to the secondary amine functionality of the repeat unit of polyamic acid (S703) was calculated using the formulae following:

Molar Ratio of Functionality

$$= \frac{\text{Number of moles of acid group in Oligomer TX-CA}}{\text{Number of moles of amide group in repeat unit of polyamic acid}}$$
$$= \frac{(\text{Weight / molecular weight of Oligomer TX-CA}) \times 1.8}{(\text{Weight / molecular weight of repeat unit}) \times 2}$$

The mixtures were heated in an oil bath for 1 hour at 60°C in a reflux condition (this will be referred to as a pre-reaction step). They were then cast onto glass slides and vacuum dried at 80°C for 4 hours, followed by four consecutive steps of post curing, each of 30 minutes duration at 120°C, 150°C, 250°C and 300°C, respectively.

The films were detached from the glass-slides by immersing them in boiling water for between 50 and 90 minutes, and were then further vacuum dried in a vacuum oven at 80°C for a day. These formulations are labelled according to the table specified below:

Oligomer %	Coding
0	Control PI
5	PI-TX-CA (5)
10	PI-TX-CA (10)
20	PI-TX-CA (20)
30	PI-TX-CA (30)

Table 3.1: Coding for the mixtures of Oligomer TX-CA and S703.

3.7.1 Effect of Solvent

The additional amount of NMP included in the systems (i.e. the level of dilution) was thought to play a significant role in achieving miscibilisation between the two polymeric components and in reducing the viscosity of the overall mixtures. In the attempt to evaluate its effect, a series of samples were produced in the same way as above, but dilution with NMP was not carried out on the original Skybond 703 solution.

3.7.2 Effect of Pre-Reaction Temperature

The pre-reaction step described above aimed in "grafting" the oligomer onto the backbone of the polyamic acid through external imidisation as mentioned previously. In an attempt to evaluate the effect of the pre-reaction temperature, a series of samples were prepared as above, but pre-reaction was carried out at 80°C instead of 60°C.

3.7.3 Visual Examinations

For all the S703/Oligomer TX-CA mixtures, the miscibility was first assessed visually at different stages of the preparation process. Placing the glass slides containing the cast samples over a white background allowed the determinations of transparency or opacity to be made more accurately.

3.7.4 Morphological Studies

The morphology of the cured polyimide/Oligomer TX-CA mixtures was evaluated using a scanning electron microscope (SEM) coupled with energy dispersive x-ray microanalysis (EDXA) – Leica Cambridge Instrument Stereo 360. The specimens were fractured with a hammer after immersing in liquid nitrogen for 20 minutes and glued to a stub with colloidal silver. A layer of gold was sputtered on the specimen to impart surface conductivity. The cross-section of the samples was examined.

3.8 Preparation of Modified Perfluoroether Polyimides with Epoxy Functionalised Oligomer (Oligomer TX-CA-E8)

Oligomer TX-CA-E8 solution was first diluted with toluene from 50% w/w to 20% w/w concentration. 1 phr TPP with respect to the weight of telechelic E828 in Oligomer TX-CA-E8, was then added. The original polyamic acid S703, was first diluted with NMP to 50% w/w concentration and then further diluted with toluene to 20% concentration.

Samples were prepared by mixing various weight fractions of diluted Oligomer TX-CA-E8 solution with the diluted S703, varying from 2.5% to 15% w/w with respect to the amount of Oligomer TX-CA-E8 in the final mixtures.

Oligomer TX-CA-E8 was expected to undergo esterification with the carboxylic functionality of the polyamic acid through its epoxy termination. Similarly, as in the previous modification with the acid functionalised oligomer, the molar ratio of the epoxy functionality of Oligomer TX-CA-E8 to that of the repeat unit of polyamic acid (S703) was calculated with a similar formula as follows:

Molar Ratio of Functionality

$$= \frac{\text{Number of moles of epoxide group in Oligomer TX-CA-E8}}{\text{Number of moles of carbonyl group in repeat unit of polyamic acid}}$$

$$= \frac{(\text{Weight / molecular weight of Oligomer TX-CA-E8}) \times 1.8}{(\text{Weight / molecular weight of repeat unit}) \times 2}$$

The mixtures were cast onto glass slides and cured with the following schedule:

- (i) 15 hours in vacuum at room temperature
- (ii) 120°C for half an hour
- (iii) 150°C for half an hour

- (iv) 250°C for half an hour
- (v) 300°C for half an hour

The films were then detached from the glass slides by immersing them in boiling water for about an hour and subsequently dried in a vacuum oven at 80°C for a day. These formulations were then labelled according to the table below:

Oligomer %	Coding
0	Control PI
2.5	PI-TX-CA-E8 (2.5)
5	PI-TX-CA-E8 (5)
10	PI-TX-CA-E8 (10)
15	PI-TX-CA-E8 (15)

Table 3.2: Coding for the mixtures of Oligomer TX-CA-E8 and S703.

3.8.1 Effect of Omitting Toluene Dilution in the Modification of the Polyamic Acid

As described above, toluene was used to dilute both the Oligomer TX-CA-E8 solution and the NMP diluted Skybond 703, from 50% w/w to 20% w/w.

In this study, a series of samples were prepared in the same way to that described above, except that no dilution with toluene was carried out.

3.8.2 Effect of Pre-Reaction Conditions Prior to Curing

In an attempt to enhance the “grafting” reaction of the perfluoroether oligomer onto the polyamic acid, a pre-reaction step was introduced in the preparation protocol. This involved the mixing of the diluted Oligomer TA-CA-E8 solution with diluted S703 at the weight ratio of 0.4 : 1. The mixture was then divided into two portions so that they can be evaluated separate with two different pre-reaction temperatures of

60°C and 80°C, respectively. The mixtures were heated for 6 hours with stirring in a reflux condition.

After the pre-reactions, a series of polyimide samples, containing overall different levels of perfluoroether oligomer modifications were prepared respectively, by diluting the pre-reacted mixture with more polyamic acid solution (Skybond 703).

The glass transition temperatures of the cured samples were determined using a conventional DSC. The detailed thermal characteristics of the samples were evaluated using MTDSC. Their fractographic morphology was examined using SEM.

3.9 Preparation of a Prehydrolysed Alkoxysilane Solution

Based on previous results [188-191] on the preparation of various organic-inorganic hybrids, the molar composition of this solution was as follows:

TEOS	1
Ethanol	1.05
H ₂ O	3
Acid	variable
GOTMS	0.12

Since TEOS is insoluble in water, ethanol was used as a co-solvent. The molar ratio of water to TEOS was maintained at 3 : 1 to ensure that the added water participates completely in the hydrolysis reaction. It was anticipated that the unreacted alkoxy group would also be hydrolysed by water liberated from subsequent condensation reaction. The molar ratio of ethanol to water was maintained at 0.35. To obtain a homogeneous and consistent solution (i.e. optically transparent), the order of mixing the individual ingredient is extremely important. Water is not miscible with the alkoxides. Hence, TEOS and GOTMS must first be allowed to dissolve in ethanol before water is added. Acid was always added last to ensure homogeneous catalysis and to avoid precipitation. Both hydrochloric acid (HCl) and p-toluene sulphonic acid (TSA) were used for the hydrolysis. The acid/TEOS molar ratio was maintained at 0.048 for HCl and 0.16 for TSA, respectively.

3.10 Hybridisation of Polyimides Modified with Perfluoroether Oligomer

Silica based polyimide hybrids were prepared by mixing solutions of polyamic acid containing various concentrations of Oligomer TX-CA-E8 with the respective prehydrolysed alkoxysilane solution. The intended silica content for each sample was fixed at 30% w/w. For all samples, heating was carried out at 80°C for 10 minutes. They were then cast onto glass slides and cured with the following schedule:

- (i) 80°C in vacuum for 15 hours
- (ii) 150°C for half an hour
- (iii) 250°C for half an hour
- (iv) 300°C for half an hour

The thermal characteristic of all the samples was evaluated using MTDSC. In addition to SEM, the morphologies of all the samples were also examined using Transmission Electron Microscope (TEM). The samples were first encapsulated in an epoxy resin before being ultra-microtomed in water at room temperature. The TEM used is a Jeol 100CX model.

3.11 Production of Composites

Skybond S703 based polyimides are brittle without fibre reinforcement, even in the presence of morphological modifier such as the modified perfluoroether oligomers used in this project. In addition, bulk samples are difficult to prepare due to the need of removing solvents and condensation volatiles liberated during imidisation. For these reasons, direct evaluation of their mechanical properties was not possible using the usual conventional method.

However, as a matrix resin for advanced composites such as carbon fibre reinforcement, Skybond 703 represents considerable versatility due to its ease of fabrication with its low viscosity and unparalleled high temperature performance, especially when compared to the more common epoxy based system.

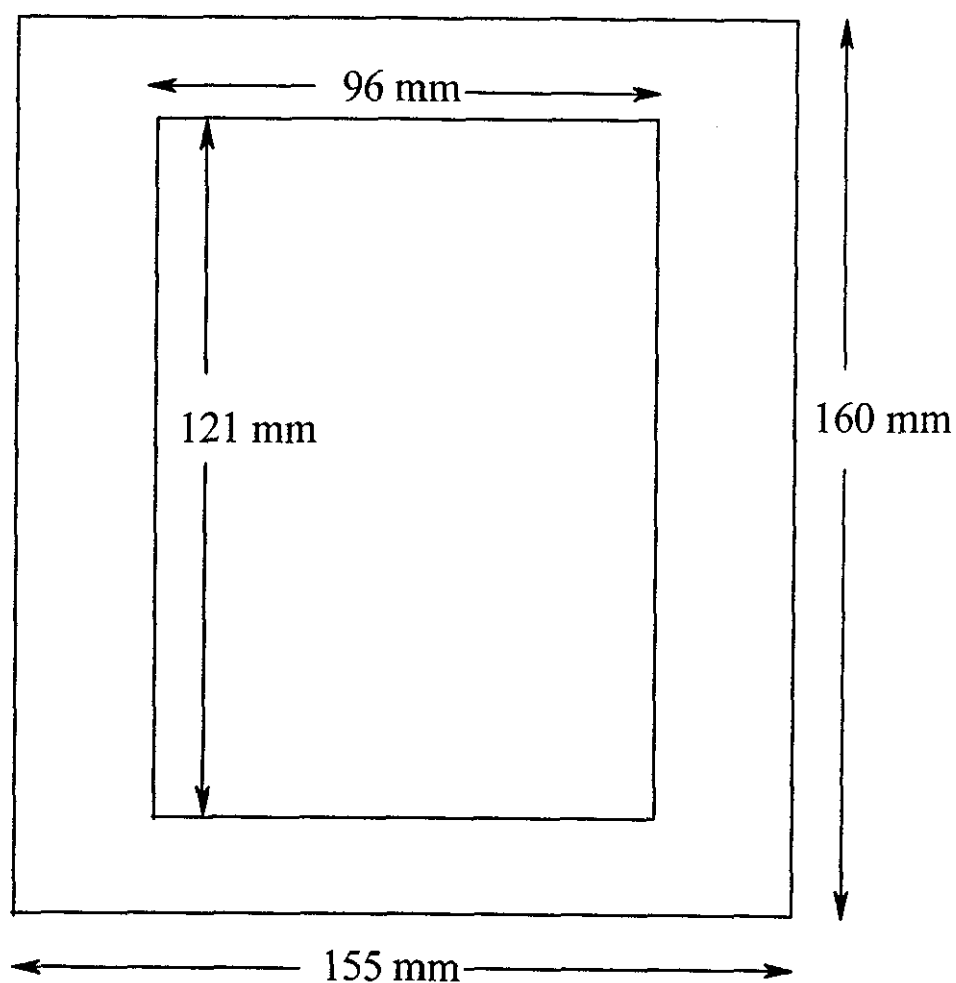
In this project, the mechanical properties of the modified polyimides are studied in a form of unidirectional carbon fibre composites, produced using a filament winding method developed in IPTME, based on previous works. Both hybridised and non-hybridised formulations of polyimides resin containing various concentrations of Oligomer TX-CA-E8 (as described earlier in the chapter) were evaluated.

The carbon fibre winding process and the resin impregnation were carried out manually completely. It is a tedious and time-consuming operation and is inevitably highly dependent on the skill and experience of the maker. For these reasons, several steps were taken during fabrication in order to ensure that the properties of each composite were consistent and comparable. With respect to the matrix resin, the precautionary steps taken were as follows:

- The pot-life of the resin mixtures was substantially prolonged and its reactivity stabilised by partially immersing the mixture container in a bowl containing ice, water and salt.
- The usable life of the resin mixtures was restricted to 2 hours. A “fresh pot” was prepared if the time was exceeded. In the case of hybrids, the “pot-life” time was reduced to only 20 minutes.
- A standard 100 mm by 25 mm glass tube was used to contain the resin mixtures.

The actual fabrication involved the careful winding of the carbon fibre tape on the standardised steel frame to a thickness of 1.6 mm and the rest of the geometry shown in figure 3.1. Impregnation of the resin was carried out using a spatula at each layer. The desired thickness was obtained by repeating the procedure several times to build-up the required number of layers. Thermal imidisation of the polyimide precursor was carried out using compression moulding. The precautionary steps taken with respect to the filament winding operation were as follows:

- Each layer of winding was standardised with 17 loops with the carbon fibre tape partially overlapping each other.



Figures 3.1: Geometries of the standardised steel frame used in the winding of the carbon fibre during composites fabrication.

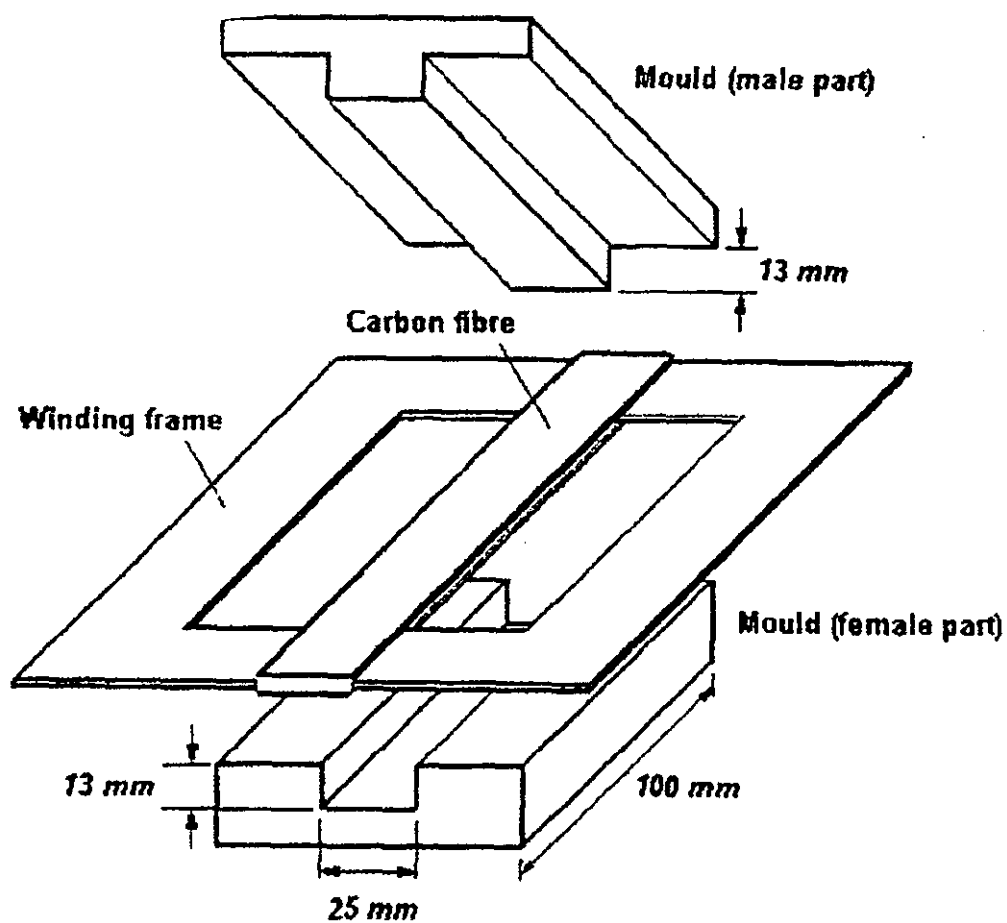
- Intermittence readjustment of the position of the carbon fibre tape on the steel frame, and partially unwinding and rewinding of the loop was completely avoided.
- Care was taken to ensure that all the loops were kept taut consistently throughout the whole operation. A large metal clip was used on the top end of the winding on the steel frame to hold the fibres loops in tension during resin impregnation.
- Approximately 2 ml of resin was applied at each layer or each application stage. This amount was gauged by marking the resin tube accordingly for each volumetric level.
- Thorough wetting of the resin onto the fibre was carried out by gliding the flat surface of the spatula used along the fibre gently and slowly without applying any pressure.

The final properties of the composites are considerably dependent on the ways in which the prepregs are dried and moulded. In this project an open-ended leaky mould was used. A three dimensional set-up of the mould and the winding frame is shown in figure 3.2. Different drying and moulding procedures were evaluated in order to determine the effects of moulding conditions on the properties of the final composites.

Method I

In this method, the winding and resin impregnation process was carried out continuously without stoppage until the 7 layers of fibres were accumulated. This essentially means that the resin solution was hardly allowed to dry throughout the whole hand lay-up process and hence should remain relatively wet and retain a relatively low viscosity during subsequent moulding. Although limited drying was carried out at the end of the winding procedure by placing the winded specimen in a vacuum oven at 80°C for an hour, the bulk of the specimen should still contain a relatively high amount of solvents. The subsequent steps are as follows:

- Transfer prepregs onto the leaky mould (preheated).
- Heated in an oven at 120°C for 1 hour. The mould was lightly compressed by placing a 5.5 kg metal plate on top of it.
- Transfer to compression moulding machine.



Figures 3.2: Schematic diagram of the leaky mould and the winding frame used for the production of carbon fibre composites.

- 150°C under contact pressure for 3 minutes.
- 150°C under 10 MPa for 45 minutes.
- Release pressure for 3 minutes.
- Ramp from 150°C to 300°C at approximately 7°C/min and 10 MPa moulding pressure.
- Moulding at 300°C for 30 minutes at the same moulding pressure.

Method II

The use of leaky mould inevitably results in the partial loss of the resin impregnated during compression moulding. This is due to the resin being squeezed out at both ends of the mould and hence will always reduce the level of composites resin content so that they are lower than the amount impregnated during hand lay-up. In practice, the degree of squeeze out is primarily dependent on the following factors:

- The geometry of the mould
- The pressure applied during moulding
- The viscosity / flowability of the resin

In this method, an attempt was made to increase the resin content of the composites by trying to control the latter two factors, as well as increase the amount of resin impregnated during hand lay-up. The same mould as in method I was used, although a longer mould may potentially reduce resin loss.

Correspondingly, at each layer interval, after the resin material was manually impregnated into the fibre using a spatula, the windings on the frame were allowed to dry in a fume cupboard for 15 minutes at room temperature before being spread again with a fresh amount of resin. The next layer of winding was laid immediately and the procedure was then repeated to pile up 7 layers of carbon fibre on the frame. Further drying was then carried out in vacuum at 80°C for 1 hour after the laminar build up. The samples were then placed into a mould and curing was carried out under pressure by initially placing a 5.5 kg metal plate on top of the mould at 120°C for 1 hour. The

samples were then transferred onto a pre-heated compression-moulding machine and moulded with the following schedule:

- 150°C under a contact pressure for 15 minutes.
- 150°C under a pressure 10 MPa for 30 minutes.
- Release pressure for 3 minutes.
- Ramp from 150°C to 250°C at approximately 7°C/min and 10 MPa moulding pressure.
- Moulding at 250°C for 1 hour under a pressure of 10 MPa.
- Ramp from 250°C to 300°C at approximately 7°C/minutes and 10 MPa moulding pressure.
- Moulding at 300°C for 1 hour under a pressure of 10 MPa.

Method III

Method III is essentially the same as method II, except that 30 minutes of drying time (instead of 15 minutes) was used at each of the layer interval and compression moulding of the prepreg was carried out the next day.

3.12 Properties Evaluation of Carbon Fibre Composites

3.12.1 Cutting Composites to Size for Various Analyses

Cooled moulded samples were cut from the steel frame using a hand-held high speed cutter wheel - Dremel multi-purpose power tool. A 22 mm diameter diamond blade, operating with a rotational speed of 1500 rpm was used. Cutting were carried out 2 to 3 mm away from each end of the moulded section, thereby reducing the length of the released specimens from 121 mm (mould dimension) to about 115 mm.

Subsequent cutting of the specimens were carried out using a precision Struers Accutom-5 cutting machine with a 125 mm diameter aluminium oxide wheel. Samples were mounted onto a gripping arm, which is programmable for 3 dimensional X, Y, Z co-ordinated movement. The cutting wheel was set with a

rotational speed of 3000 rpm. Cutting was carried out very slowly with a lateral speed of 3 mm/min, with the cutting wheel being cooled continuously with jetting coolant during the cutting operation.

3.12.2 Thermomechanical Characterisation

This study was carried out using a dynamic mechanical analyser. A Polymer Laboratories MKII equipment was used. Specimens, 1.5 and 3 mm thick and 6 mm wide, were mounted onto a small frame and attached to a short single cantilever bending head with a span of 8 mm; (span/thickness ratio = 2.7 to 5). Specimens were evaluated in the transverse direction of the fibres in order to emphasize the mechanical of the matrix in the composites. Tests were carried out from -100°C to 300°C with a heating rate of $3^{\circ}\text{C}/\text{min}$ and in a nitrogen environment. A frequency of 1 Hz was used.

3.12.3 Mechanical Testing

Both flexural and interlaminar shear tests were carried out.

An interlaminar shear test is in effect a 3-point bending test in which a very low span to thickness ratio of 5:1 at the maximum is used. This aims to maximise the level of shear relative to flexural stress in the specimen being tested. It is based on the British Standard BS2782: Part3: Method 341A: 1977 and it is especially suited to fibre-reinforced composites, giving a good indication of the interfacial strength between matrix and the fibres.

The inter-laminar shear strength was calculated from an average of at least 3 specimens, according to the formula

$$\sigma_i = \frac{0.75F}{bd}$$

Where: σ_I = inter-laminar shear strength (MPa)
 F = force at yield or at first fracture (N)
 b = specimen width (mm)
 d = specimen thickness (mm).

In the flexural test, the testing mode is very similar to the interlaminar shear test, except that a much wider span to thickness ratio of at least 15:1 was used. At least 3 specimens were used from each formulation and the formulae used were that of the structural types from beam theory of elastic materials i.e.

$$\text{Flexural modulus (in MPa)} = mL^3/(4bd^3)$$

$$\text{Flexural strength (in MPa)} = 3 PL/(2bd^2)$$

Where: P = load at break (N)
 m = gradient from origin (N/mm)
 L = span (mm)
 d = thickness (mm)
 b = width (mm)

3.12.4 Morphological Examinations

Cross-sections of the composites were evaluated using scanning electron microscopy (SEM). A small sample of about 3 mm by 6 mm was cut and encapsulated edge-wise in a slow-setting acrylic resin and hand grinded until the cross-section of the sample emerged. The surface was then progressively smoothed using progressively finer grit size sandpapers in running water.

The highly uniform surfaces were then subsequently polished to a highly gloss finish on a polishing wheels at 250 rpm using a water-based diamond suspensions of 6 μm and 1 μm particle sizes. This stage of the preparation was found to be most crucial and took up to 2 hours to obtain the best result, especially with specimen

containing high perfluoroether content. Intermittent observations under a reflective light microscope were constantly made to assess the quality of the finishing.

The polished surfaces were then gold-sputtered and examined using a Cambridge 360 Steroscan electron microscope.

3.12.5 Thermogravimetric Analysis

The decomposition weight-loss characteristics of polyimide-carbon fibre composites were found to be rather complex and peculiar when the pyrolysis of the samples was carried out in a furnace, as there was a lack of reproducibility of the weight-loss results. In addition to the fact that the major decomposition temperature of the resin and the fibre are very close, it is presumed that this may result also from the changes in reaction orders due to:

- Inconsistent heating rate
- Small fluctuation of temperature in the furnace
- Inconsistent air circulation

These limitations were then overcome by using an instrument thermogravimetric analyser (TGA). Reproducibility was found to be within 3 %.

The mass of the samples used in the TGA was close to the upper volumetric limit permissible, restricted only by the size of the platinum sample holder. This was to ensure that accurate and representative compositions of the composite samples were available for analysis.

The analyses were carried out using a TA Instrument Hi-Rev Modulated TGA 2950 Thermogravimetric Analyser. The testing environment was continuously purged by a steady flow of air at 60 cm³/min. The samples were heated from room temperature to 600°C with a heating rate of 50°C /min and were then kept isothermally at 600°C for 20 minutes.

4 RESULTS

4.1 Telechelic Modifications of Hydroxyl-Terminated Perfluoroether Oligomer

4.1.1 Acid Functionalisation Using Chlorendic Anhydride

Chlorendic anhydride (CA) is completely insoluble in the liquid hydroxyl terminated perfluoroether oligomer (Oligomer TX). Consequently, the acid functionalisation reaction of these two reactants (see page 57 for reaction schematic) can only occur on the surfaces of the CA crystals.

It was not surprising, therefore, to find that by grinding the CA powder down to finer particles, the required time for the esterification reaction to be completed could be shorten dramatically. This enhanced efficiency of the reaction has the important advantage of minimising the risk of polymerisation of the acid functionalised perfluoroether oligomer at the later stages.

Due to the insolubility of CA in the reaction medium, the reaction end point can be determined reliably by monitoring the disappearance of CA powder in the reaction mixture.

4.1.2 Epoxy Functionalisation Using Epoxy Resin

The acid functionalised perfluoroether oligomer (Oligomer TX-CA) is a high viscosity fluid and was found to be immiscible with the high viscosity epoxy resin, E828, over a wide composition range.

In order to minimise polymerisation, reactions between E828 and Oligomer TX-CA (which can easily occur as both reactants are difunctional in nature), and to ensure that the catalytic action of triphenylphosphine (TPP) was effective and uniform in the reaction mixture, the epoxy functionalisation process was carried out in an NMP/toluene solution with an E828/Oligomer TX-CA molar ratio equal to 2. The

excess quantity of E828 would allow statistically an end-capping reaction to occur predominately in a fully miscibilised mixture and hence essentially avoiding linear polymerisation.

4.2 Fourier Transform Infrared Spectroscopy

4.2.1 Qualitative Analysis

The telechelic modifications of Oligomer TX involving the two consecutive steps of acid and epoxy functionalisations were followed by FTIR. The respective spectra are shown in figure 4.1.

Spectrum (a) corresponds to the hydroxyl-terminated perfluoroether oligomer (Oligomer TX). The absorbance peak for the hydroxyl-terminal at around 3400 cm^{-1} is clearly visible.

Spectrum (b) corresponds to the acid functionalised perfluoroether oligomer (Oligomer TX-CA). The peak at around 3400 cm^{-1} can be seen to be reduced significantly owing to the terminal hydroxyl of the oligomer being consumed by the esterification reaction with chlorendic anhydride (CA). A new peak appeared around $3200\text{ to }3100\text{ cm}^{-1}$, corresponding to the introduction of carboxylic acid group as a result of the esterification.

Spectrum (c) corresponds to the epoxy functionalised perfluoroether oligomer (Oligomer TX-CA-E8). The epoxide ring-opening reaction induced by the carboxylic functionality reintroduces the hydroxyl group back to the oligomer. This mechanism is clearly reflected in the spectrum with the disappearance of the carboxylic acid peak at around 3200 cm^{-1} and the reappearing of hydroxyl peak at around 3400 cm^{-1} .

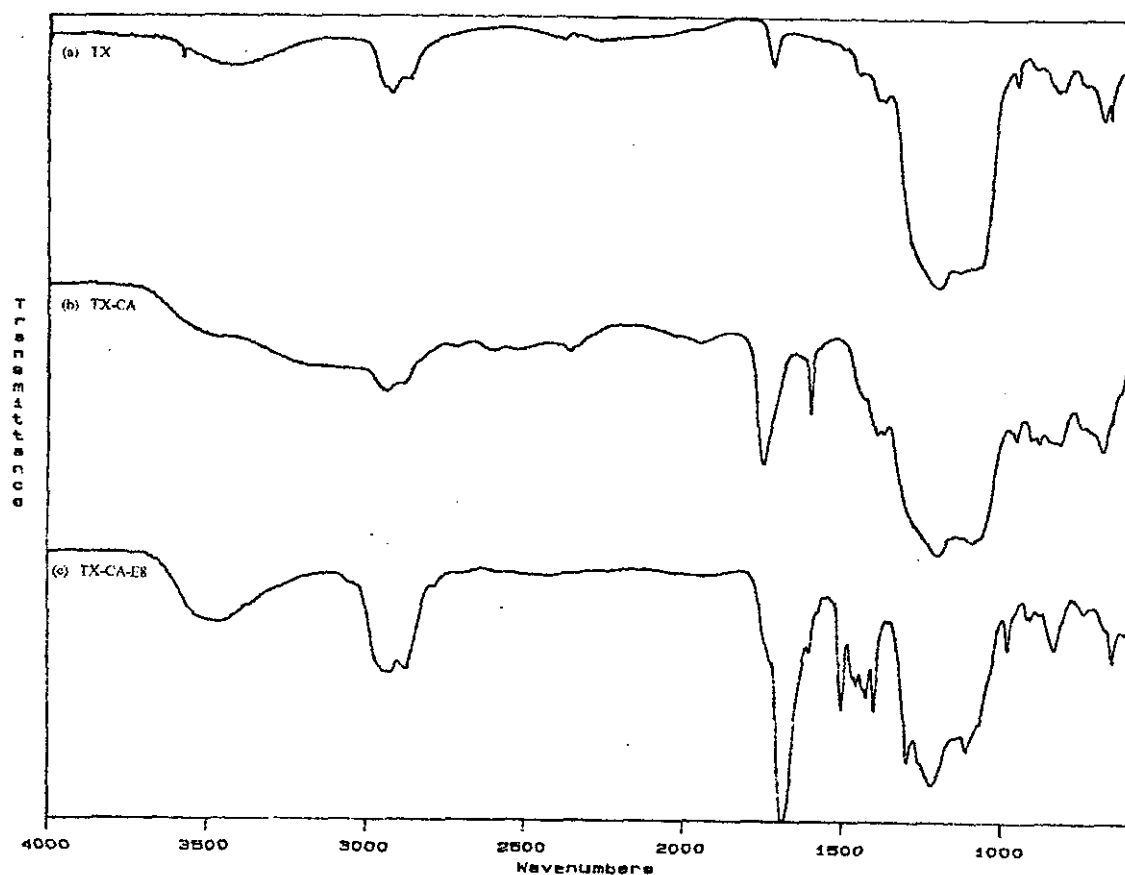


Figure 4.1: FTIR spectra following the telechelic modification reactions of perfluoroether oligomer. Spectra (a), (b) and (c) correspond to Oligomer TX, Oligomer TX-CA and Oligomer TX-CA-E8, respectively.

4.2.2 Quantitative Analysis

The FTIR spectrum of E828 is shown in figure 4.2. The absorption peaks at around 1500 cm^{-1} and 914 cm^{-1} (corresponding to the respective aromatic ring and epoxide group) are highlighted. (These optical densities were used for computation of Epoxy Index [EI], see page 58).

The change in EI as a function of reaction time, i.e. the epoxy functionalisation of perfluoroether oligomer with E828, is shown in figure 4.3. The decreasing value of EI clearly indicates that the epoxide groups of E828 are consumed in the reaction, confirming that chain extension of the perfluoroether oligomer had taken place.

The EI value can be seen to reach a plateau after about 2.5 hours, consequently this reaction step was subsequently standardised at 3 hours.

4.3 Miscibility of Mixtures

4.3.1 Mixtures of Acid Functionalised Perfluoroether Oligomer and Polyamic Acid

Effect of NMP Dilution

The following table shows the visual observations made on films of various Oligomer TX-CA modified S703 casted on glass slides. The effect of NMP dilution of the original Skybond 703 is also shown.

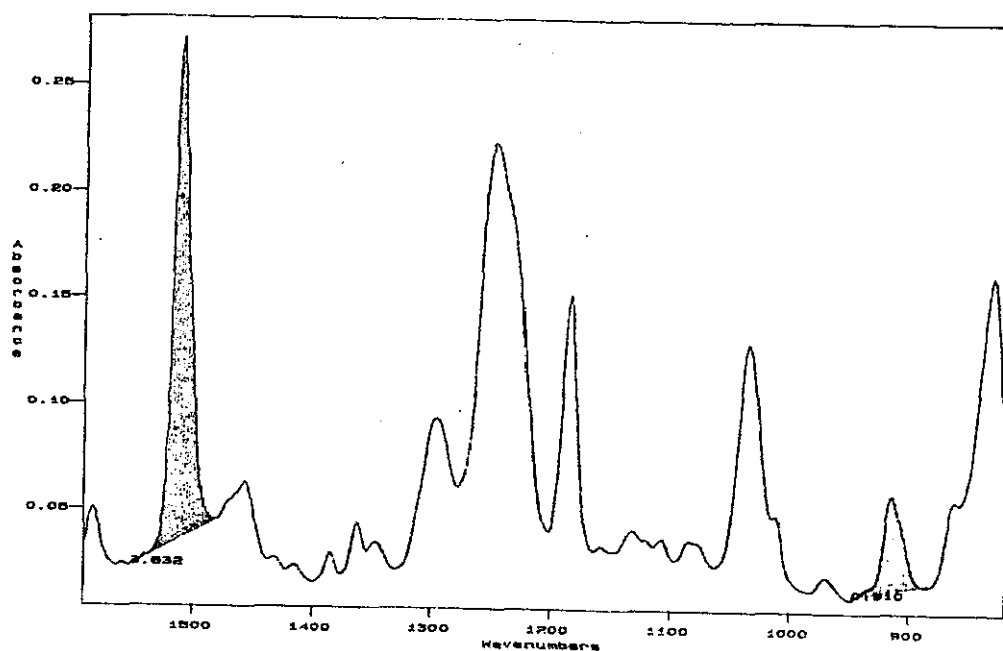


Figure 4.2: FTIR spectrum of original epoxy resin, E828. The integration of the epoxide group around 914 cm^{-1} and the aromatic band around 1500 cm^{-1} were used in the calculation of Epoxy Index (EI).

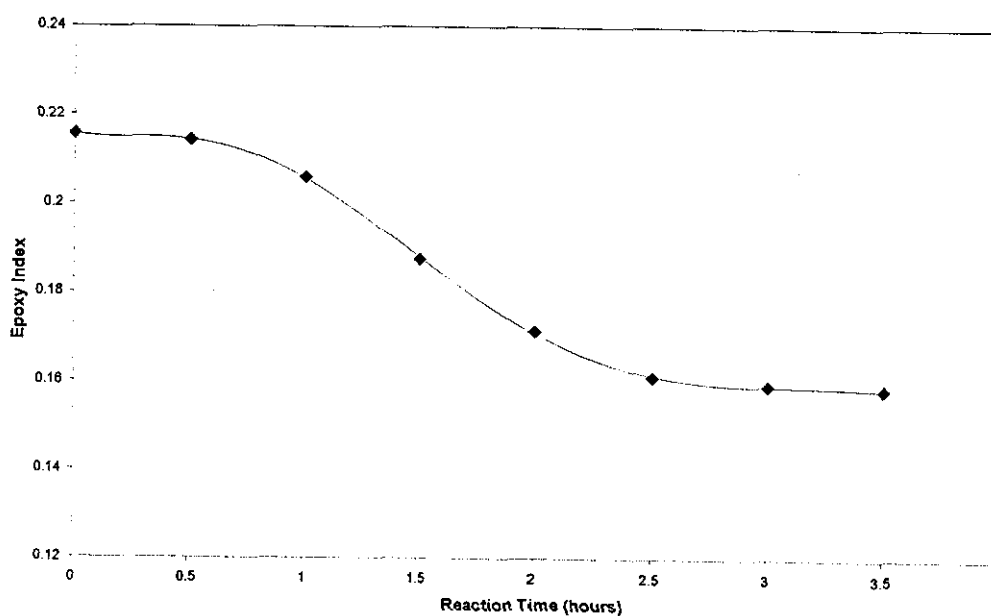


Figure 4.3: Plot showing the effect of reaction time on the epoxy index of the functionalised perfluoroether oligomer.

No.	Perfluoroether Modification %	RT ₁	60°C	RT ₂	120°C	150°C
1	0%	T	T	T	T	T
2	10% (U)	O	O	T	T	O
3	20% (U)	O	O	O	O	O
4	30% (U)	O	O	O	O	O
5	5% (D)	O	O	O	T	O
6	10% (D)	O	O	T	T	O
7	20% (D)	T	O	T	T	O
8	30% (D)	O	O	T	T	O

Table 4.1: Visual observations on PAA modified with various concentrations of acid functionalised perfluoroether oligomer at different stages of preparation.

Note:

- The perfluoroether modification column indicates the weight fraction (in percentages) of the perfluoroether oligomer in the PAA.
- Sample number 1 was a control. Samples number 2 (U) to number 4 (U) were undiluted samples and sample number 5 (D) to number 8 (D) were diluted samples.
- RT₁ refers to the observation made initially at room temperature, prior to the pre-reaction.
- The 60°C column indicates the observation made immediately at the end of pre-reaction step, which was carried out at 60°C. The glass slides were preheated in an oven at the pre-reaction temperature before the samples were cast to ensure that temperature differential effects were eliminated. The optical assessments of the samples were carried out within the first 20 seconds after casting to avoid errors due to the excessive evaporation of solvents.
- RT₂ is the observation at room temperature after allowing the mixtures to cool down (in their enclosed glass tubes) from 60°C subsequent to the reaction.
- T and O denote transparent and opaque observation, respectively.

- g) The last 2 columns (120°C and 150°C) represent the results obtained for the first two heating steps of imidisation reaction. The optical assessments were made upon cooling to room temperature from the respective heating step.

From table 4.1, it can be observed that dilution with NMP did not result in miscibilisation immediately in almost all the mixtures, except for sample number 7, which contained 20 wt% of the perfluoroether modifier. This result, therefore, indicates that the acid functionalised Oligomer TX-CA is still highly immiscible with the polyamic acid, even in the presence of high concentration of co-solvent, i.e. NMP.

However, the NMP dilution seems to enhance the efficiency of the pre-reaction significantly. Upon cooling from the reaction temperature, almost all the mixtures became miscible, except for sample number 5, which contained 5 wt% of the perfluoroether modifier. It is, therefore, important to note from this observation that miscibilisation between Oligomer TX-CA and S703 can only be achieved in this approach through chemical reaction, i.e. grafting.

Increasing the pre-reaction temperature from 60°C to 80°C did not result in any difference in the optical appearance.

The opacity of all the samples after the heat treatment at 150°C indicates that phase-separation occurs as a result of imidisation reactions.

4.3.2 Mixtures of Epoxy Functionalised Perfluoroether Oligomer and Polyamic Acid

Use of Triphenylphosphine

Triphenylphosphine (TPP) was used to catalyse the ring opening reaction of the terminal epoxy groups of Oligomer TX-CA-E8 with the reactive functionalities of the polyamic acid, i.e. carboxylic groups or amide in the backbone structure.

The catalyst TPP was first dissolved in Oligomer TX-CA-E8 before mixing with polyamic acid in order to ensure that it would locate itself around the epoxy groups and enhance its catalytic efficiency.

In the presence of TPP, the miscibilisation of the polyamic acid and Oligomer TX-CA-E8 was instantaneous. However, in the absence of TPP, the dissolution of the two components did not occur even with prolonged mechanical stirring at room temperature. It is important to note that although no TPP was added in the mixing of TX-CA-E8 with the polyamic acid, an equivalent amount of TPP was present in Oligomer TX-CA-E8 as a component for the preparation of TX-CA-E8. This indicates that TPP is not a true catalyst for the reaction of epoxy groups with carboxylic acid groups but an actual participant of the reaction.

Toluene Dilution and Pre-reaction

Number	PFO Modified %	RT	Dried	120°C	150°C
1	0%	T	T	T	T
2	2.5%	T	O	O	O
3	5%	T	O	O	O
4	10%	T	O	O	O
5	15%	T	O	O	O
6	2.5% (60°C)	T	T	H	O
7	5% (60°C)	T	T	H	O
8	10% (60°C)	T	T	O	O
9	15% (60 °C)	T	H	O	O
10	2.5% (80°C)	T	T	T	O
11	5% (80°C)	T	T	T	T
12	10% (80°)	T	T	T	T
13	15% (80°)	T	T	T	H

Table 4.2: Visual observations on PAA modified with various concentrations of epoxy functionalised perfluoroether oligomer at different stages of preparation. All the samples shown in this table were initially diluted with toluene.

Note:

- a) H = Hazy, T = transparent, O = opaque.
- b) The epoxy-functionalised perfluoroether (PFO) modification column indicates the weight fraction (in percentages) of Oligomer TX-CA-E8 in PAA.
- c) Sample number 1 was a control. Sample numbers 2 to 5 were mixtures prepared with no pre-reaction step. In Samples 6 to 13, the respective weight fraction of perfluoroether was obtained through dilution with unmodified PAA from a 40 wt% concentrated mixture after pre-reaction (see section 3.8.2). Sample numbers 6 to 9 were mixtures prepared with pre-reaction at 60°C. Sample numbers 10 to 13 were prepared with pre-action at 80°C.
- d) RT refers to the observations made initially at room temperature, upon cooling from the pre-reaction step.
- e) Dried refers to the observations made at room temperature after the samples were dried in the vacuum oven at 60°C for a day.
- f) The last two columns (120°C and 150°C) represent the observation results obtained after the temperature at which the first two heating steps of imidisation reaction were carried out. The optical assessments were made upon cooling to room temperature from the respective heating step.

In the absence of toluene, Oligomer TX-CA-E8 was found to have very limited miscibility with PAA, even in solution. The mixtures of both components, irrespective of composition, were dark and opaque. However, in the presence of toluene, very clear and transparent mixtures were formed (see RT results of table 4.2). This observation clearly indicates that toluene is an effective co-solvent for both components.

From table 4.2, it can be observed that Oligomer TX-CA-E8 and PAA were not miscible without co-solvents. This is deduced from the fact that phase separation was found to occur readily in samples 2 to 5 after drying. To a certain extent, this observation is consistent with the effect of toluene dilution discussed in the paragraph above.

It was also discovered that pre-heating these mixtures individually at 80°C enhanced the miscibility slightly, but was not as effective as the dilution method (see note (b) of table 4.2), i.e. the resulting mixtures were optically less transparent than the corresponding samples 10 to 13 shown in table 4.2.

The result in table 4.2 clearly showed that pre-reaction at 80°C was more effective in sustaining miscibility in the mixtures during imidisation. The darkening and the opacity of Samples 6 to 9 indicates the on-set of significant phase-separation when the PAA imidised at 120°C and 150°C.

All the samples of table 4.2 became very dark after being heated at temperature above 150°C and visual transparency assessment was no longer possible.

4.3.3 Mixtures of Epoxy-Functionalised Perfluoroether Oligomer, Polyamic Acid and Prehydrolysed Alkoxysilane Solution

All mixtures containing various concentrations of perfluoroether and a fixed concentration of prehydrolysed alkoxysilane were found to be fully miscible after heating at 80°C for 10 minutes.

The addition of alkoxysilane solution reduced the viscosity of all the mixtures substantially. The transparency of all the samples were found to be very high with a significantly lower level of darkness as compared to previous mixtures with no addition of alkoxysilane.

Vacuum drying and imidisation did not result in observable phase separation. A reasonable level of transparency was still present in all the mixtures after they were fully imidised at 300°C. Consequently, the presence of the co-continuous polysiloxane nanodomains can be considered to be the main factor that prevents the precipitation of the perfluoroether component into microdomains.

4.4 Morphology of Imidised Films

4.4.1 Scanning Electron Microscopy of Non-Hybridised Films

SEM micrographs (A) and (B) shown in figure 4.4 were the cross-sections of fractured surfaces of unmodified polyimide, based on Skybond 703. The morphologies were that of a typical brittle material with smooth surfaces and sharp fracture lines.

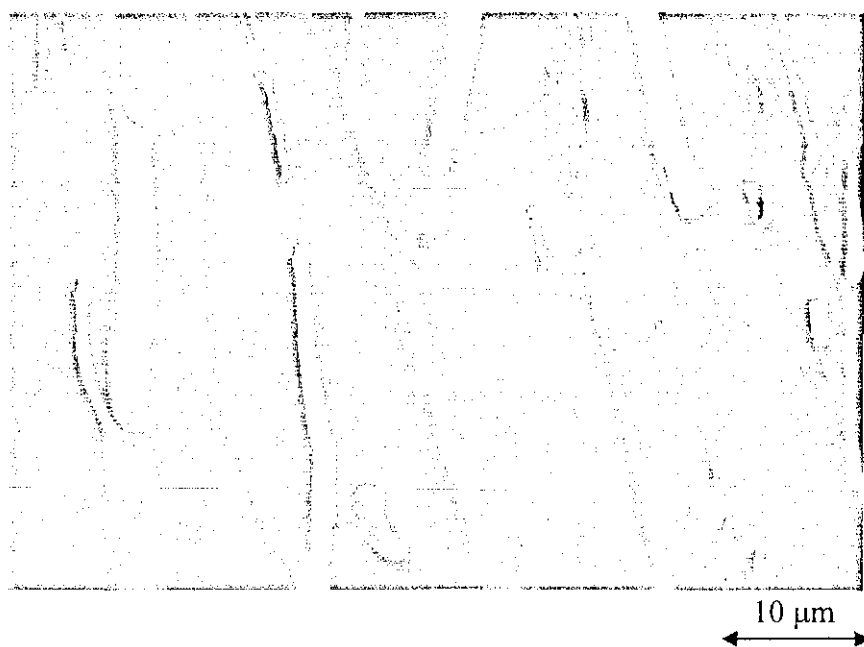
SEM micrographs (C) to (F) shown in figures 4.5 to 4.8 were those of polyimides modified with Oligomer TX-CA. A heterophase morphology, with irregular precipitation, can be observed. The particle size distribution was found to be very wide with the upper part of the scale in the region of about 10 μm . The fracturing process during samples preparation seems to cause some of the particles to deform, resulting in the formation of shear bands surrounding them (see figure 4.8).

SEM micrographs (G) to (I) shown in figure 4.9 were those of Oligomer TX-CA-E8 modified polyimides. It was found that the morphology of the fracture surfaces did not differ distinctively with varying perfluoroether content from 2.5 wt% to 15 wt%. A relatively regular heterogeneous morphology can be observed, particularly at higher magnification.

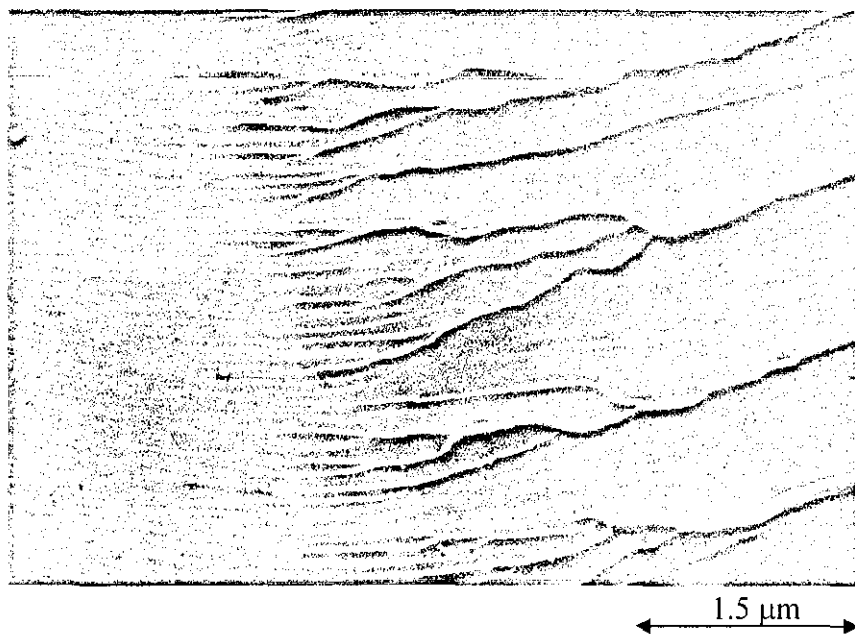
4.4.2 Transmission Electron Microscopy of Hybridised Films

TEM micrographs (J) and (K) of figure 4.10 showed the featureless morphology of a fully imidised S703. No heterogeneity can be seen in the material, even in very high magnification.

TEM micrographs (L) to (N) of figure 4.11 showed the morphology of a polyimide-silica hybrid at various magnifications. Evenly dispersed heterogeneity can be observed, reflecting the fine nanostructure of the silica phase. Although the morphology was slightly obscure, it can still be seen that the primary domain size of the silica phase is in the region of 10 and 20 nanometres.



(A)



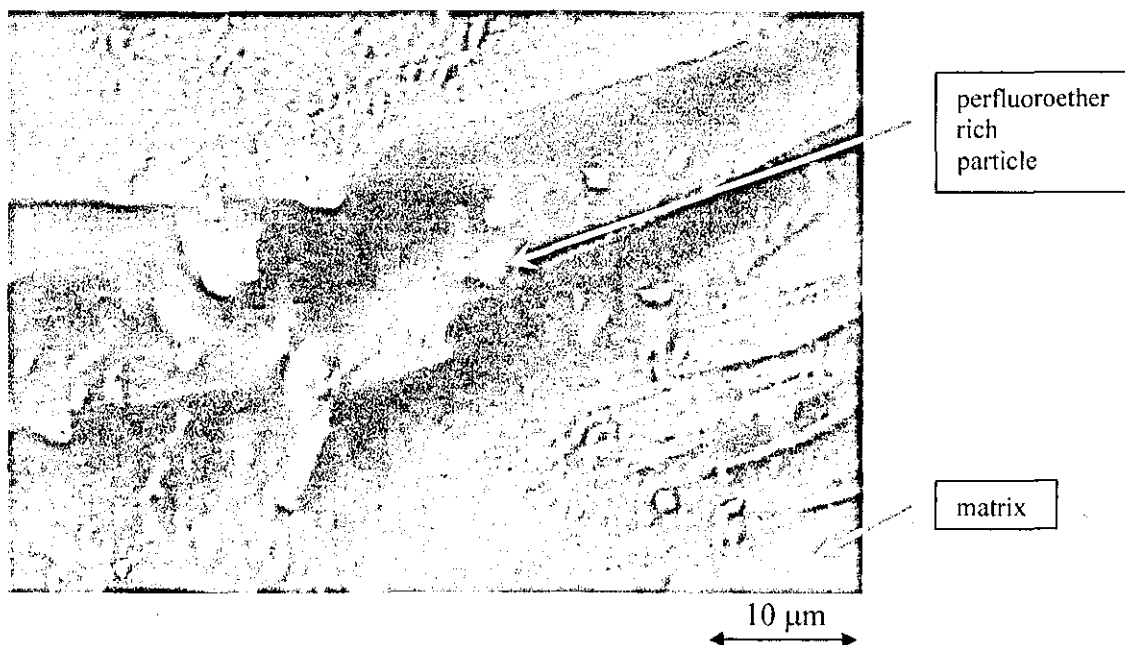
(B)

Figure 4.4: SEM micrographs (A and B) of unmodified polyimide films, showing the cross-section of fractured surfaces.



(C)

Figure 4.5: SEM micrograph showing the morphology of the fractured surface of a perfluoroether modified polyimide film containing 2.5 wt% of Oligomer TX-CA.



(D)

Figure 4.6: SEM micrograph showing the morphology of the fractured surface of a perfluoroether modified polyimide film containing 5 wt% of Oligomer TX-CA.

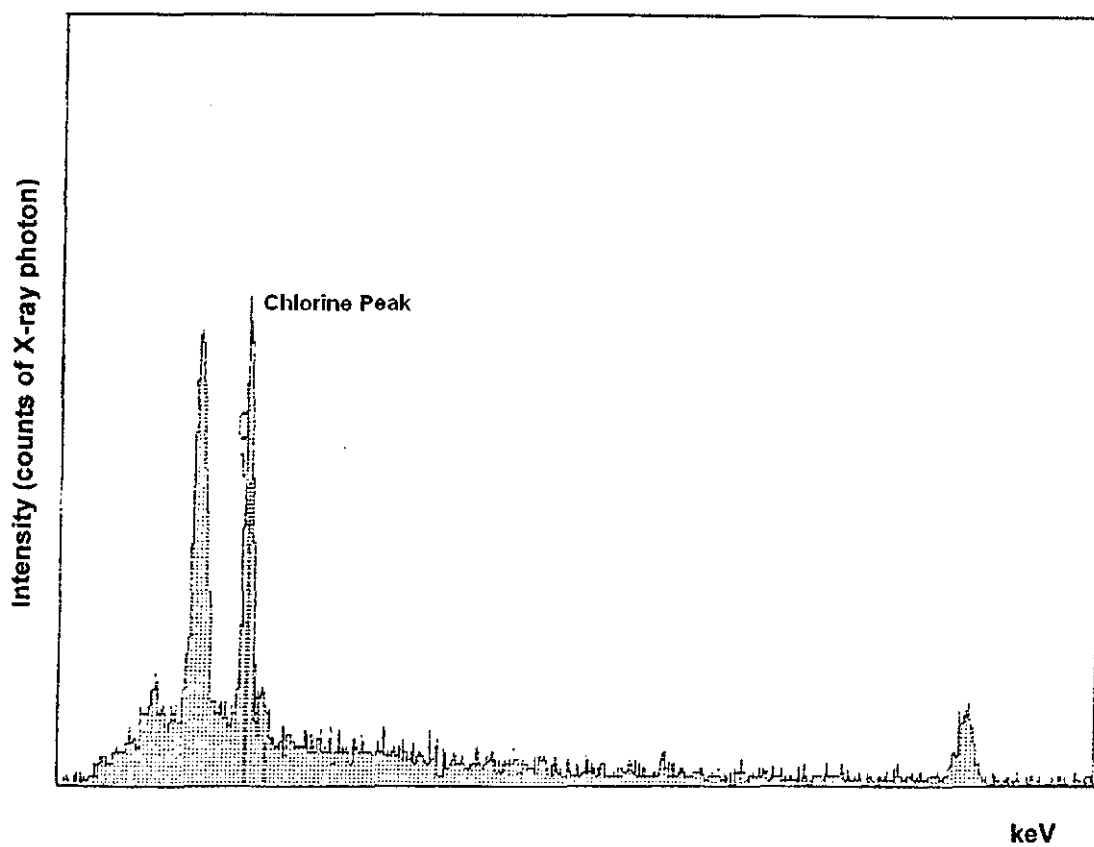


Figure 4.6A: Localised EDX analysis carried out of the particle region of the fracture surface of figure 4.6.

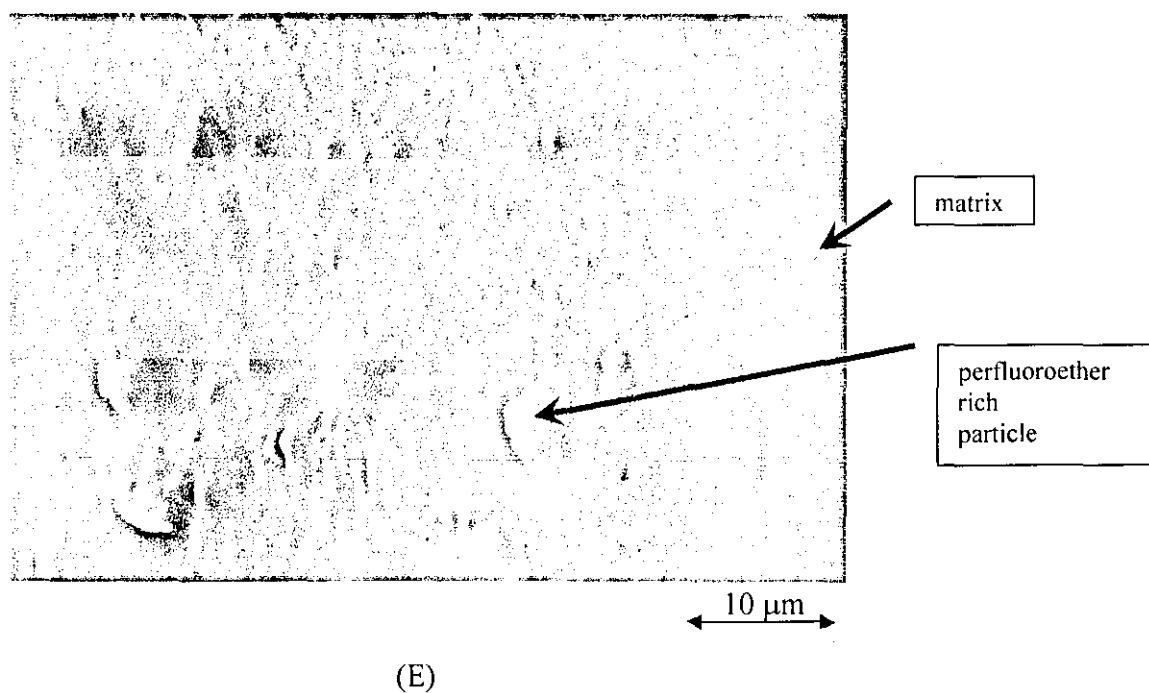


Figure 4.7: SEM micrograph showing the morphology of the fractured surface of a perfluoroether modified polyimide film containing 10 wt% of Oligomer TX-CA.

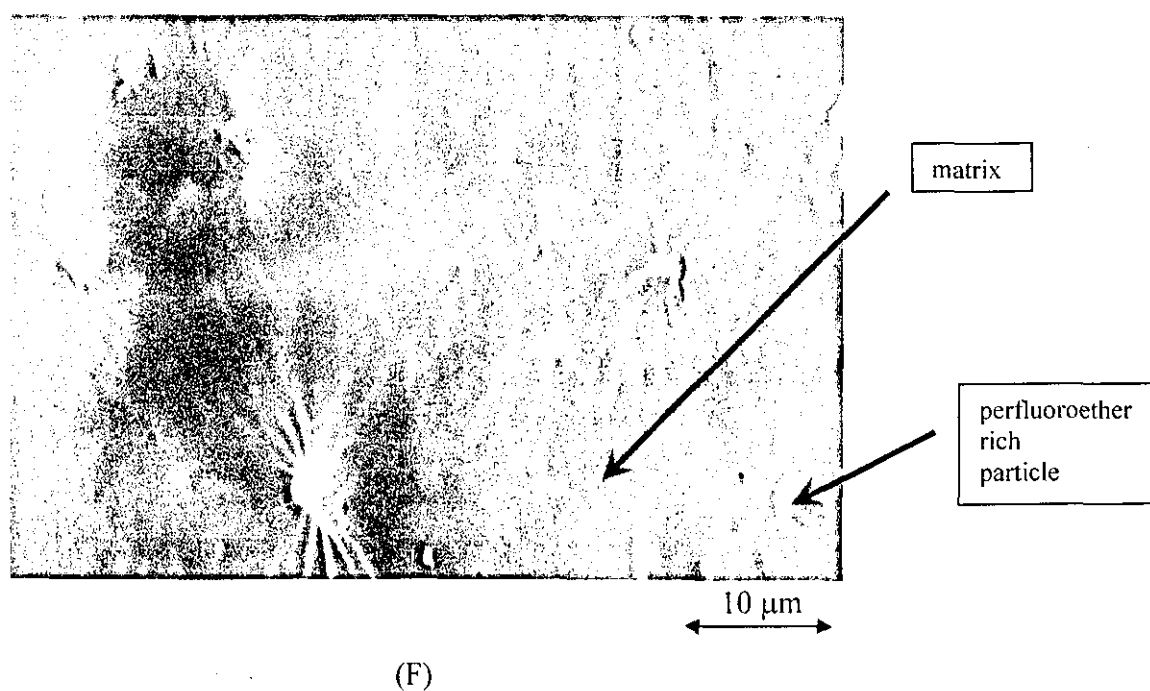


Figure 4.8: SEM micrograph showing the morphology of the fractured surface of a perfluoroether modified polyimide film containing 15 wt% of Oligomer TX-CA.

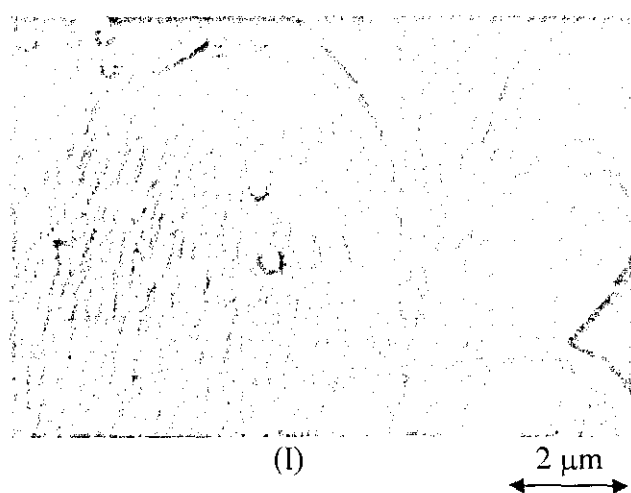
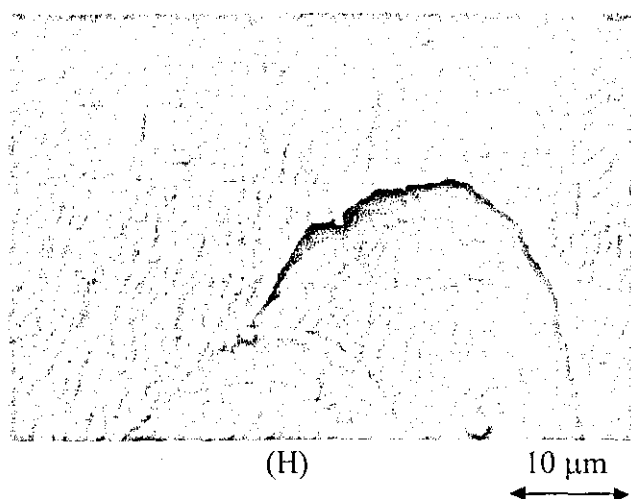
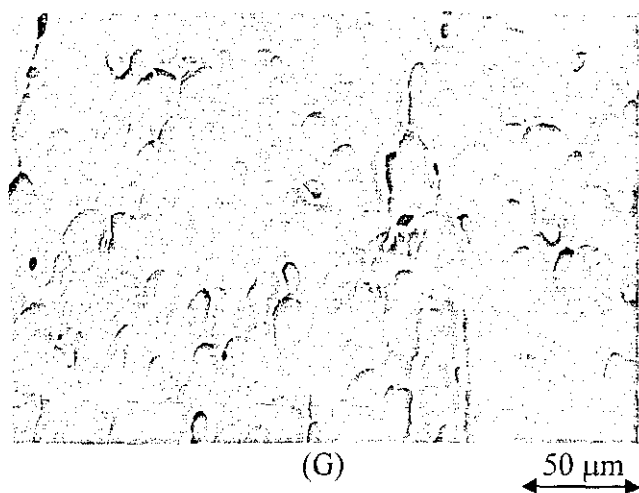
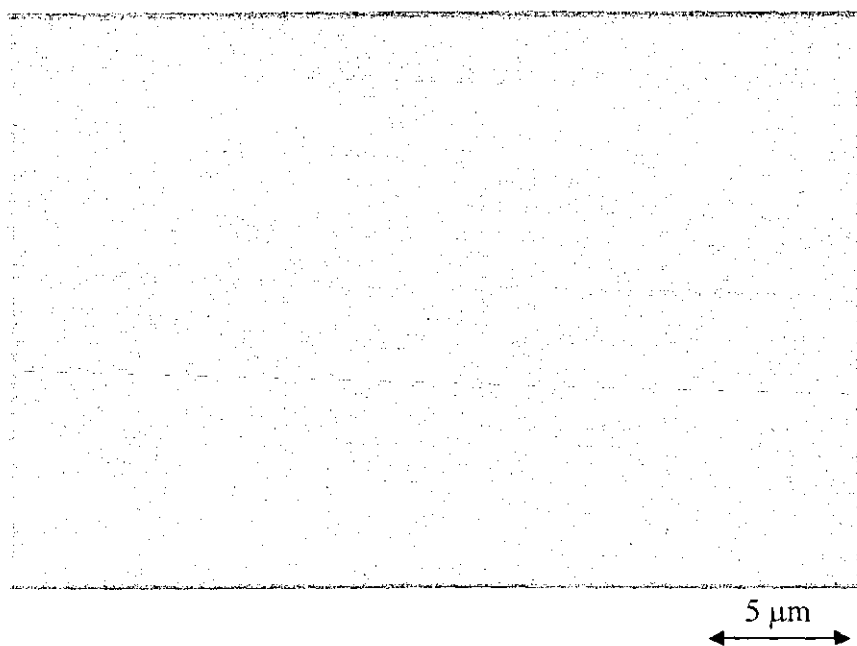
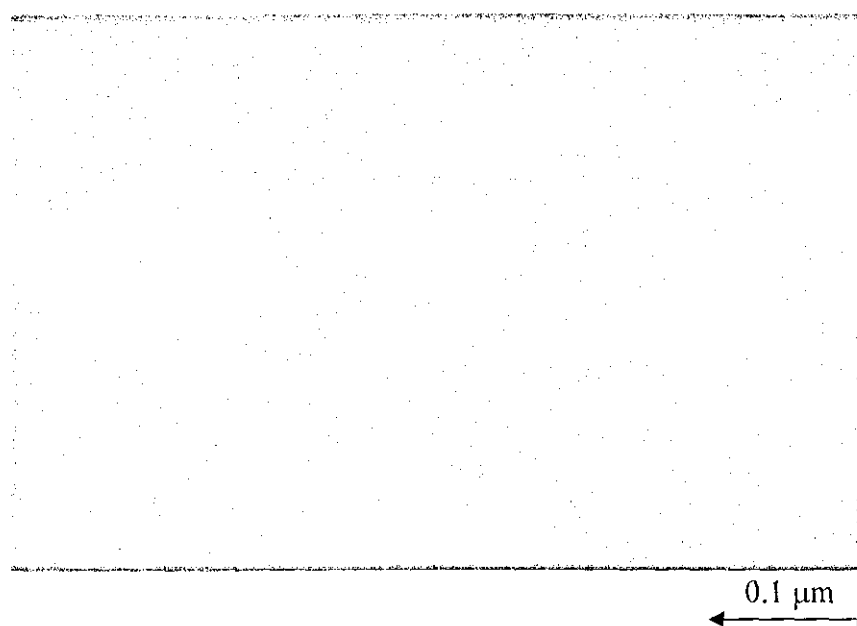


Figure 4.9: SEM micrographs showing the morphology of the fractured surface of perfluoroether modified polyimide film containing 15 wt% of Oligomer TX-CA-E8. Three different magnifications were illustrated.



(J)



(K)

Figure 4.10: TEM micrographs of (J and K) of unmodified polyimide films at two different magnifications.

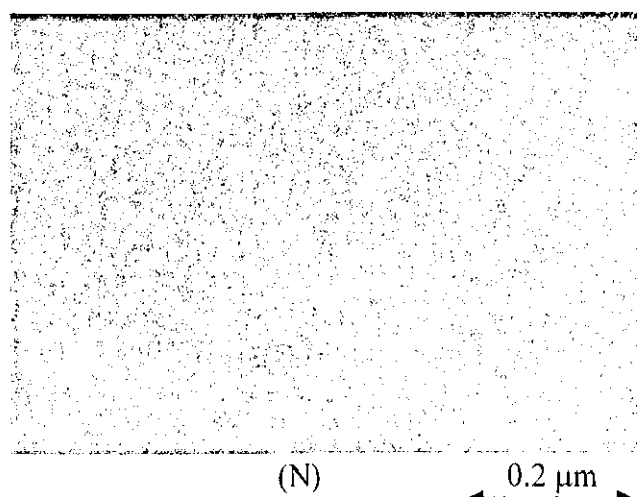
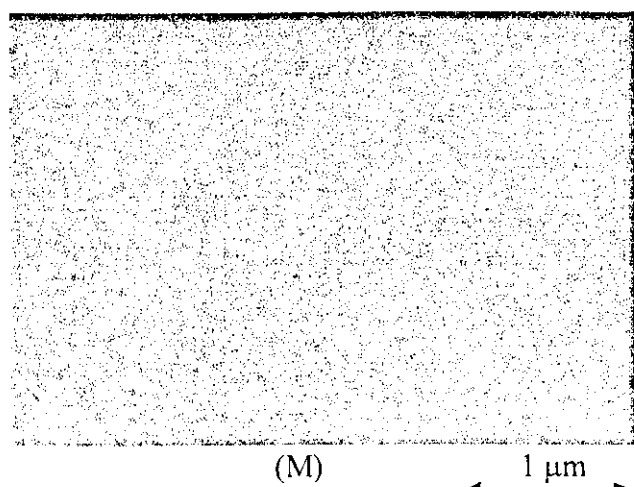
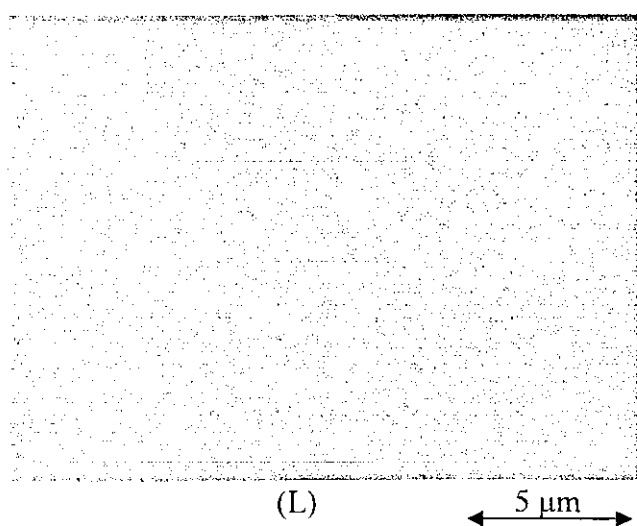


Figure 4.11: TEM micrographs (L, M and N) of polyimide hybrids containing 30 wt% of silica. No perfluoroether modifier was present in this system. Three different magnifications were shown.

Figures 4.12 to 4.15 showed the TEM micrographs of perfluoroether modified polyimides containing different concentrations of Oligomer TX-CA-E8, varying from 2.5 wt% to 15 wt%. The morphological heterogeneity resulting from the immiscibility between the perfluoroether Oligomer and the polyimide was clearly shown. Diffused precipitation of dispersed particulation can be observed. The concentration of these particles increases progressively with increasing perfluoroether content. Their particle sizes also seem to increase progressively from a few nanometres at 2.5 wt% of Oligomer TX-CA-E8 modification, to about 20 nanometre at 15 wt% of Oligomer TX-CA-E8 modification. At the upper level of modification with perfluoroether, the phase separation domain became very diffused and irregular in shape and seems to show some level of co-continuity.

Figures 4.16 to 4.19 showed the TEM micrographs of perfluoroether modified polyimide-silica hybrids containing the various concentrations of Oligomer TX-CA-E8. A more regular morphological heterogeneity is clearly evident in all the samples evaluated. In fact, their morphologies contain the combined features of both of the binary systems, i.e. the unmodified polyimide-silica hybrid and the non-hybridised polyimide modified with Oligomer TX-CA-E8.

4.5 Thermal Analysis Using Modulated Temperature Differential Scanning Calorimetry

4.5.1 Characterisation of Epoxy Functionalised Perfluoroether Oligomer

The MTDSC thermogram of Oligomer TX-CA-E8 is shown in figure 4.20 and figure 4.21. As a comparison, the heat flow signal transitions of Oligomer TX-CA-E8 from conventional DSC is shown in figure 4.22 in which no distinct thermal events can be observed. On the other hand, the MTDSC technique allowed the glass transition region of the oligomer to be clearly detected with a peak temperature (T_g) at around -53°C. This temperature was determined using a Gaussian curve fitting technique (see figure 4.21). The convoluted shape of the transition was found to be reproducible and was a reflection of the complexity of the molecular structure of telechelic modified perfluoroether oligomer. From the Gaussian calculation, the change in specific heat capacity (ΔC_p) at this region can be estimated to be around 0.21 J/g/°C.

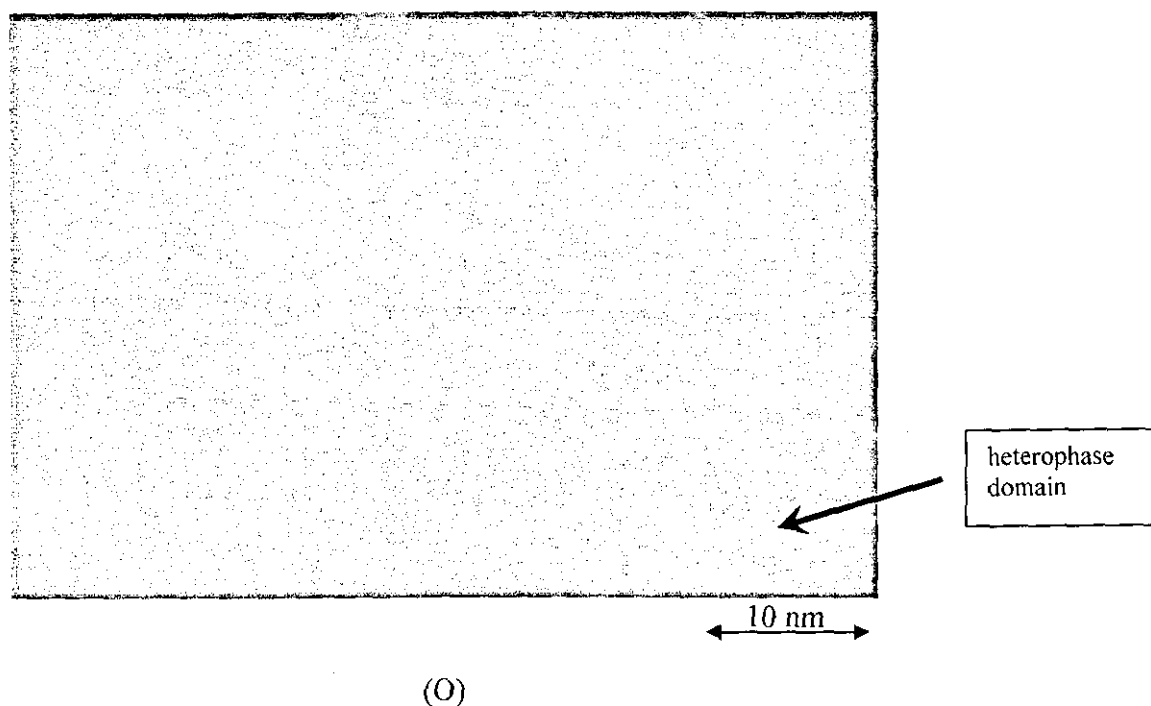


Figure 4.12: TEM micrograph showing the morphology of a perfluoroether modified polyimide film containing 2.5 wt% of Oligomer TX-CA-E8.

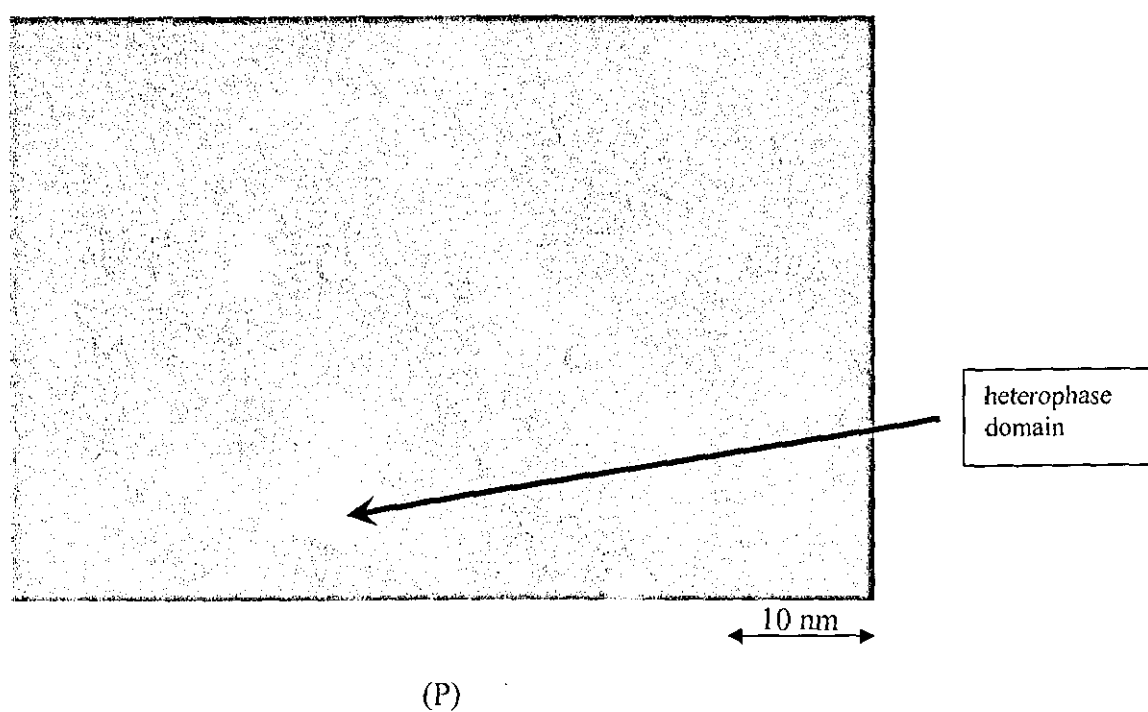
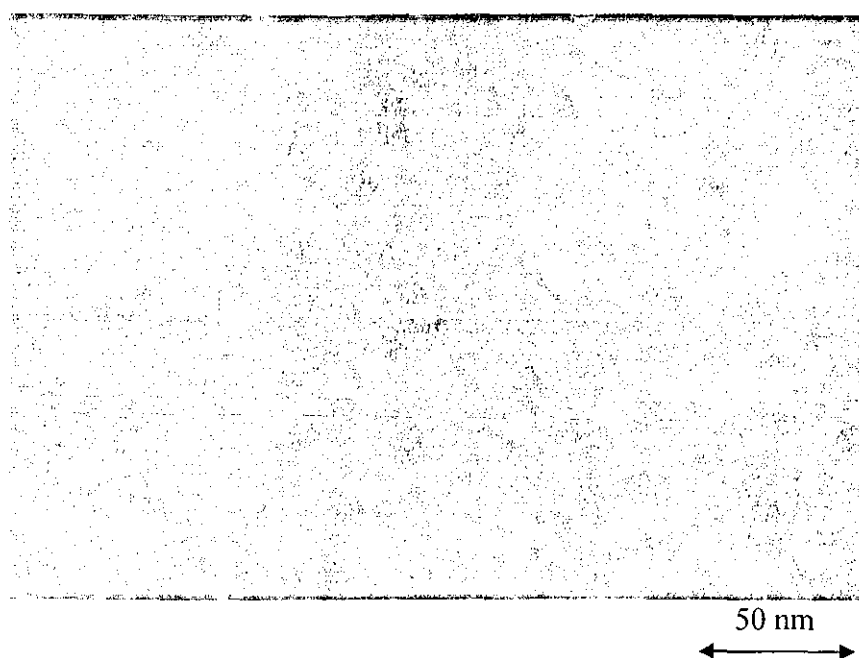
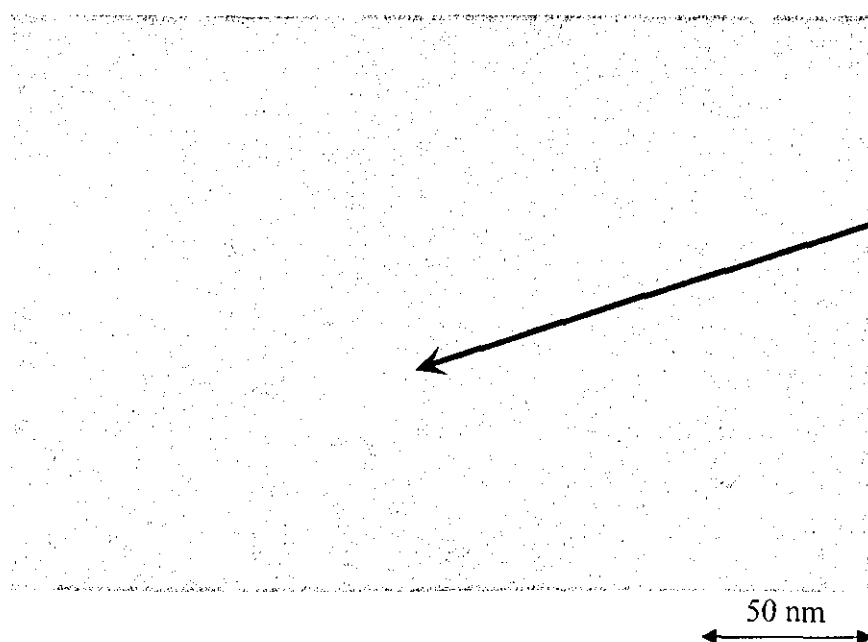


Figure 4.13: TEM micrograph showing the morphology of a perfluoroether modified polyimide film containing 5 wt% of Oligomer TX-CA-E8.



(Q)

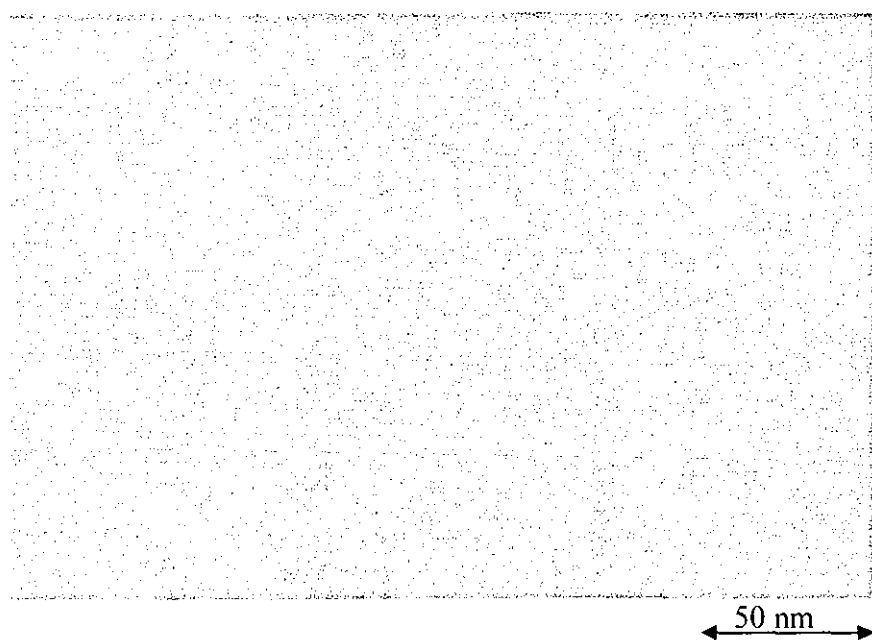
Figure 4.14: TEM micrograph showing the morphology of a perfluoroether modified polyimide film containing 10 wt% of Oligomer TX-CA-E8.



hint of co-continuity in the multiphase morphology

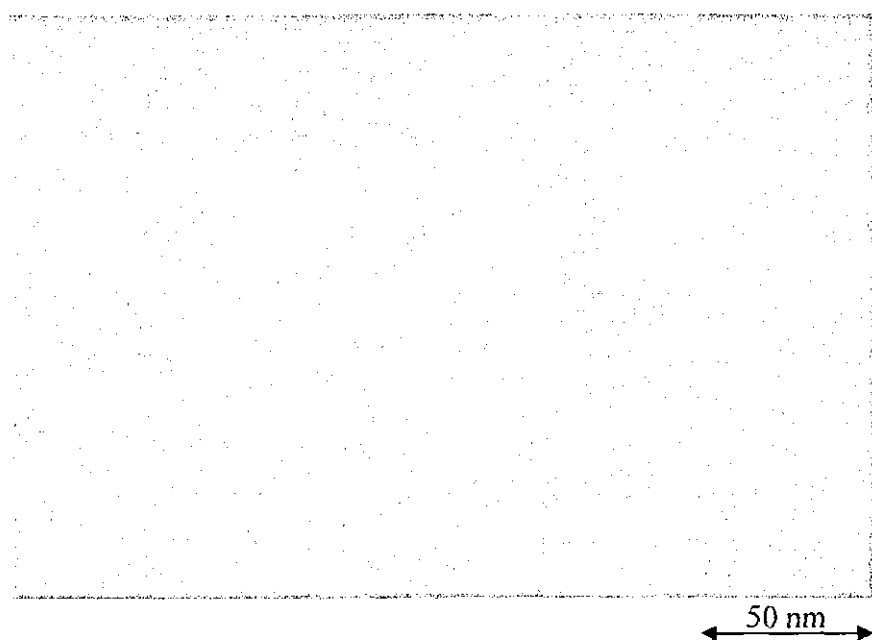
(R)

Figure 4.15: TEM micrograph showing the morphology of a perfluoroether modified polyimide film containing 15 wt% of Oligomer TX-CA-E8.



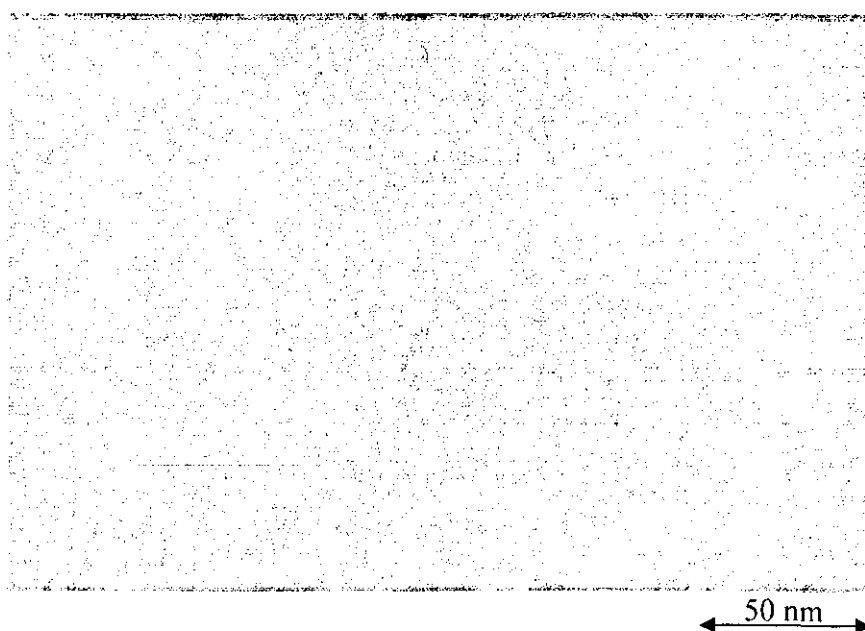
(S)

Figure 4.16: TEM micrograph showing the morphology of a perfluoroether modified polyimide-silica hybrid containing 2.5 wt% of Oligomer TX-CA-E8.



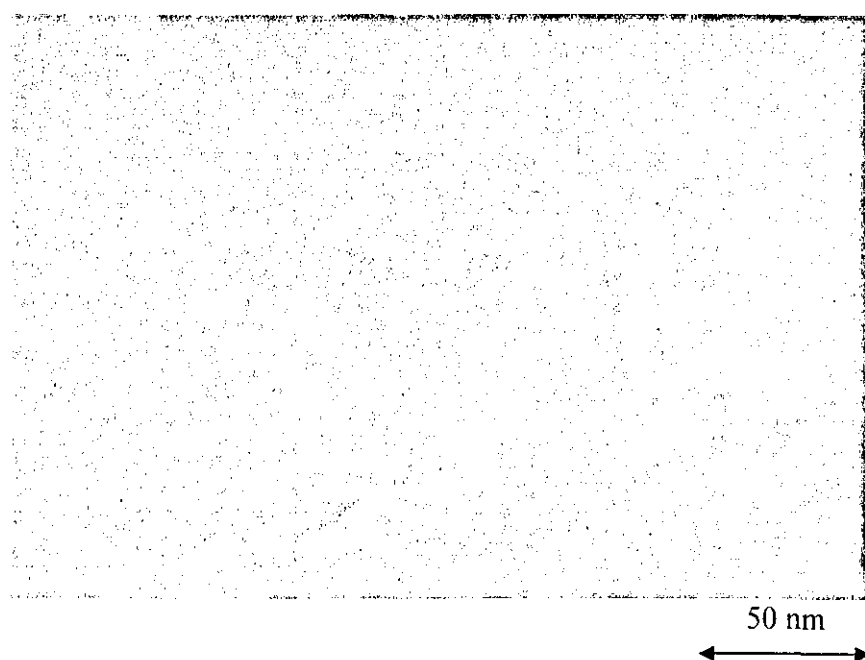
(T)

Figure 4.17: TEM micrograph showing the morphology of a perfluoroether modified polyimide-silica hybrid containing 5 wt% of Oligomer TX-CA-E8.



(U)

Figure 4.18: TEM micrograph showing the morphology of a perfluoroether modified polyimide-silica hybrid containing 10 wt% of Oligomer TX-CA-E8.



(V)

Figure 4.19: TEM micrograph showing the morphology of a perfluoroether modified polyimide-silica hybrid containing 15 wt% of Oligomer TX-CA-E8.

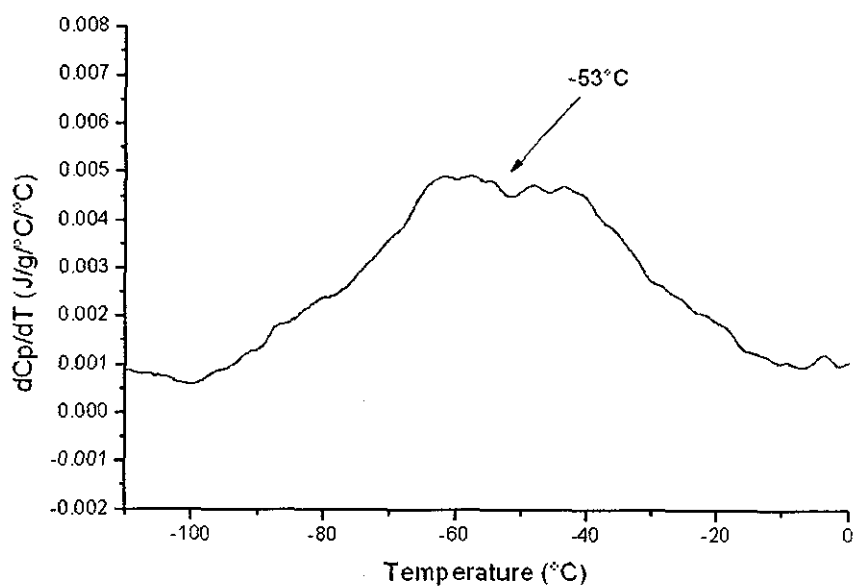


Figure 4.20: MTDSC thermogram of Oligomer TX-CA-E8, showing the derivative specific heat capacity.

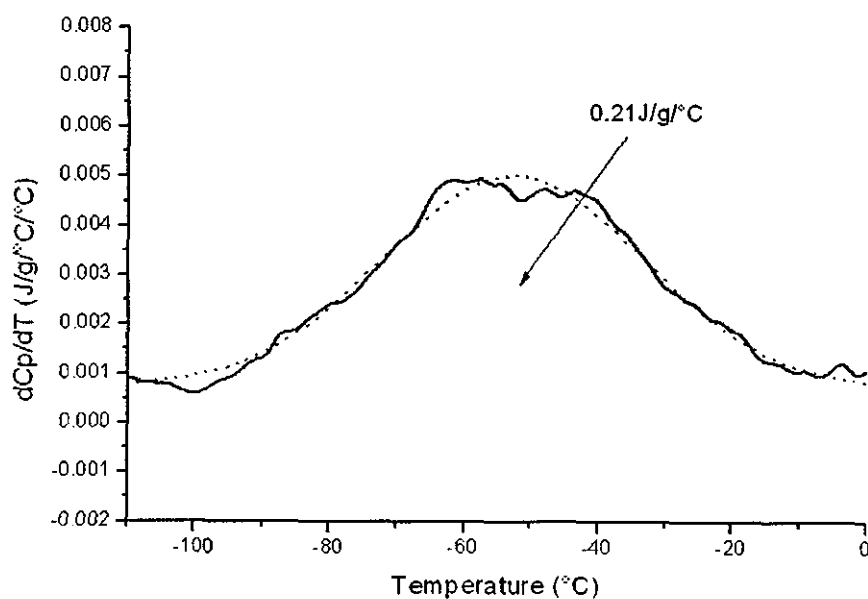


Figure 4.21: MTDSC thermogram of Oligomer TX-CA-E8 and the result of Gaussian curve fitting.

Based on the results obtained, the benefit of superimposing a temperature modulation on an underlying heating rate (i.e. the principle of MTDSC) was clearly evident with the enormous increase in sensitivity in the thermal data.

4.5.2 Thermal Evaluation of Uncured Mixtures of Polyamic Acid and Epoxy Functionalised Perfluoroether Oligomer

Figures 4.23 to 4.32 show the MTDSC thermograms with the temperature derivative of specific heat capacity signal (ΔC_p) of pre-cured films (80°C). These were casting of polyamic acid modified with Oligomer TX-CA-E8. A second transition can clearly be observed at around -5°C for the unmodified film and the film containing 2.5 wt% of perfluoroether. At higher level of perfluoroether modification, this transition was found to move to a slightly higher temperature of around 0°C. Using the Gaussian curve fitting technique, the specific heat capacity of this transition can be estimated in all the formulations.

Progressive heating above this transition reveals a series of complicated events. In the unmodified film (see figure 4.23), two sharp dips were observed at around 85°C and 120°C, which are associated with the sudden liberation of toluene and NMP, respectively. The reductions in specific heat capacity in these two events were, therefore, the result of spontaneous chain restriction due to volatisation of these two solvents consecutively. These two dips were not detectable in all the films, which contained the perfluoroether modifier.

Very convoluted signals were observed at higher temperature around 140°C to 160°C, which are attributed to the combined effects of further solvent evaporation of NMP through decomplexation from the amic acid and imidisation reactions. The patterns of these signals are very different from one formulation to another. Deconvoluted interpretation of the individual event is very difficult (figures 4.24 to 4.32).

Figures 4.33 and 4.34 show the change in specific heat capacity and their peak temperatures of the low temperature transitional event as a function of perfluoroether content. The trends of the two plots were very similar to each other.

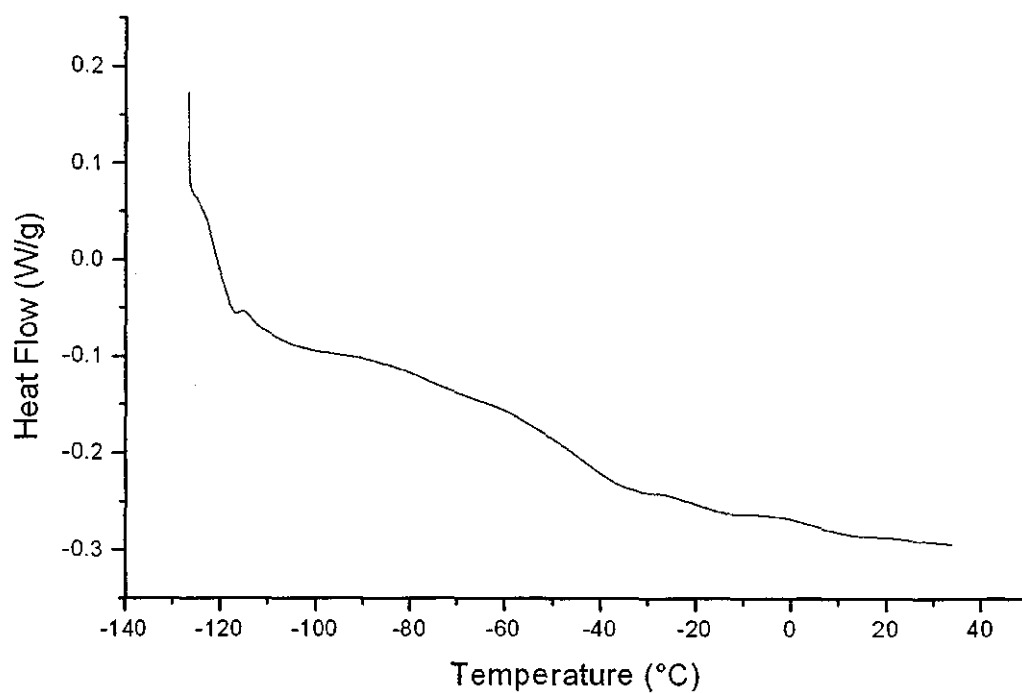


Figure 4.22: DSC thermogram of Oligomer TX-CA-E8, showing the conventional heat flow signal.

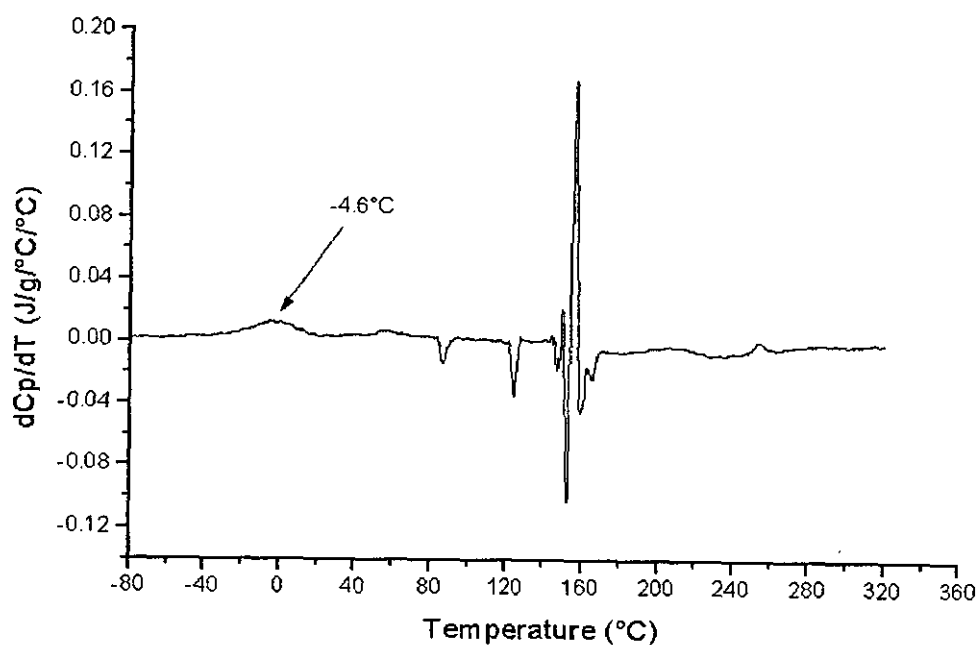


Figure 4.23: MTDSC thermogram of an unmodified uncured polyamic acid (Skybond 703) showing the derivative of specific heat capacity signal.

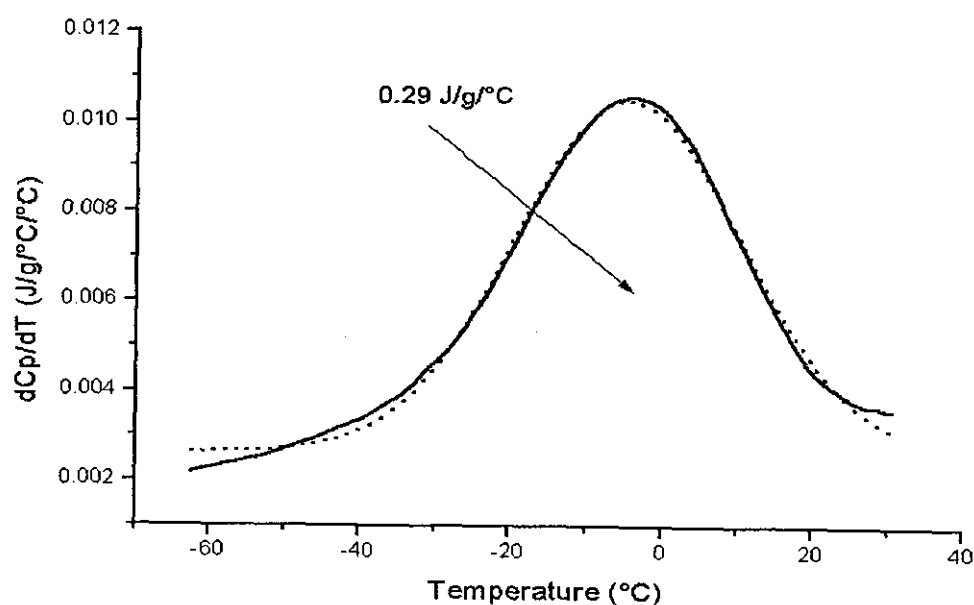


Figure 4.24: MTDSC thermogram of an unmodified uncured polyamic acid (Skybond 703) showing an enlarged region of the lower transitional region of the polymer.

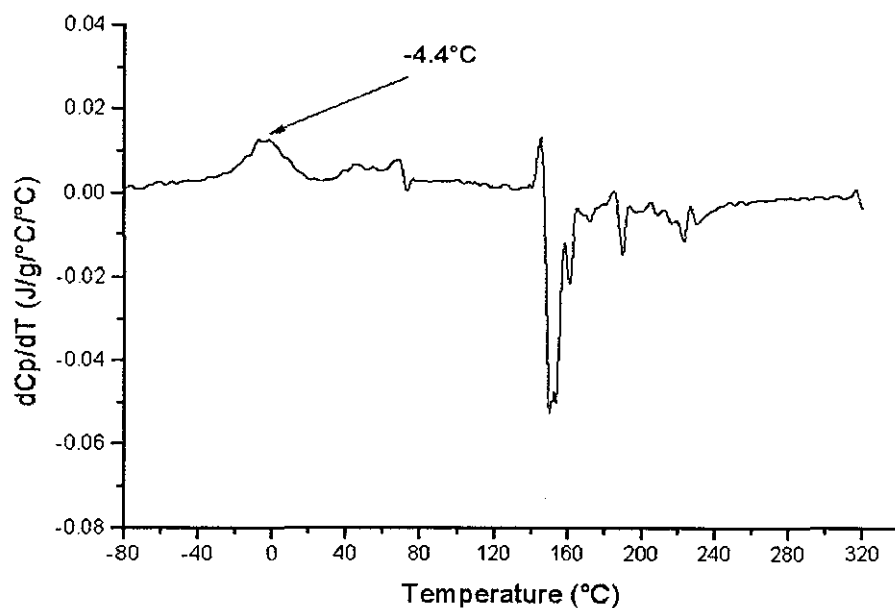


Figure 4.25: MTDSC thermogram of a 2.5 % w/w Oligomer TX-CA-E8 modified, uncured polyamic acid (Skybond 703) showing the derivative of specific heat capacity signal.

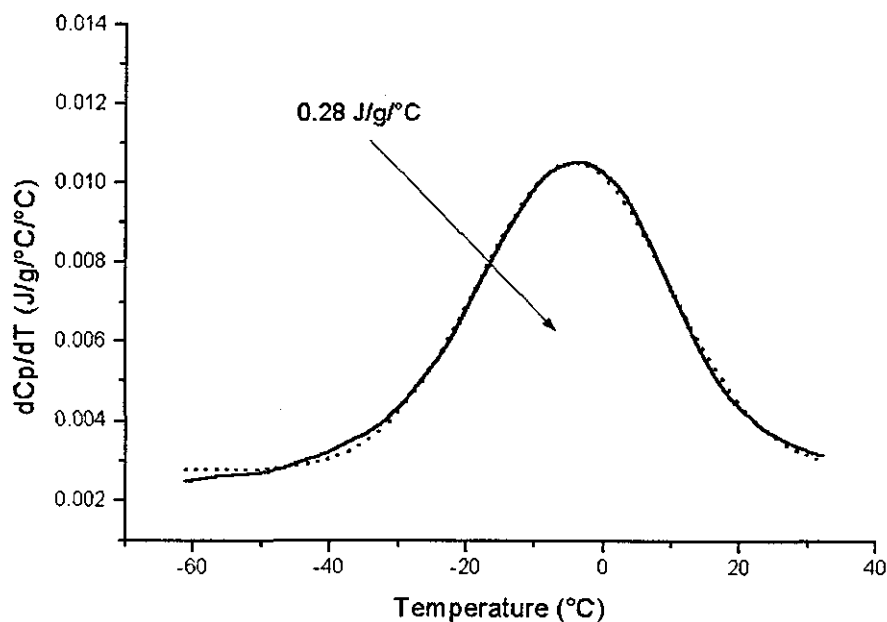


Figure 4.26: MTDSC thermogram of the 2.5% w/w modified, uncured polyamic acid (Skybond 703) showing an enlarged region of the lower transitional region of the polymer.

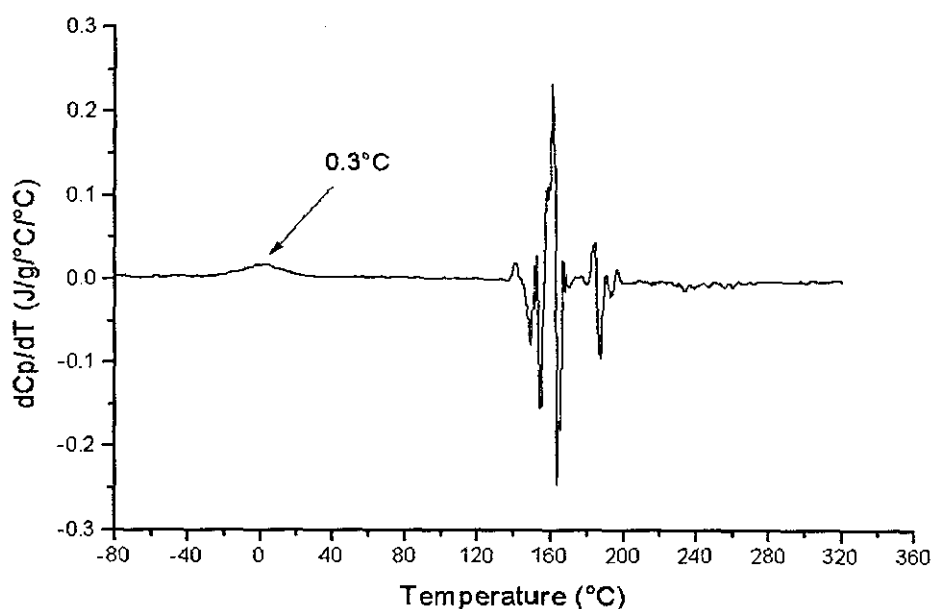


Figure 4.27: MTDSC thermogram of a 5 % w/w Oligomer TX-CA-E8 modified, uncured polyamic acid (Skybond 703) showing the derivative of specific heat capacity signal.

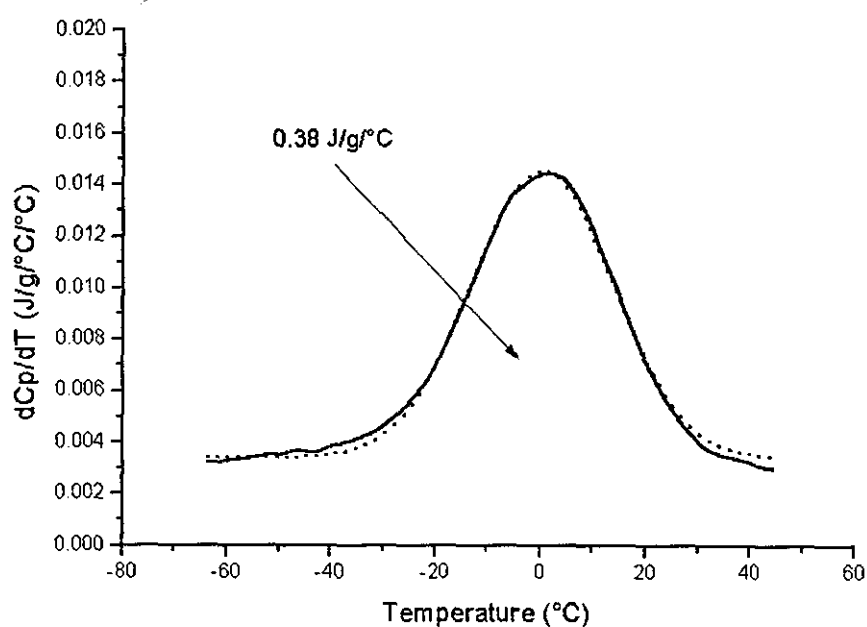


Figure 4.28: MTDSC thermogram of the 5 % w/w modified, uncured polyamic acid (Skybond 703) showing an enlarged region of the lower transitional region of the polymer.

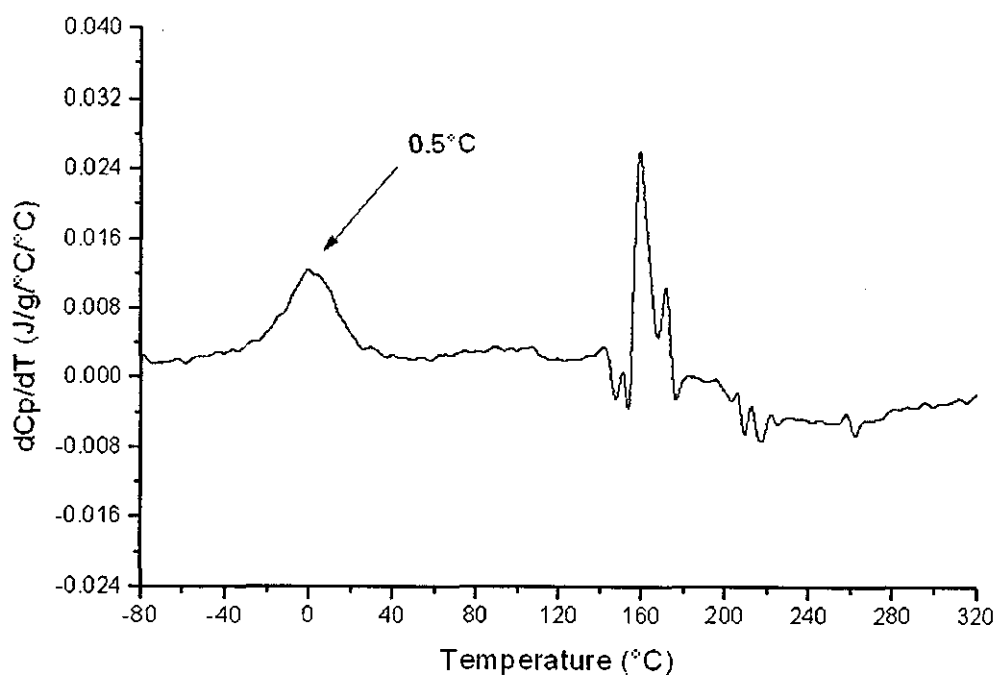


Figure 4.29: MTDSC thermogram of a 10 % w/w Oligomer TX-CA-E8 modified, uncured polyamic acid (Skybond 703) showing the derivative of specific heat capacity signal.

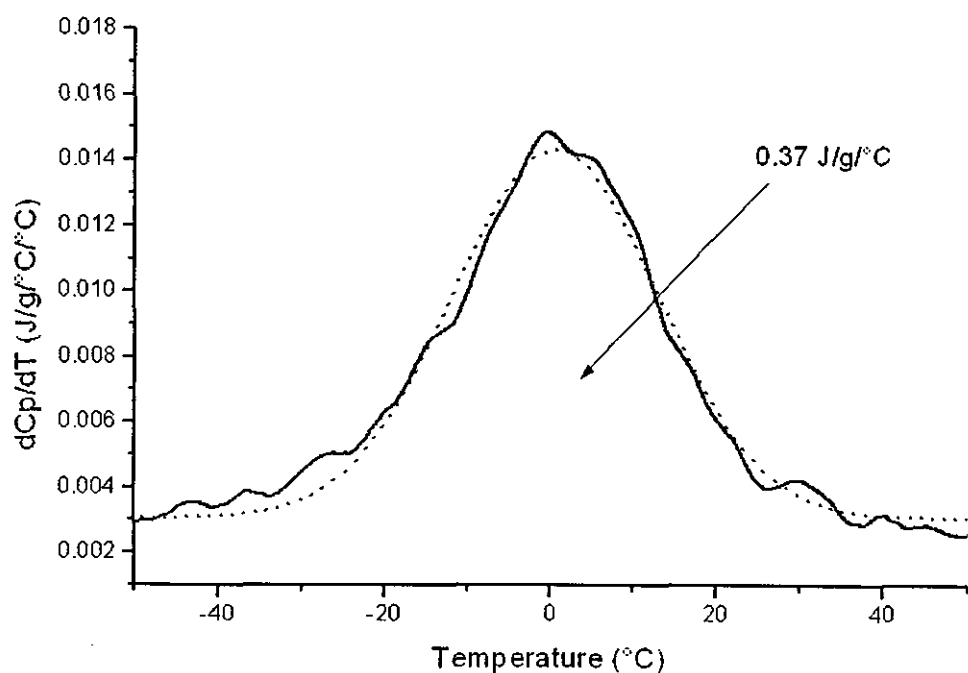


Figure 4.30: MTDSC thermogram of the 10 % w/w modified, uncured polyamic acid (Skybond 703) showing an enlarged region of the lower transitional region of the polymer.

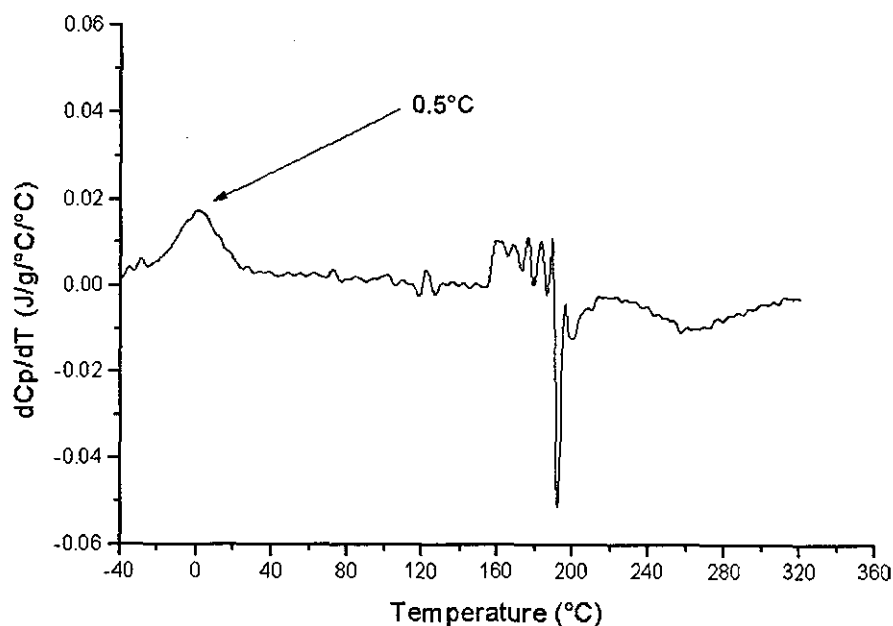


Figure 4.31: MTDSC thermogram of a 15 % w/w Oligomer TX-CA-E8 modified, uncured polyamic acid (Skybond 703) showing the derivative of specific heat capacity signal.

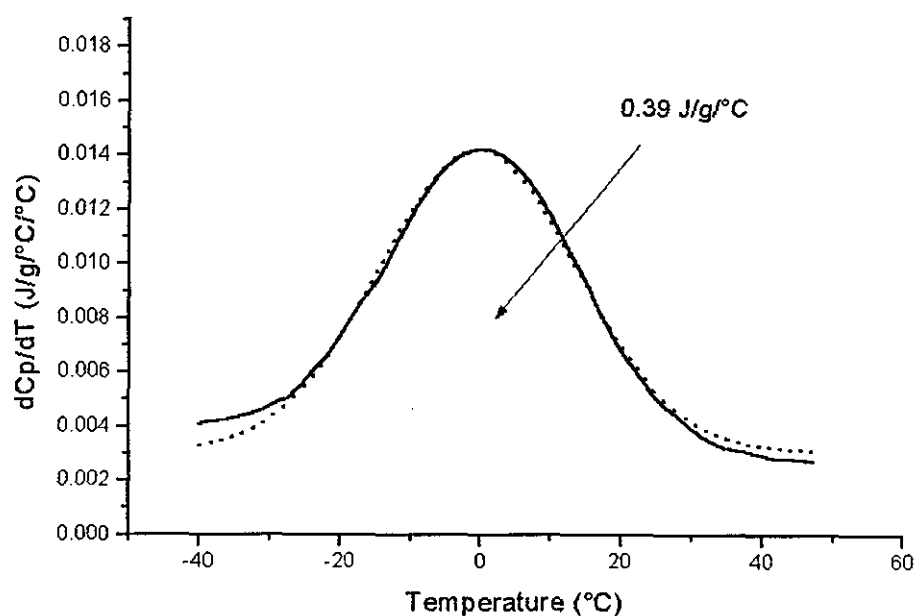


Figure 4.32: MTDSC thermogram of the 15 % w/w modified, uncured polyamic acid (Skybond 703) showing an enlarged region of the lower transitional region of the polymer.

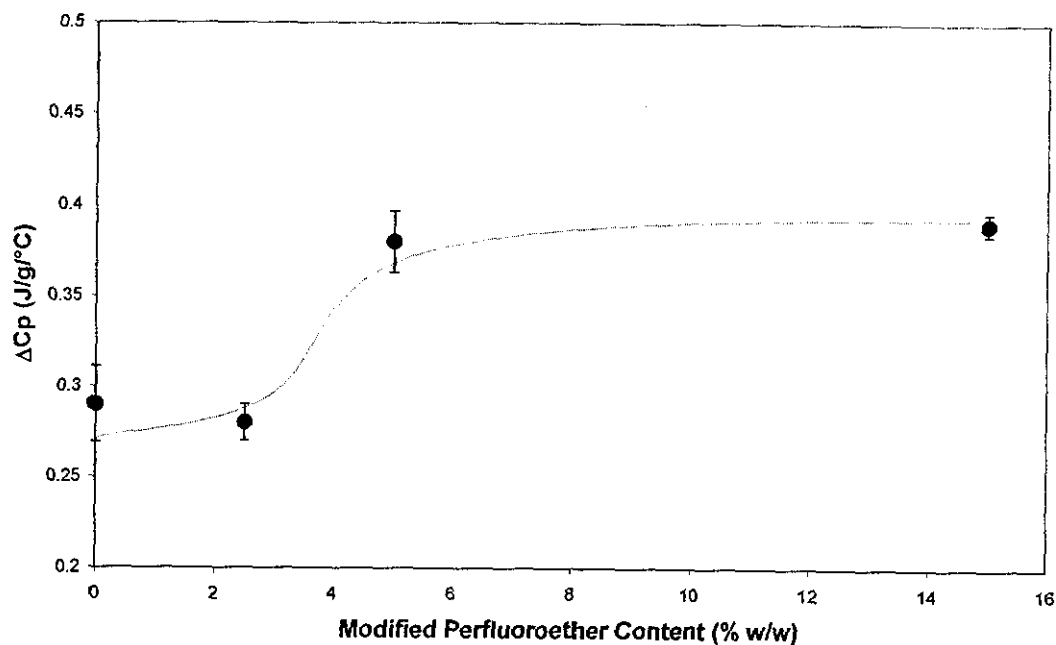


Figure 4.33: ΔC_p of the low temperature peak of the non-hybridised and uncured polyamic acid films at various modified perfluoroether concentrations.

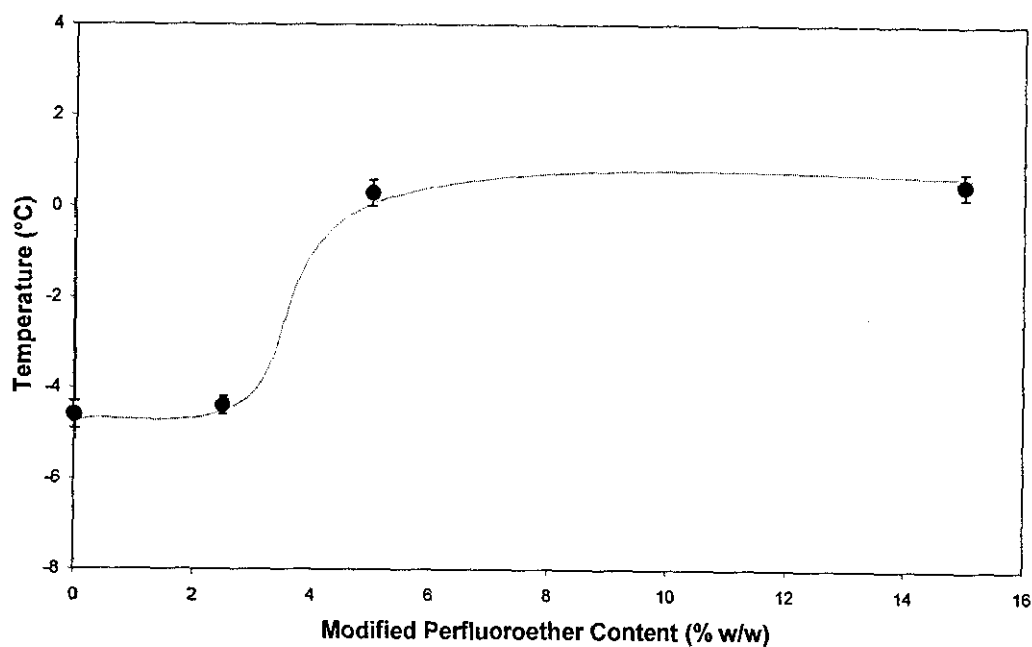


Figure 4.34: Peak temperatures of the low temperature peak of the non-hybridised and uncured polyamic acid films at various modified perfluoroether concentrations.

Figure 4.35 shows the consolidated MTDSC thermograms with the conventional heat flow signal of the same series of pre-cured films as above. The low temperature transitional event is clearly visible with the unmodified film and the film containing only 2.5 wt% of Oligomer TX-CA-E8. In contrast to the derivative specific heat capacity signal discussed above, this transition became very small in the heat flow signal with high concentration of perfluoroether in the films.

Subsequent heating above the transition resulted in a series of endothermic peaks. These signals were considerably less complicated than the derivative specific heat capacity signal, probably due to the reduced sensitivity. Three major peaks may be identified in all the formulations, as a general observation and, they started to appear after about 150°C. These endothermic peaks are very large for the case of the unmodified film, and become considerably smaller with films containing higher concentrations of perfluoroether, i.e. 10 wt% and 15 wt%. The presence of Oligomer TX-CA-E8, therefore, can be seen to facilitate the removal of the NMP through a more gradual diffusion process.

4.5.3 Thermal Evaluation of Uncured Mixtures of Polyamic Acid, Hybridising Silica and Epoxy Functionalised Perfluoroether Oligomer

Figures 4.36 to 4.44 show the MTDSC thermograms with the temperature derivative of specific heat capacity signal of pre-cured film (80°C). These were compatibilised mixture of polyamic acid, prehydrolysed alkoxysilane/silica and Oligomer TX-CA-E8.

The low temperature transition found in the non-hybridising films discussed earlier can also be detected in the films studied in this section. In addition, the overall trend of the thermograms of all the films were considerably simpler as well. The convoluted signal of the non-hybridising films at temperature above 150°C was replaced by a straight-forward dip.

Figures 4.45 and 4.46 show the change in specific heat capacity and their peak temperatures of the low temperature transitional event as a function of perfluoroether content. The transition was not detectable in the film containing 15 wt% of

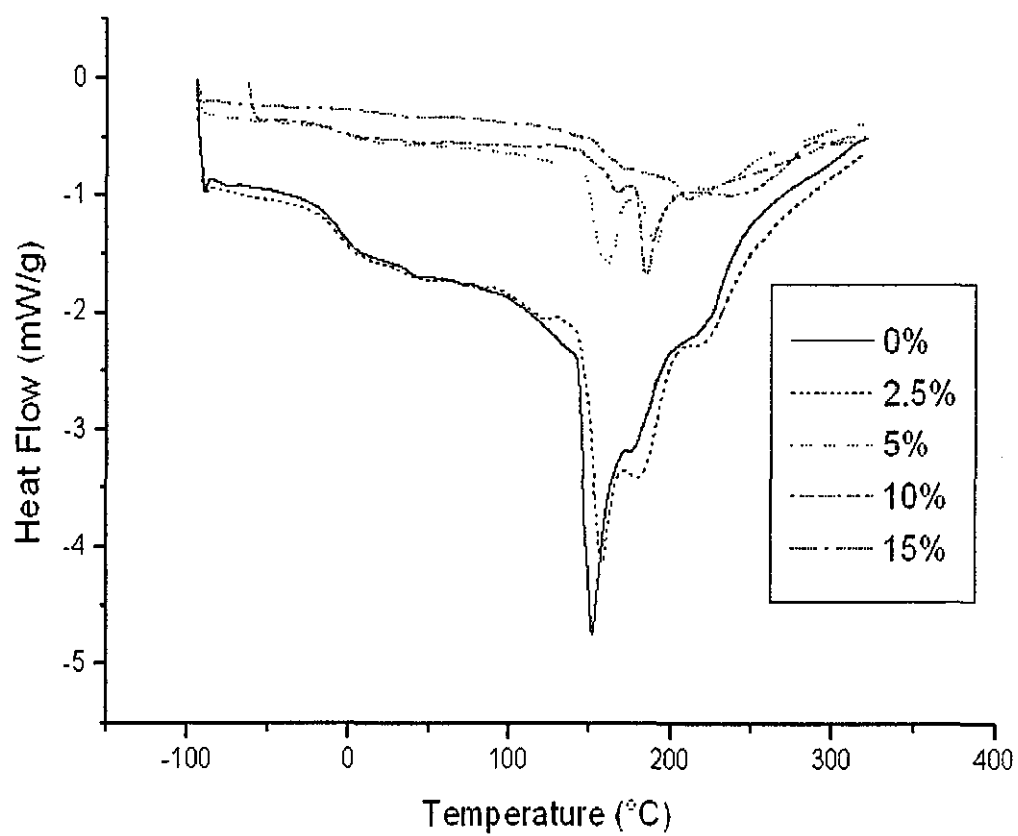


Figure 4.35: MTDSC thermograms showing the heat flow signals of uncured and non-hybridised films of polyamic acid at various concentrations of perfluoroether.

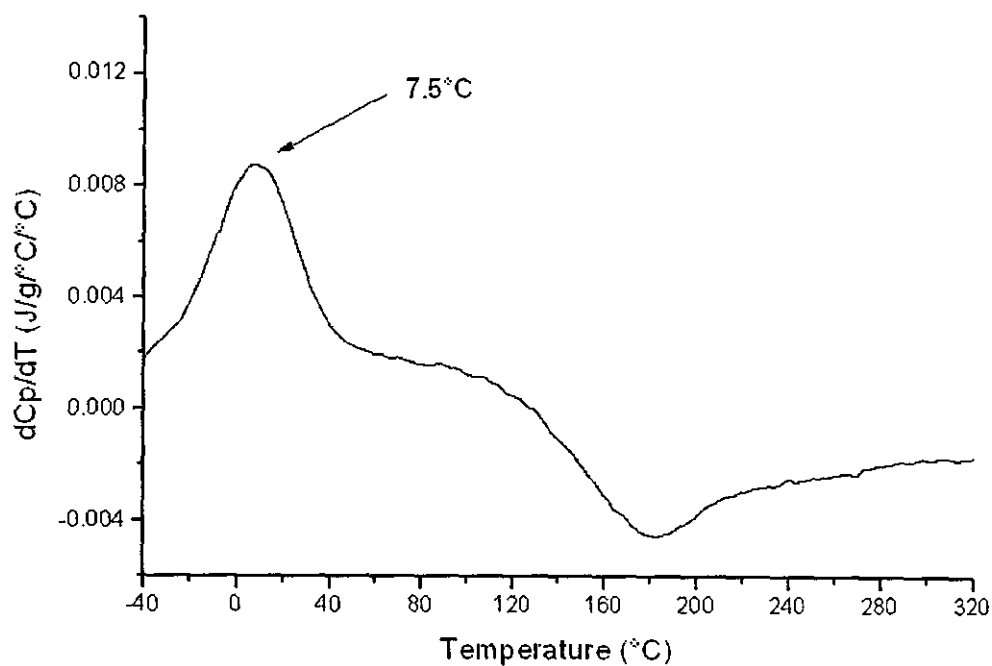


Figure 4.36: MTDSC thermogram of an uncured polyamic acid-silica hybrid containing no perfluoroether modifier. The derivative specific heat capacity signal is shown.

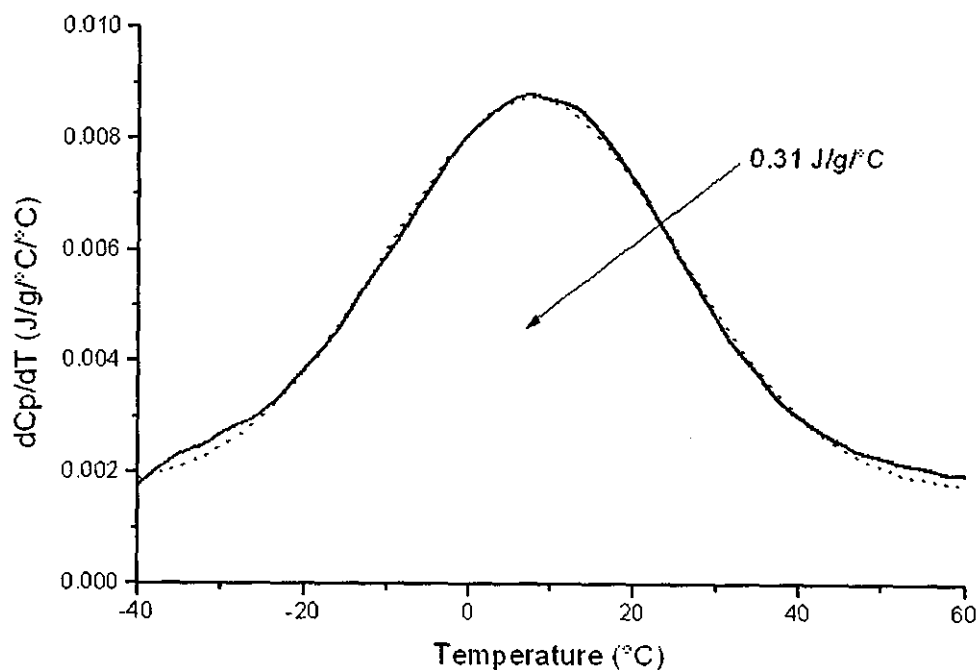


Figure 4.37: MTDSC thermogram of the above, showing an enlarged region of the lower transition and the result of Gaussian curve fitting.

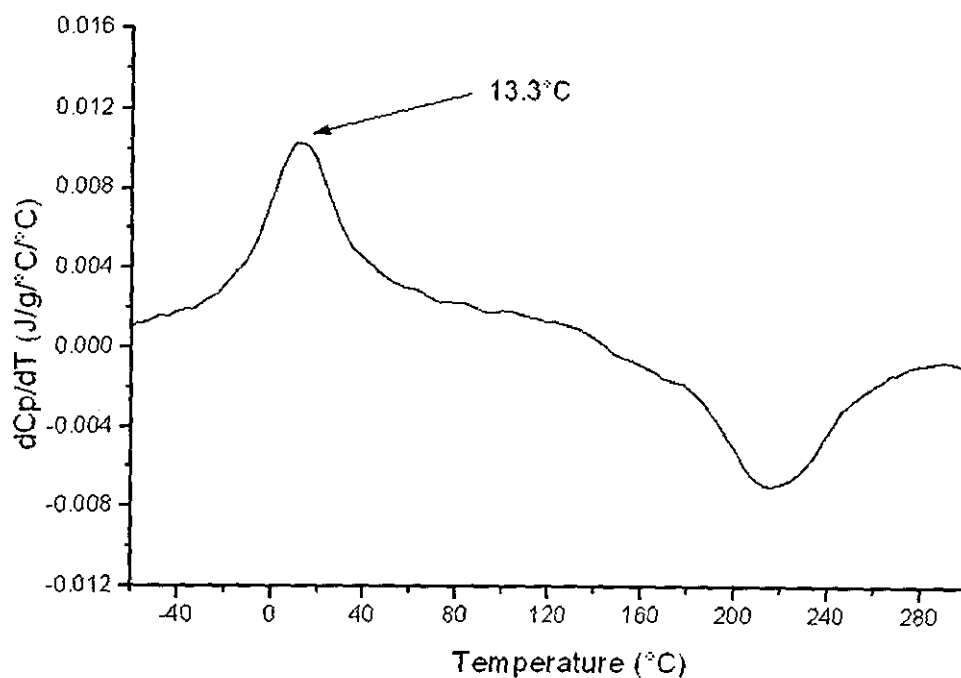


Figure 4.38: MTDSC thermogram of an uncured polyamic acid-silica hybrid containing 2.5 wt% of perfluoroether modifier. The derivative specific heat capacity signal is shown.

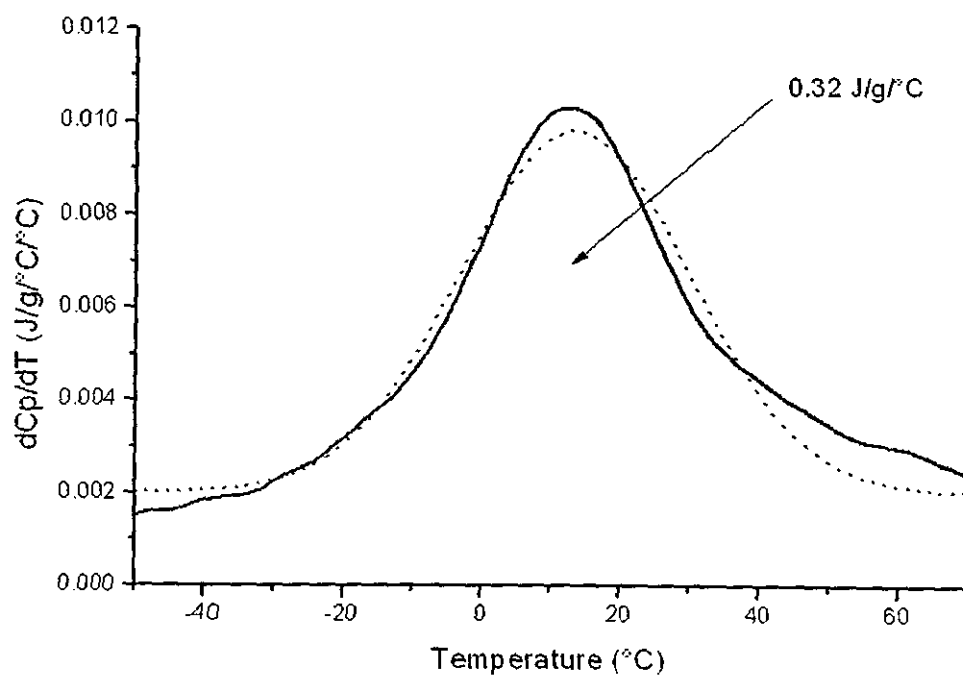


Figure 4.39: MTDSC thermogram of the above, showing an enlarged region of the lower transition and the result of Gaussian curve fitting.

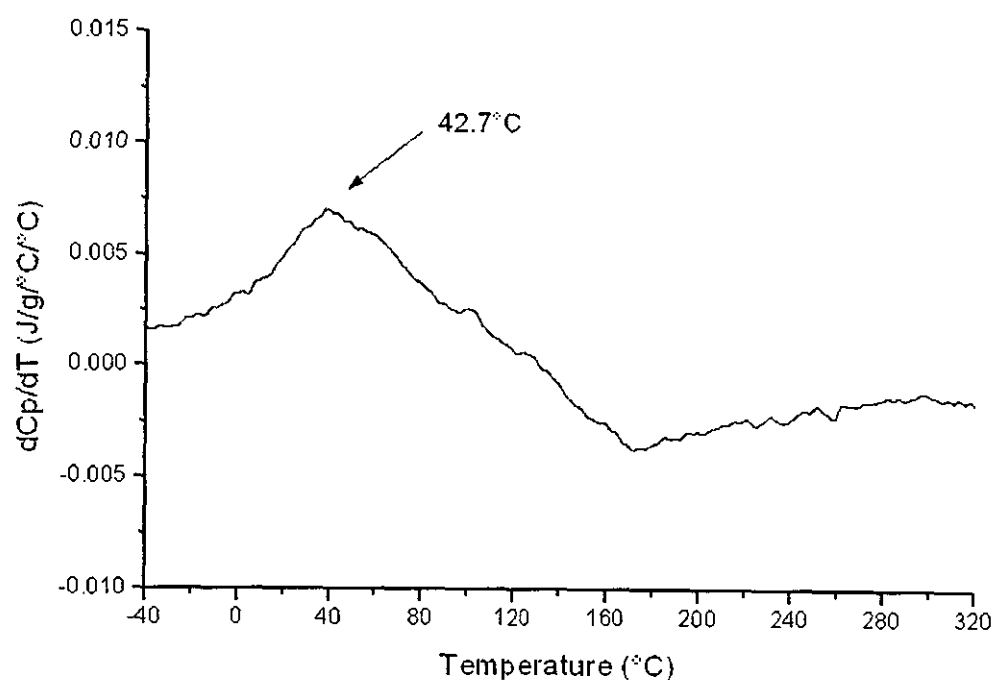


Figure 4.40: MTDSC thermogram of an uncured polyamic acid-silica hybrid containing 5 wt% of perfluoroether modifier. The derivative specific heat capacity signal is shown.

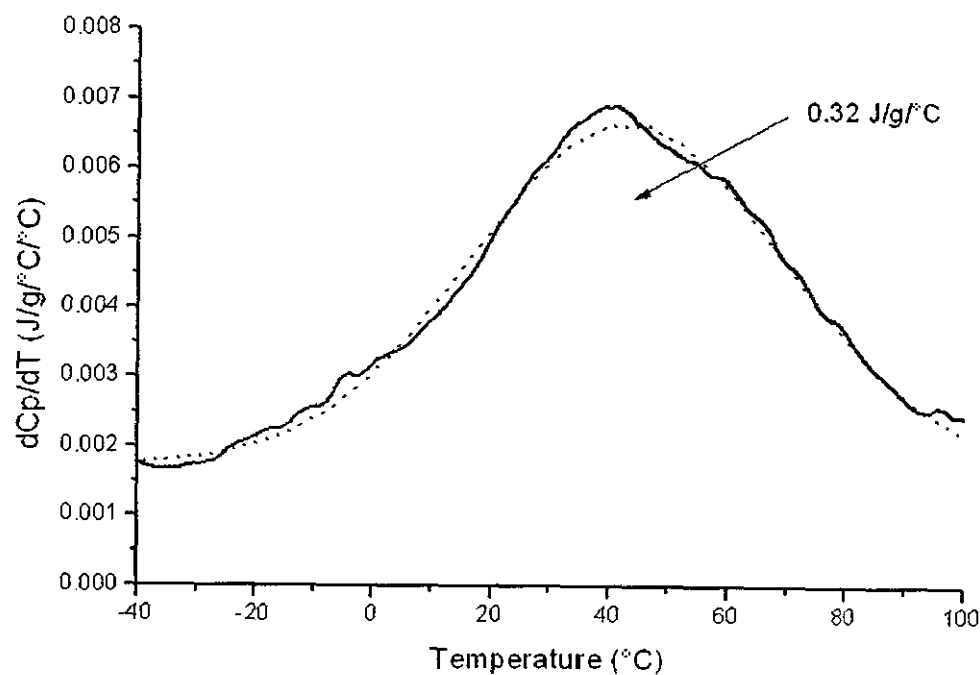


Figure 4.41: MTDSC thermogram of the above, showing an enlarged region of the lower transition and the result of Gaussian curve fitting.

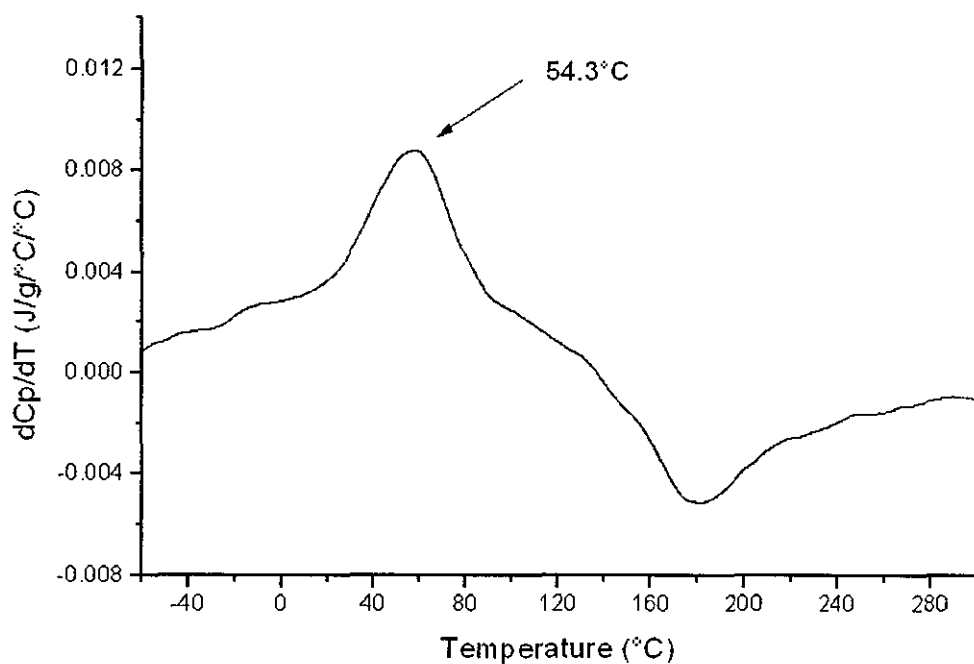


Figure 4.42: MTDSC thermogram of an uncured polyamic acid-silica hybrid containing 10 wt% of perfluoroether modifier. The derivative specific heat capacity signal is shown.

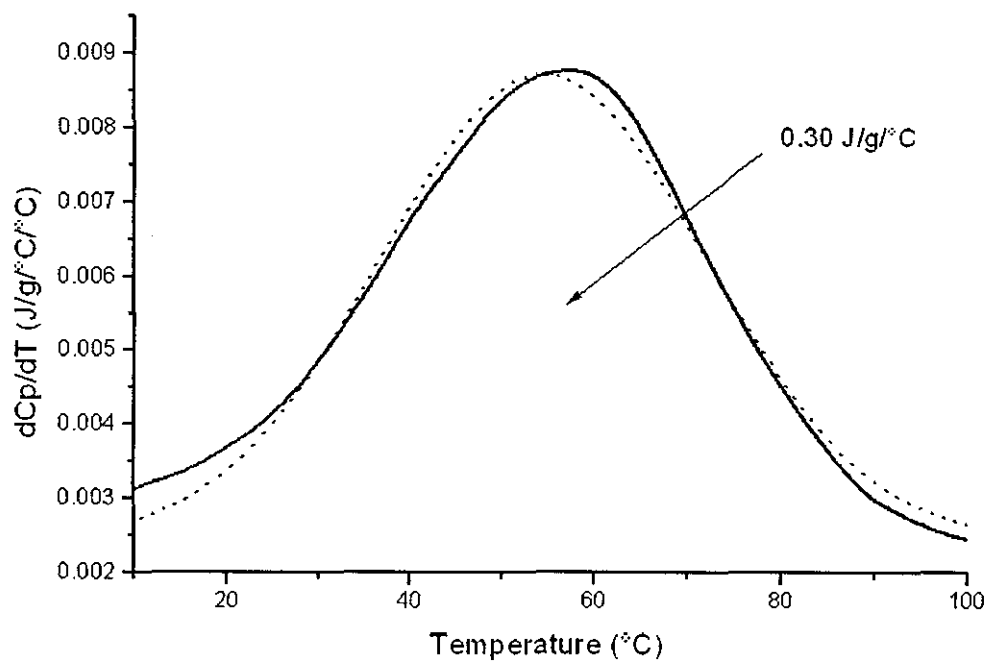


Figure 4.43: MTDSC thermogram of the above, showing an enlarged region of the lower transition and the result of Gaussian curve fitting.

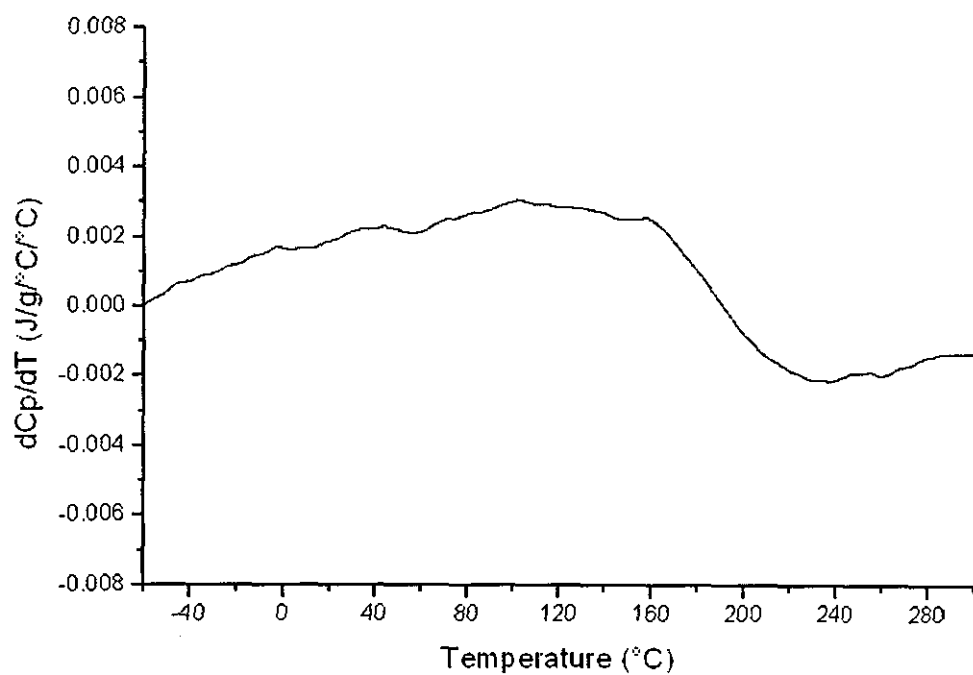


Figure 4.44: MTDSC thermogram of an uncured polyamic acid-silica hybrid containing 15 wt% of perfluoroether modifier. The derivative specific heat capacity signal is shown.

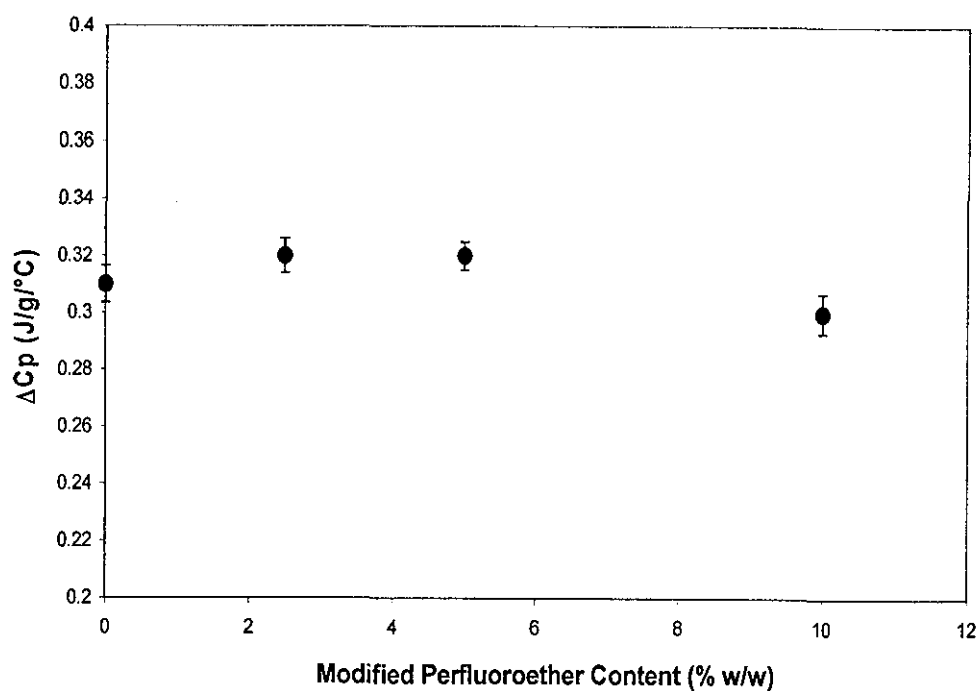


Figure 4.45: ΔC_p of the low temperature peak of the hybridised films at various concentrations of perfluoroether modification.

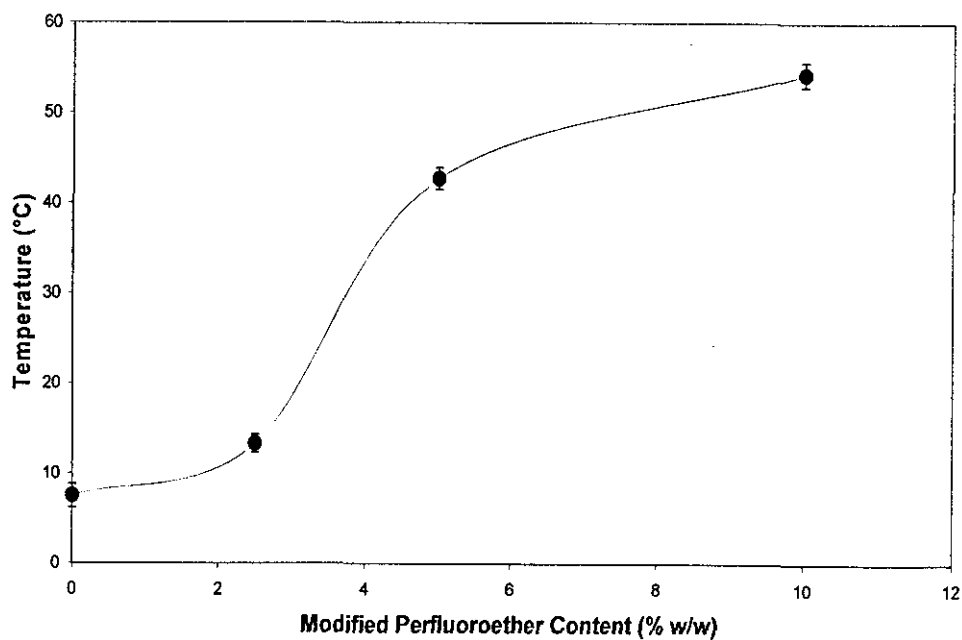


Figure 4.46: Peak temperatures of the low temperature peak of the hybridised films at various concentrations of perfluoroether modification.

Oligomer TX-CA-E8 and hence was not included in the plots. The trend of the change in peak temperature value has some resemblance to their non-hybridising equivalent, discussed earlier (see figure 4.34). A similar stepwise increase in the transitional peak temperature value occurs at around 2.5 to 5 wt% modification level of Oligomer TX-CA-E8. However, the trend of the derivative specific heat capacity plot was not showing any similarity with the corresponding non-hybridising films. In fact, no significant changes in the derivative specific heat capacity signal can be detected with increasing perfluoroether content, except for a large reduction above 12% perfluoroether content.

Figure 4.47 shows the consolidated MTDSC thermograms with the conventional heat flow signal of DSC of the above films. The low temperature transitions of the films were visible, particularly those with lower level of modification of perfluoroether. The overall trend of the signals of all the films was quite simple with a very large peak at temperature slightly above 150°C, which also reduced in size progressively with increasing perfluoroether content. This is associated with a more gradual loss of NMP.

Figure 4.48 shows the comparison of conventional heat flow signal between an unmodified polyamic acid and a polyamic acid containing the hybridising silica. Both samples did not contain any perfluoroether modifier. It is clear that the endotherm produced by the hybrid is considerably smaller, which again is associated with a more gradual loss of NMP starting at lower temperatures.

4.5.4 Thermal Evaluation of Fully Imidised Films of Polyimides and Polyimide-Silica Hybrids Modified with Epoxy Functionalised Perfluoroether Oligomer

Figures 4.49 to 4.58 show the MTDSC thermograms with temperature derivative of the specific heat capacity signal of polyimide film containing various concentrations of Oligomer TX-CA-E8. The thermograms of the hybrid equivalent of the films are shown in figures 4.59 to 4.68.

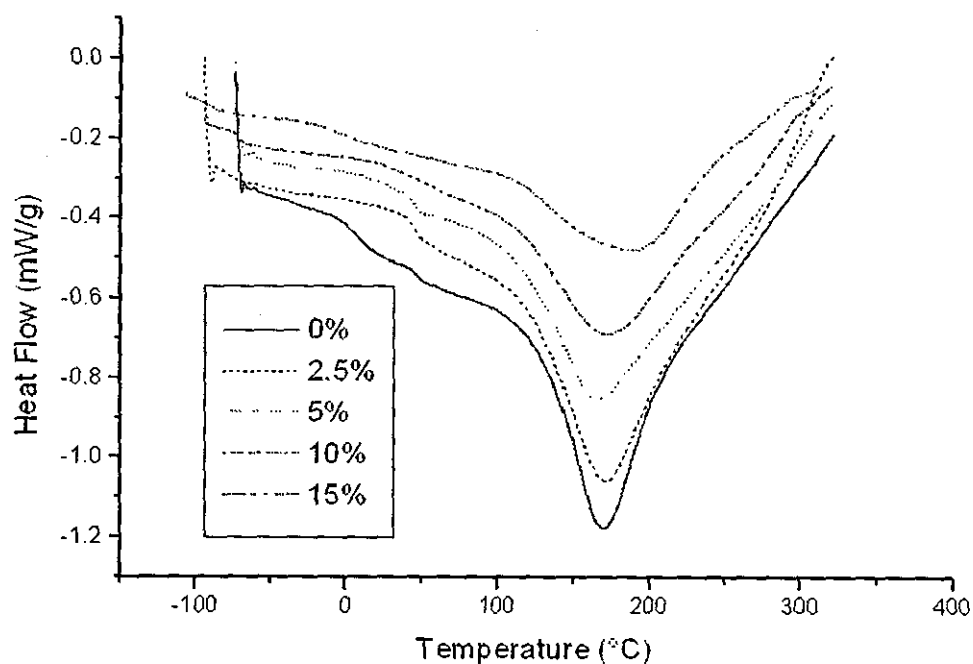


Figure 4.47: MTDSC thermograms showing the conventional heat flow signals of the uncured and hybridised polyamic acid film at various concentrations of perfluoroether modification.

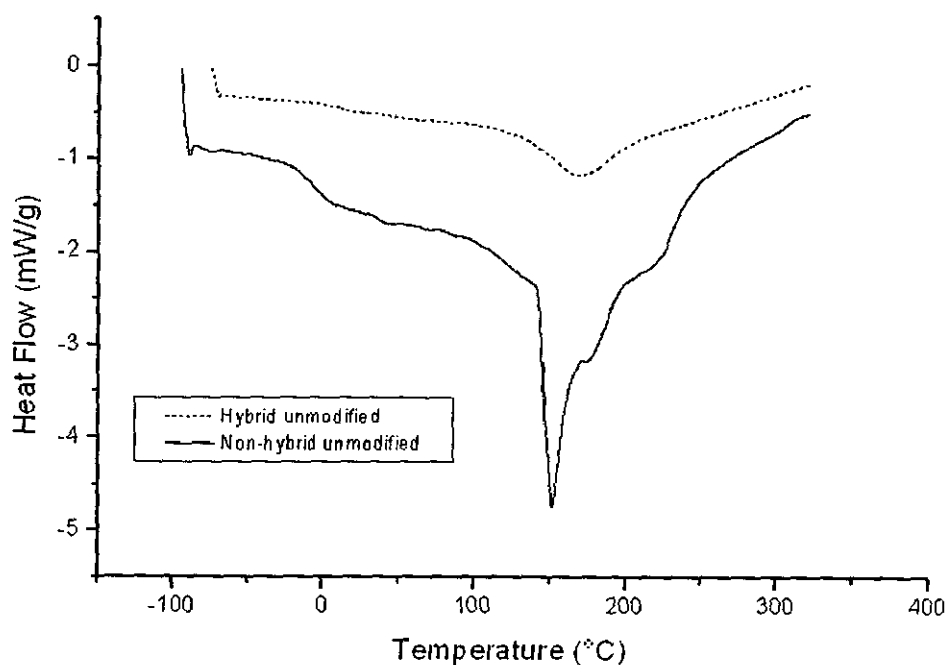


Figure 4.48: MTDSC thermograms comparing the heat flow signal between a hybridised and a non-hybridised polyamic acid films.

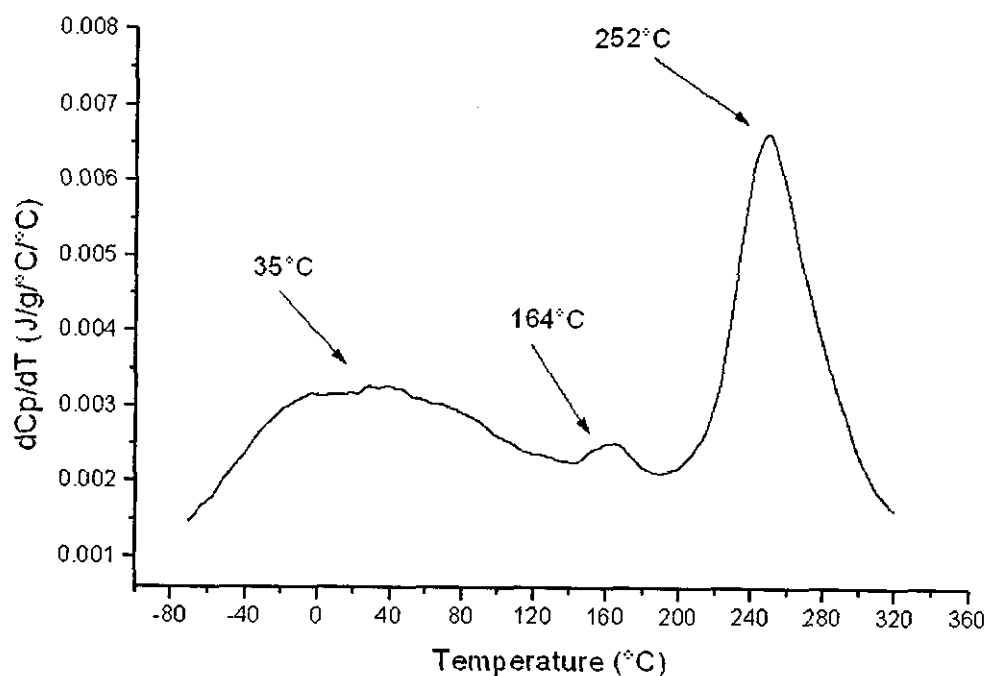


Figure 4.49: MTDSC thermogram showing the derivative specific heat capacity signal of a cured and non-hybridised polyimide film containing no perfluoroether modifier.

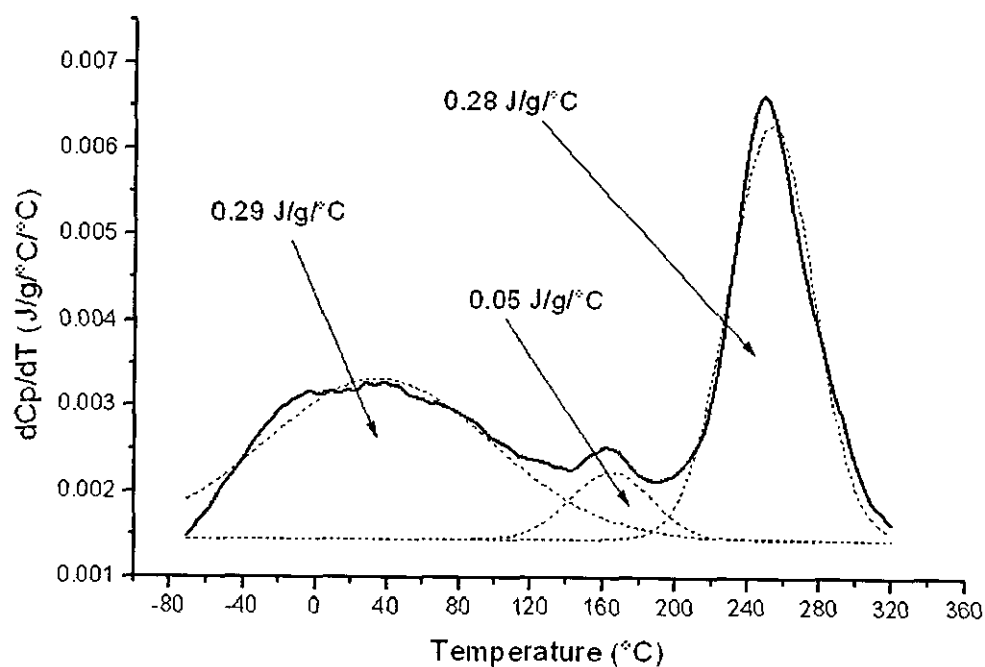


Figure 4.50: MTDSC thermogram of the above, showing the results of Gaussian curve fitting.

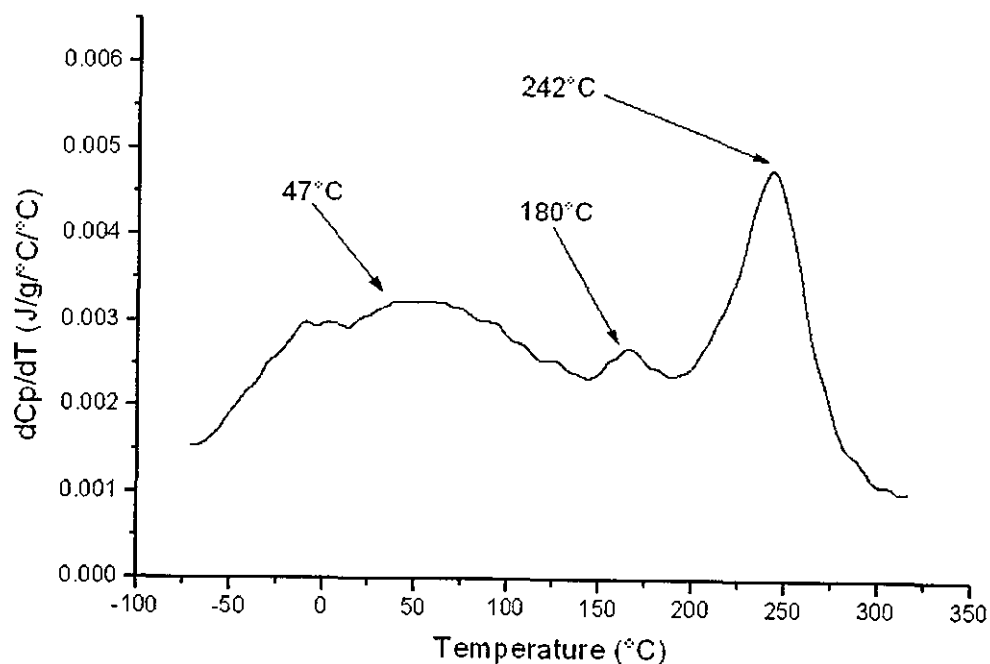


Figure 4.51: MTDSC thermogram showing the derivative specific heat capacity signal of a cured and non-hybridised polyimide film containing 2.5 wt% perfluoroether modifier

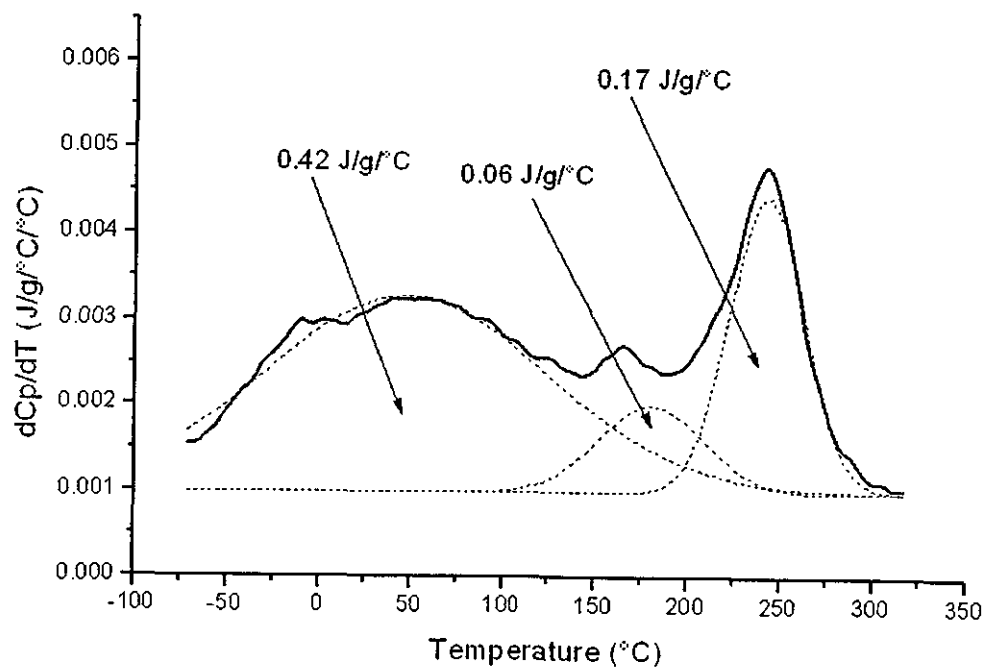


Figure 4.52: MTDSC thermogram of the above, showing the results of Gaussian curve fitting.

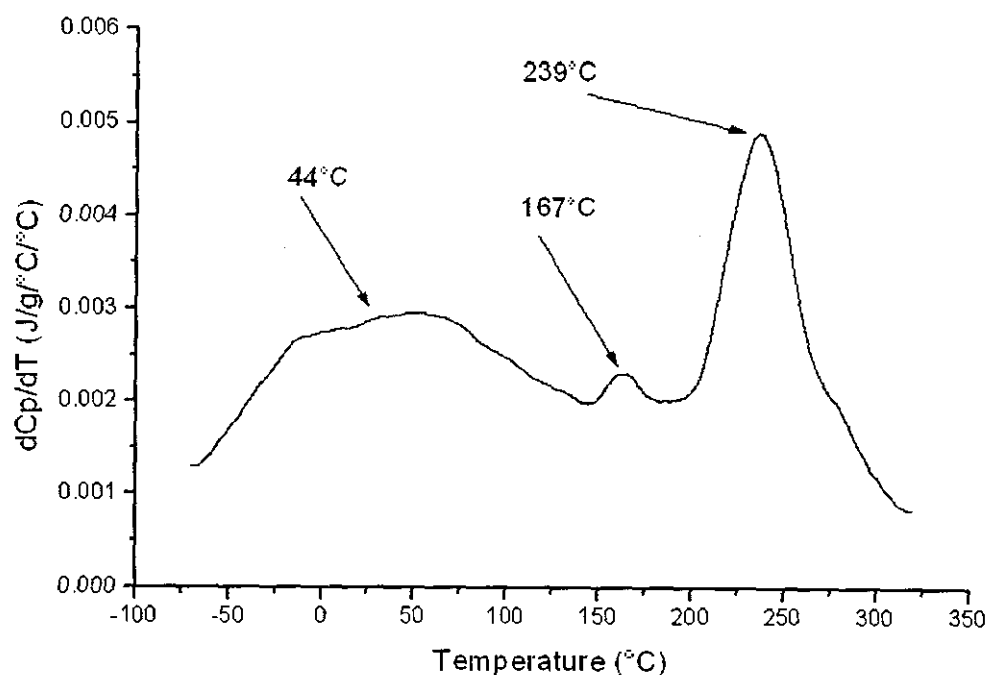


Figure 4.53: MTDSC thermogram showing the derivative specific heat capacity signal of a cured and non-hybridised polyimide film containing 5 wt% perfluoroether modifier

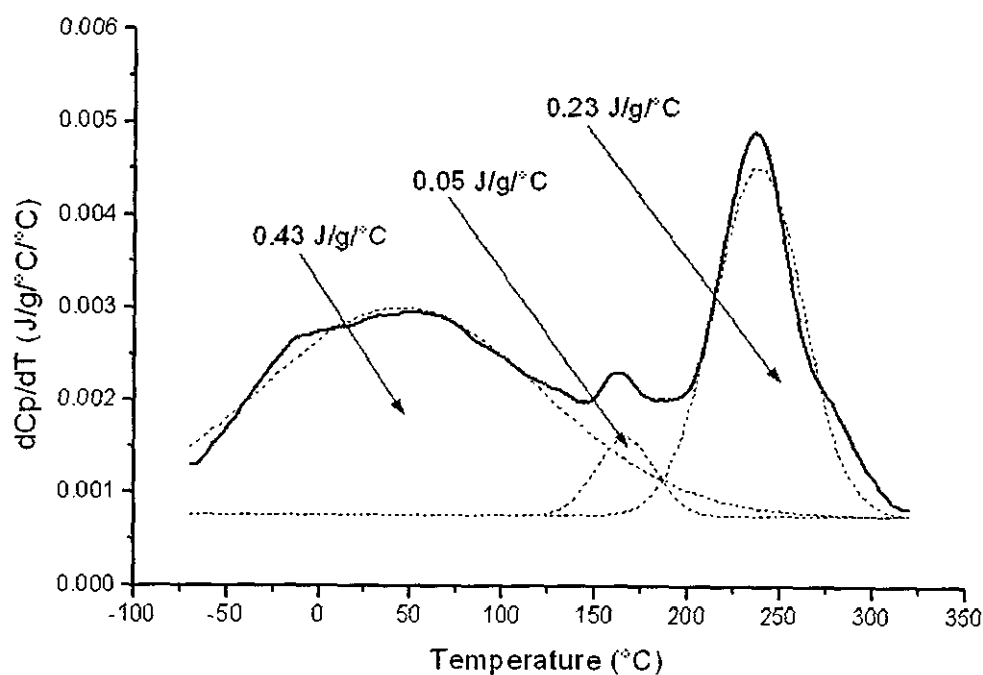


Figure 4.54: MTDSC thermogram of the above, showing the results of Gaussian curve fitting.

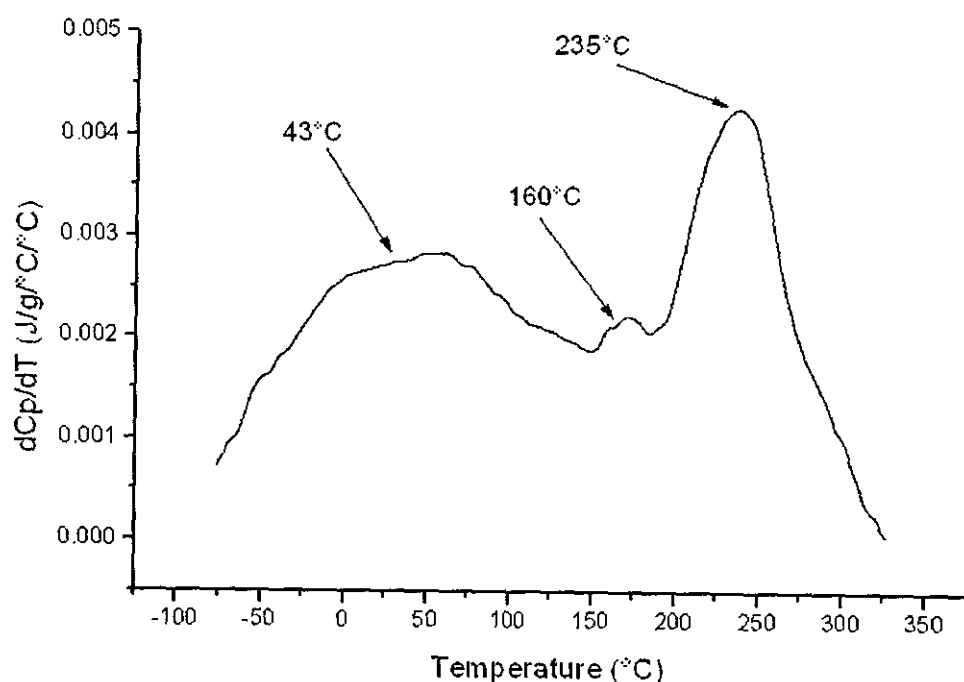


Figure 4.55: MTDSC thermogram showing the derivative specific heat capacity signal of a cured and non-hybridised polyimide film containing 10 wt% perfluoroether modifier

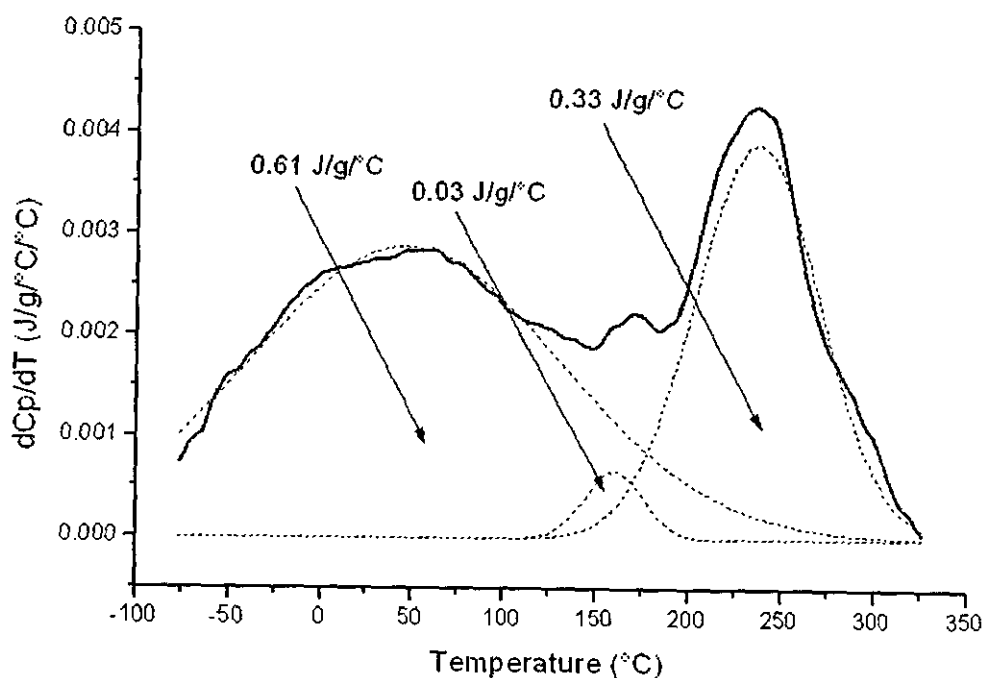


Figure 4.56: MTDSC thermogram of the above, showing the results of Gaussian curve fitting.

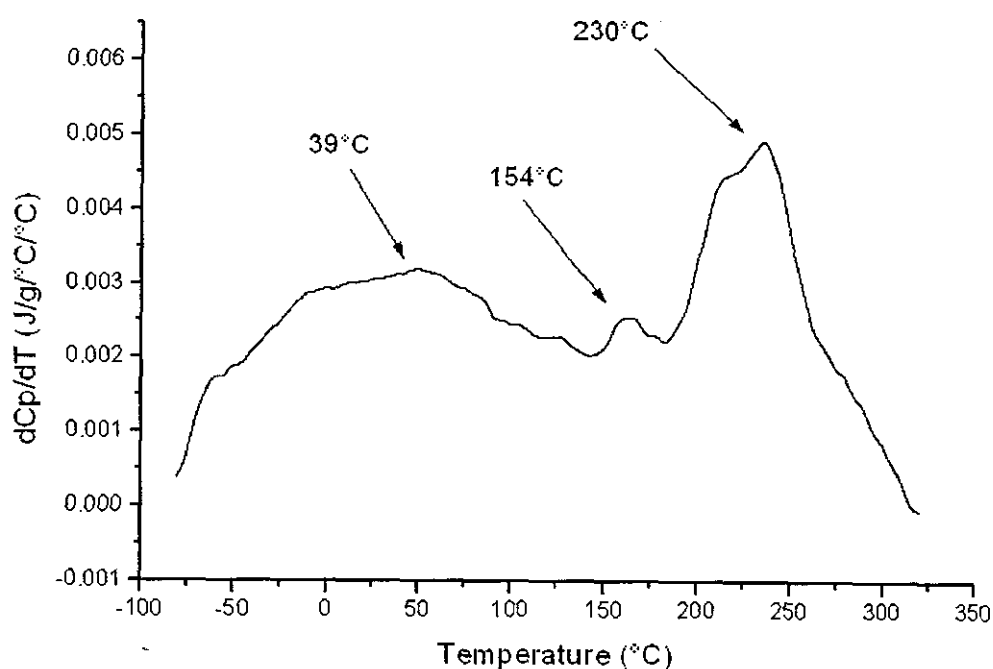


Figure 4.57: MTDSC thermogram showing the derivative specific heat capacity signal of a cured and non-hybridised polyimide film containing 15 wt% perfluoroether modifier

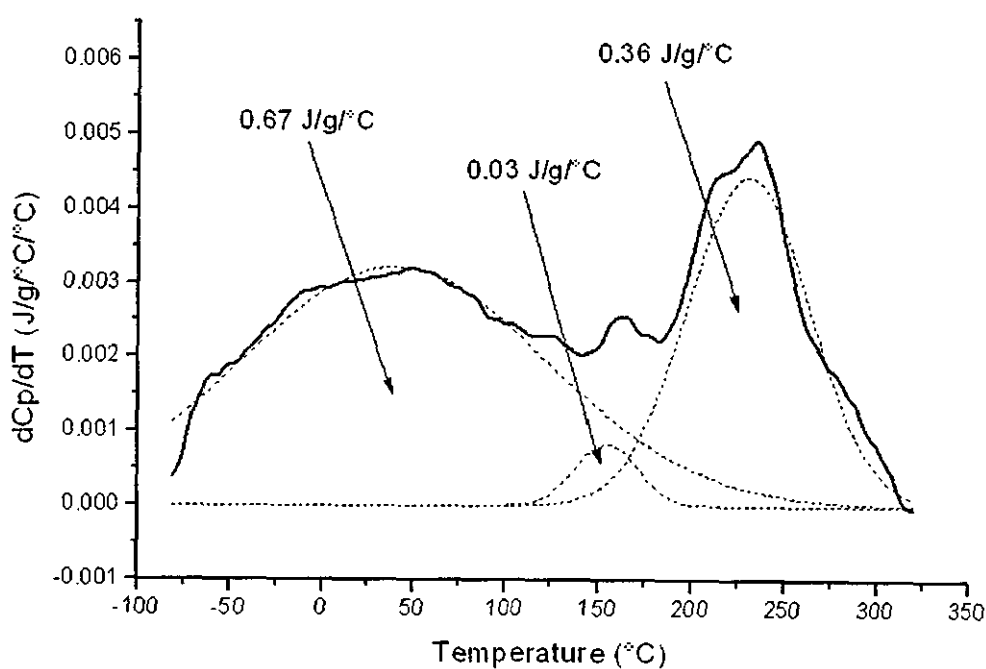


Figure 4.58: MTDSC thermogram of the above, showing the results of Gaussian curve fitting.

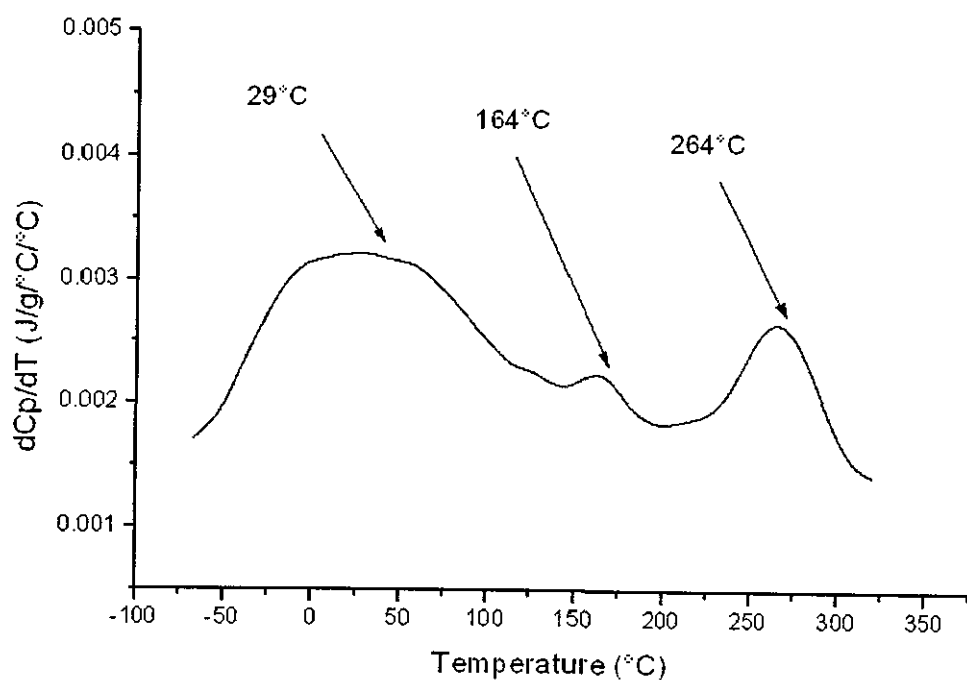


Figure 4.59: MTDSC thermogram showing the derivative specific heat capacity signal of a cured and hybridised polyimide film containing no perfluoroether modifier.

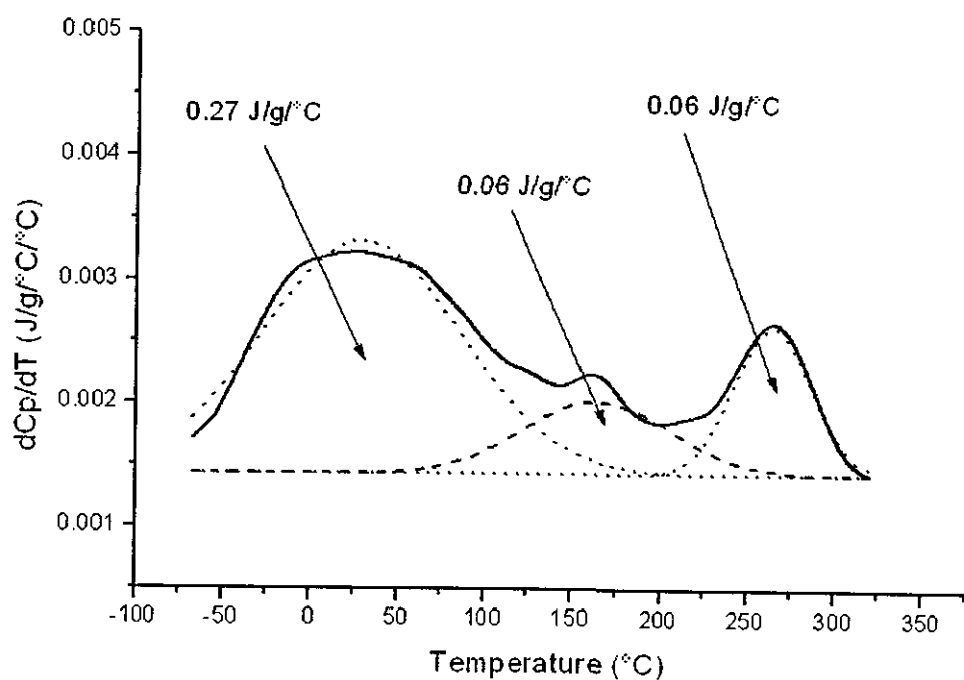


Figure 4.60: MTDSC thermogram of the above, showing the results of Gaussian curve fitting.

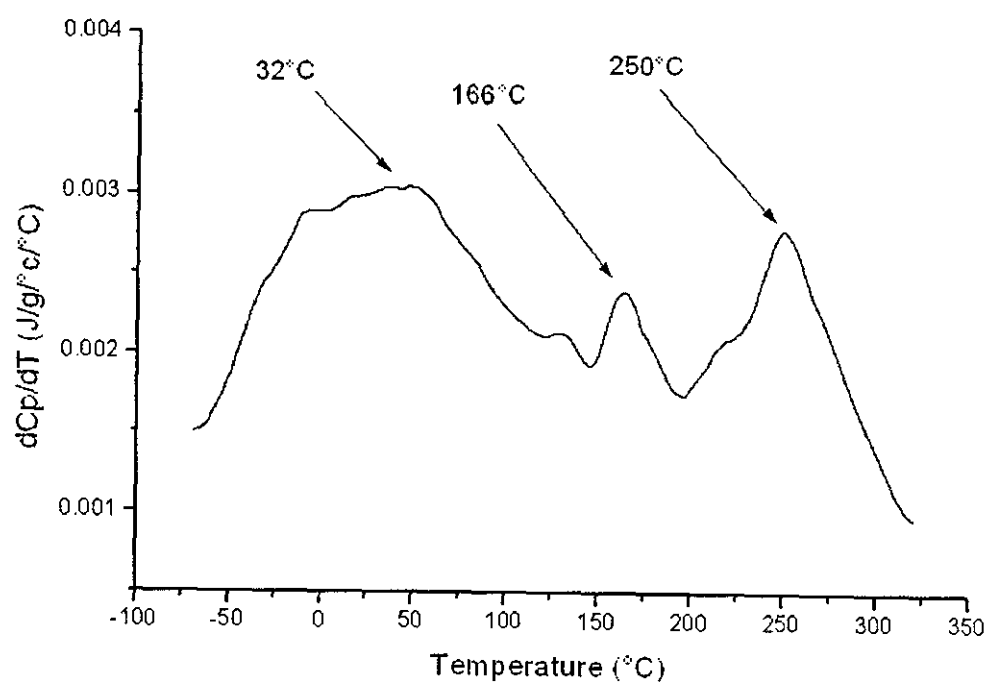


Figure 4.61: MTDSC thermogram showing the derivative specific heat capacity signal of a cured and hybridised polyimide film containing 2.5 wt% perfluoroether modifier.

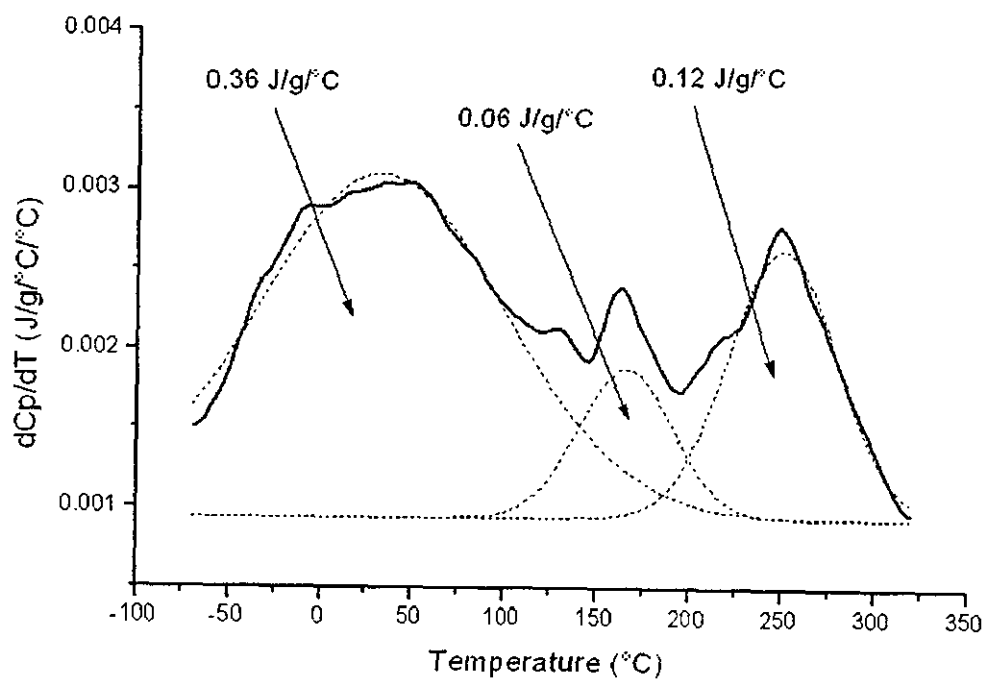


Figure 4.62: MTDSC thermogram of the above, showing the results of Gaussian curve fitting.

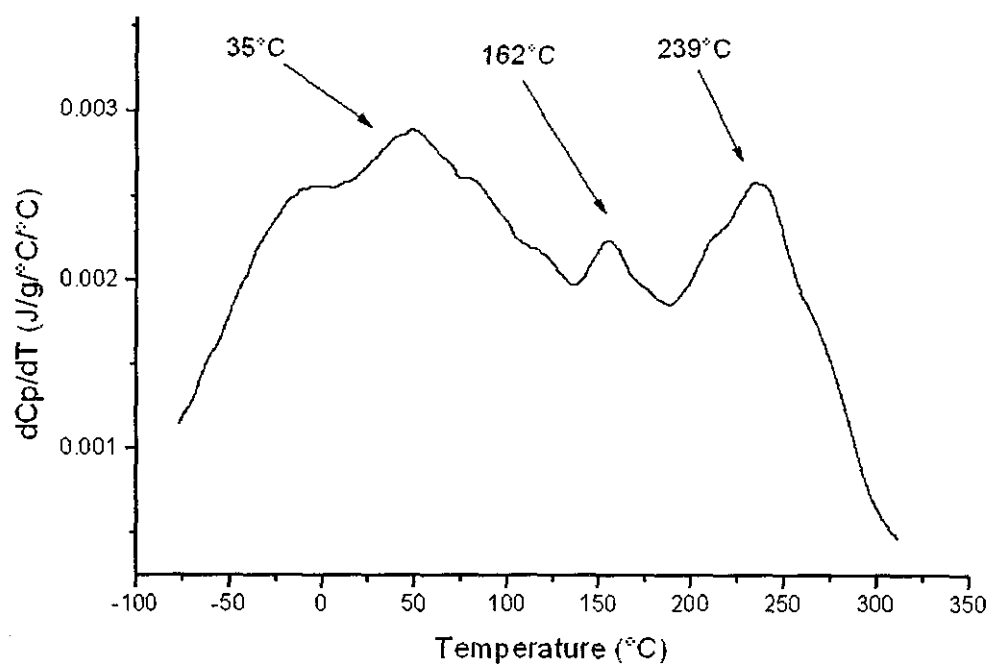


Figure 4.63: MTDSC thermogram showing the derivative specific heat capacity signal of a cured and hybridised polyimide film containing 5 wt % perfluoroether modifier.

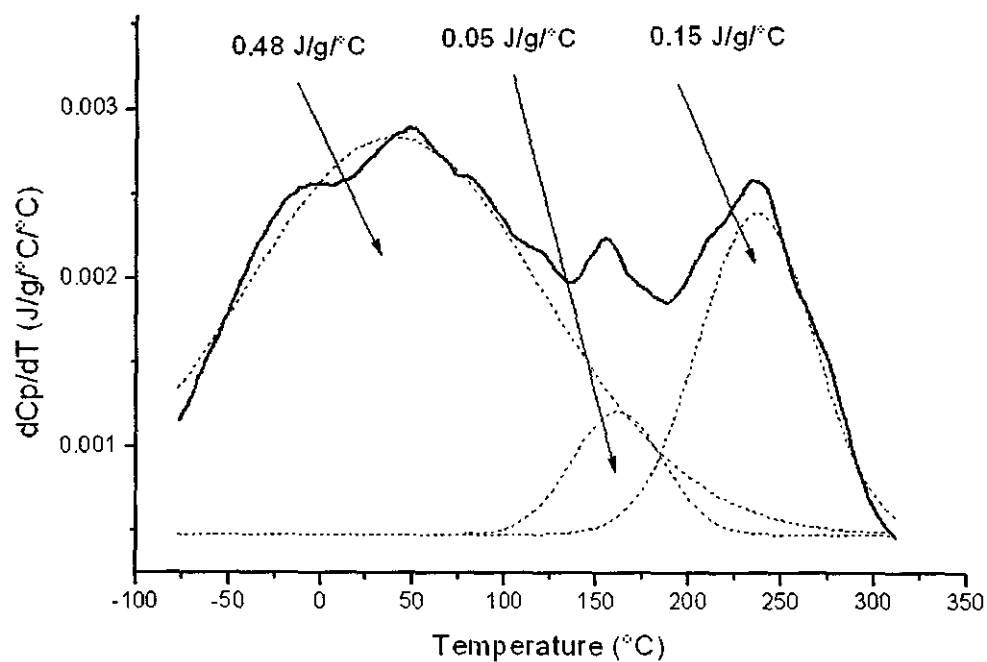


Figure 4.64: MTDSC thermogram of the above, showing the results of Gaussian curve fitting.

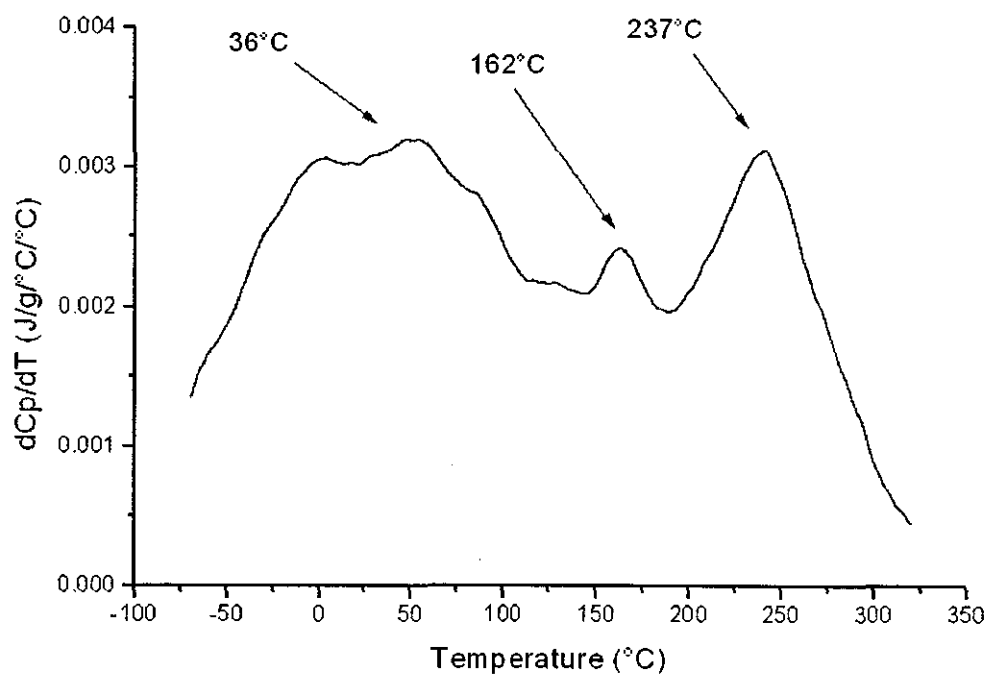


Figure 4.65: MTDSC thermogram showing the derivative specific heat capacity signal of a cured and hybridised polyimide film containing 10 wt% perfluoroether modifier.

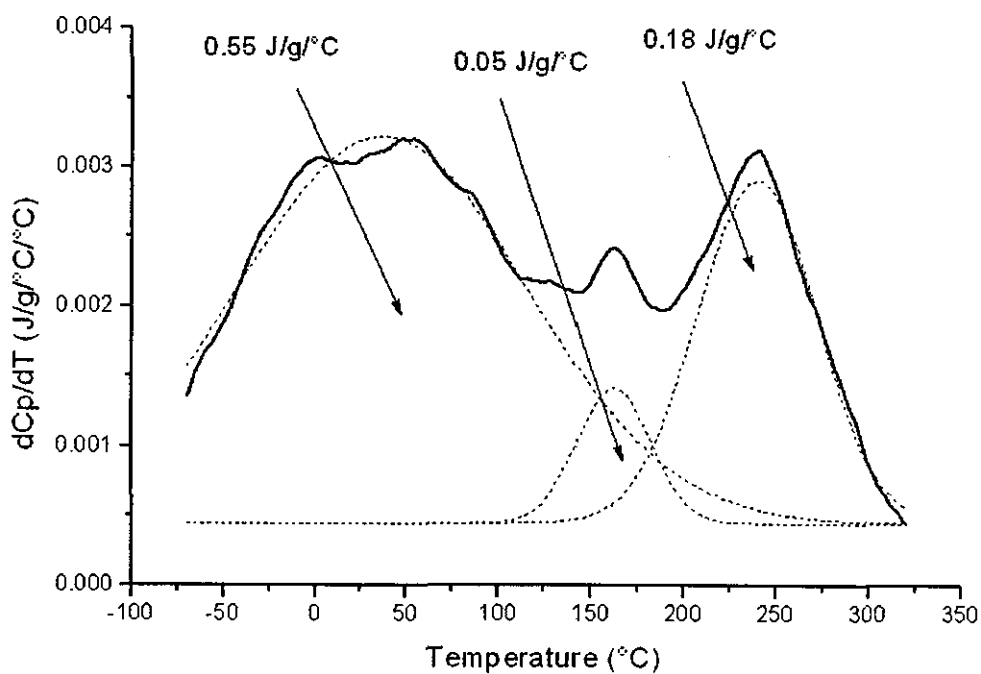


Figure 4.66: MTDSC thermogram of the above, showing the results of Gaussian curve fitting.

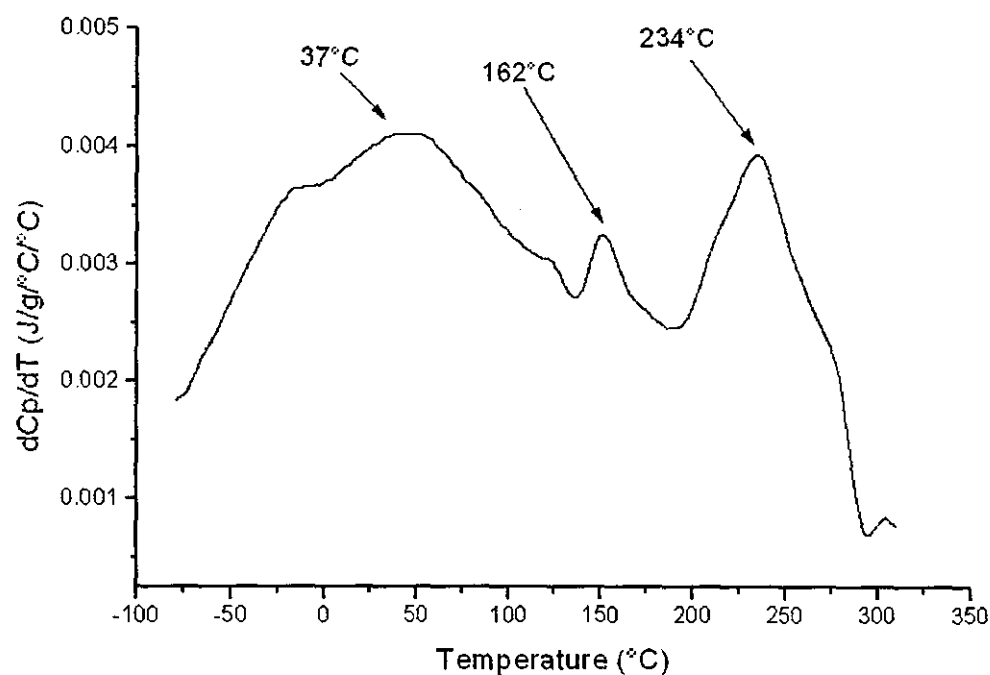


Figure 4.67: MTDSC thermogram showing the derivative specific heat capacity signal of a cured and hybridised polyimide film containing 15 wt% perfluoroether modifier.

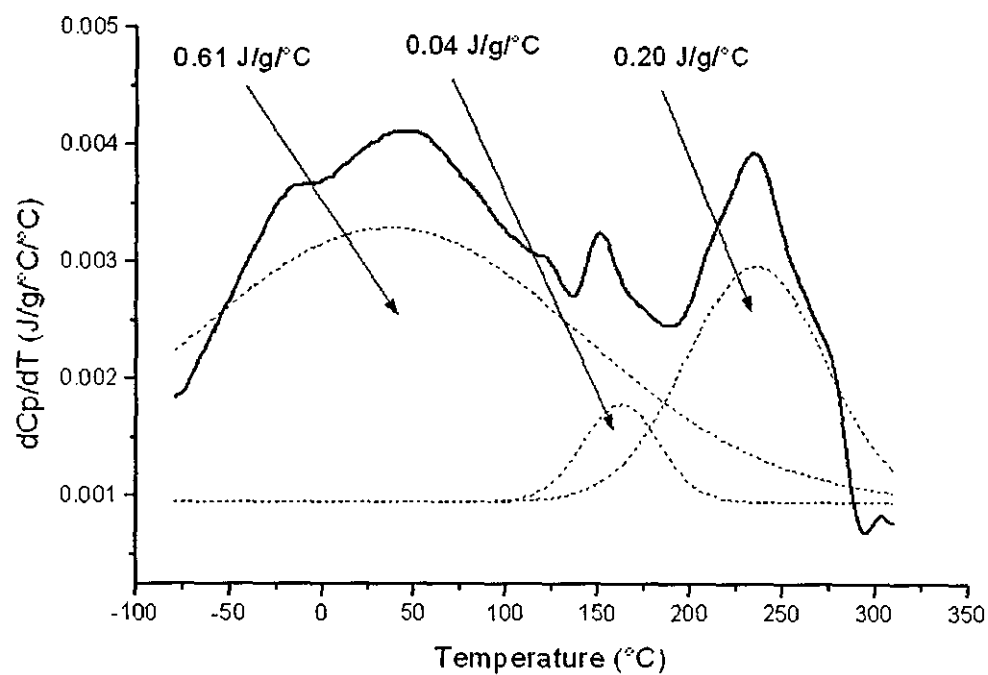


Figure 4.68: MTDSC thermogram of the above, showing the results of Gaussian curve fitting.

In all the thermograms, three major peaks can be found. Using the Gaussian Curve fitting technique, the temperature of all the peaks and their respective changes in specific heat capacity can be estimated.

4.6 Thermal Analysis of Carbon Fibre Composites Using Thermogravimetry

Thermogravimetric analysis was found to be effective in quantifying the composition of the composites evaluated, in particular the resin content and the volatiles.

4.6.1 Weight-Loss Characteristics of Resins

Figures 4.69 and 4.70 show the isothermal weight-loss characteristics of an unmodified polyimide film and its hybrid at 600°C. A simple weight-loss step can be observed in both of the samples. The residue shown in figure 4.70 reflect the 30 wt % of silica present the hybrid.

4.6.2 Weight-Loss Characteristics of Carbon Fibre Composites of Perfluoroether Modified Polyimide and Polyimide-Silica Hybrids Prepared Using Different Methods

Method I

From the point of view of comparison with subsequent methods of producing composite (to be discussed later), this method of composite preparation can be characterised by the continuous impregnation approach, i.e. the thickness of the composites was built up in one step, compiling all the layers continuously up to the final thickness.

Figure 4.71 shows weight-loss result of an unmodified polyimide composite. Two weight-loss steps can be seen. Assuming the first step was due to the volatilisation of solvent, the resin content of the composite is only slightly more than 5 wt%. In addition, the solvent content in the composite was 23 wt% relative to the amount of resin.

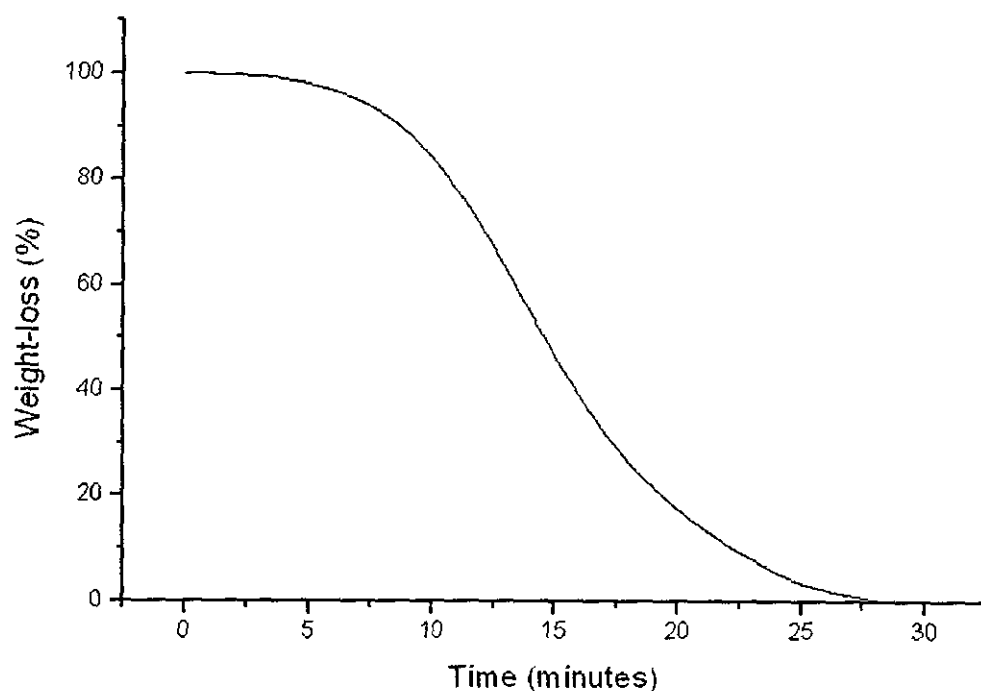


Figure 4.69: Isothermal thermogravimetric weight-loss characteristic of fully imidised unmodified polyimide film. (Temperature = 600°C).

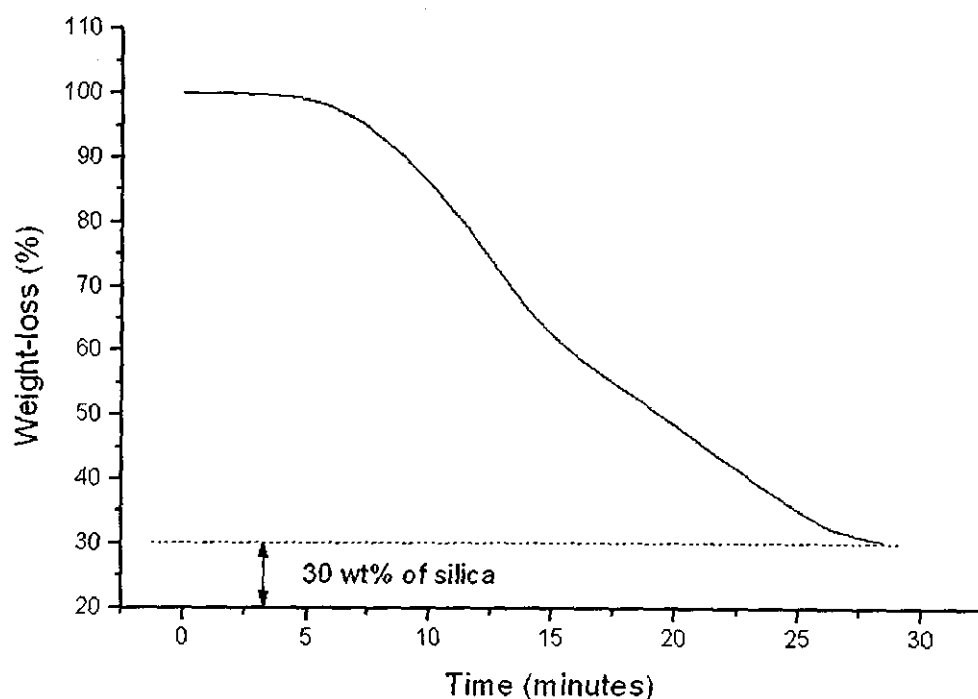


Figure 4.70: Isothermal thermogravimetric weight-loss characteristic of fully imidised unmodified polyimide-silica hybrid film. (Temperature = 600°C).

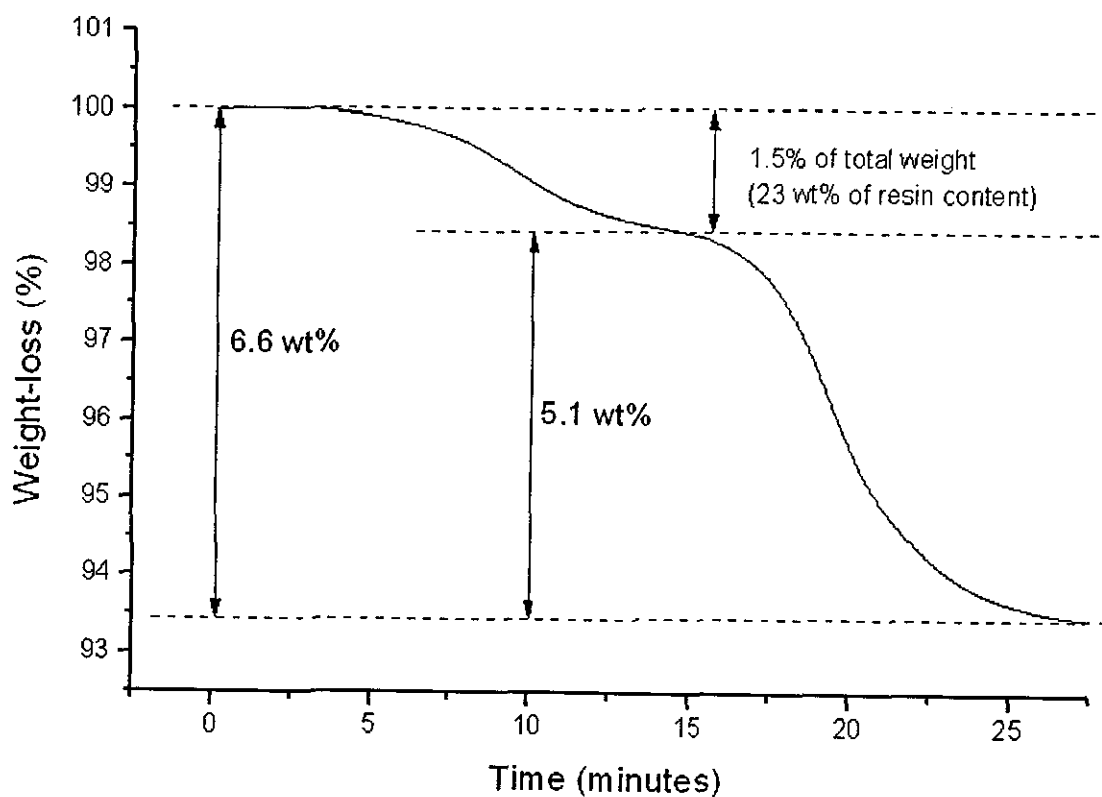


Figure 4.71: Isothermal thermogravimetric weight loss characteristic of the unmodified polyimide-carbon fibre composite, produced using method I. (Temperature = 600°C).

Figures 4.72 to 4.74 show weight-loss results of composites impregnated with perfluoroether modified polyimide, polyimide-silica hybrid and perfluoroether modified polyimide-silica hybrid. A similar two weight-loss steps was observed again in all the samples. The resin content in all the samples was also very small at approximately 5 wt% level. However, the solvent contents were found to be reduced considerably to levels just slightly above 10 wt% with respect to the amount of the resin. The magnitude of the reduction in solvent content can be appreciated easily in figure 4.75, showing the consolidated results of all the samples of method I.

Method II

The preparation of the composites by method II can be characterised by the “multiple steps” approach for the resin impregnation in the fibres. A 15 minutes interval was allowed between each layer for the drying of solvents during the building up of the composite pre-preg.

Figure 4.76 shows the weight-loss characteristic of an unmodified polyimide composites. Again, two weight-loss steps can be seen. However, in comparison to all the samples in method I, the resin content has approximately doubled to about 11 wt% in this sample. In addition, a lesser proportion of solvent of around 10 wt%, as compared to the previous unmodified composite was observed. More importantly, this reduction in solvent content was achieved even in the absence of silica and perfluoroether modifier.

The weight-loss characteristic of the composite of polyimide-silica hybrid is shown in figure 4.77. Some surprising results can be noted here. The increase in resin content was smaller than for the non-hybridised system above, being only 8 wt% approximately. Although two major weight-loss steps were observed again, a gradual, but progressive weight-loss trend can be seen before the first weight-loss step. This trend was not observed in the earlier samples, both in method I and II. Perhaps more importantly, the solvent content was very high, even though the hybridised silica was present in the system, in amounts of about 25 wt% with respect to the resin content.

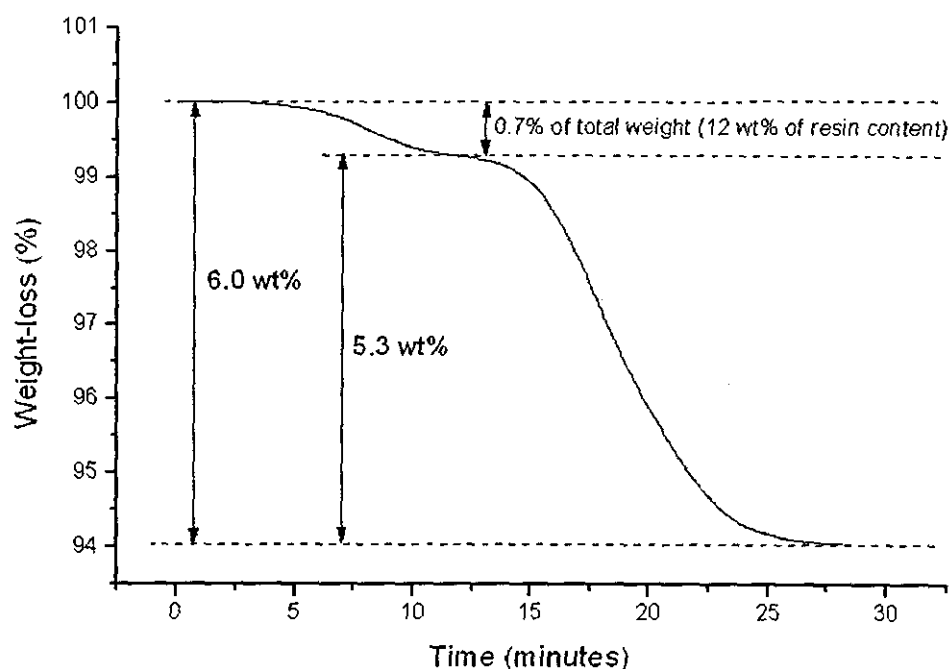


Figure 4.72: Isothermal thermogravimetric weight-loss characteristic of the polyimide-carbon fibre composite containing 10 wt% of perfluoroether modifier. The composite is produced using method I. (Temperature = 600°C).

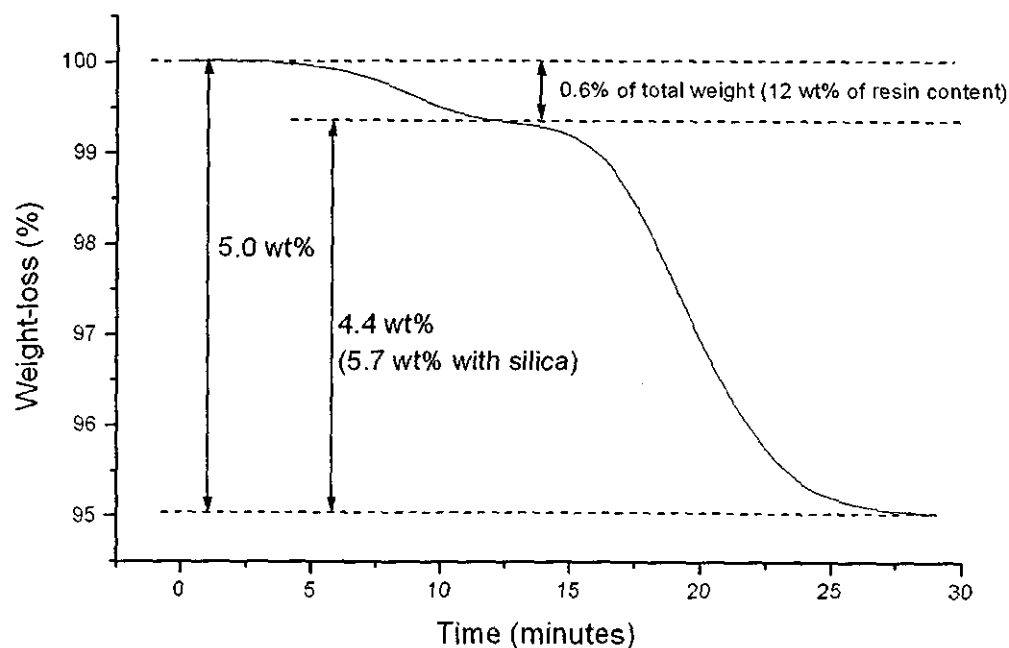


Figure 4.73: Isothermal thermogravimetric weight-loss characteristic of the polyimide-carbon composite hybridised with 30 wt% of silica. The composite is produced using method I. (Temperature = 600°C).

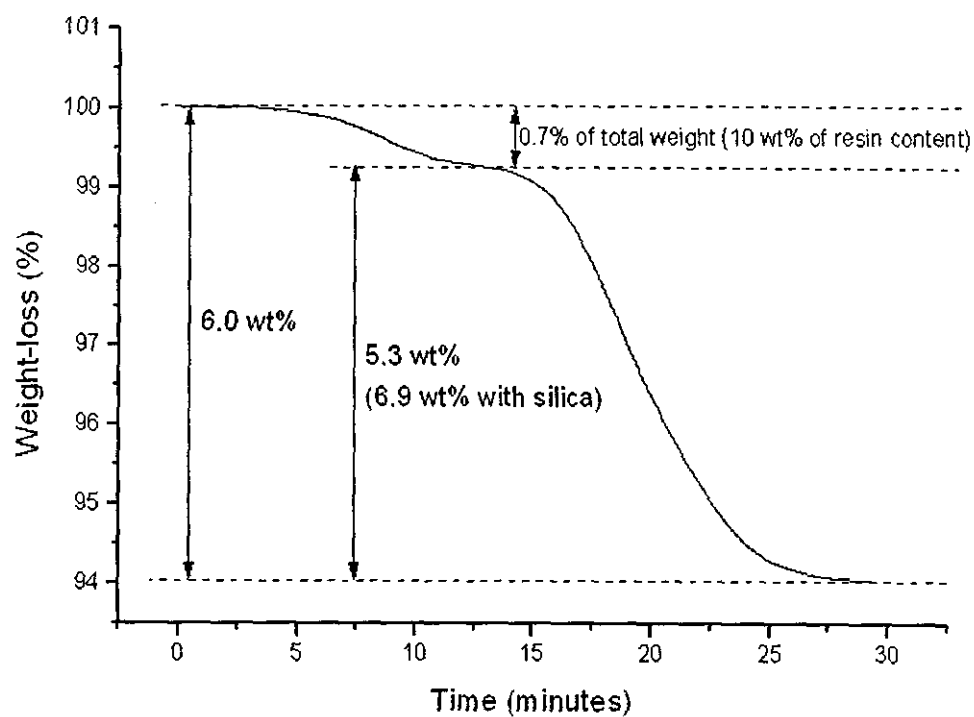


Figure 4.74: Isothermal thermogravimetric weight-loss characteristic of polyimide-carbon composite hybridised with 30 wt% of silica and modified with 10% of perfluoroether. The composite is produced using method I. (Temperature = 600°C).

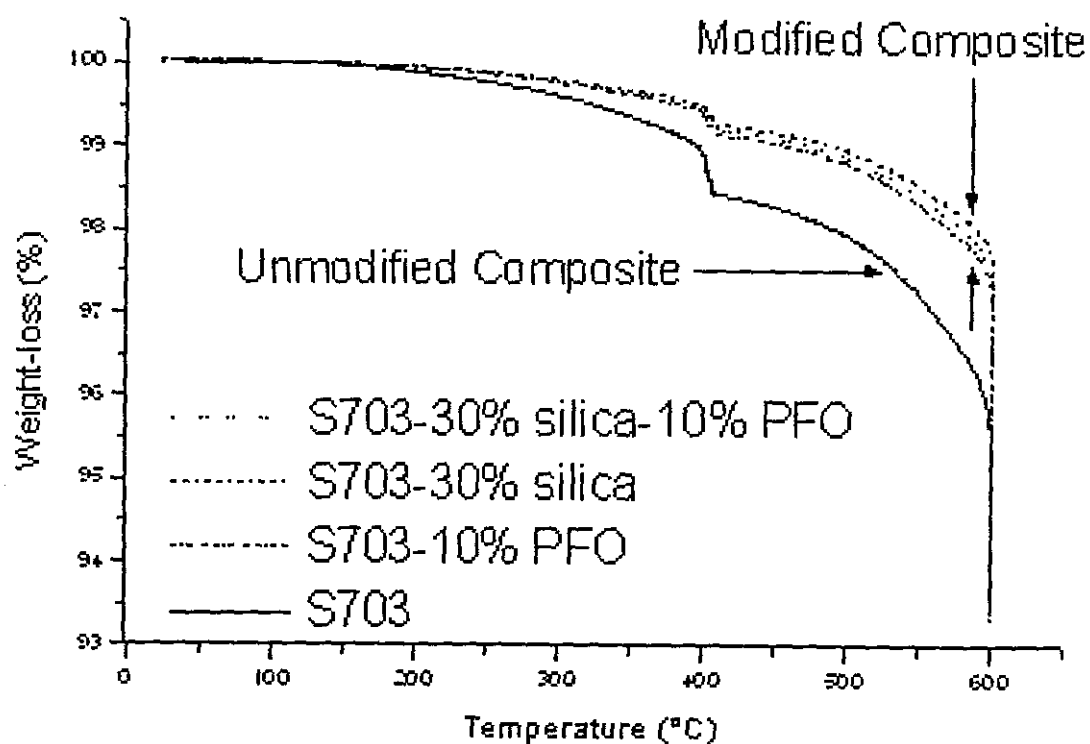


Figure 4.75: Thermogravimetric weight-loss characteristics of all the method I composites analysed. (Temperature = 600°C).

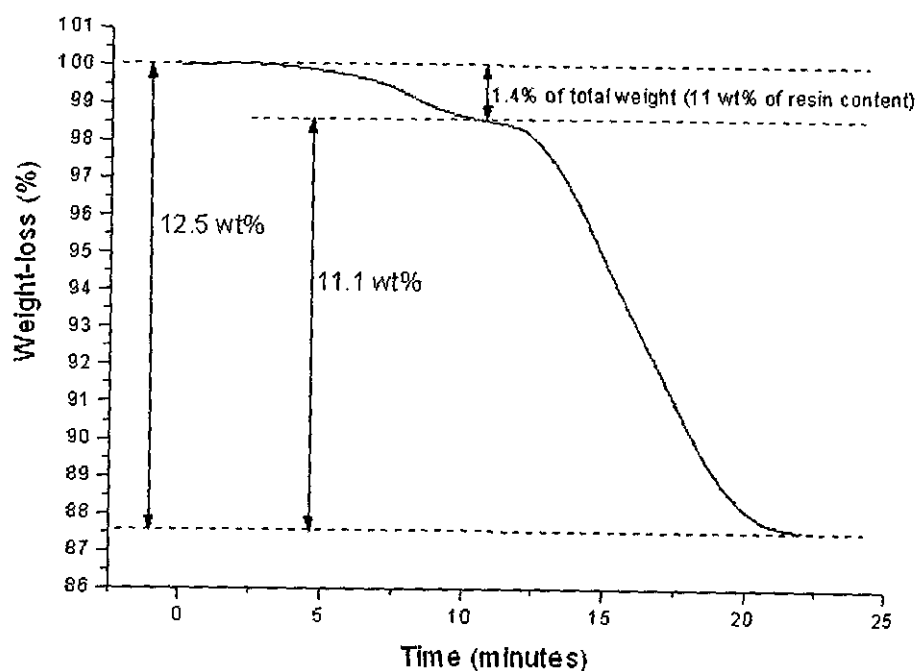


Figure 4.76: Isothermal thermogravimetric weight loss characteristic of the unmodified polyimide-carbon fibre composite, produced using method II. (Temperature = 600°C).

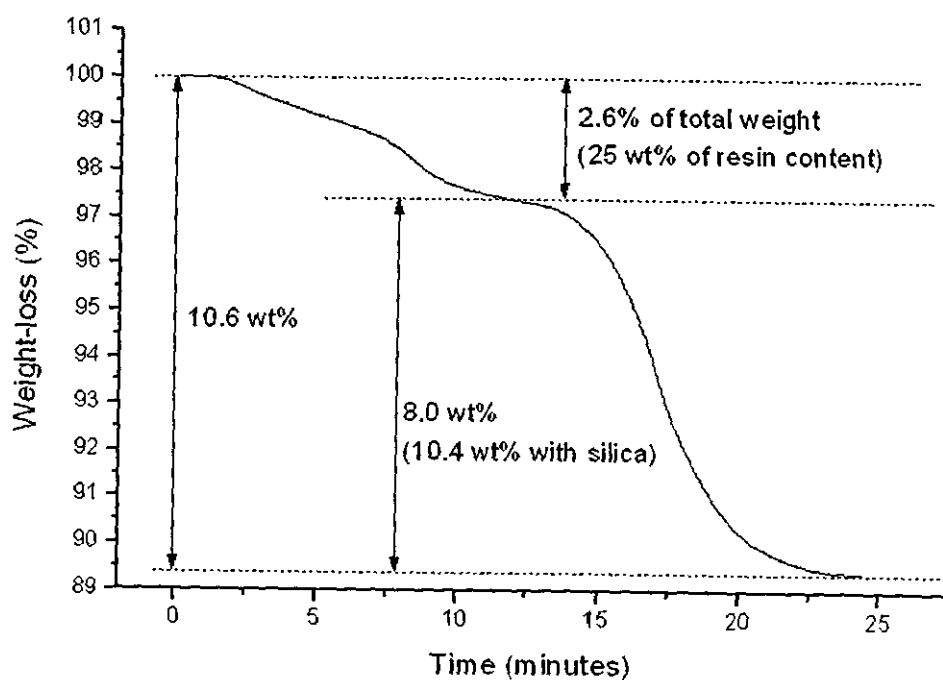


Figure 4.77: Isothermal thermogravimetric weight-loss characteristic of the polyimide-carbon composite hybridised with 30 wt% of silica. The composite is produced using method II. (Temperature = 600°C).

The weight-loss characteristic of the composite of polyimide modified with 10 wt% of perfluoroether modifier is shown in figure 4.78. A notable resin content of around 12 wt% with relative low solvent content of about 8 wt% of the resin content can be observed.

The weight-loss result of the composite shown in figure 4.79 is that of the polyimide hybridised with silica and modified by perfluoroether. Expectedly, the weight-loss characteristic reflecting the combined effects of the above three samples was observed. In particular, the general weight-loss trend before the first weight-loss step can also be observed.

4.6.3 Effects of Acid Catalyst

In the following two thermograms, the weight-loss characteristics of two special composites are detailed. They were obtained for composites based on polyimide-silica hybrids. However, the silica was hybridised using p-toluene sulphonic acid (TSA) instead of hydrochloric acid, which was used in all the hybrids discussed earlier.

Figure 4.80 shows the weight-loss characteristic of the composite of polyimide-silica hybrid. In comparison to result of the equivalent hybrid (see figure 4.77) prepared using HCl, the resin content of the composites is relatively high at around 12 wt% with only about half the amount of solvent at around 12 wt%. The weight-loss curve also seemed to show 3 weight-loss steps. However, the rather obscure first step was probably similar or equivalent to the gradual weight-loss trend demonstrated by all the hybrid samples.

Figure 4.81 shows the weight-loss characteristic of the composite of polyimide-silica hybrid (TSA type) modified with 10 wt% of Oligomer TX-CA-E8. Again, the presence of the perfluoroether modifier seems to increase the resin content and reduces the solvent content slightly.

The consolidated results of all the samples prepared using method II were shown in figure 4.82. The enlarged illustration of the first weight-loss step is shown in

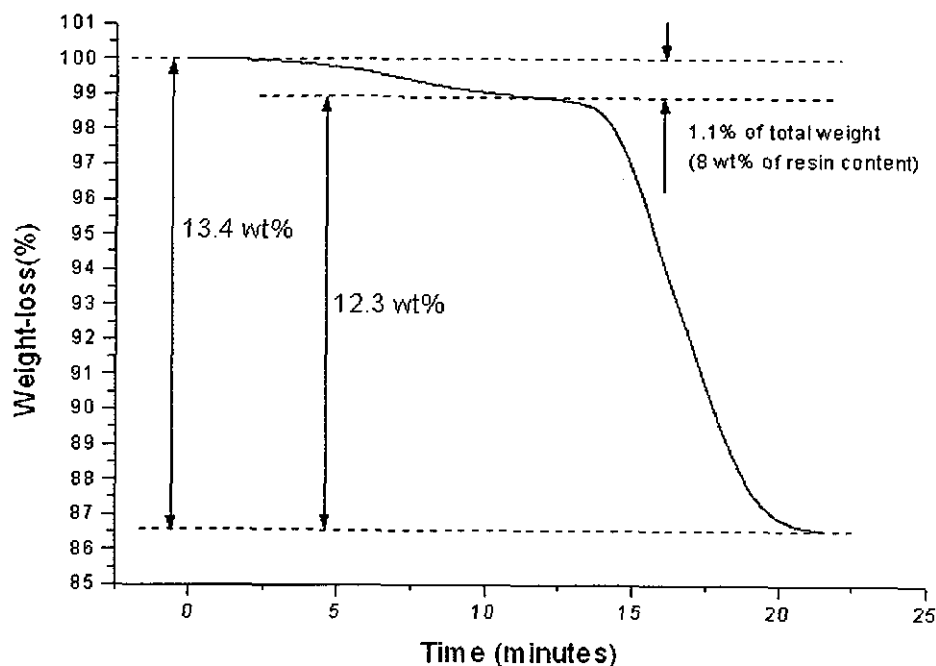


Figure 4.78: Isothermal thermogravimetric weight-loss characteristic of the polyimide-carbon fibre composite containing 10 wt% of perfluoroether modifier. The composite is produced using method II. (Temperature = 600°C).

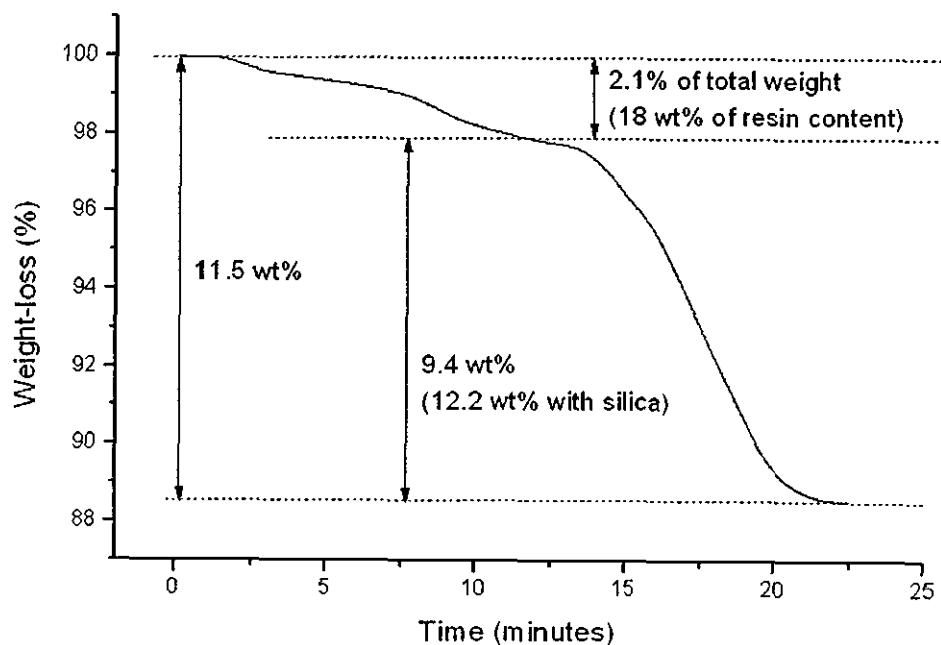


Figure 4.79: Isothermal thermogravimetric weight-loss characteristic of polyimide-carbon composite hybridised with 30 wt% of silica and modified with 10% of perfluoroether. The composite is produced using method II. (Temperature = 600°C).

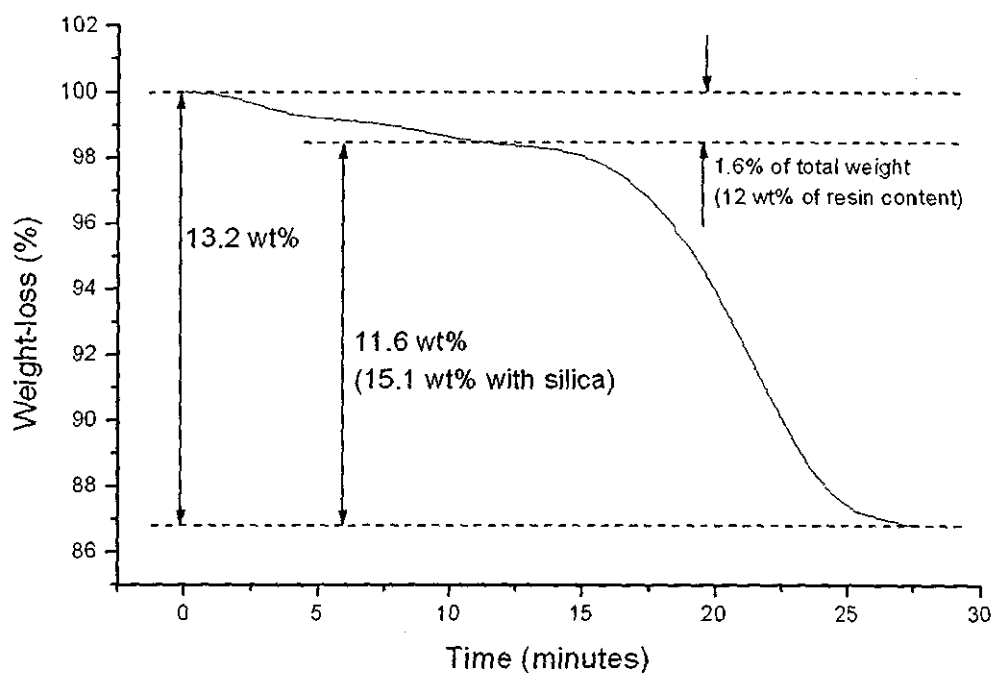


Figure 4.80: Isothermal thermogravimetric weight-loss characteristic of the polyimide-carbon composite hybridised with 30 wt% of silica (TSA type). The composite is produced using method II. (Temperature = 600°C).

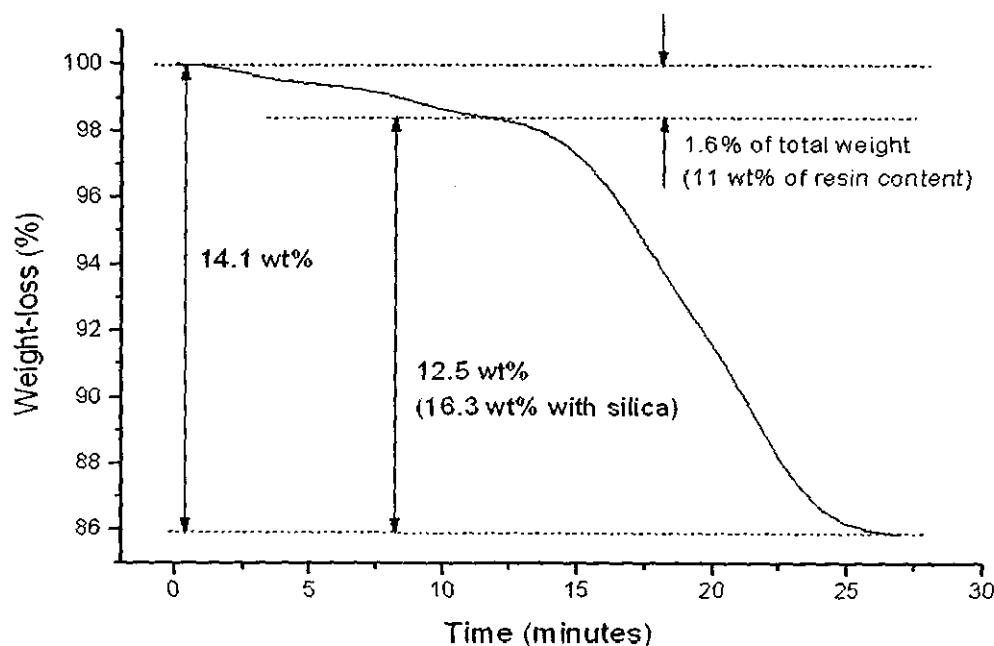


Figure 4.81: Isothermal thermogravimetric weight-loss characteristic of polyimide-carbon composite hybridised with 30 wt% of silica and modified with 10% of perfluoroether (TSA type). The composite is produced using method II. (Temperature = 600°C).

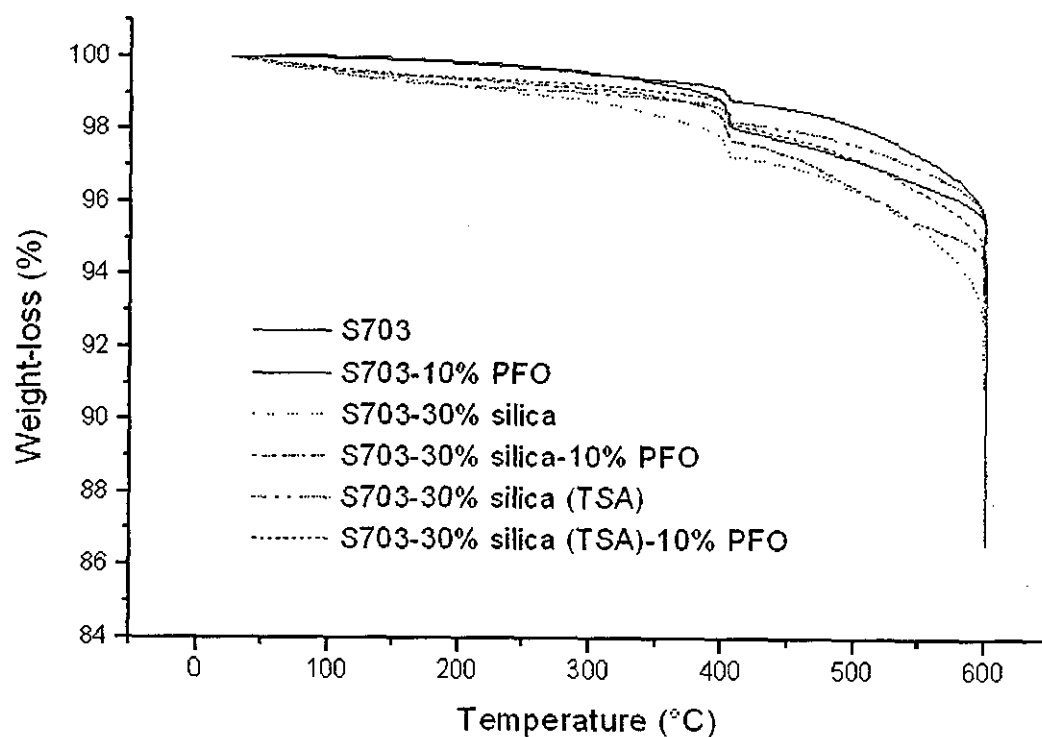


Figure 4.82: Thermogravimetric weight-loss characteristics of all the method II composites analysed. (Temperature = 600°C).

figure 4.83. In the non-hybrid, the ability of the perfluoroether modifier in reducing the solvent content is clear. Hybridisation catalysed by HCl increased the solvent content, whereas in the case of hybridisation using TSA, the solvent content was very similar to the unmodified polyimide. Figure 4.84 shows the characteristic of the samples before the first weight-loss step. The presence of the gradual weight-loss trend in all the hybrid samples was clearly evident.

Method III

The procedure for composites prepared using method III included an elaborated drying regime to remove the solvent during the resin impregnation stage. A 30 minutes interval was allowed at each layer. In addition, compression moulding was carried out on the following day and hence allowed substantial amount of time for further drying after impregnation.

Figure 4.85 shows the weight-loss characteristic of the composite pre-preg using of the unmodified polyimide. The resin content was high with rather low solvent content. Both characteristics were further enhanced with perfluoroether modification (see figure 4.86). In the presence of the perfluoroether modifier, more than 15 wt% resin content, with less than 3 wt% solvent, was achieved, i.e. 3 times more resin than samples of method I.

In the case of pre-pregs of composites with polyimide of hybrids (see figures 4.87 and 4.88), the solvent content remained relative high.

The consolidated results were shown in figure 4.89. The drastic difference in the weight-loss between the non-hybridised samples and the hybrids is very clear.

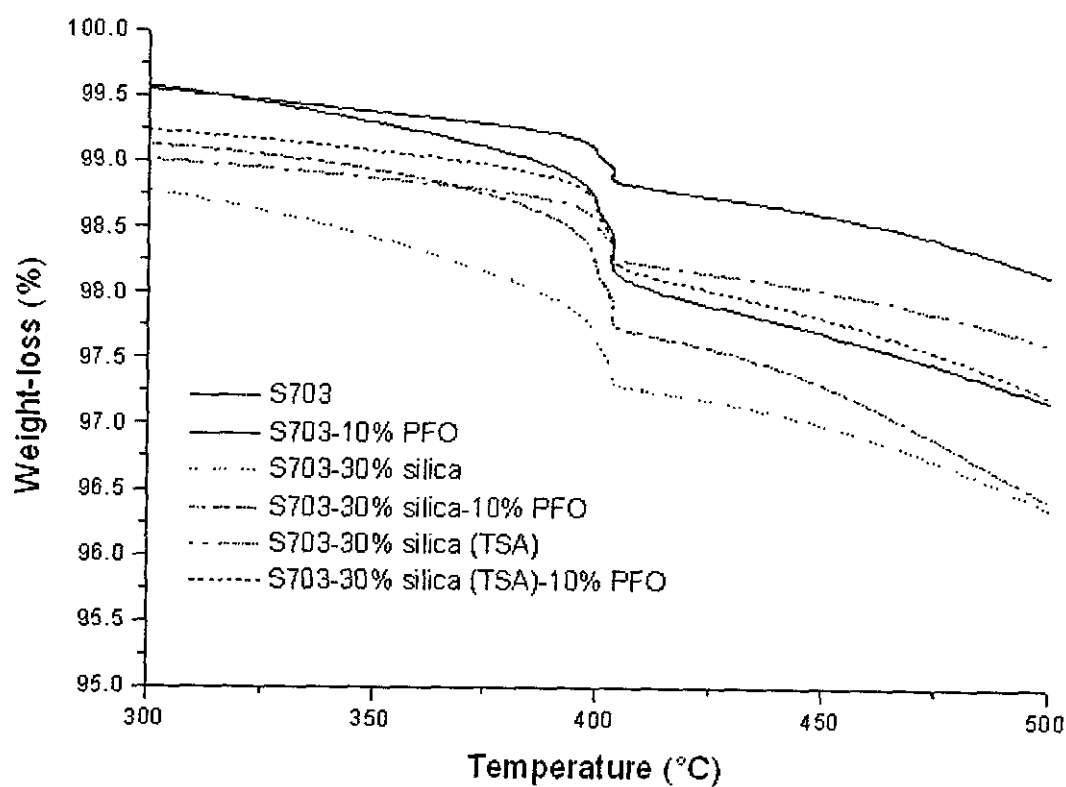


Figure 4.83: Thermogravimetric weight-loss characteristics of all the method II composites analysed showing temperature range from 300 °C to 500°C.

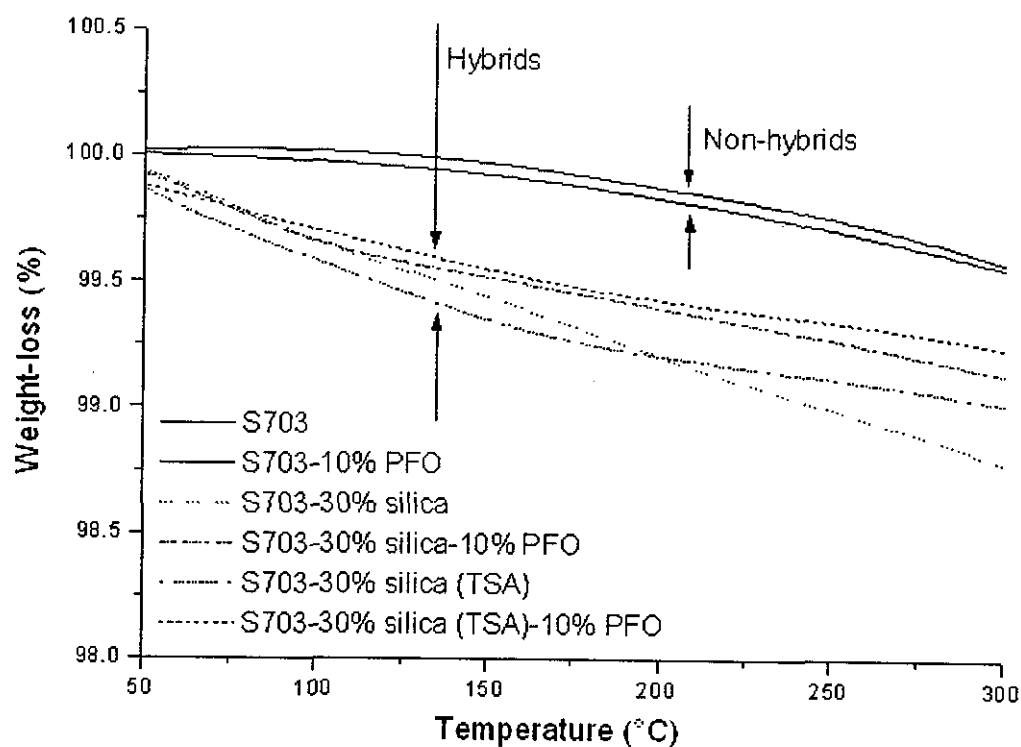


Figure 4.84: Thermogravimetric weight-loss characteristics of all the method II composites analysed showing temperature range from 50 °C to 300°C.

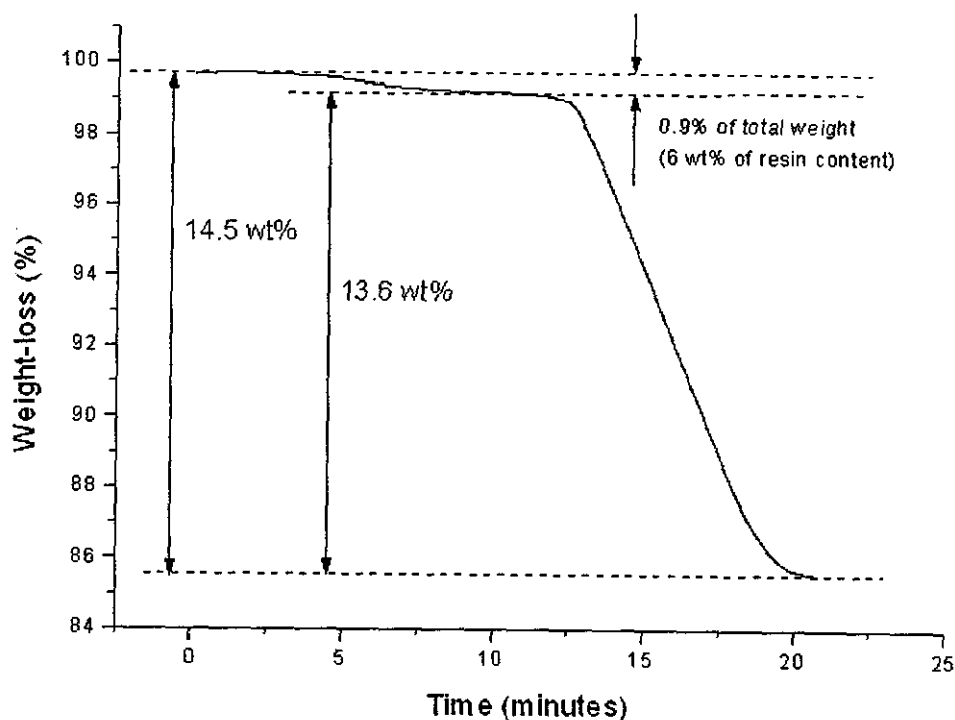


Figure 4.85: Isothermal thermogravimetric weight loss characteristic of the unmodified polyimide-carbon fibre composite, produced using method III. (Temperature = 600°C).

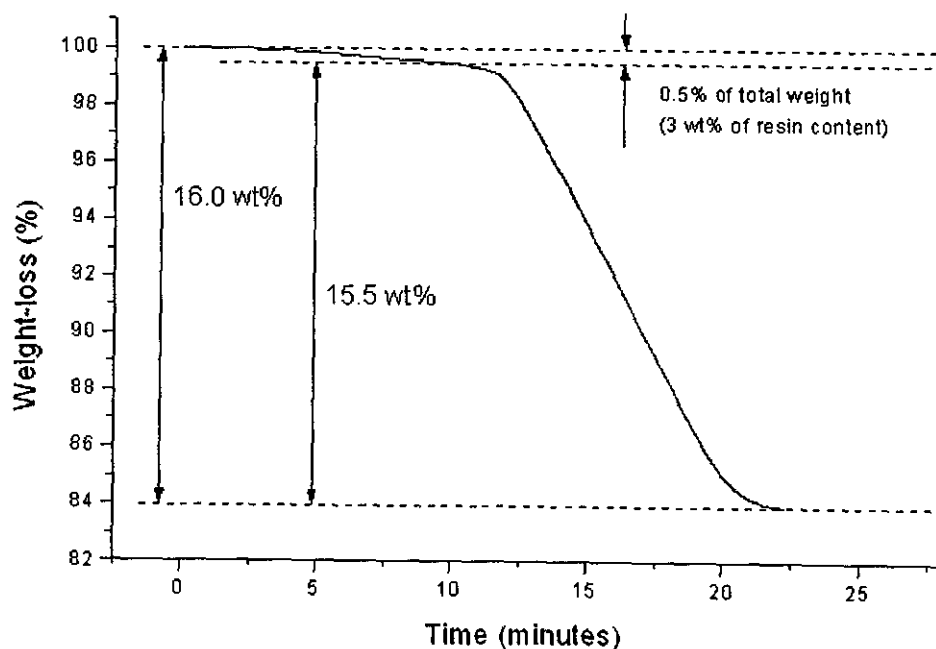


Figure 4.86: Isothermal thermogravimetric weight loss characteristic of the polyimide-carbon fibre composite containing 10 wt% of perfluoroether modifier, produced using method III. (Temperature = 600°C).

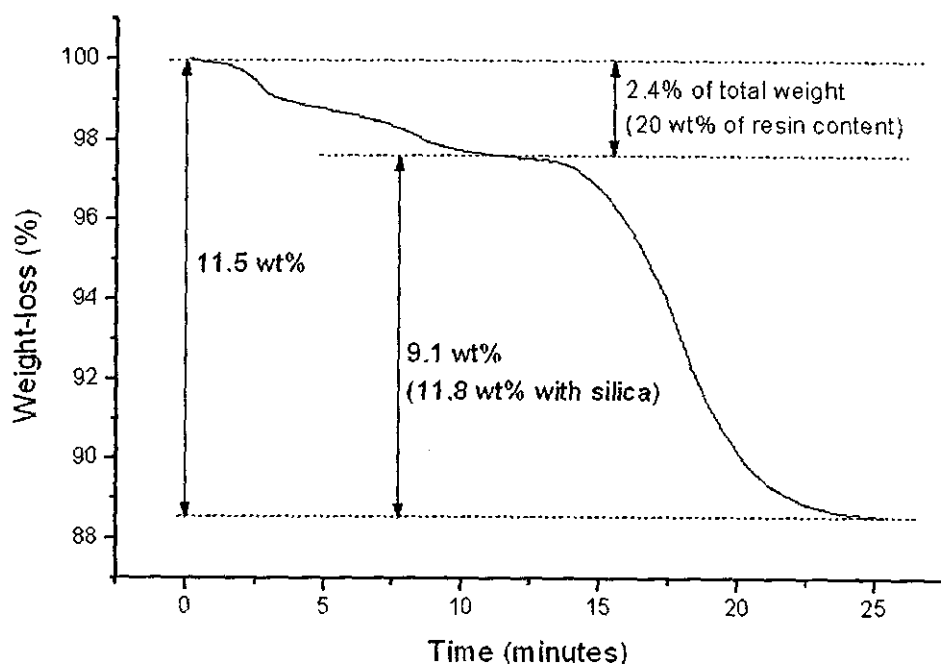


Figure 4.87: Isothermal thermogravimetric weight-loss characteristic of the polyimide-carbon fibre composite hybridised with 30% silica. The composite is produced using method III. (Temperature = 600°C).

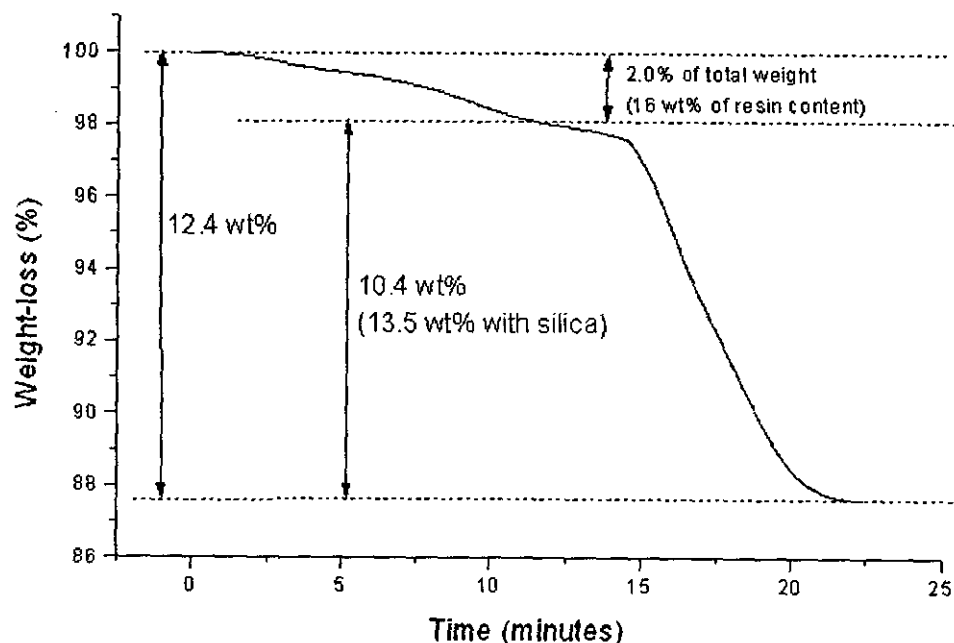


Figure 4.88: Isothermal thermogravimetric weight-loss characteristic of polyimide-carbon composite hybridised with 30 wt% of silica and modified with 10% of perfluoroether. The composite is produced using method III. (Temperature = 600°C).

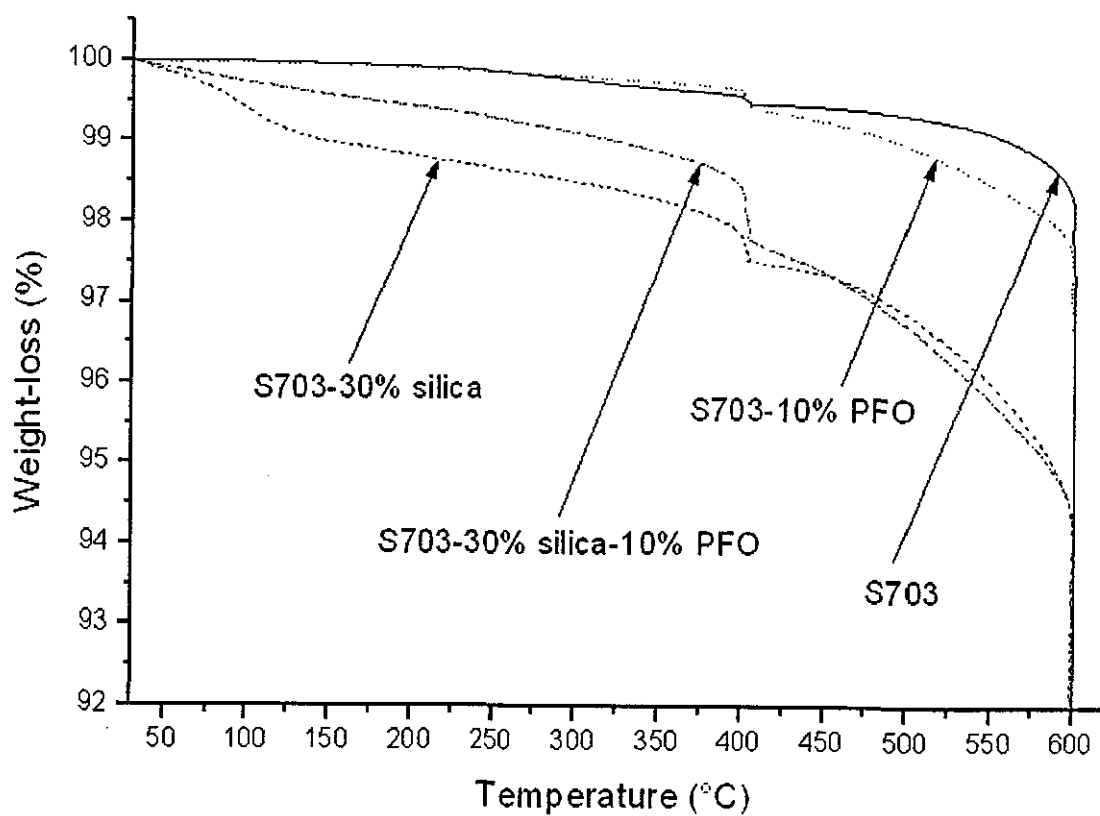


Figure 4.89: Thermogravimetric weight-loss characteristics of all the method II composites analysed. (Temperature = 600°C).

4.7 Mechanical and Thermomechanical Properties of the Composites

Method I

Figures 4.90 and 4.91 show the DMTA transverse storage modulus and corresponding $\tan \delta$ results for the non-hybridised polyimide composite samples modified with various concentrations of perfluoroether modifier. In comparison with the control (i.e. composite of unmodified polyimide), the storage moduli of the rest of the samples were relatively low, particularly the formulations with 2.5 wt% and 5 wt% of perfluoroether content, which were an order of magnitude lower. In addition, their $\tan \delta$ baselines were also noticeable higher than the control, while their $\tan \delta$ peaks showed a substantial reduction in temperature and height.

The storage modulus and $\tan \delta$ results of the 10% formulation are more difficult to explain. The reduction in modulus is substantially less drastic than the other modifications, i.e. 2.5% and 5%, while the $\tan \delta$ peak height was even higher than the control.

Figures 4.92, 4.93 and 4.94 show the flexural strength, flexural modulus and interlaminar shear strength results of the polyimide composites at the various concentrations of perfluoroether modification, respectively. A substantial improvement in these properties can clearly be seen with an increasing level of perfluoroether content. A stepwise increase in trend was observed in the properties between 2.5% and 5% modification.

Figures 4.95 and 4.96 show the DMTA storage modulus and $\tan \delta$ results of the hybrid samples modified with various concentrations of perfluoroether modification, respectively. Although the reduction in storage modulus was rather substantial with increasing concentration of perfluoroether modification, it was significantly less drastic as compared with the non-hybridised formulation as shown in figure 4.90. The considerable improvement in damping capacity of the samples with increasing level of perfluoroether modification can clearly be seen from the upward shift in the

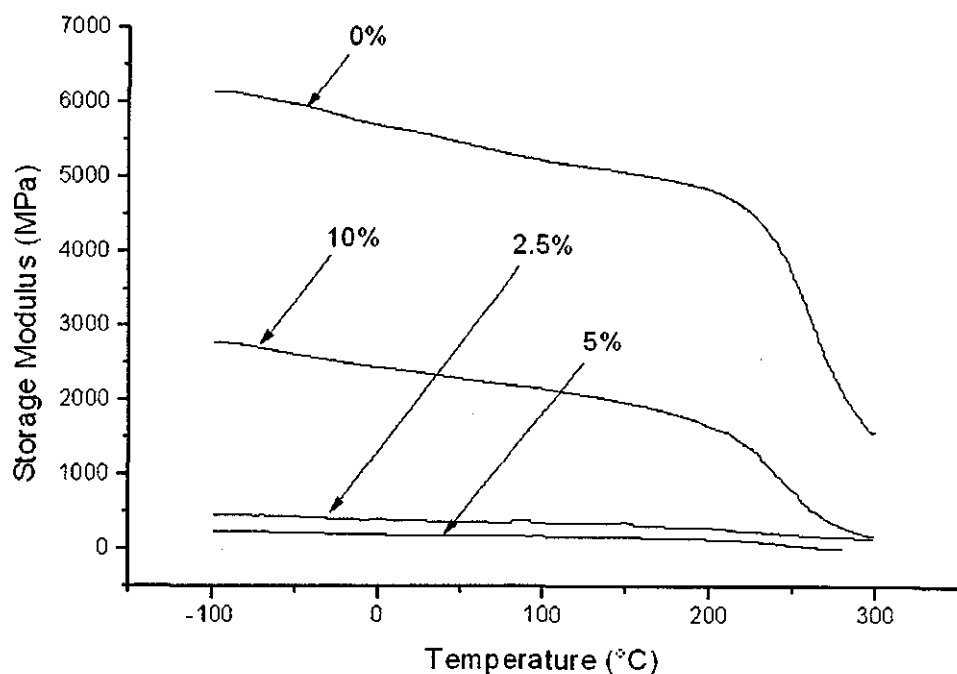


Figure 4.90: DMTA thermograms showing the transverse storage moduli of method I polyimide-carbon fibre composites at various concentrations of perfluoroether modification.

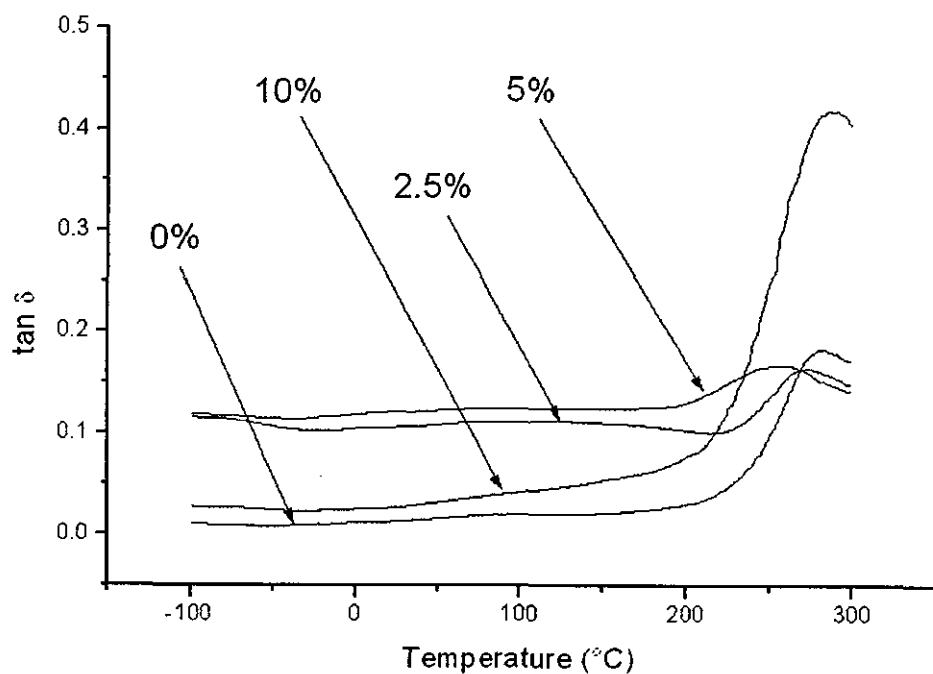


Figure 4.91: DMTA thermograms showing the $\tan \delta$ of method I polyimide-carbon fibre composites at various concentrations of perfluoroether modification.

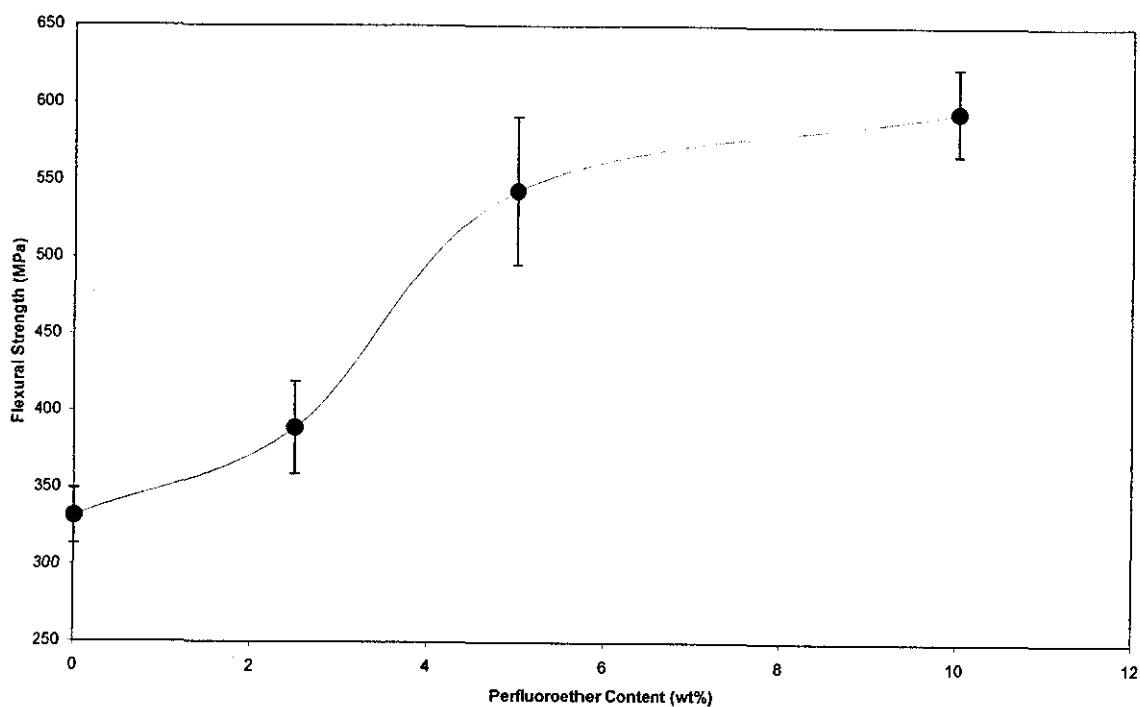


Figure 4.92: Flexural strength of method I polyimide-carbon fibre composites at various concentrations of perfluoroether modification.

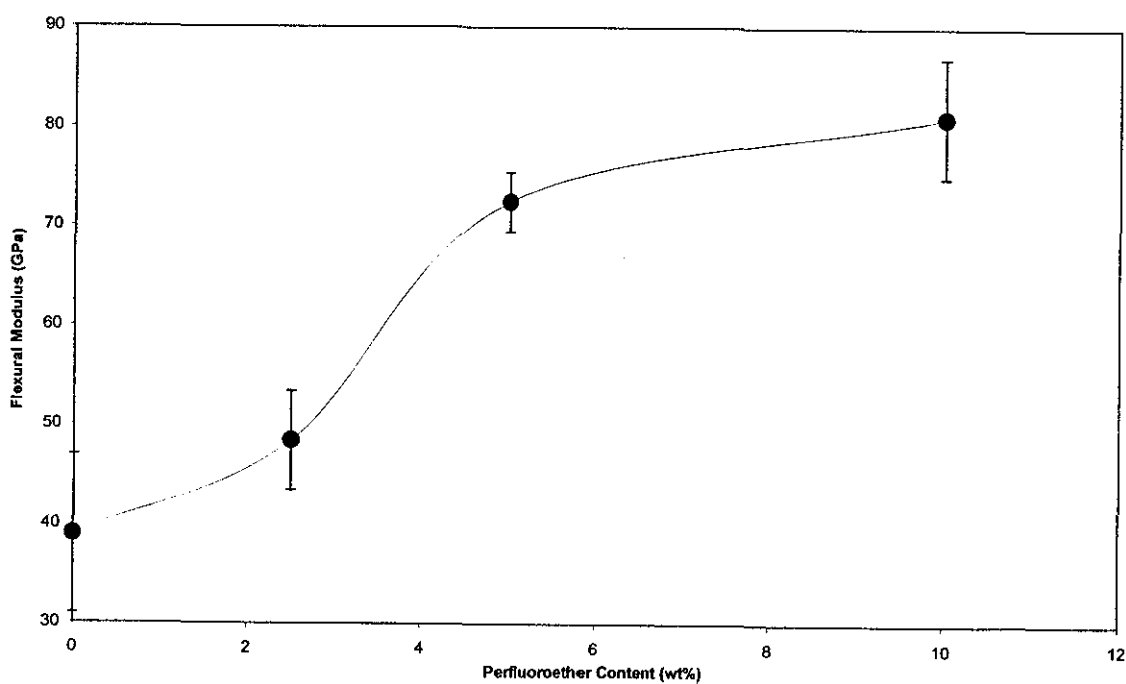


Figure 4.93: Flexural modulus of method I polyimide-carbon fibre composites at various concentrations of perfluoroether modification.

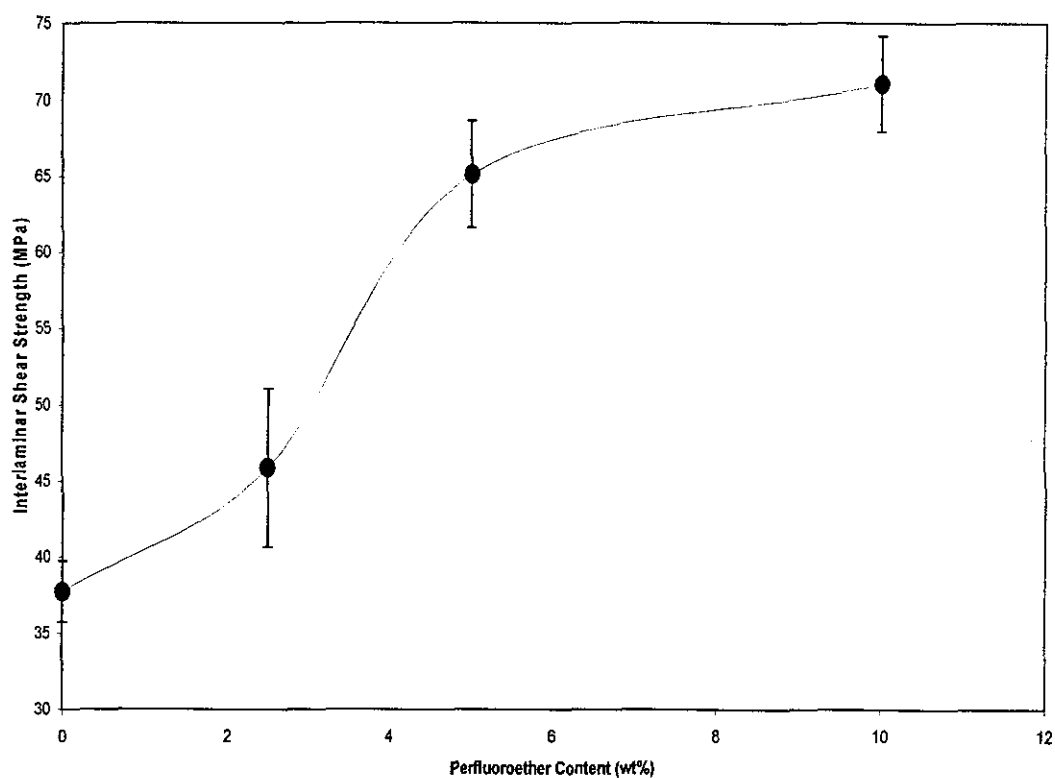


Figure 4.94: Interlaminar shear strength of method I polyimide-carbon fibre composites at various concentrations of perfluoroether modification.

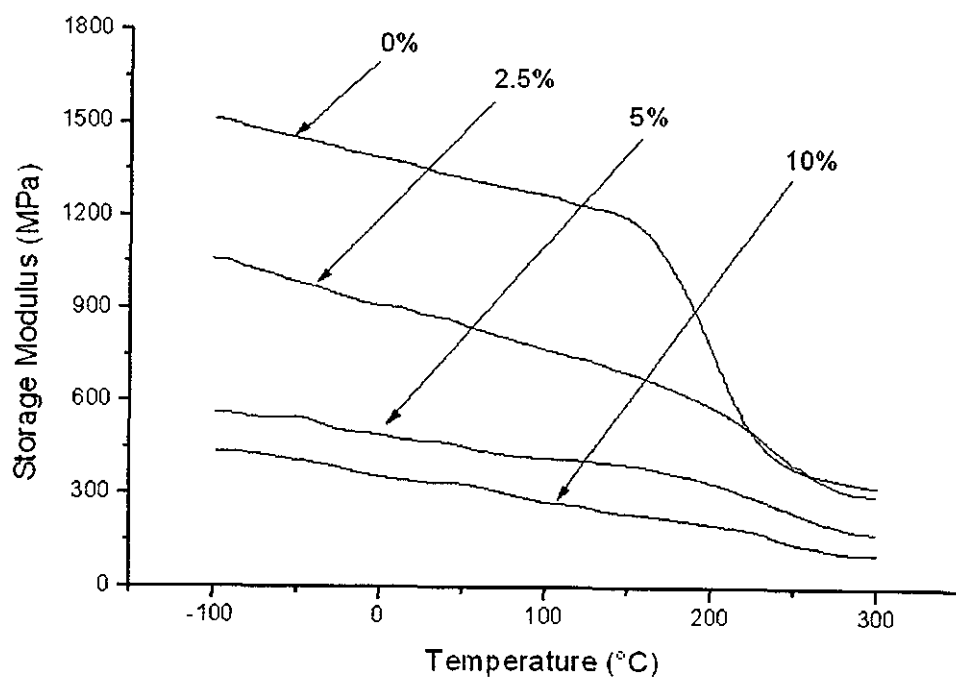


Figure 4.95: DMTA thermograms showing the transverse storage moduli of method I hybrid carbon fibre composites at various concentrations of perfluoroether modification.

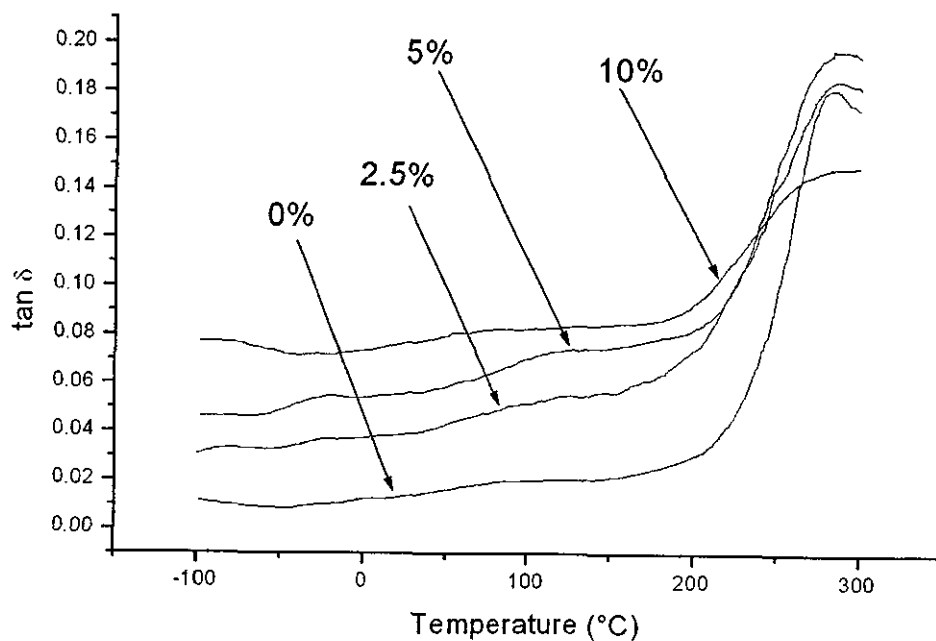


Figure 4.96: DMTA thermograms showing the $\tan \delta$ of method I hybrid carbon fibre composites at various concentrations of perfluoroether modification.

$\tan \delta$ baselines. More significant is that this enhanced damping was achieved without any reduction in the glass transition temperature.

Figures 4.97, 4.98 and 4.99 show the flexural strength, flexural modulus and interlaminar shear strength of the samples modified with various concentrations of perfluoroether modification, respectively. The declining trends in the properties were rather drastic with increasing modification. A drastic step change was observed in all the properties at around 5% modification.

Method II

Figures 4.100 and 4.101 show the DMTA storage modulus and $\tan \delta$ results of the non-hybridised polyimide composites at the various concentrations of perfluoroether modification. It is worth noting that in addition to the longer drying time than method I, imidisation under compression was conducted more thoroughly through the introduction of an additional heating step at 250°C for 1 hour. The improvement in the damping capacity of the samples can be observed clearly from the progressive increase in both the $\tan \delta$ baseline and peak height with increasing level of perfluoroether modification. A substantial increase in glass transition temperature can also be observed in all the formulations as compared to the control. An expected reduction in storage modulus as a result of plasticisation of perfluoroether modification was observed. It should be noted that this reduction in properties was less significant than all the systems reported in method I.

Figures 4.102, 4.103 and 4.104 show the flexural strength, flexural modulus and interlaminar shear strength of the samples at various concentrations of modifications. All properties showed an immediate reduction with the addition of the perfluoroether modifier.

In method II, two different type of hybrid based composites were prepared, corresponding HCl hydrolysed and TSA hydrolysed samples.

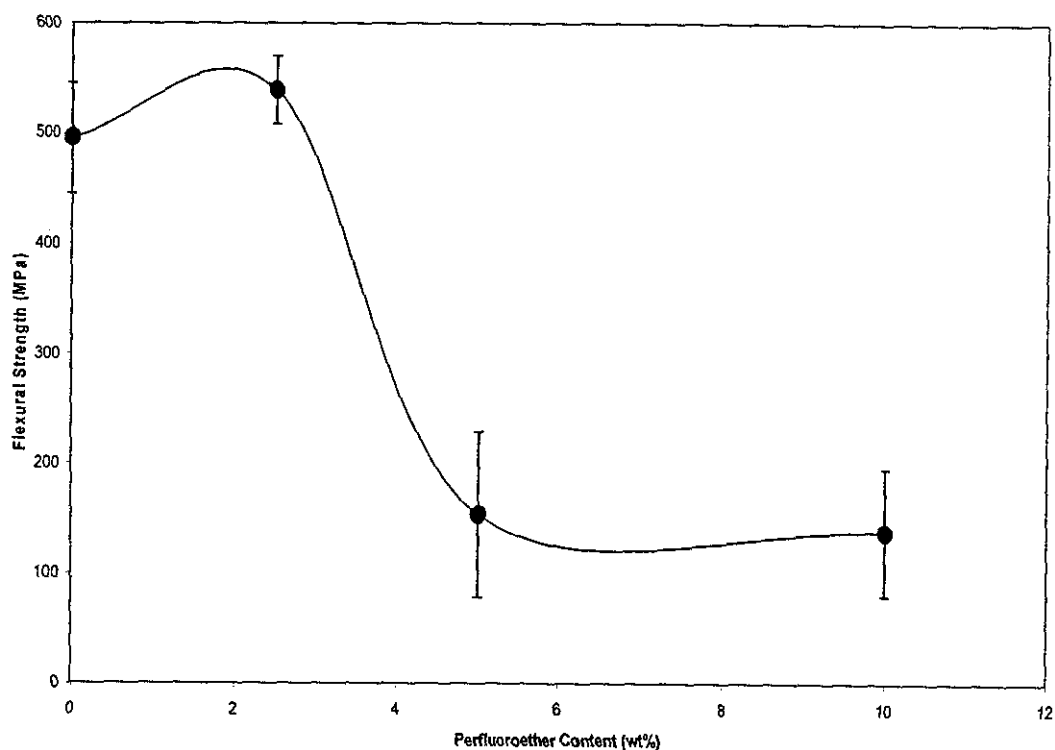


Figure 4.97: Flexural strength of method I hybrid carbon fibre composites at various concentrations of perfluoroether modification.

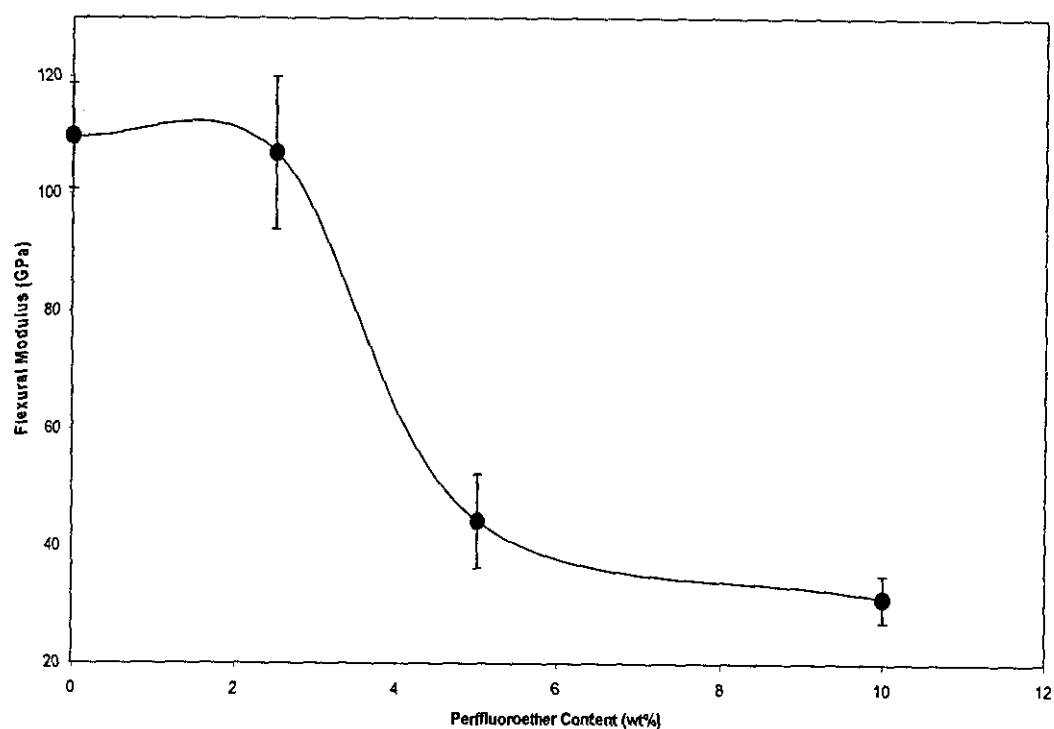


Figure 4.98: Flexural modulus of method I hybrid carbon fibre composites at various concentrations of perfluoroether modification.

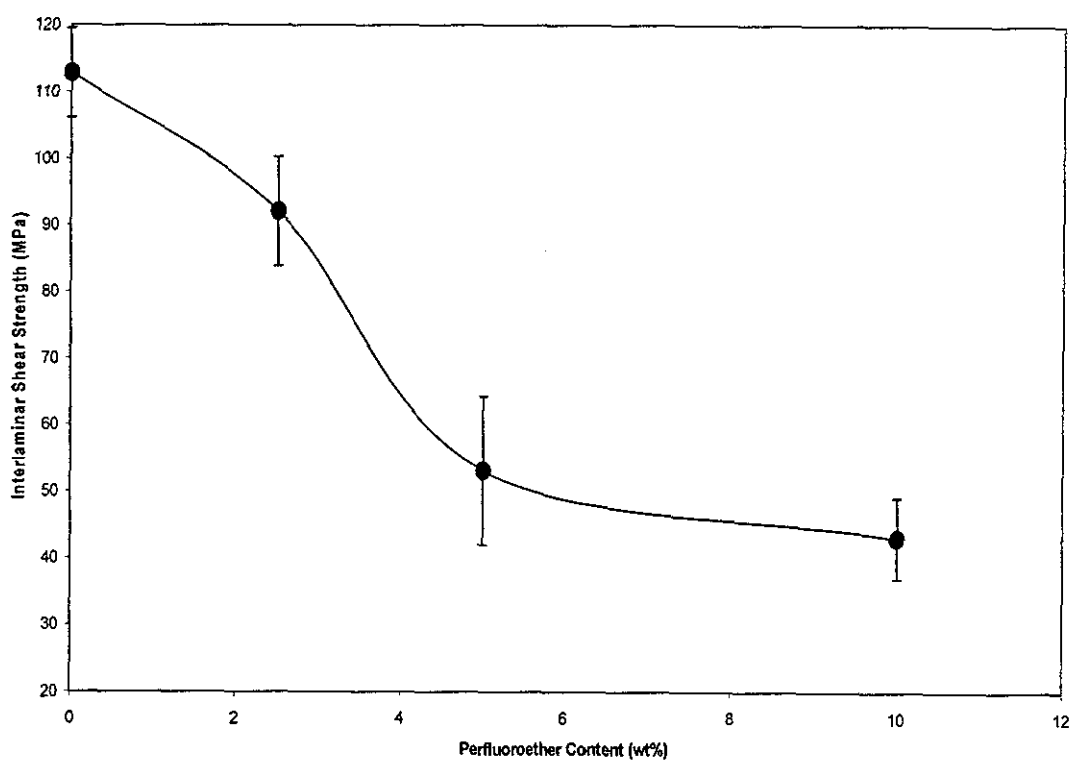


Figure 4.99: Interlaminar shear strength of method I hybrid carbon fibre composites at various concentrations of perfluoroether modification.

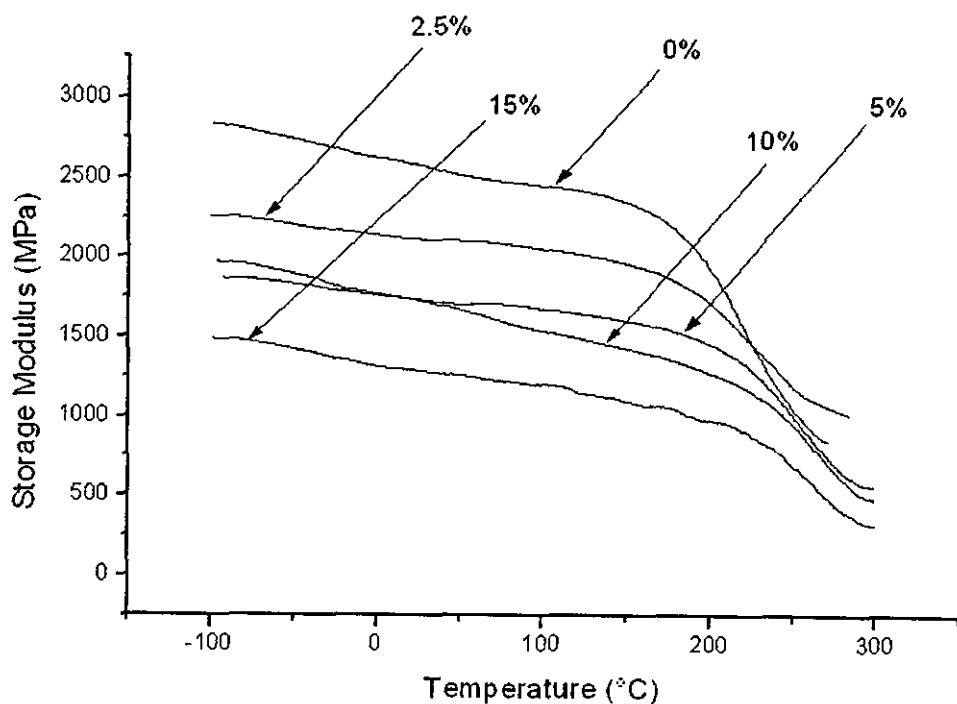


Figure 4.100: DMTA thermograms showing the transverse storage moduli of method II polyimide-carbon fibre composites at various concentrations of perfluoroether modification.

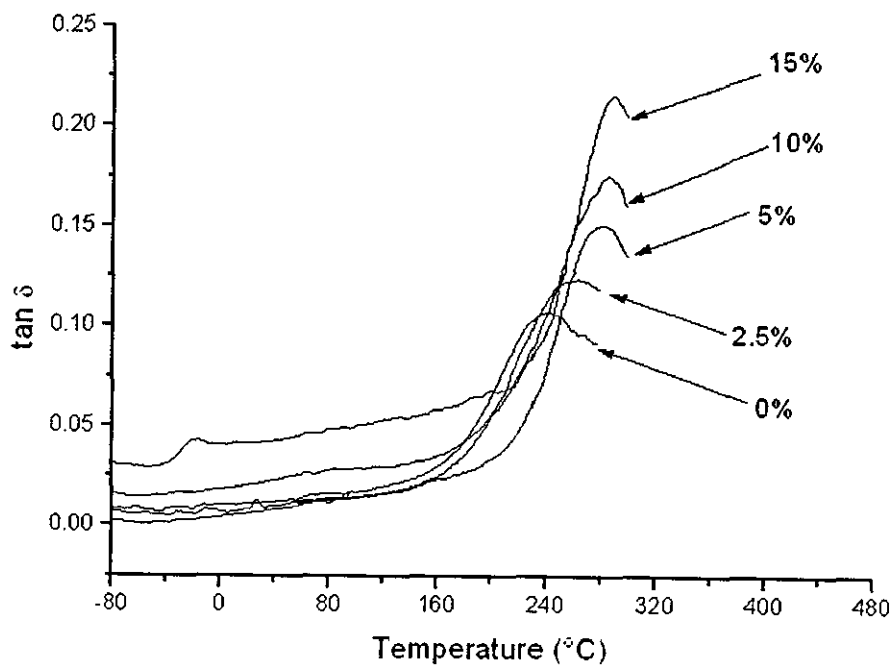


Figure 4.101: DMTA thermograms showing the $\tan \delta$ of method II polyimide-carbon fibre composites at various concentrations of perfluoroether modification.

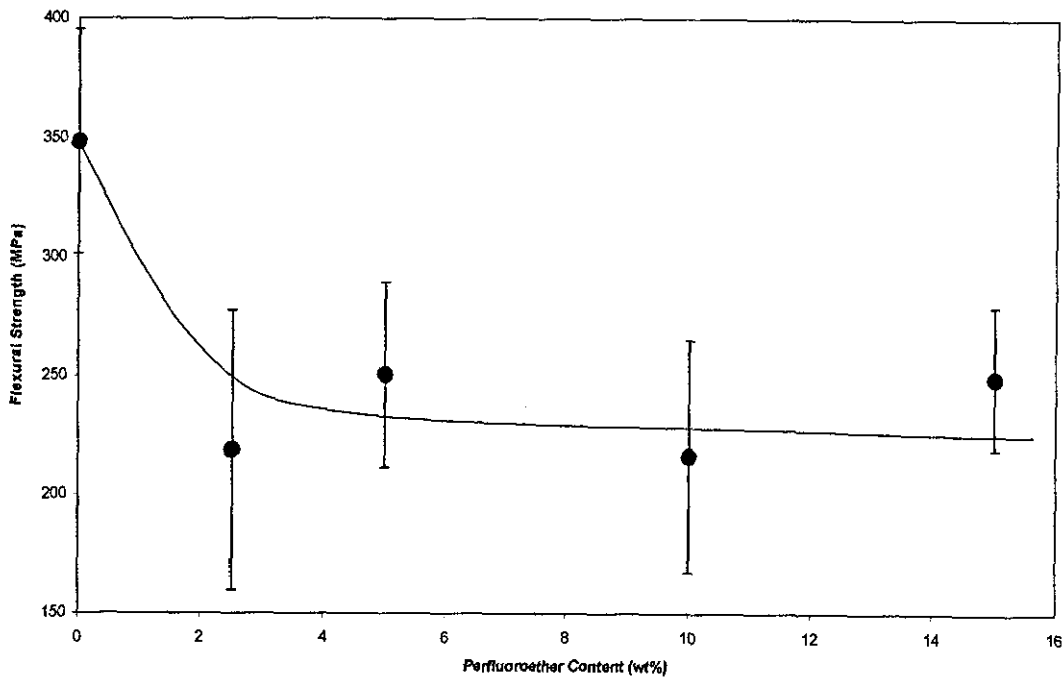


Figure 4.102: Flexural strength of method II polyimide-carbon fibre composites at various concentrations of perfluoroether modification.

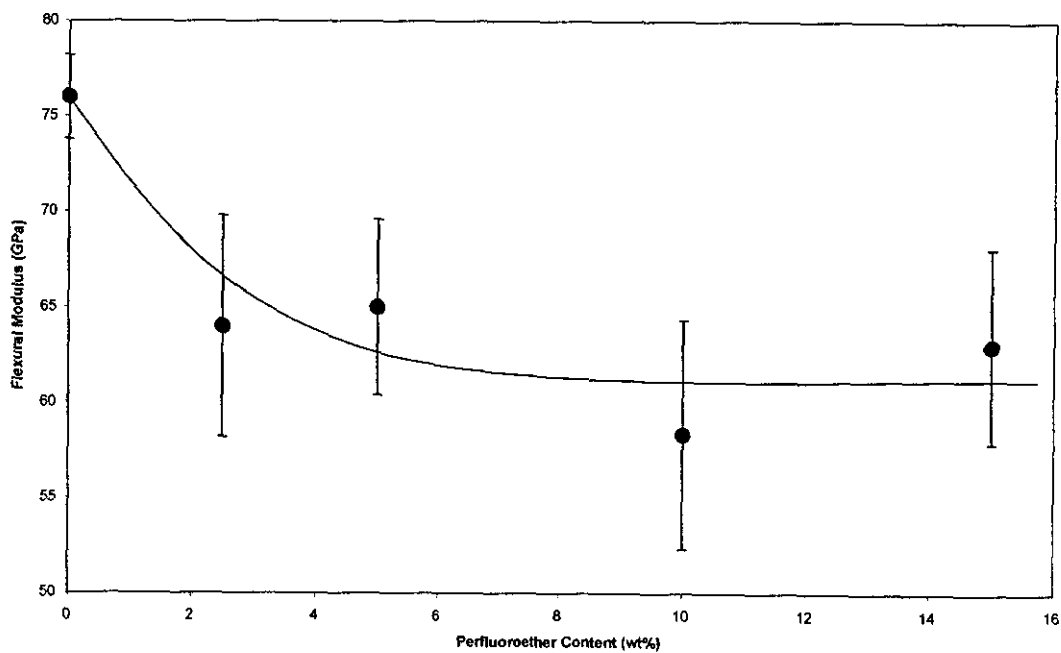


Figure 4.103: Flexural modulus of method II polyimide-carbon fibre composites at various concentrations of perfluoroether modification.

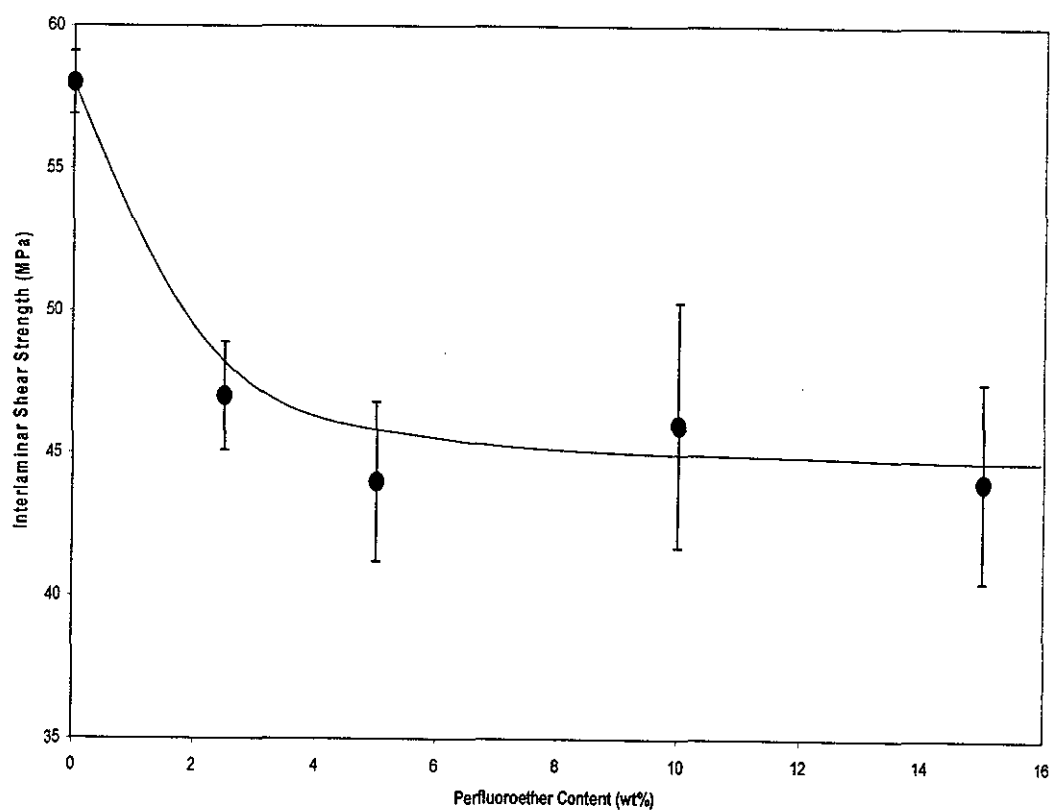


Figure 4.104: Interlaminar shear strength of method II polyimide-carbon fibre composites at various concentrations of perfluoroether modification.

In the case of HCl type samples, the DMTA storage modulus and $\tan \delta$ results are shown in figures 4.105 and 4.106, respectively. Samples with various concentrations of perfluoroether were compared. In the $\tan \delta$ results, a very prominent peak can be observed in all the samples, except 15% formulation, at around -20°C , which is extremely large in the unmodified and 2.5% formulation. With increasing perfluoroether content, the size of the peak decreased drastically and is not detectable at 15% modification level. The storage moduli of all the samples were very low. Increasing the perfluoroether content in the composites show a noticeable increase in the modulus from extremely low figures that are below 100 MPa.

Figures 4.107, 4.108 and 4.109 show the flexural strength, flexural modulus and interlaminar shear strength results of the HCl type samples, respectively. A progressive increase in all the properties as a function of increasing perfluoroether concentration can be observed.

In the case of TSA type samples, the DMTA storage modulus and $\tan \delta$ results are shown in figures 4.110 and 4.111, respectively. The storage modulus of the control sample, i.e. 0% concentration of perfluoroether, is very high, in excess of 8 GPa. However, the addition of perfluoroether modifier into the system is demonstrated to have a very significant effect in the storage modulus of composite, i.e. the reduction in the modulus is enormous with increasing perfluoroether modification. In order to reveal more details in the thermogram, the individual storage modulus results for each sample are shown in figures 4.112 to 4.116. A gradual reduction in modulus can be observed in all the formulations, but no obvious transition or thermal event was detected. The progressive and noticeable increase in damping capacity of the composites can be clearly illustrated from the $\tan \delta$ results, where a large upward shift in the baseline can be observed with increasing perfluoroether concentration.

Figures 4.117, 4.118 and 4.119 show the flexural strength, flexural modulus and interlaminar shear strength of TSA type samples at various concentrations of perfluoroether modification. The significant increase in all the properties as a function of increasing perfluoroether modification can clearly be observed.

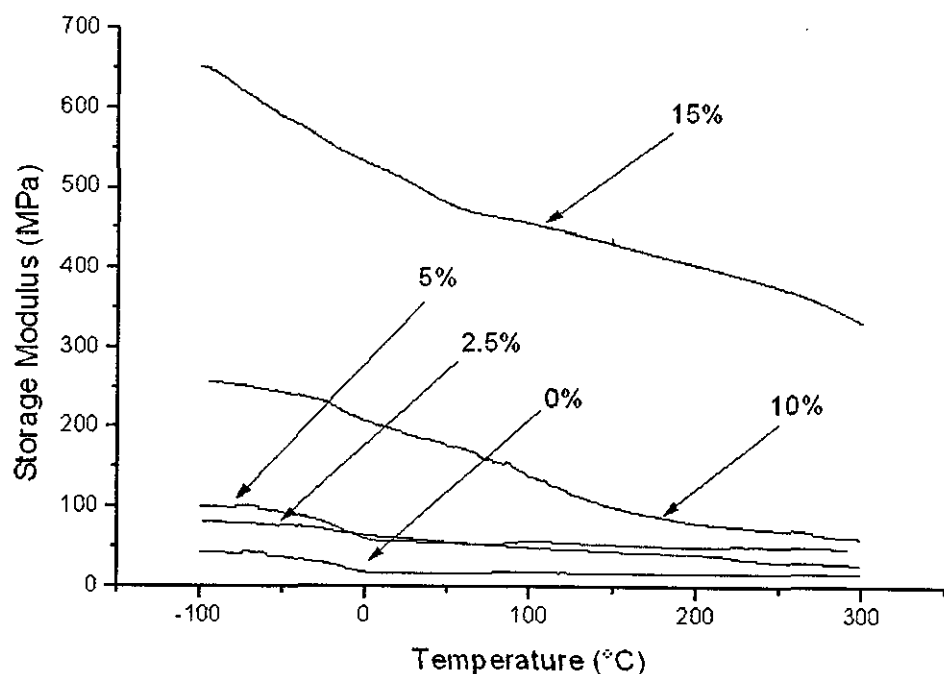


Figure 4.105: DMTA thermograms showing the transverse storage moduli of method II polyimide-silica hybrid (HCl type) carbon fibre composites at various concentrations of perfluoroether modification.

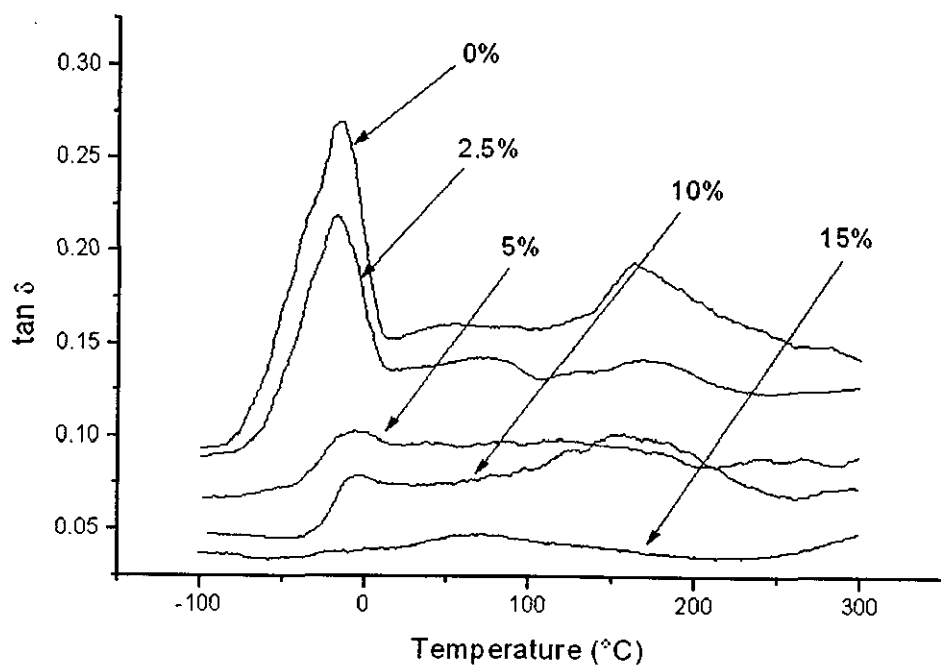


Figure 4.106: DMTA thermograms showing tan δ of method II polyimide-silica hybrid (HCl type) carbon fibre composites at various concentrations of perfluoroether modification.

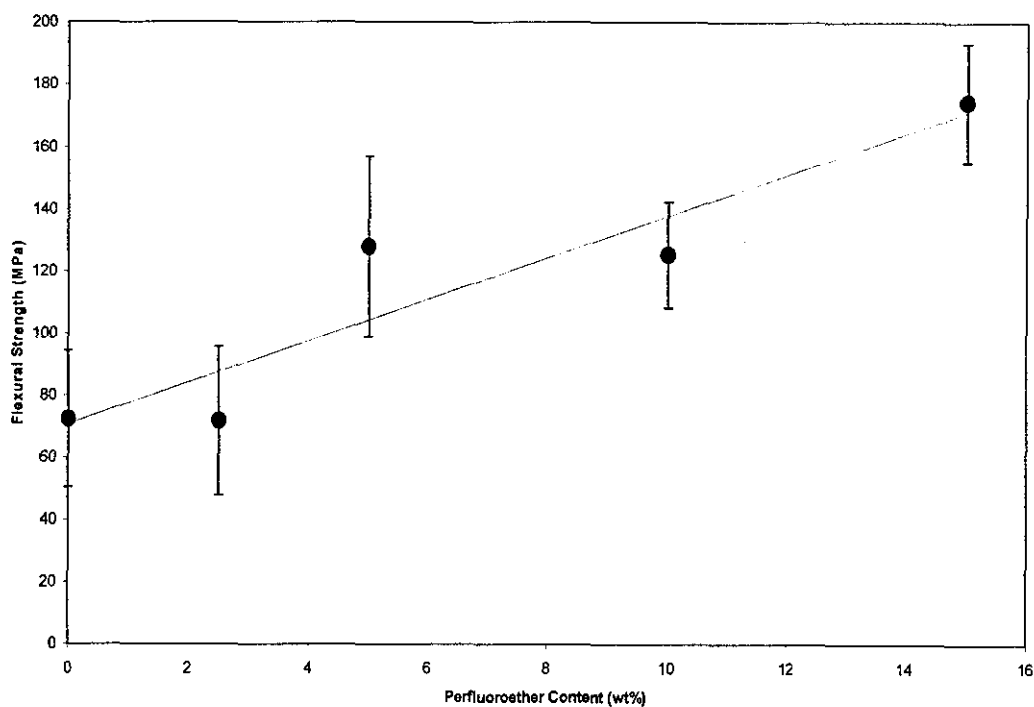


Figure 4.107: Flexural strength of method II polyimide-silica hybrid (HCl type) carbon fibre composites at various concentrations of perfluoroether modification.

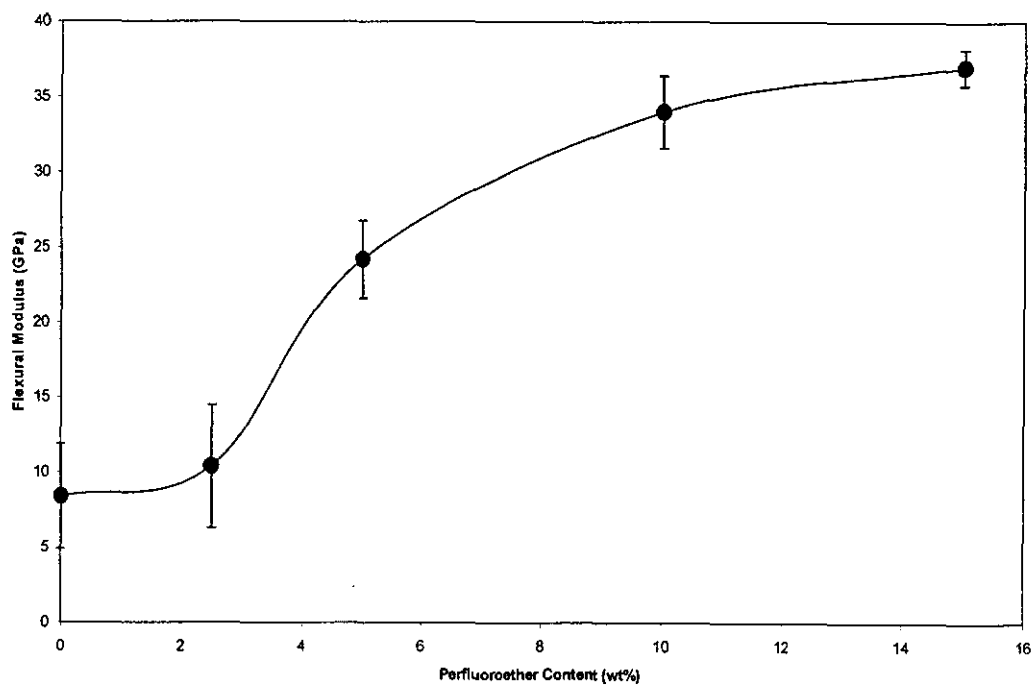


Figure 4.108: Flexural modulus of method II polyimide-silica hybrid (HCl type) carbon fibre composites at various concentrations of perfluoroether modification.

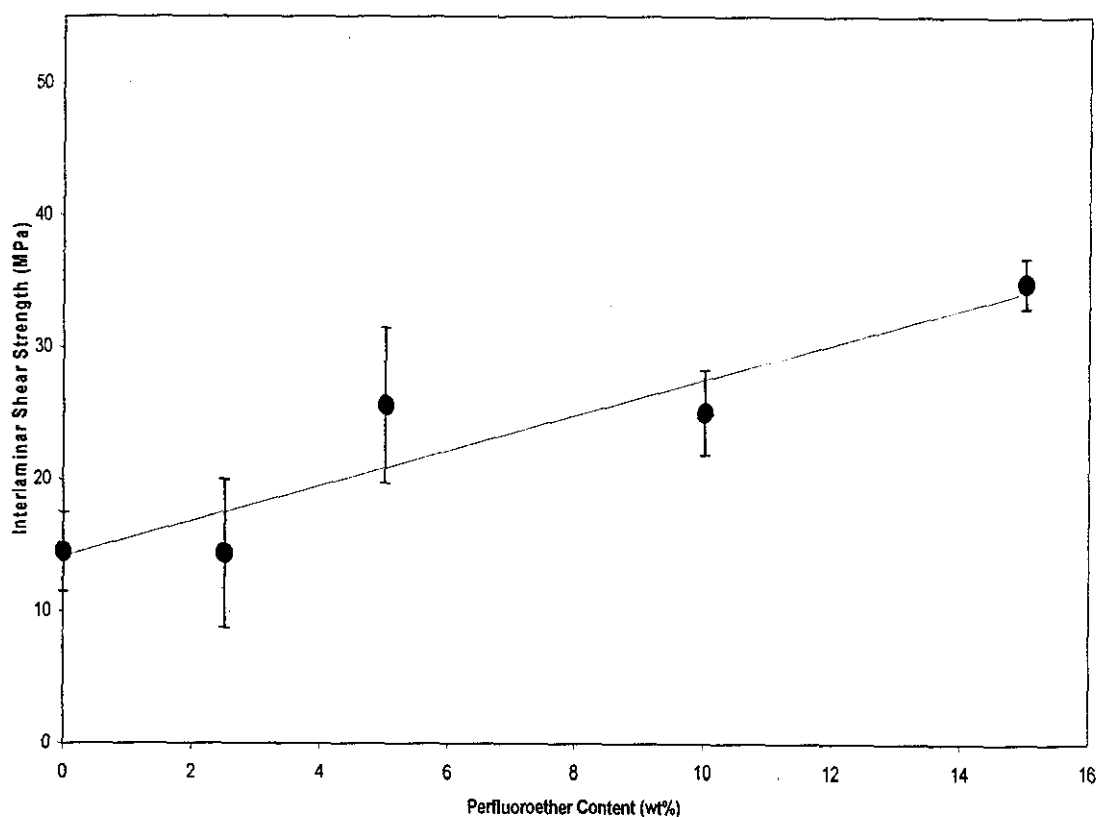


Figure 4.109: Interlaminar shear strength of method II polyimide-silica hybrid (HCl type) carbon fibre composites at various concentrations of perfluoroether modification.

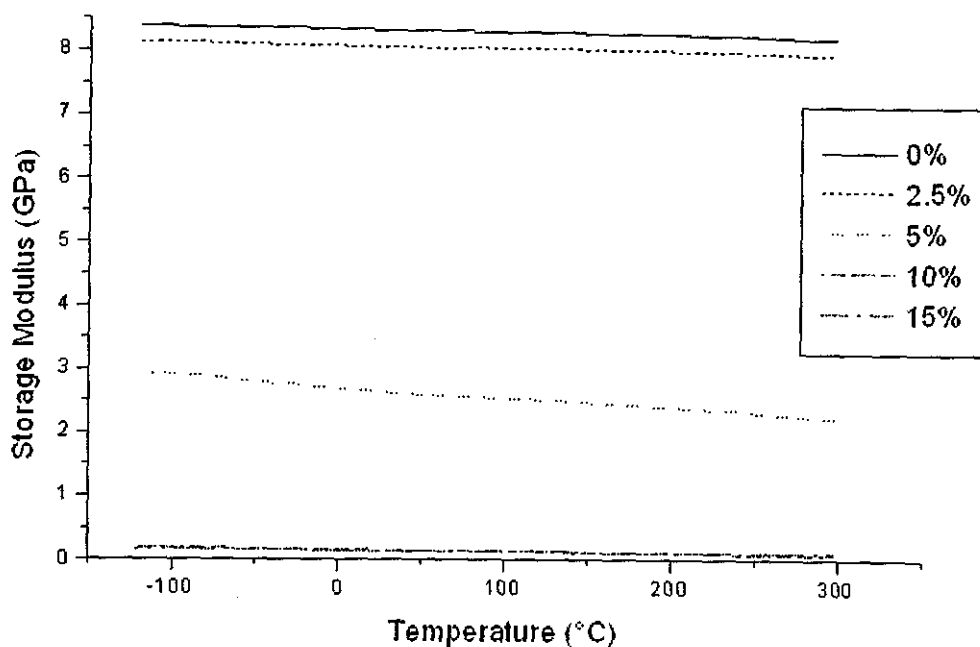


Figure 4.110: DMTA thermograms showing the transverse storage moduli of method II polyimide-silica hybrid (TSA type) carbon fibre composites at various concentrations of perfluoroether modification.

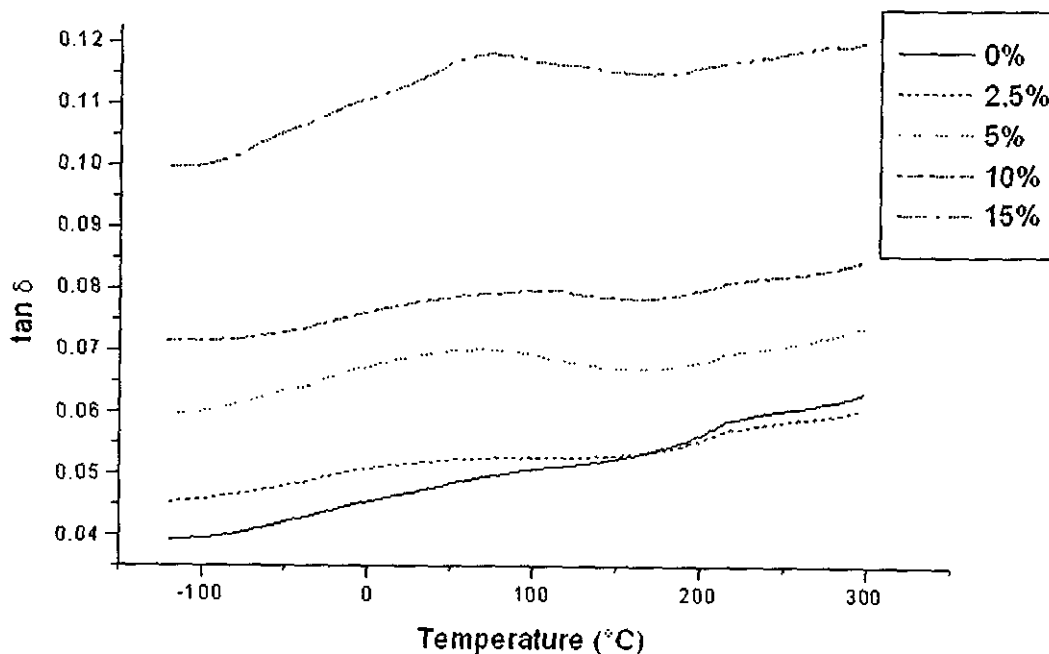


Figure 4.111: DMTA thermograms showing the tan δ of method II polyimide-silica hybrid (TSA type) carbon fibre composites at various concentrations of perfluoroether modification.

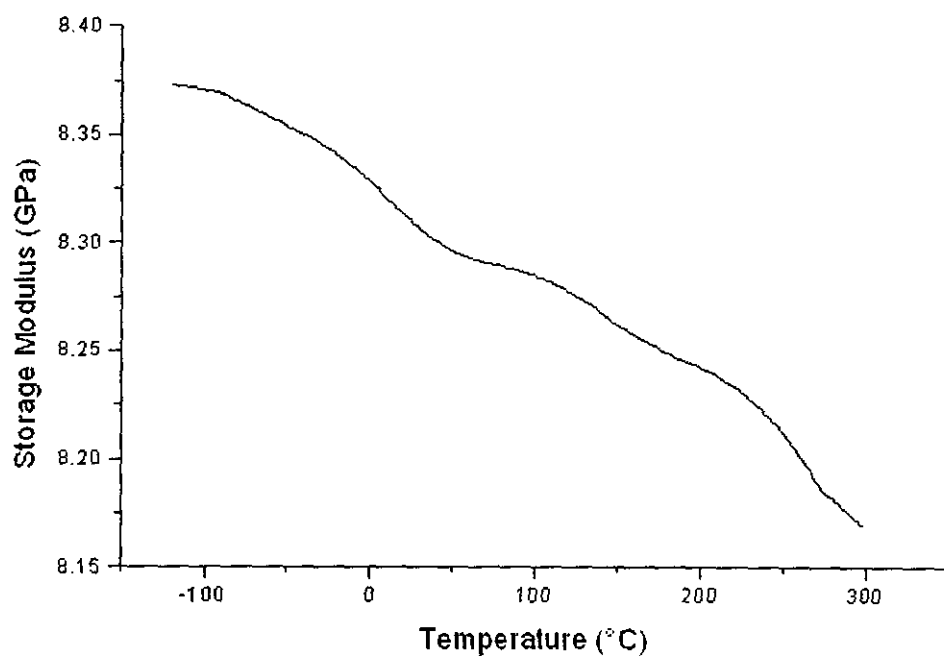


Figure 4.112: DMTA thermograms showing the transverse storage modulus of method II polyimide-silica hybrid (TSA type) carbon fibre composites at 0 wt% concentrations of perfluoroether modification.

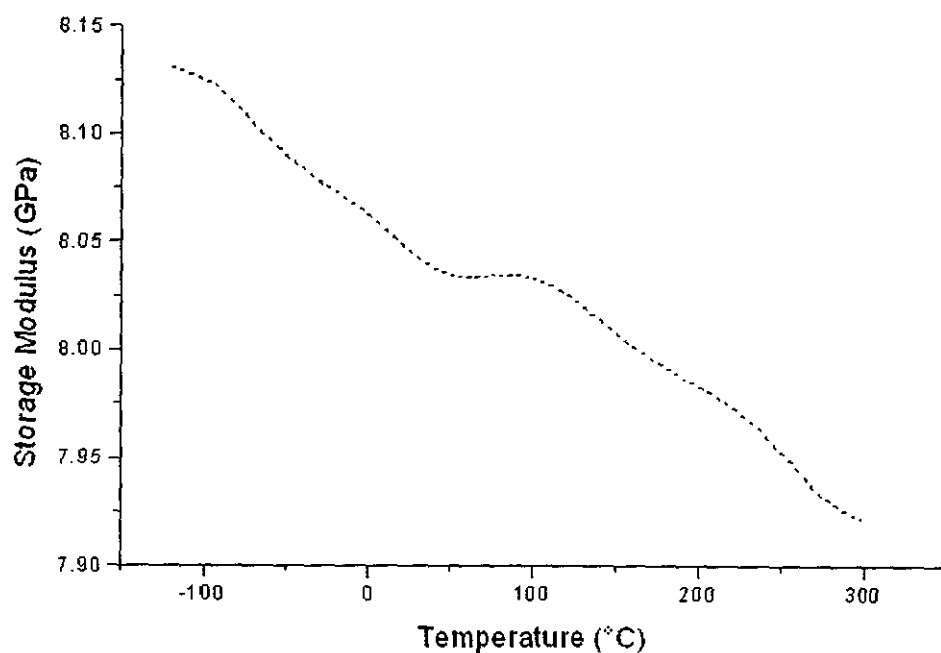


Figure 4.113: DMTA thermograms showing the transverse storage modulus of method II polyimide-silica hybrid (TSA type) carbon fibre composites at 2.5 wt% concentrations of perfluoroether modification.

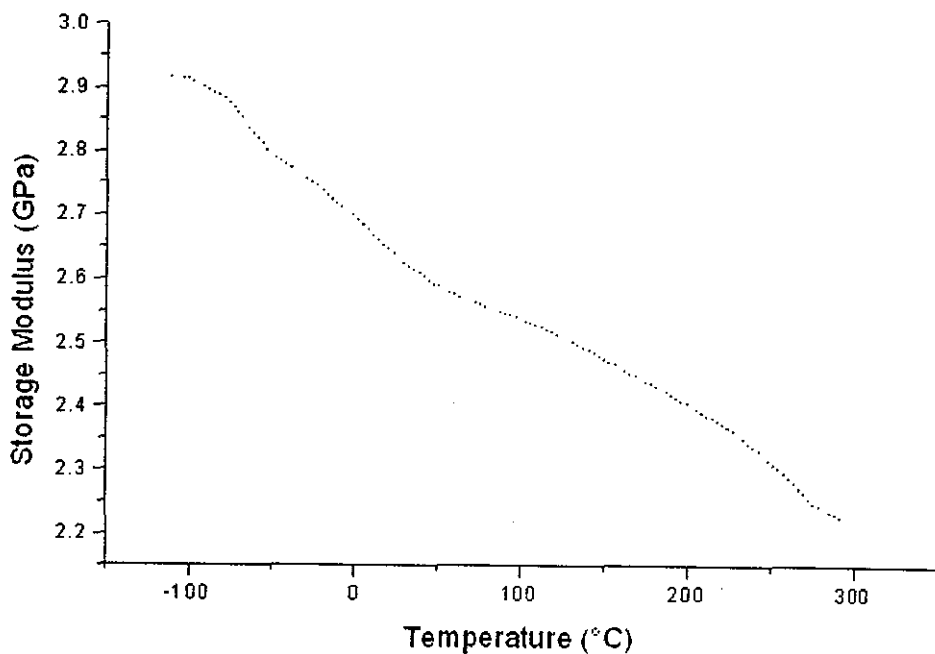


Figure 4.114: DMTA thermograms showing the transverse storage modulus of method II polyimide-silica hybrid (TSA type) carbon fibre composites at 5 wt% concentrations of perfluoroether modification

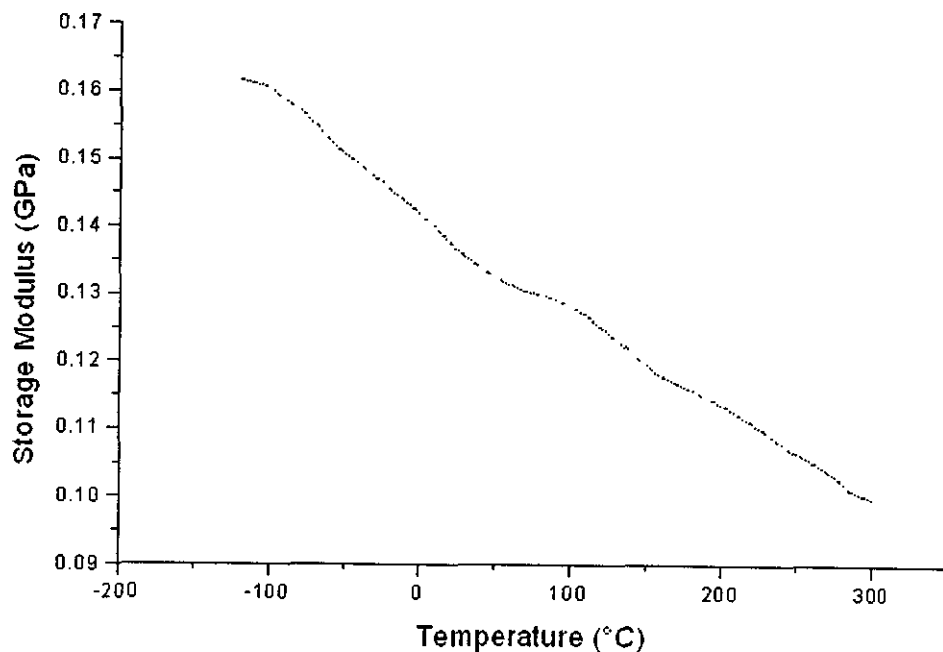


Figure 4.115: DMTA thermograms showing the transverse storage modulus of method II polyimide-silica hybrid (TSA type) carbon fibre composites at 10 wt% concentrations of perfluoroether modification

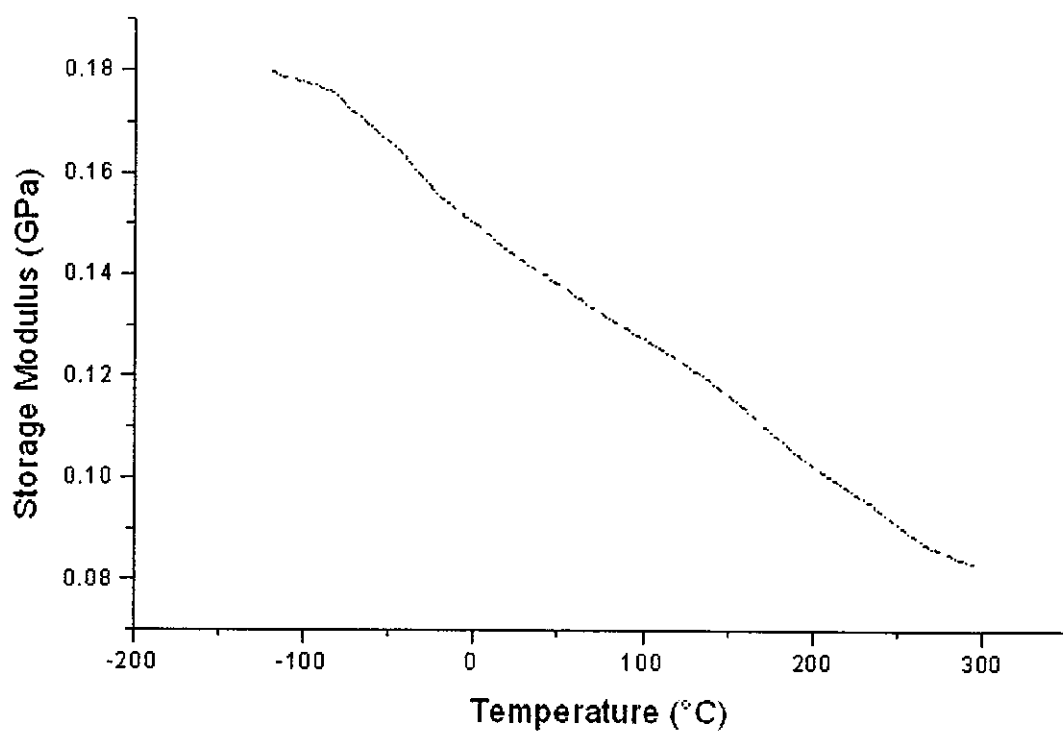


Figure 4.116: DMTA thermograms showing the transverse storage modulus of method II polyimide-silica hybrid (TSA type) carbon fibre composites at 15 wt% concentrations of perfluoroether modification

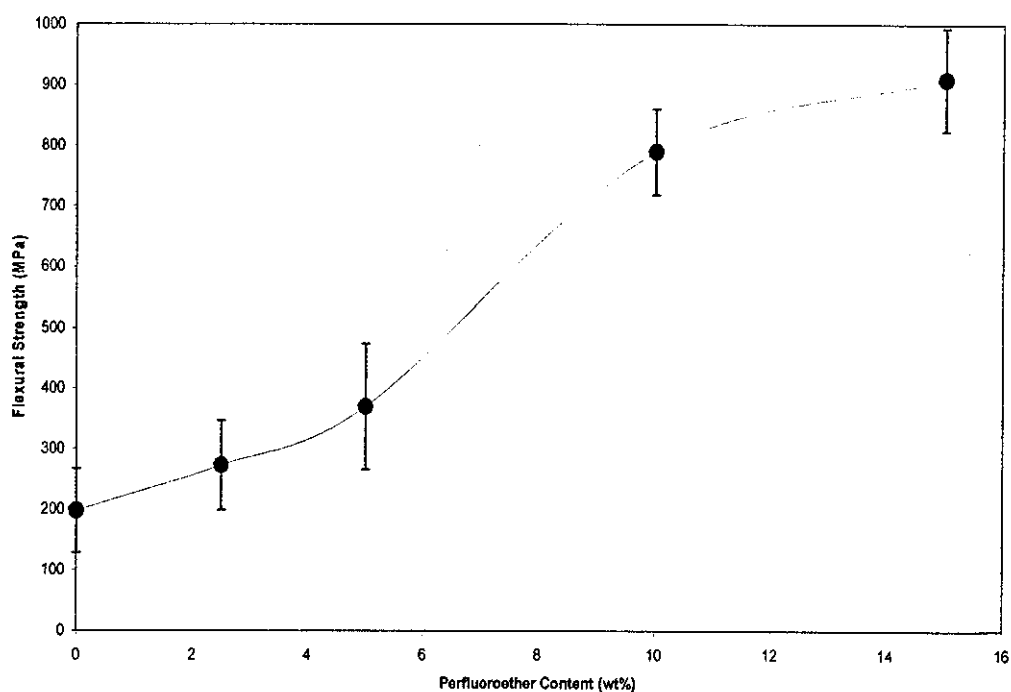


Figure 4.117: Flexural strength of method II polyimide-silica hybrid (TSA type) carbon fibre composites at various concentrations of perfluoroether modification

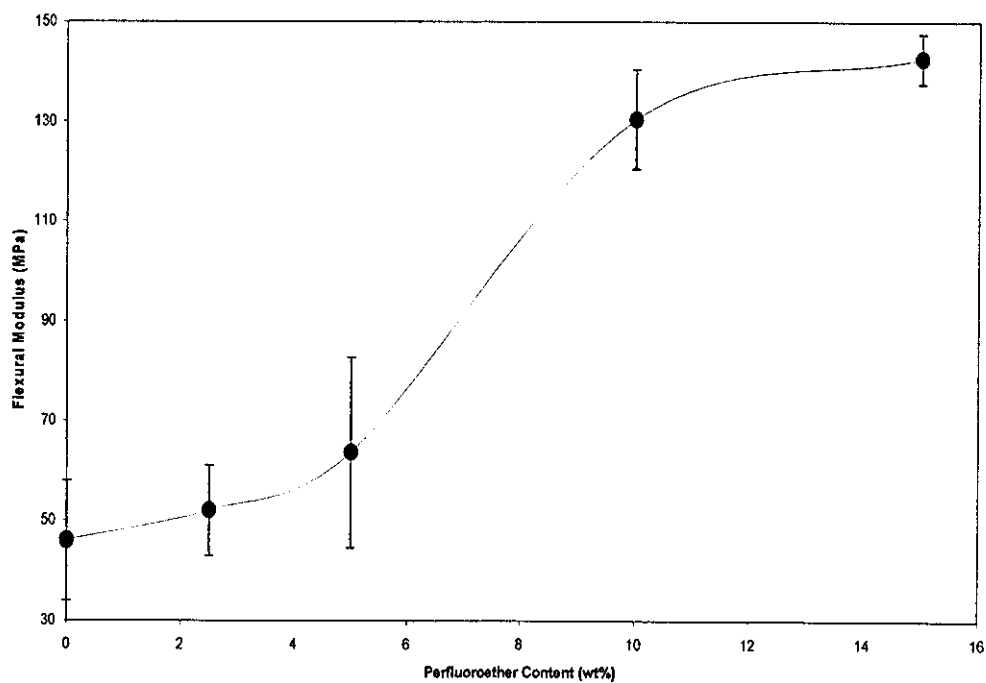


Figure 4.118: Flexural modulus of method II polyimide-silica hybrid (TSA type) carbon fibre composites at various concentrations of perfluoroether modification

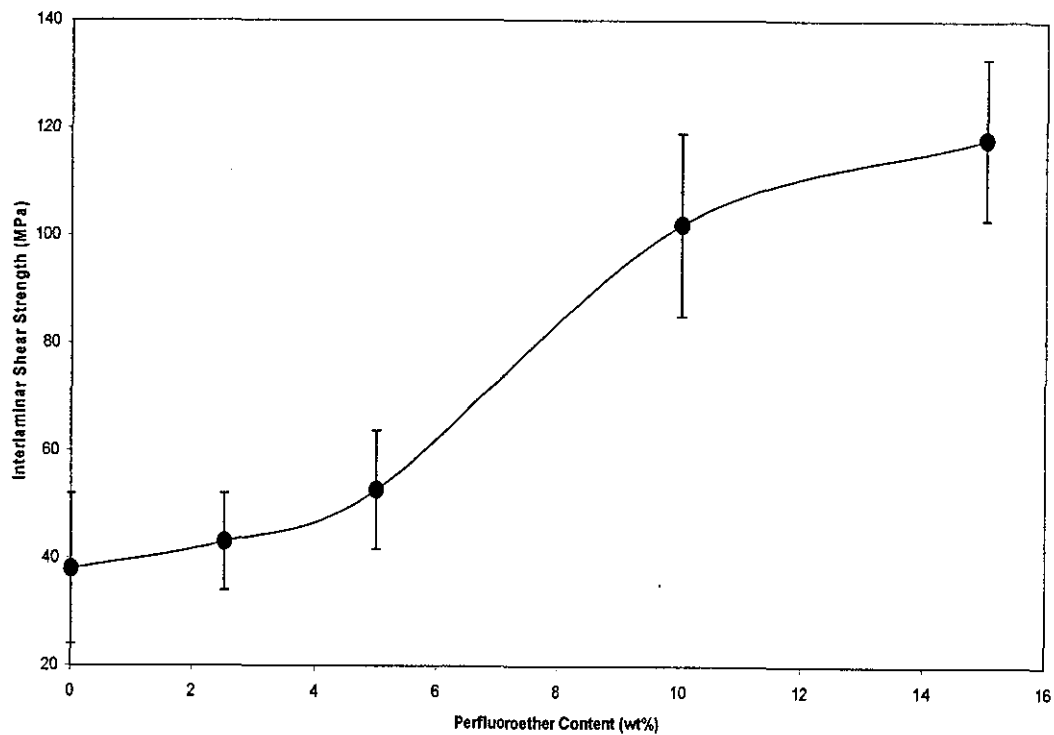


Figure 4.119: Interlaminar shear strength of method II polyimide-silica hybrid (TSA type) carbon fibre composites at various concentrations of perfluoroether modification

Method III

Figures 4.120 and 4.121 show the DMTA storage modulus and $\tan \delta$ results of the non-hybridised polyimide composite samples at various concentrations of perfluoroether modification. The reduction in storage modulus of the composites is very drastic with increasing perfluoroether content. In the $\tan \delta$ results, the increase in damping capacity as a result of perfluoroether modification is very clear. Interestingly at 2.5% and 5% perfluoroether modification, a 50°C to 60°C increase in glass transition can be observed. At 10% modification, the damping capacity became very large and the sharp glass transition of the polyimide disappeared from the analysis temperature range. A very broad energy absorbing band appear instead, which ranges from about -40°C to about 200°C.

Figures 4.122, 4.123 and 4.124 show the flexural strength, flexural modulus and interlaminar shear strength results of the composites at various concentrations of perfluoroether modification. All properties show a considerable drop with increasing perfluoroether modification.

Figures 4.125 and 4.126 show the DMTA storage modulus and $\tan \delta$ results of the hybrid samples at various perfluoroether modification levels. As can be observed, the improvement in storage modulus is significant with increasing perfluoroether content. In $\tan \delta$ results, a very large peak can be observed in the unmodified sample, i.e. 0% concentration of perfluoroether. The addition of perfluoroether clearly shown to remove the peak. At 10% modification, the peak became undetectable.

A progressive increase in flexural modulus, flexural strength and interlaminar shear strength in the composites with increasing perfluoroether modification can be observed in figures 4.127 to 4.129, respectively.

4.8 Scanning Electron Microscopy of the Composites

The SEM micrographs of a selection of the composites produced are shown in figures 4.130 to 4.141.

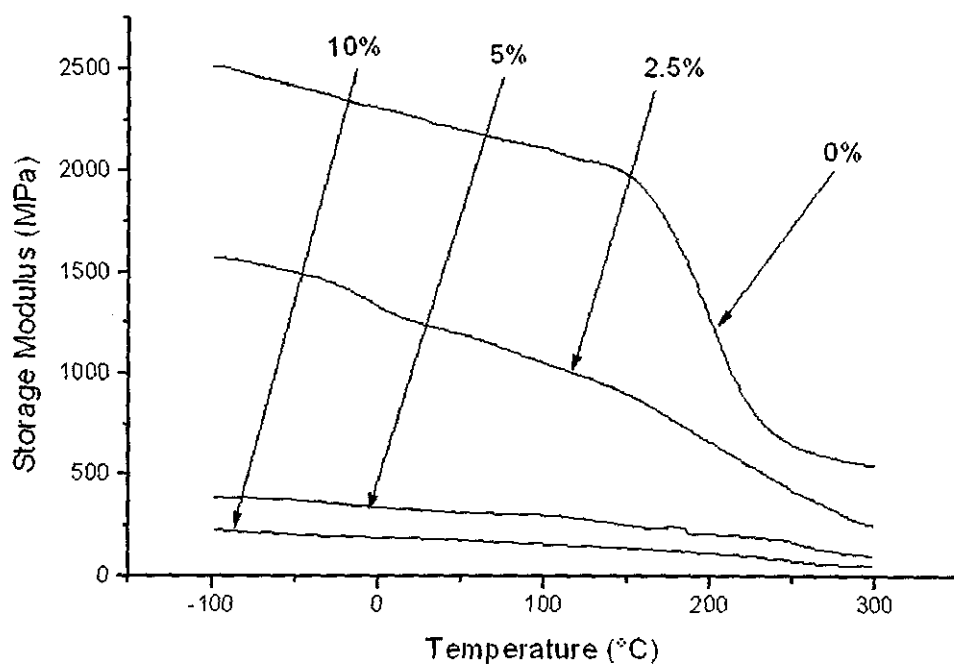


Figure 4.120: DMTA thermograms showing the transverse storage moduli of method III polyimide-carbon fibre composites at various concentrations of perfluoroether modification.

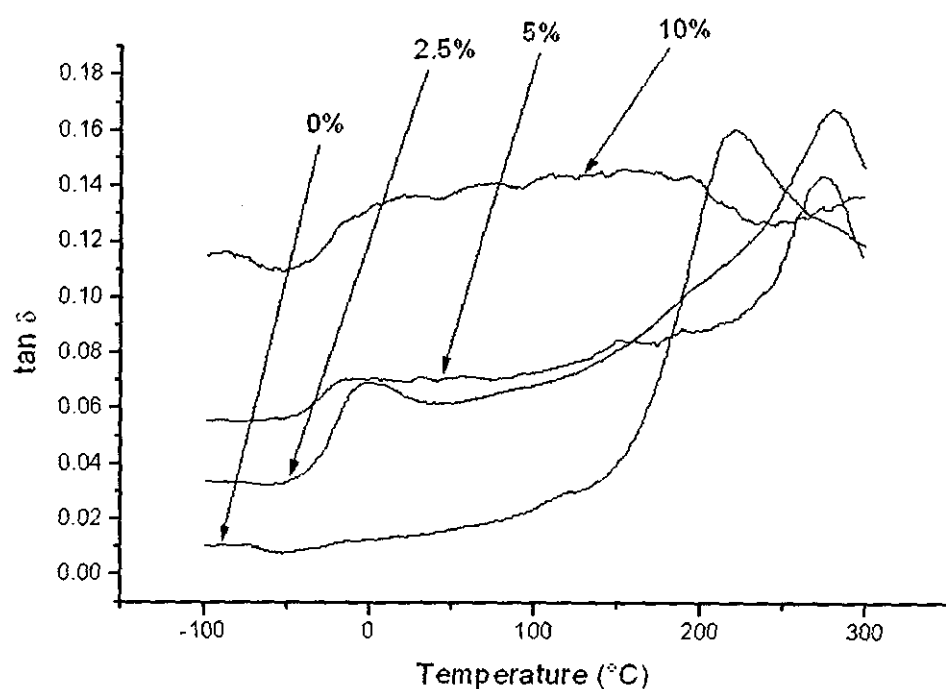


Figure 4.121: DMTA thermograms showing the $\tan \delta$ of method III polyimide-carbon fibre composites at various concentrations of perfluoroether modification.

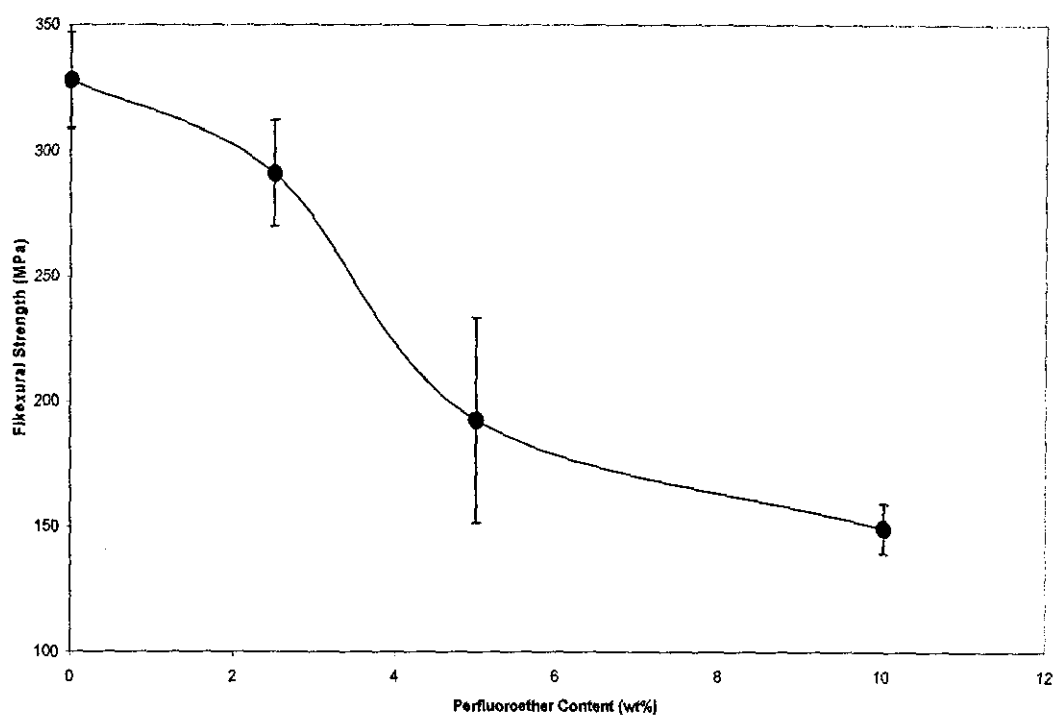


Figure 4.122: Flexural strength of method III polyimide-carbon fibre composites at various concentrations of perfluoroether modification.

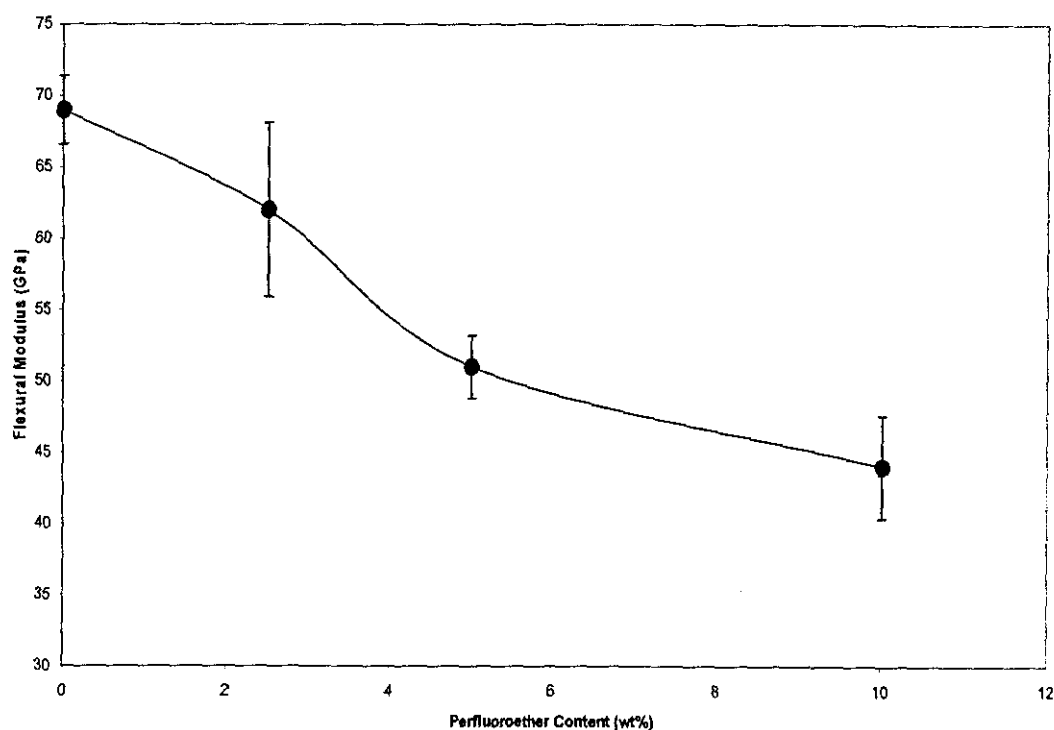


Figure 4.123: Flexural modulus of method III polyimide-carbon fibre composites at various concentrations of perfluoroether modification.

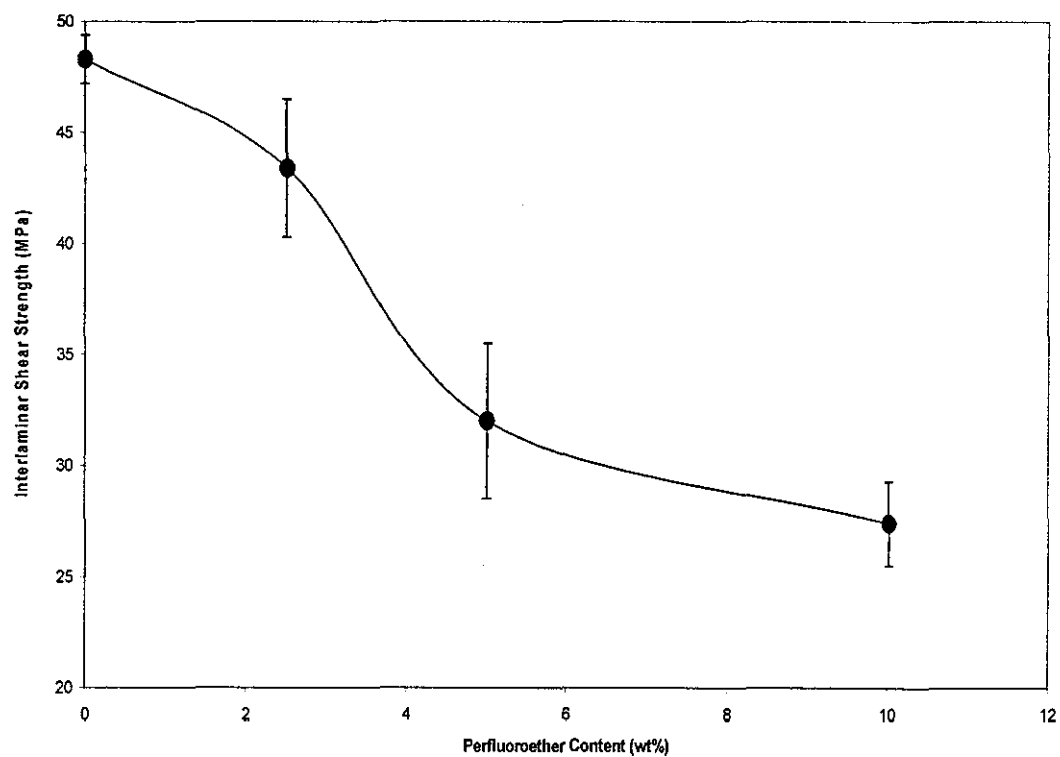


Figure 4.124: Interlaminar shear strength of method III polyimide-carbon fibre composites at various concentrations of perfluoroether modification.

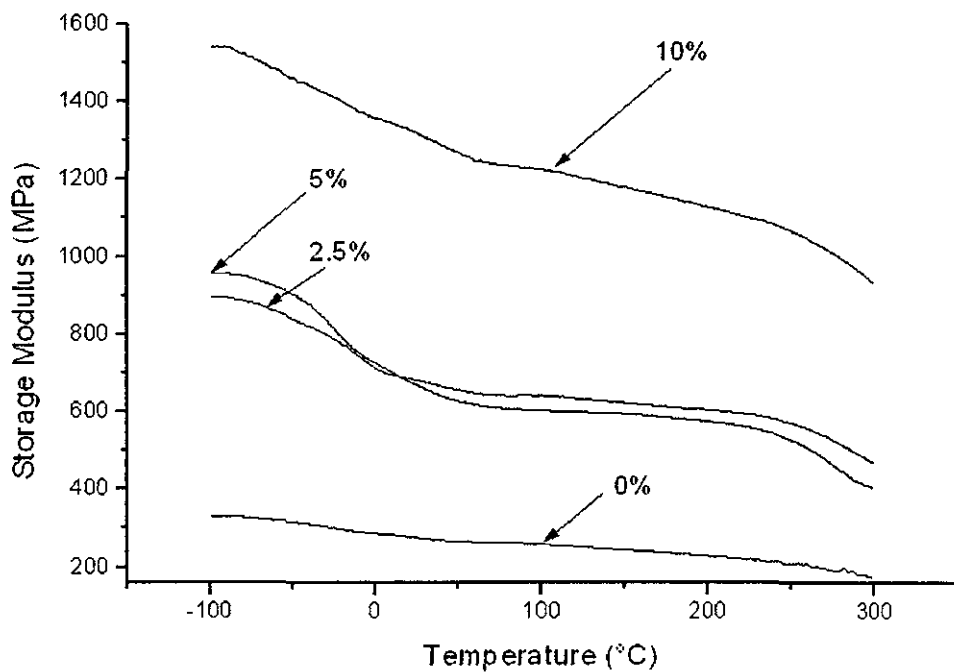


Figure 4.125: DMTA thermograms showing the transverse storage moduli of method III hybrid carbon fibre composites at various concentrations of perfluoroether modification.

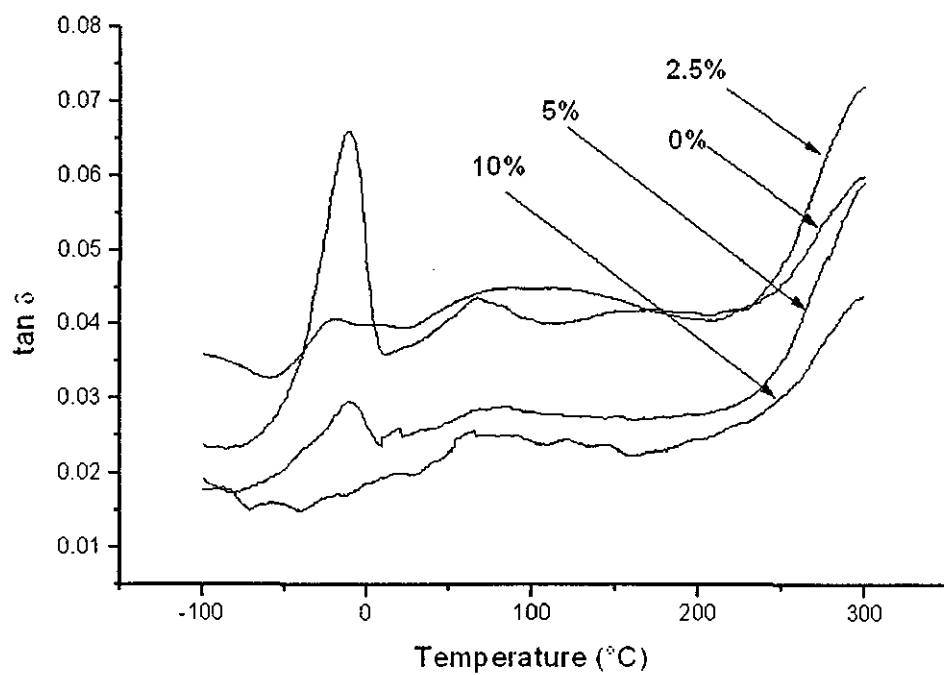


Figure 4.126: DMTA thermograms showing the $\tan \delta$ of method III hybrid carbon fibre composites at various concentrations of perfluoroether modification.

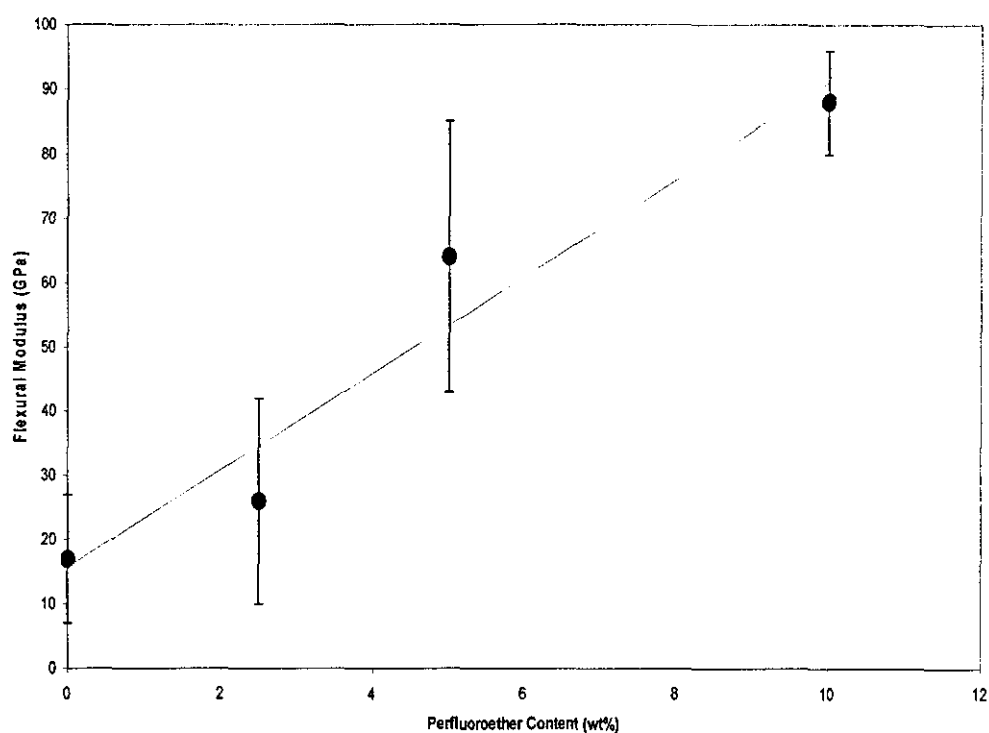


Figure 4.127: Flexural modulus of method III hybrid carbon fibre composites at various concentrations of perfluoroether modification.

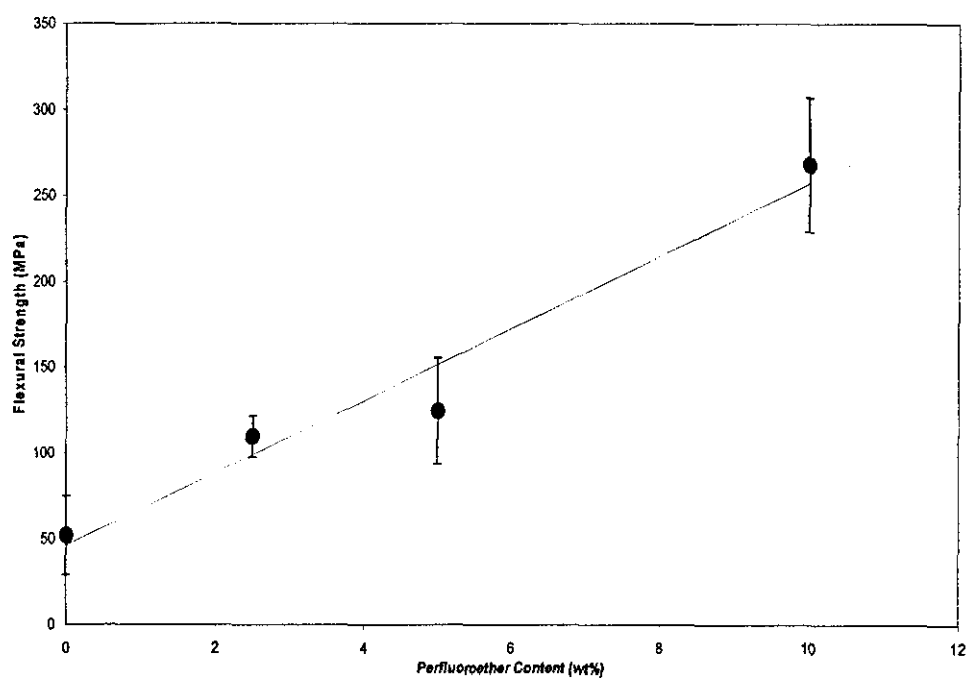


Figure 4.128: Flexural strength of method III hybrid carbon fibre composites at various concentrations of perfluoroether modification.

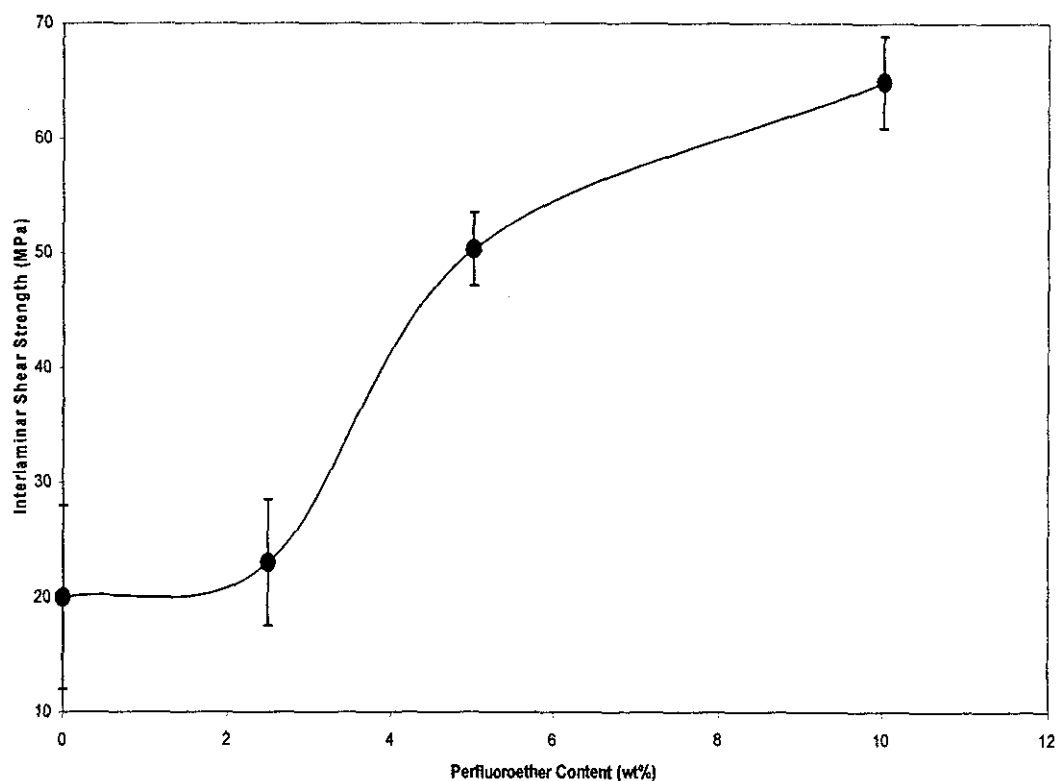


Figure 4.129: Interlaminar shear strength of method III hybrid carbon fibre composites at various concentrations of perfluoroether modification.

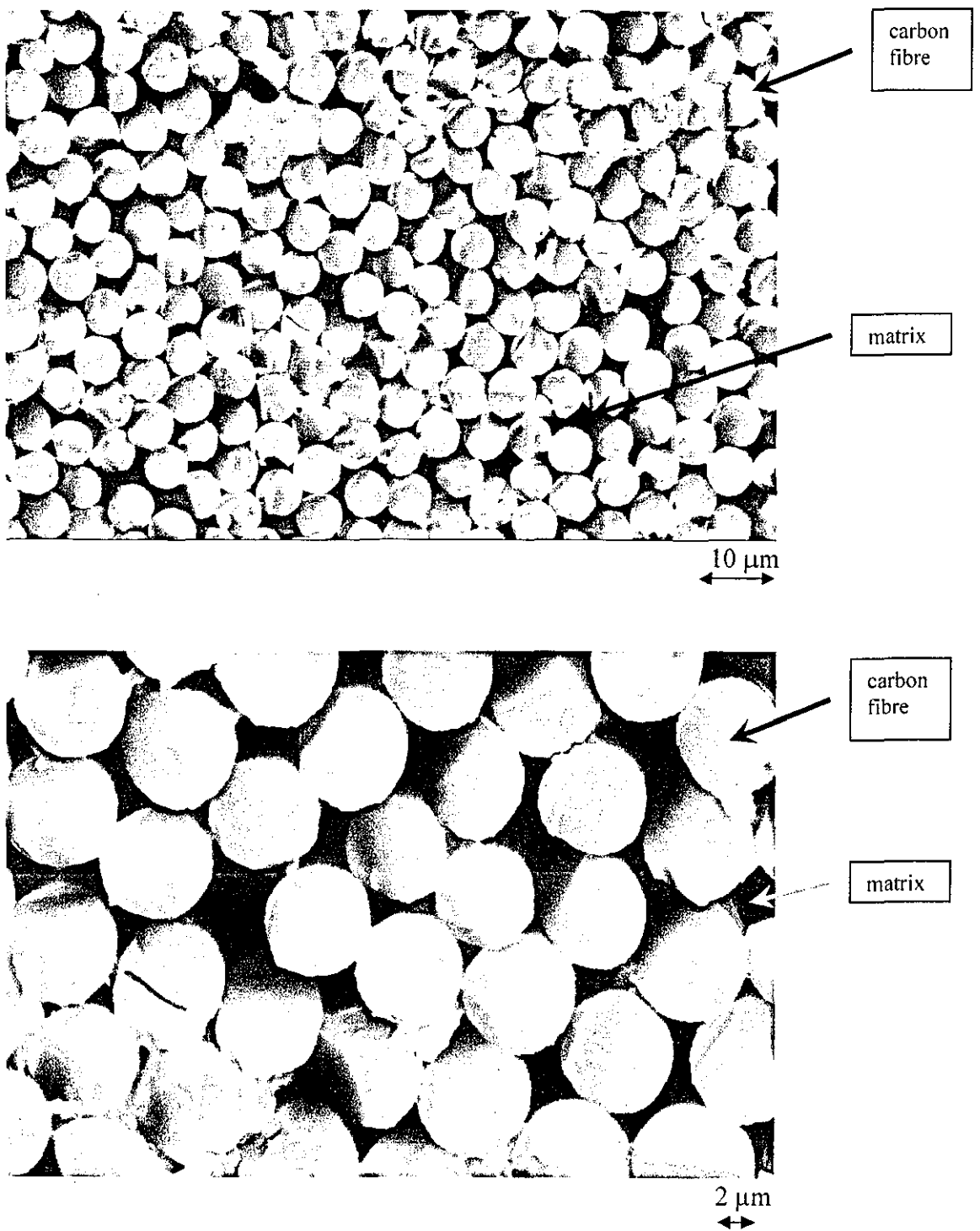


Figure 4.130: Composite produced using method I. SEM micrograph showing the cross-section of the composite with matrix containing unmodified polyimide.

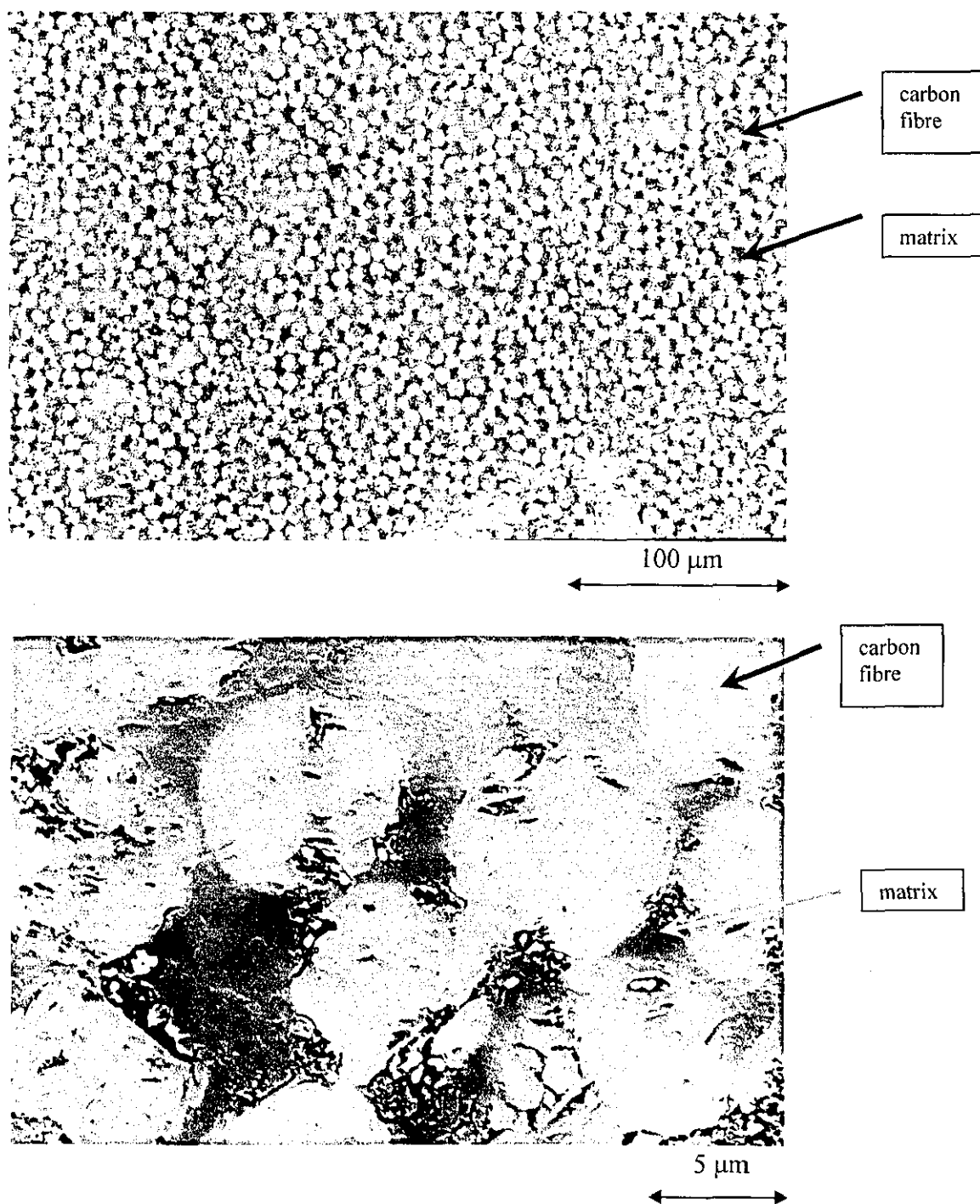


Figure 4.131: Composite produced using method I. SEM micrograph showing the cross-section of the composite with matrix containing polyimide modified with 10% of perfluoroether.

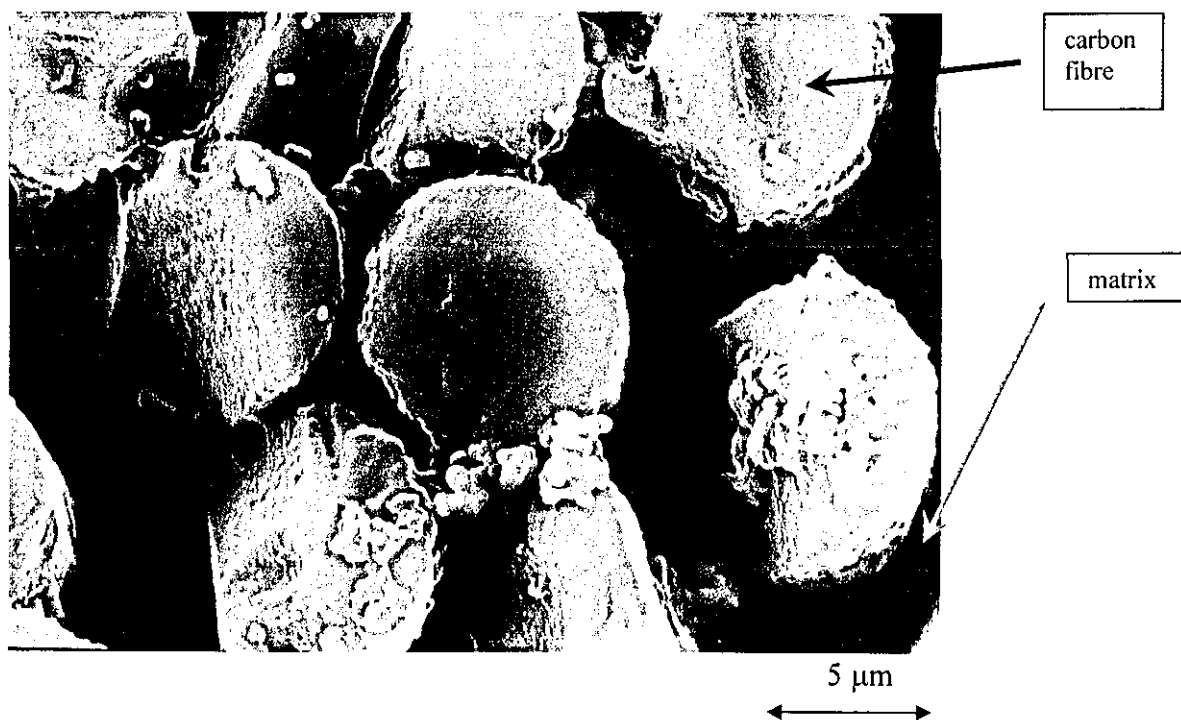
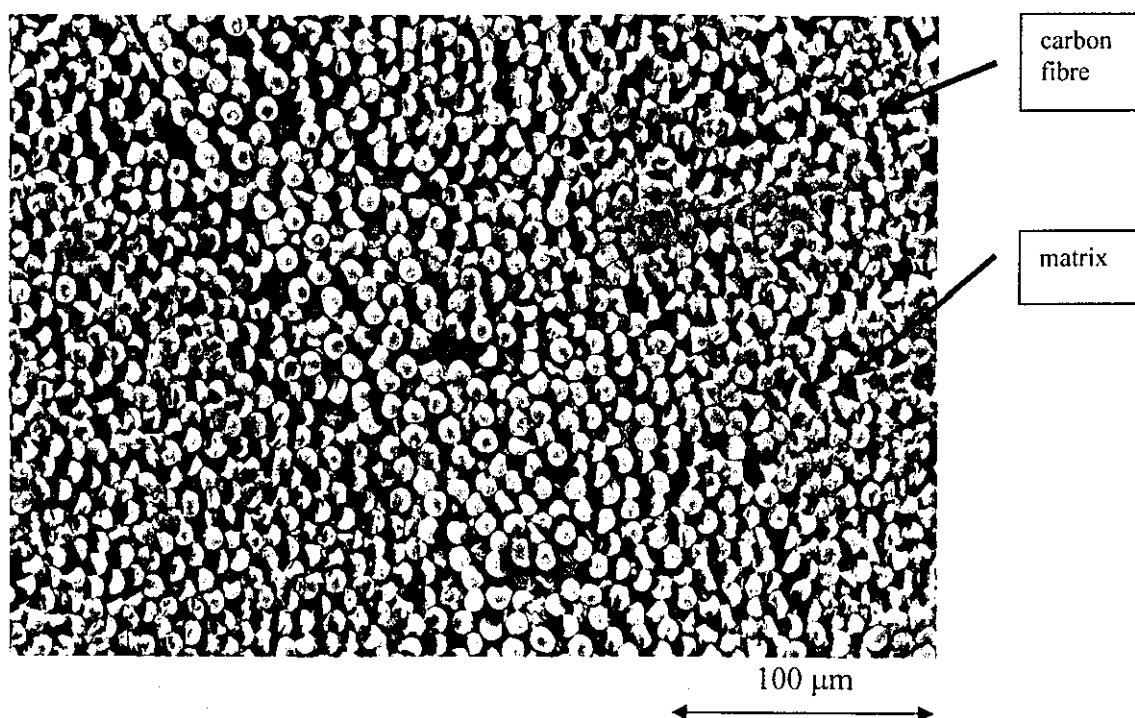


Figure 4.132: Composite produced using method I. SEM micrograph showing the cross-section of the composite with matrix containing unmodified polyimide hybridised with 30% silica.

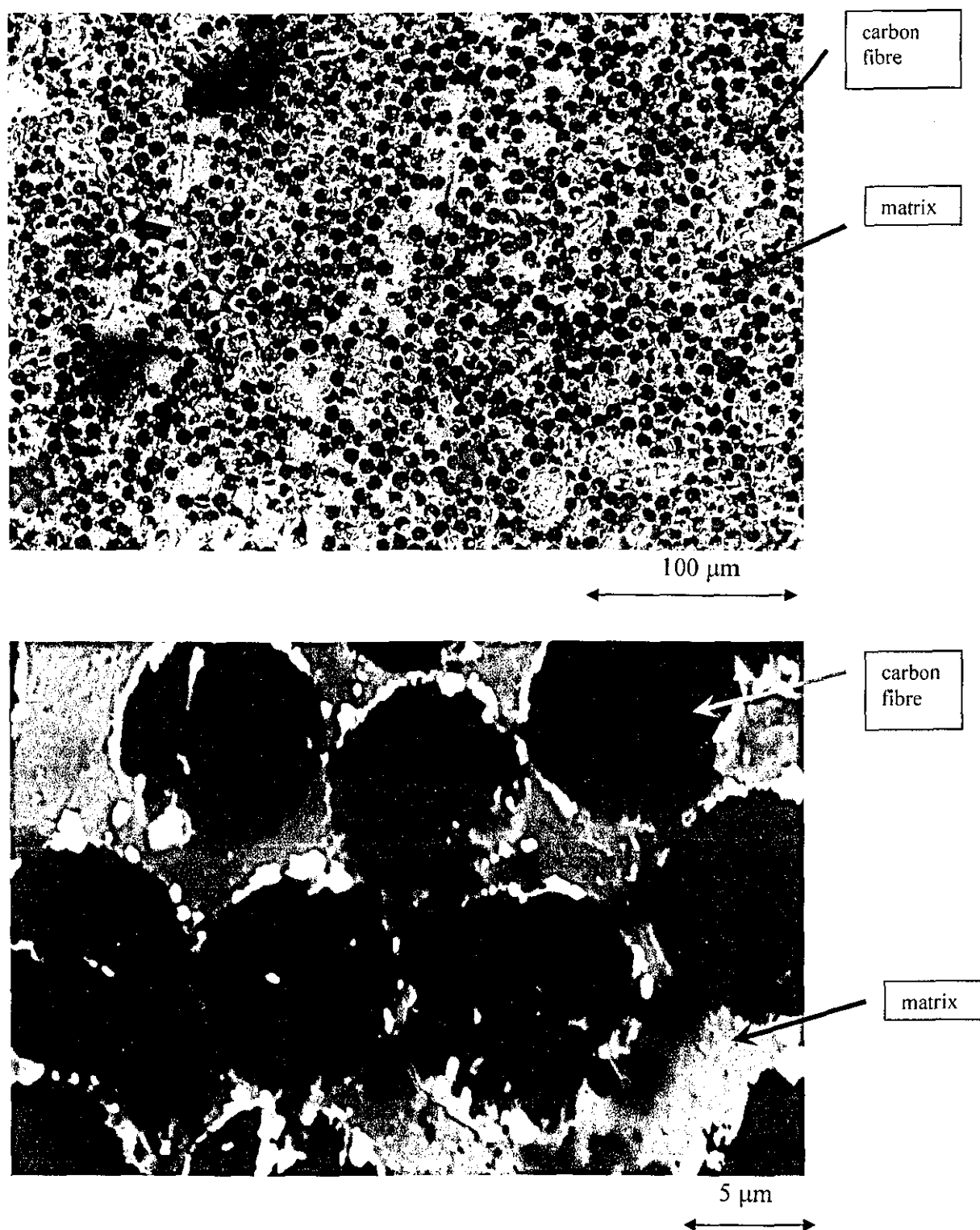


Figure 4.133: Composite produced using method I. SEM micrograph showing the cross-section of the composite with matrix containing polyimide modified with 5% of perfluoroether and hybridised with 30% silica.

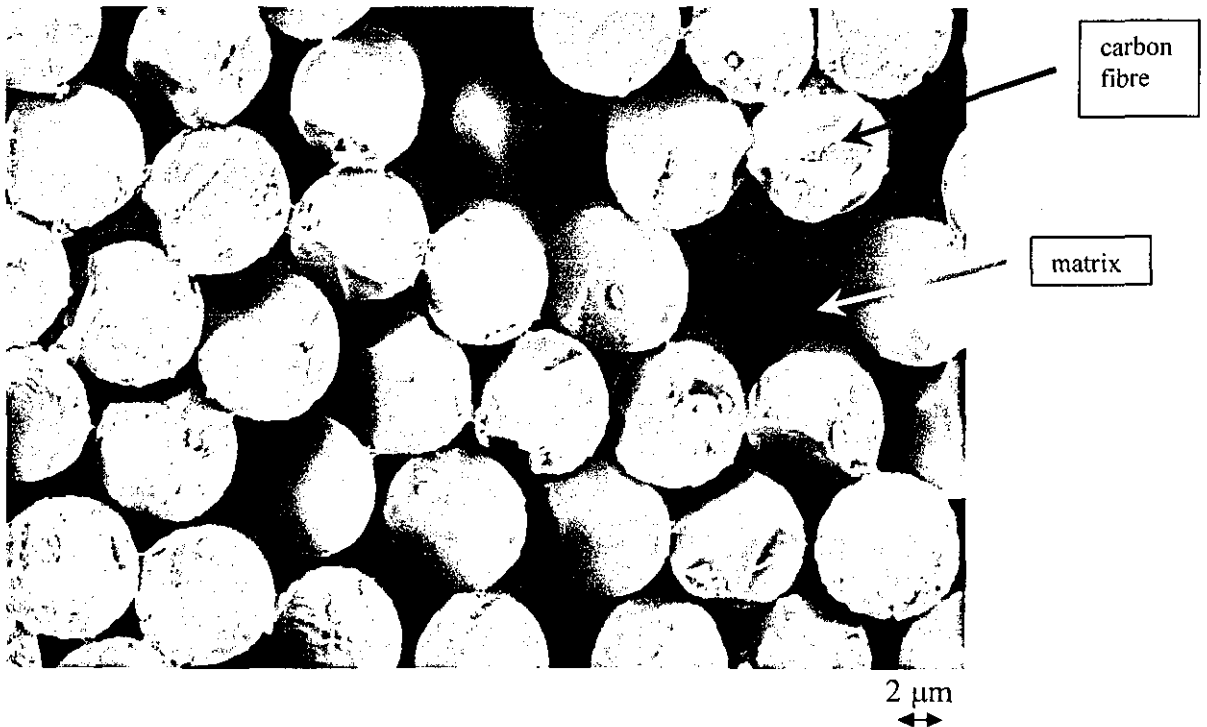
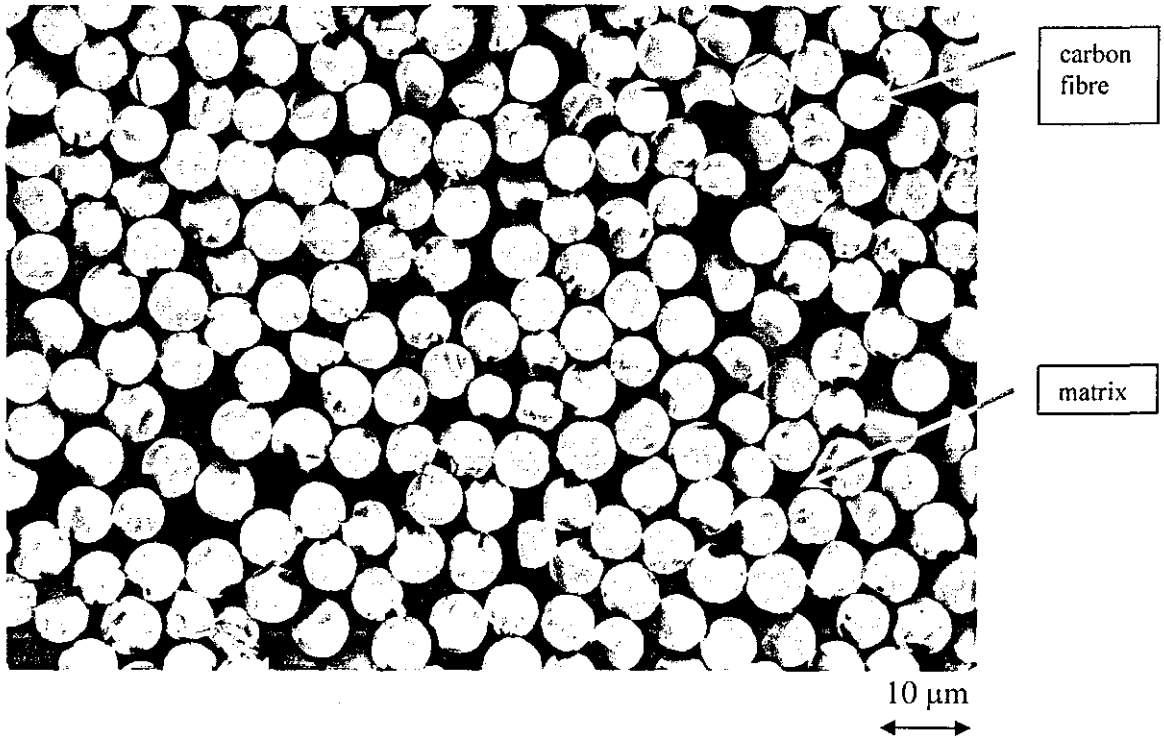


Figure 4.134: Composite produced using method II. SEM micrograph showing the cross-section of the composite with matrix containing unmodified polyimide.

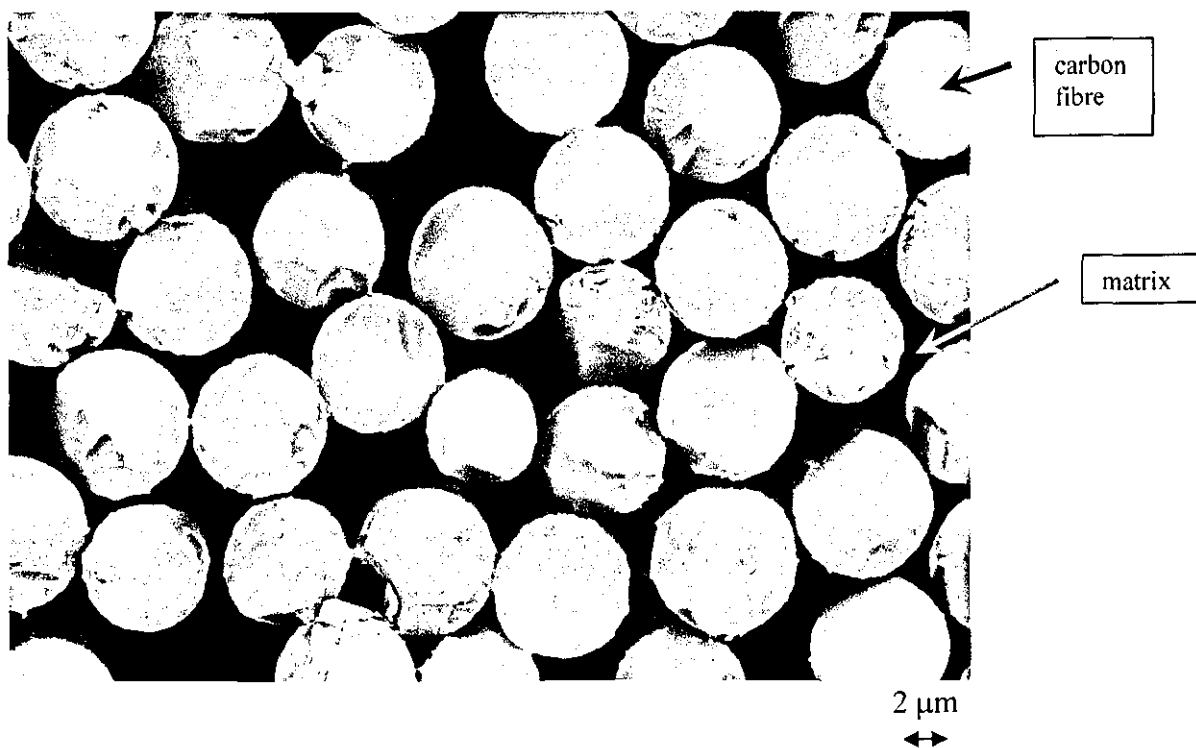
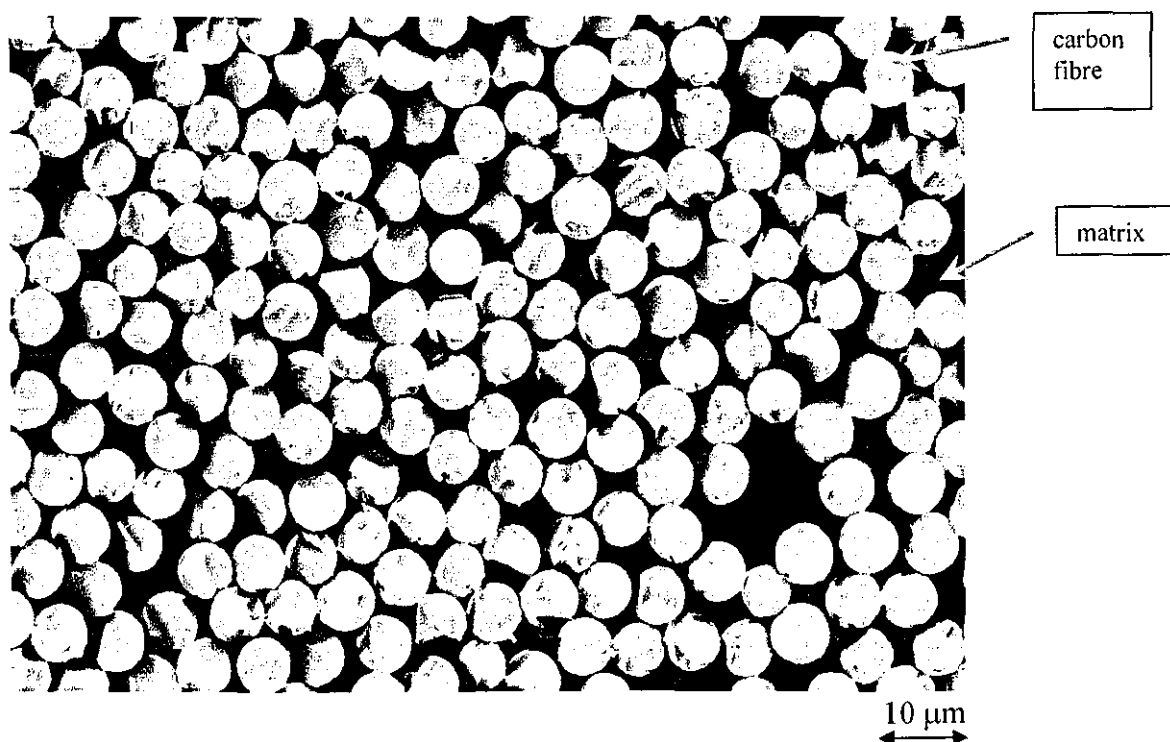


Figure 4.135: Composite produced using method II. SEM micrograph showing the cross-section of the composite with matrix containing polyimide modified with 10% of perfluoroether.

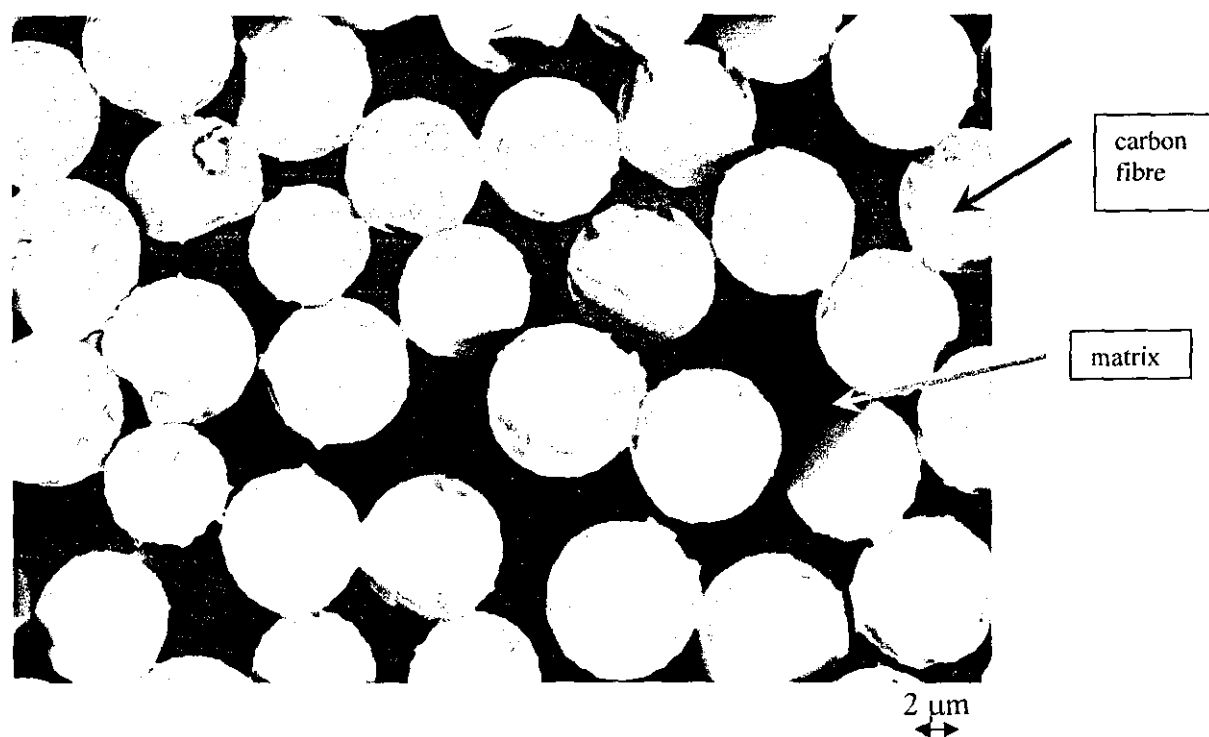
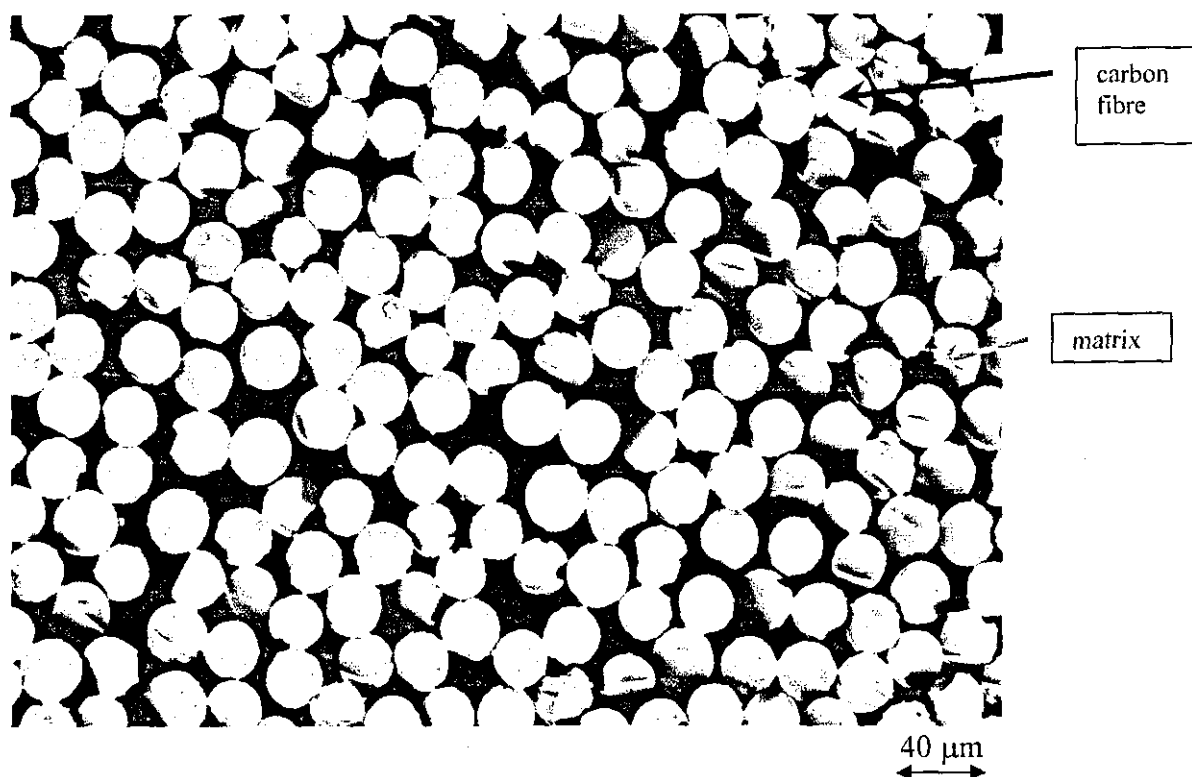


Figure 4.136: Composite produced using method III. SEM micrograph showing the cross-section of the composite with matrix containing unmodified polyimide.

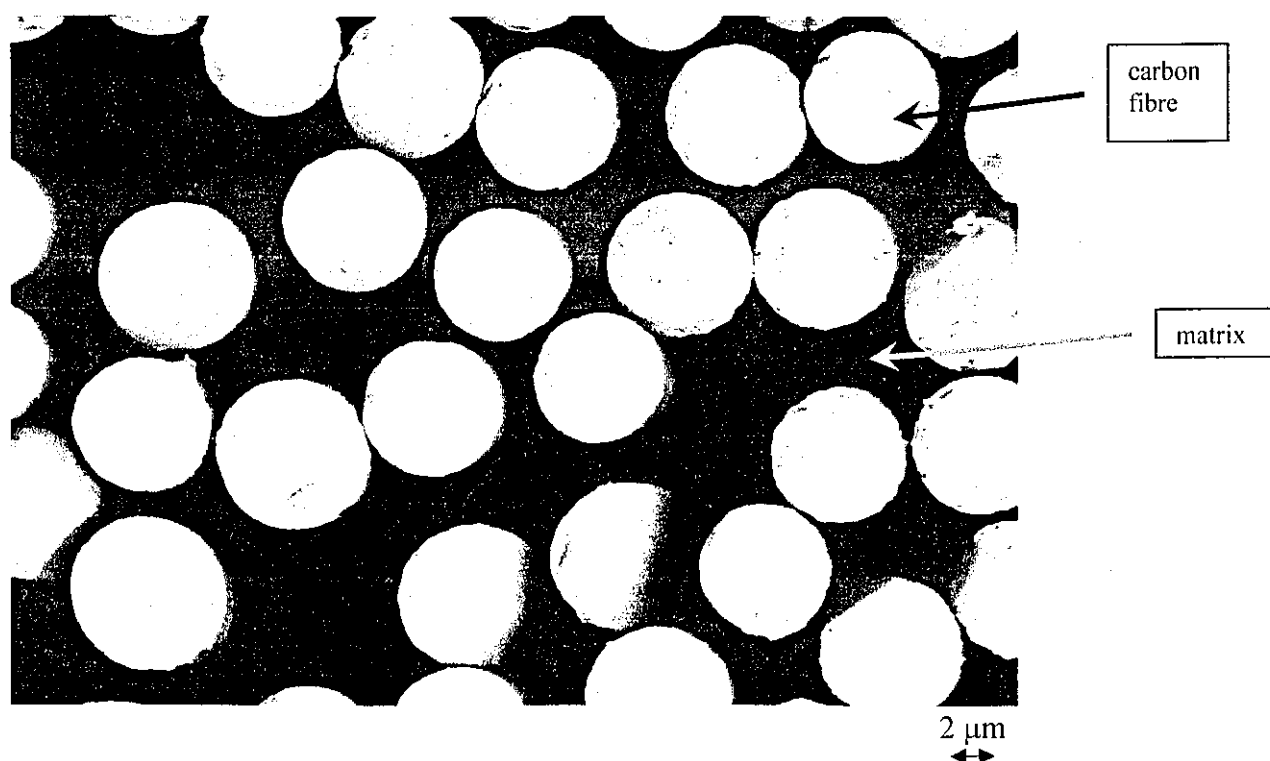
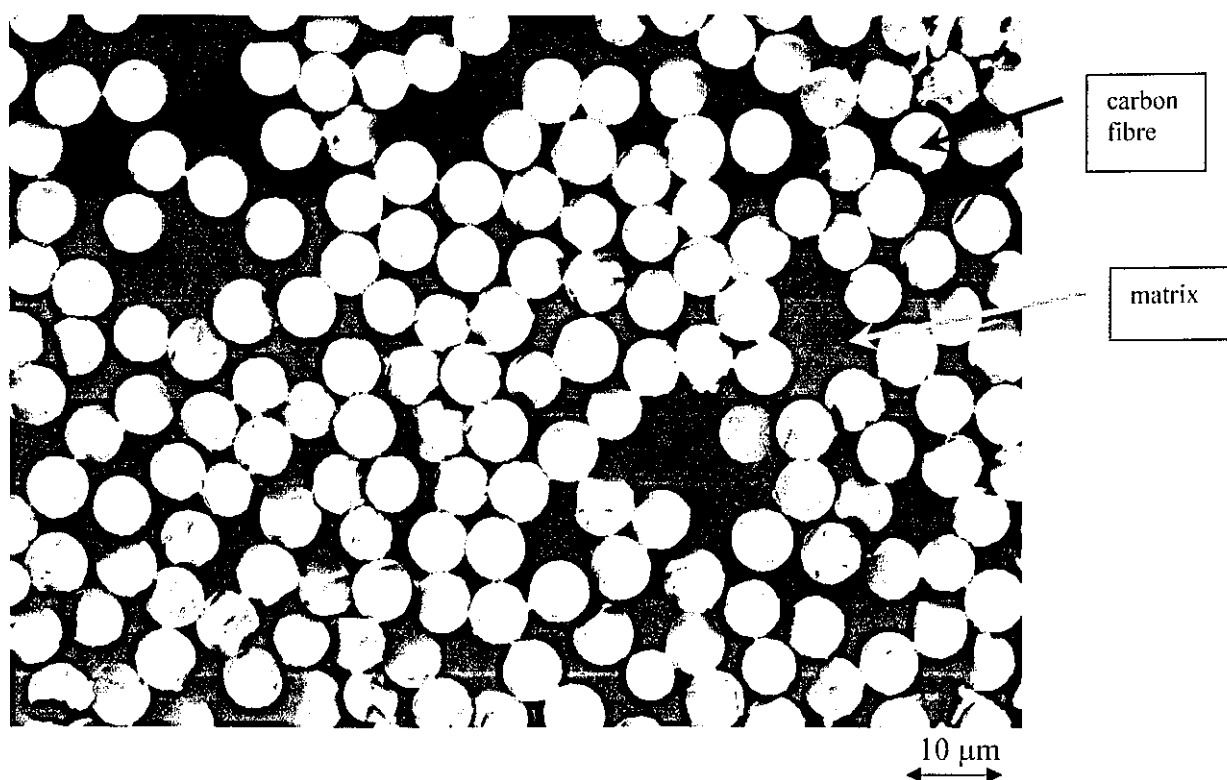


Figure 4.137: Composite produced using method III. SEM micrograph showing the cross-section of the composite with matrix containing polyimide modified with 10% of perfluoroether.

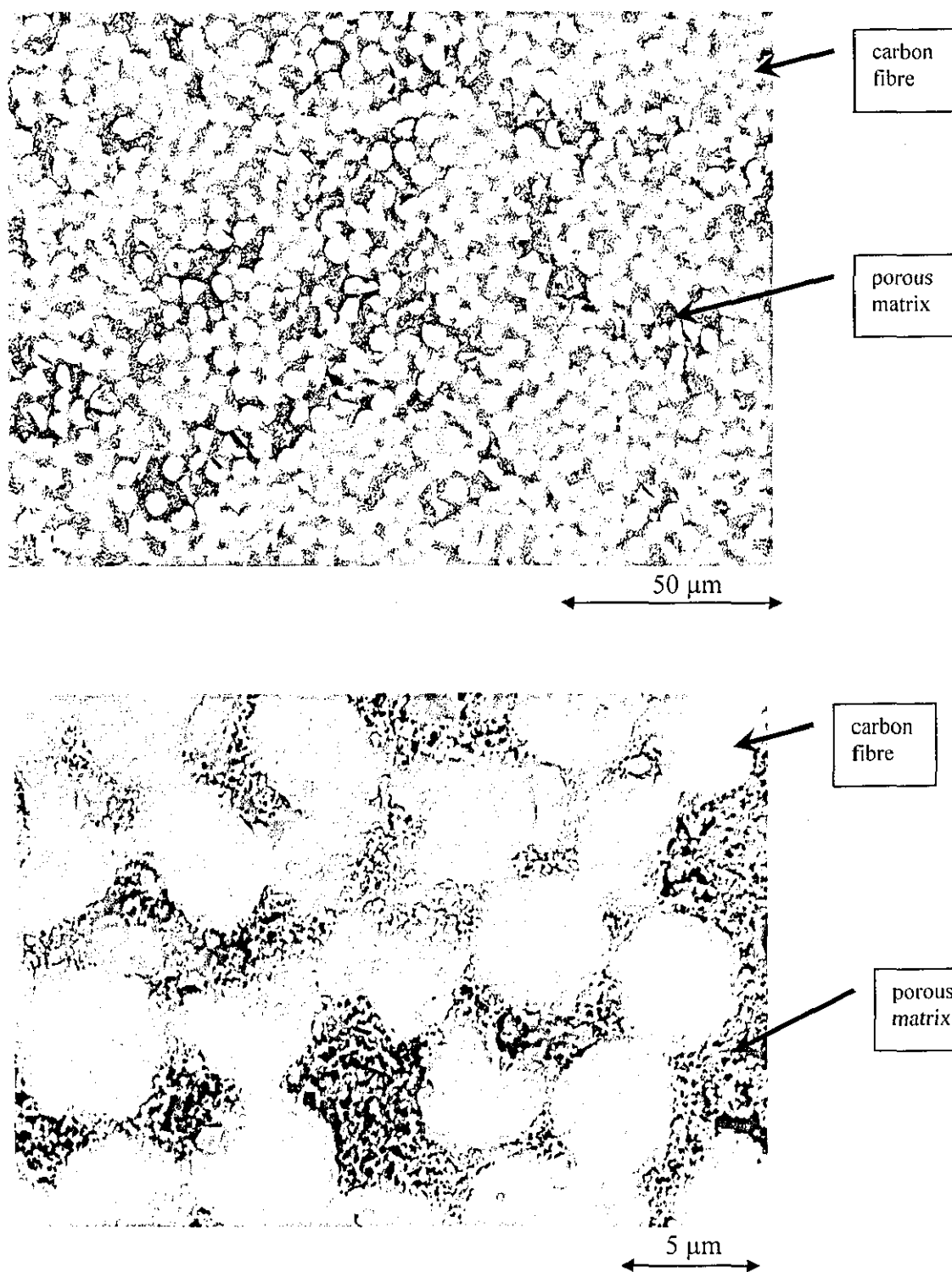


Figure 4.138: Composite produced using method III. SEM micrograph showing the cross-section of the composite with matrix containing unmodified polyimide hybridised with 30% silica.

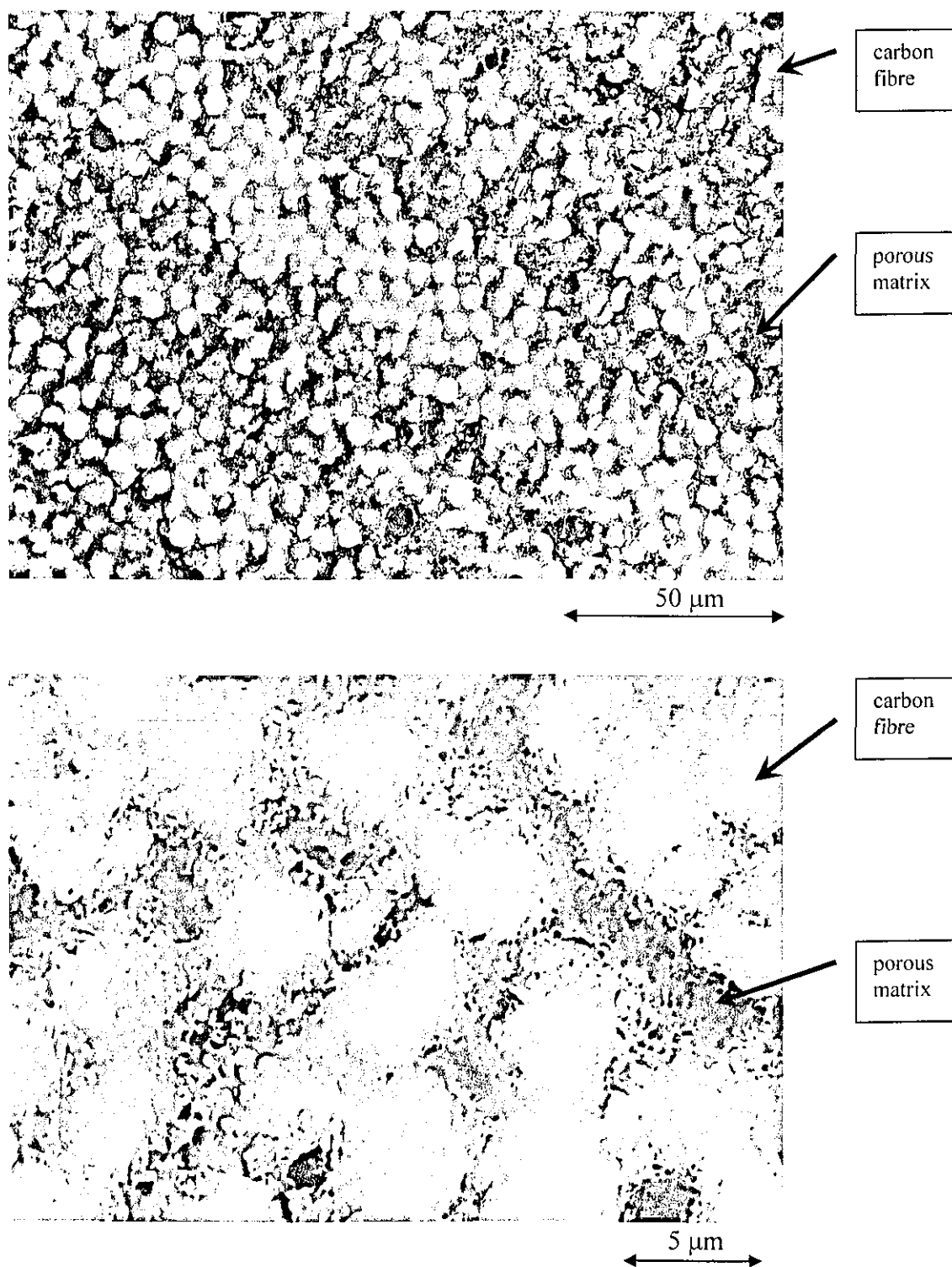


Figure 4.139: Composite produced using method III. SEM micrograph showing the cross-section of the composite with matrix containing polyimide modified with 2.5% of perfluoroether and hybridised with 30% silica.

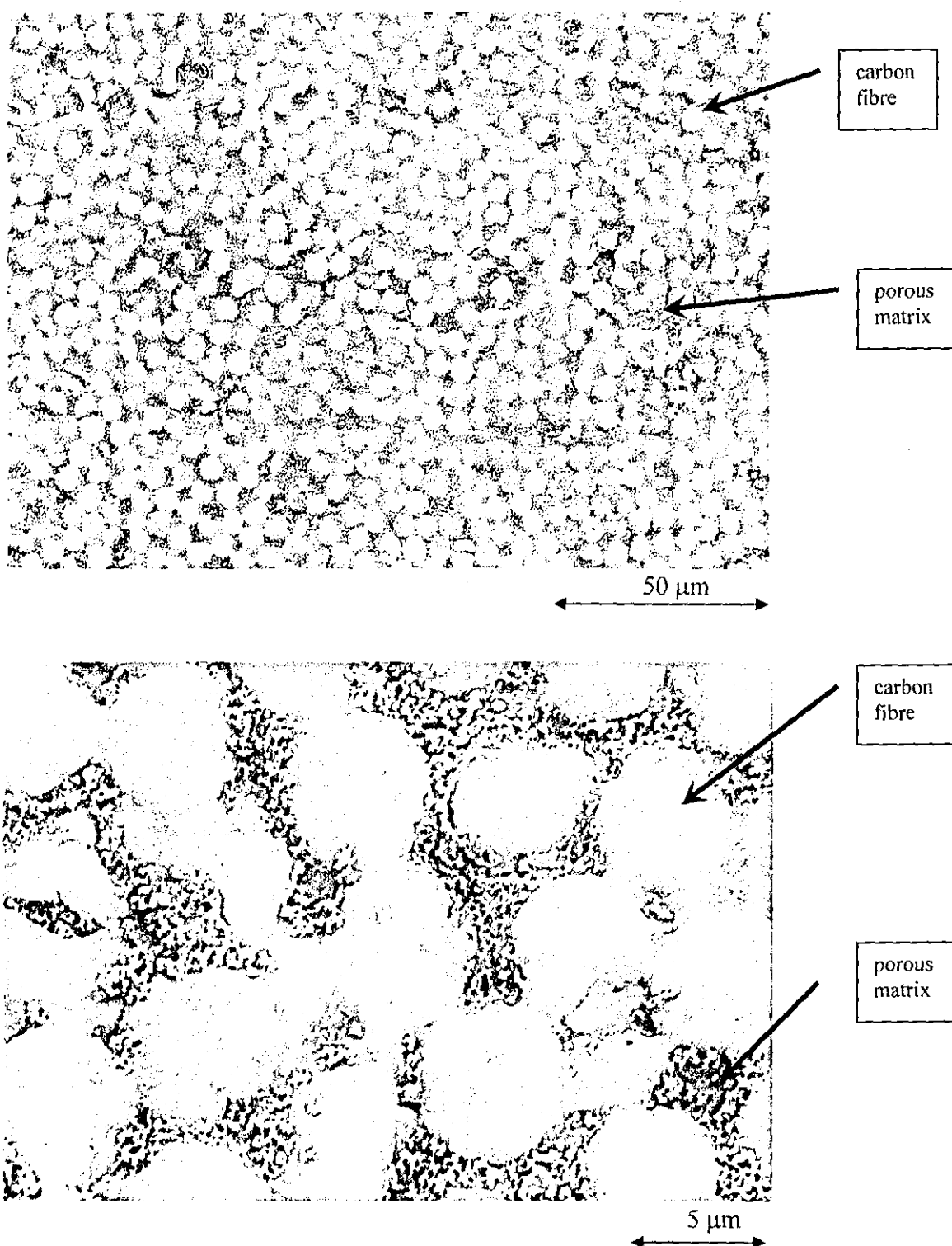


Figure 4.140: Composite produced using method III. SEM micrograph showing the cross-section of the composite with matrix containing polyimide modified with 5% of perfluoroether and hybridised with 30% silica.

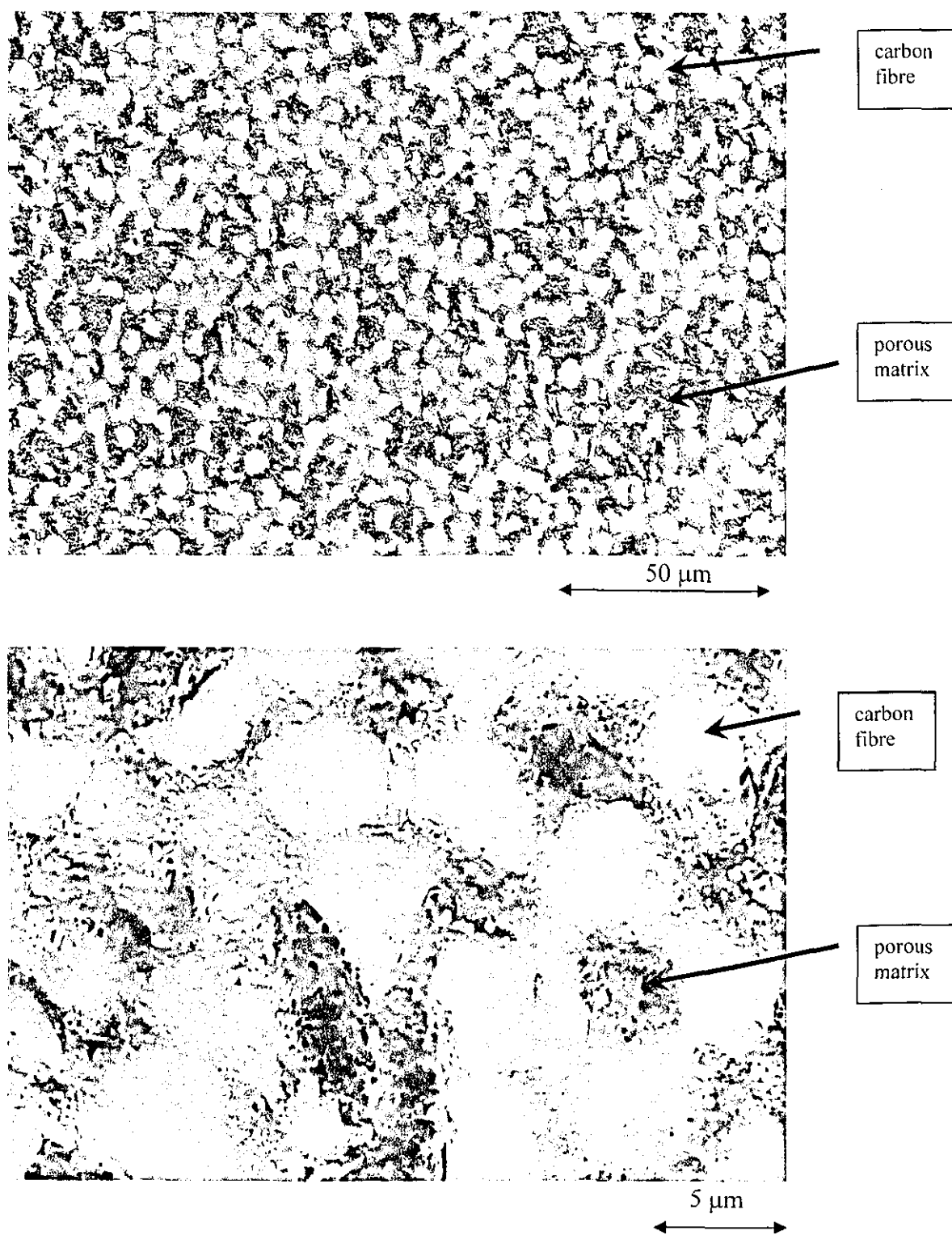


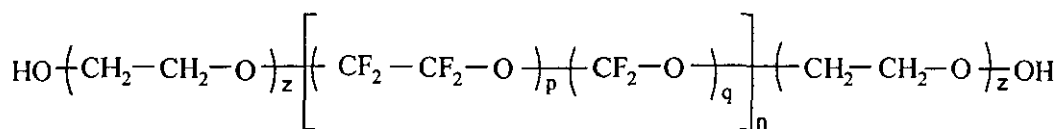
Figure 4.141: Composite produced using method III. SEM micrograph showing the cross-section of the composite with matrix containing polyimide modified with 10% of perfluoroether and hybridised with 30% silica.

5 DISCUSSION

5.1 Perfluoroether Oligomer

Fluoropolymers are known to have very high thermal stability and chemical resistance. Undoubtedly, the most well known example is polytetrafluoroethylene (PTFE) [192]. The outstanding properties of this material can be attributed to two main factors. First, the carbon-fluorine covalent bond strength is very high (485 KJ/mol), especially in comparison to hydrocarbon or carbon-hydrogen covalent bond (413 KJ/mol). Consequently, much higher energy (i.e. higher temperature) is required (in comparison to hydrocarbon) for chain scission to occur. Second, there is a high level of symmetry in the macromolecular structure. This allows the electronegativity resulted from the carbon-fluorine bond to be effectively neutralised by the opposite carbon-fluorine bond of the same carbon. The net effect is that the material has a very low polarisation and is chemically very inert [192]. In addition, these exceptional properties were further enhanced by the fact that the size of a fluorine atom is considerably bigger than both that of a carbon and hydrogen atom. The fluoro-configuration and helix conformation of the polymer chain allow the carbon backbone to be effectively protected from thermal degradation and chemical attack by the large fluorine atoms surrounding the polymer chain [193].

However, PTFE is a highly crystalline material. In addition, the main glass transition temperature (T_g) of PTFE is known to be fairly high at around 11°C and the melting temperature (T_m) is at around 330°C [193]. It is, therefore, not an ideal candidate as a morphological modifier for extremely brittle material such as polyimide, particularly from the point of view of achieving the desired level of miscibility. On the other hand, these limitations are not present in the fluoroether oligomers used in this study, while maintaining the advantages of perfluoroether polymers, i.e. high thermal stability and chemical resistance. The stereoregularity of the oligomeric chain is disturbed by the combination of perfluoroethylene oxide and perfluoromethylene oxide repeat units in the structure:



Where: p/q molar ratio = approximately 0.67

n = approximately 10

z = approximately 1.5

As a result of the lack of regularity in the molecular structure, the oligomer is completely amorphous. In addition, the ether linkages also impart a high level of flexibility to the material by having a low rotation energy barrier in the molecular structure. Hence, the Tg of the perfluoroether oligomer used in this study is around – 120°C [192].

It is important to note that ether linkages are also thermally stable and chemically inert. As such, the resulting perfluoroether possesses almost the same level of heat and chemical resistance as PTFE. The slight inferiority of perfluoroethers with respect to these properties can be mainly attributed to the chain ends. The presence of short aliphatic hydrocarbon segments and functional chain ends enhances the compatibility of the oligomer as a modifier for relatively polar materials such as epoxy resins and polyimides at the expense of thermal stability and chemical resistance.

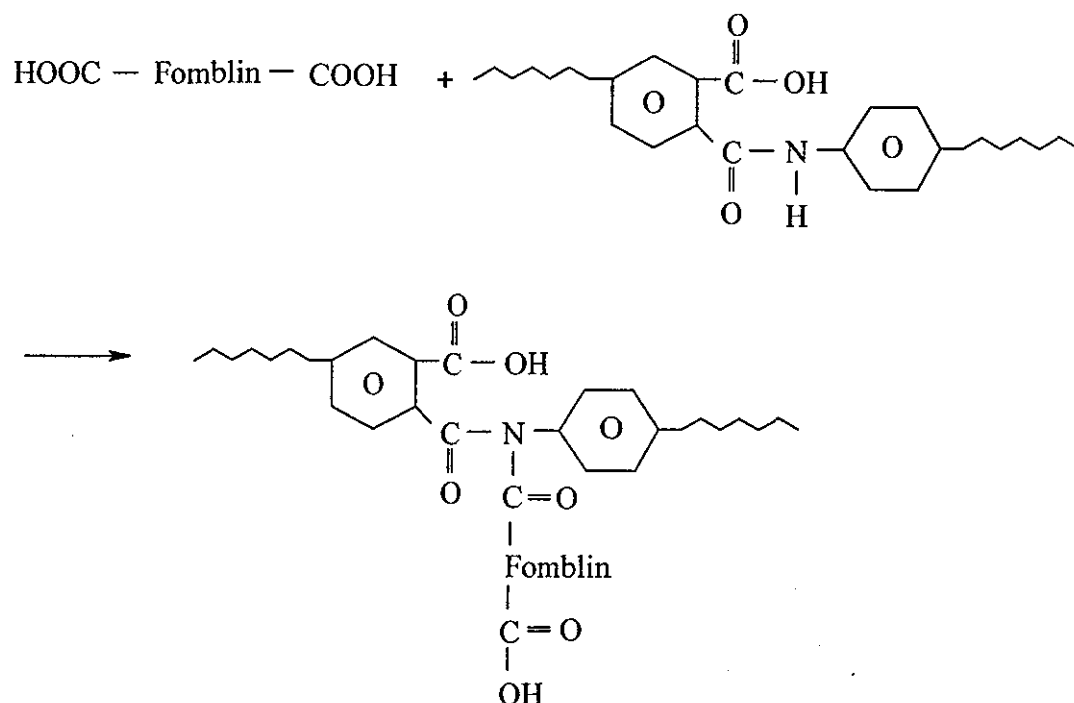
5.2 Acid Functionalisation of Perfluoroether Oligomer

The hydroxyl chain end functionality of Oligomer TX was found to be highly unreactive with polyamic acid. Mixtures of the two liquid materials were observed to phase separate readily, even with prolonged heating at elevated temperatures, to form two bulk layers with the perfluoroether oligomer sinking to the bottom of the mixing container (identified using FTIR).

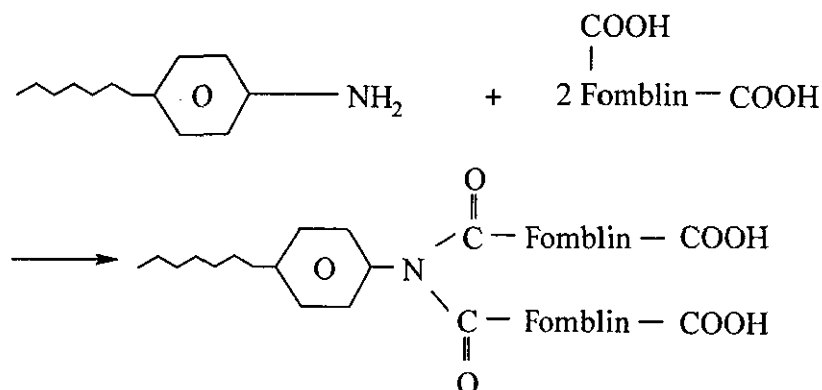
Chlorendic anhydride is a very reactive telechelic modifier and is known to react with Oligomer TX efficiently to form carboxylic chain ends [47]. This acid functionalisation reaction increased both the reactivity and polarity of the oligomer considerably and allowed it to be miscible with polyamic acid in the presence of large

quantity of solvent (see table 4.1). Miscibility in the absence of solvent can be achieved by preheating the Oligomer TX-CA/S703 mixtures in solution at elevated temperatures (two temperatures of 60°C and 80°C were studied). Two possible chemical reactions are proposed:

Intermolecular Imidisation Through Backbone Amide Group



Intermolecular Imidisation Through Chain-End Primary Amine



5.3 Epoxy Functionalisation of Perfluoroether Oligomer

The epoxy functionalisation reaction, as a consecutive telechelic modification step, has enhanced further the reactivity and miscibility of the oligomer with polyamic acid. Reactions of the epoxy groups in the perfluoro-oligomer with the acid groups of the polyamic acid should occur more readily than the reaction of the acid functionalised oligomer with the amide groups of the amic acid. At the same time, the epoxy groups would react more readily than acid groups with the amine end groups in the polyamic acid.

The above hypothesis is well supported by the resulting miscibilities shown in table 4.2. Optical transparencies were available more extensively at various stages of the mixtures studied, especially those pre-reacted at 80°C (in comparison to the miscibilities of mixtures with acid functionalised perfluoroether oligomer, discussed previous).

The reaction conversion in the form of Epoxy Index (EI) is shown in figure 4.3, which further supports the hypothesis, clearly demonstrating that a measurable concentration of epoxide groups was used up in the functionalisation reaction.

5.4 Effects of Epoxy Functionalised Perfluoroether Oligomer on Polyamic Acid and Polyamic Acid / Prehydrolysed Alkoxysilane Mixtures

5.4.1 Characteristics of Curing Mixtures

It is well known that solvents such as NMP and DMAc have a strong affinity to polyamic acid. In a typical solution of polyamic acid, both H-bonded / co-ordinated and free solvent would be present [96-100].

It has been found in this study that in the presence of the epoxidised perfluoroether oligomer, the efficiency of solvent removal during curing is significantly enhanced during curing. *This enhancement can be considered and explained in two ways: first, the perfluorinated structure, the oligomer has very little affinity for polar solvents, which would allow free solvent to be removed quite readily during heating. Second,*

it is hypothesized that the epoxy functionality of the oligomer may be capable of promoting decomplexation of the bonded solvent. NMP is known in the literature to solvate the carboxylic group of the polyamic acid and delay imidisation [102]. It is believed in this study that the co-ordinated structure of the solvent and the carboxylic acid may be substituted by the epoxy-functionality of the perfluoroether oligomer. In fact, it is thought that this is the initial step of the grafting reaction, which allows the oligomer to be eventually covalently bonded to the polyamic acid through an esterification reaction. The two effects may act in solvent removal, in so far as the perfluoro-oligomer is more "finely" dispersed in the polyamic acid as a result of the reaction of the epoxy chain ends in the perfluoroether oligomer with the amic acid.

Conceptually, the removal of free solvent would cause the glass transition temperature of the polyamic acid to increase. This presumes that the plasticising efficiency of the perfluoroether oligomer is not as high as that due to the solvent, which can be easily appreciated from the fact that the molecular weight of solvent is considerably smaller than the oligomer but also by the fact that perfluoroether oligomer is not completely soluble in the polyimide.

On the other hand, the decomplexation of solvated solvent should, theoretically, lead to an increase in the derivative specific heat capacity, ΔC_p , at the glass transition. Conceptually, ΔC_p is related to the enthalpy of segmental motion of an amorphous or disordered phase. Removal of solvent by decomplexation increases the enthalpy through the loss of plasticizing effects on segmental motion and, therefore, should cause the ΔC_p to increase.

The above hypothesis can clearly be evident from the stepwise increase in glass transition temperature and ΔC_p shown in figures 4.34 and 4.33. These stepwise changes with increasing perfluoroether content also indicate that only small amounts (i.e. between 2.5 wt% and 5 wt%) of the perfluoroether modifier are sufficient to affect the removal of both bonded and free solvent. Subsequent increases in amounts of the modifier did not result in further enhancements in solvent removal.

In the case of hybrids, the structural modification with perfluoroether did not result in any significant changes in the ΔC_p value up to 10% addition (see figure 4.45).

The efficiency of solvent removal of the perfluoroether modifier can be further evidenced in the consolidated heat flow signals of the pre-cured films shown in figure 4.47. The endothermic peaks shown as a result of solvent volatisations can be seen to reduce in size substantially with increasing perfluoroether content. In the presence of the modifier, the majority of the residual solvent was removed during the casting stage of the pre-cured films. These drastic changes suggest that some level of solvent decomplexation has also taken place in the presence of the perfluoroether oligomer during the heating process through the DSC.

Again, in the case of hybrids, the enhancement observed in solvent removal, shown in the consolidated heat flow signals (see figure 4.47) was less drastic. However, by comparing the heat flow signal of the unmodified film with that of the equivalent hybrid film (see figure 4.48), it is clear that the solvent removal has been enhanced considerably by the hybridisation. Hence, it is not difficult to appreciate that subsequent enhancement with the perfluoroether modifier become relatively moderate.

5.4.2 Characteristics of Cured Mixtures

The derivative specific heat capacity signals of cured films are considerably less complicated than the uncured films. Three major peaks may be observed in both non-hybridised and hybridised films. For ease of identification, they will be described as first peak (lowest temperature), second peak and third peak (highest temperature).

It is, however, worth noting that the first peak temperature increases considerably from -5°C to 35°C with curing. Conceptually, this can be explained from the point of view that transitional temperatures are relatively more influenced by chain mobility. During curing, the molecular chain became rigid as a result of imidisation. Consequently, chain mobility decreased and transitional temperature increased. In the case of the equivalent hybrid, a slight reduction in the specific heat capacity was

observed, i.e. $\Delta C_p = 0.27 \text{ J/g/}^\circ\text{C}$. This result suggests that some level of molecular interpenetrating network has been formed between the polyimide and the silica structure. This result is in agreement with the hypothesis proposed for the uncured films in relation to molecular interpenetrating network development in hybrids.

The effects of perfluoroether modification on the specific heat capacity of the first peak in both the hybrids and the non-hybrids are shown in figure 5.1. The miscibility level of the perfluoroether modifier can be observed to be highly consistent between the hybrids and the non-hybrids. Their specific heat capacity values increased almost linearly with the increasing perfluoroether content. The hybridisation process, therefore, did not show to affect significantly the miscibility characteristic between the polyimide phase associated with the first peak and the perfluoroether modifier. The effect of the perfluoroether modification on the temperature of the first peak is shown in figure 5.2. The plasticisation effect of the modifier is obvious with the progressive reduction in temperature as a function of the modification level.

The effects of perfluoroether modification on the specific heat capacity of the third peak are shown in figure 5.3. The specific heat capacities of all the non-hybrids are higher than their equivalent hybrids. From the point of view that this peak transition is related to molecular event associated with segmental motion, the suppression of enthalpy reflected in the specific heat capacity results of the hybrids clearly suggest that co-continuous interpenetrating network also occur at the molecular level between the inorganic oxides and the polyimides.

In the non-hybrid system, a very drastic dip was observed at 2.5 wt% modification level. This is deduced to be the result of solvent removal. With subsequent increase in perfluoroether content, the specific heat capacity increases progressively with increase miscibilisation of the perfluoroether modifier in this phase.

The results for the hybrids are simpler to interpret. No dip was observed at low modification level of perfluoroether. This can be explained from the fact that the presence of the silica domains also facilitated the removal of solvent and therefore it decreases the solvent removal effect contributed by the perfluoroether modifier. The

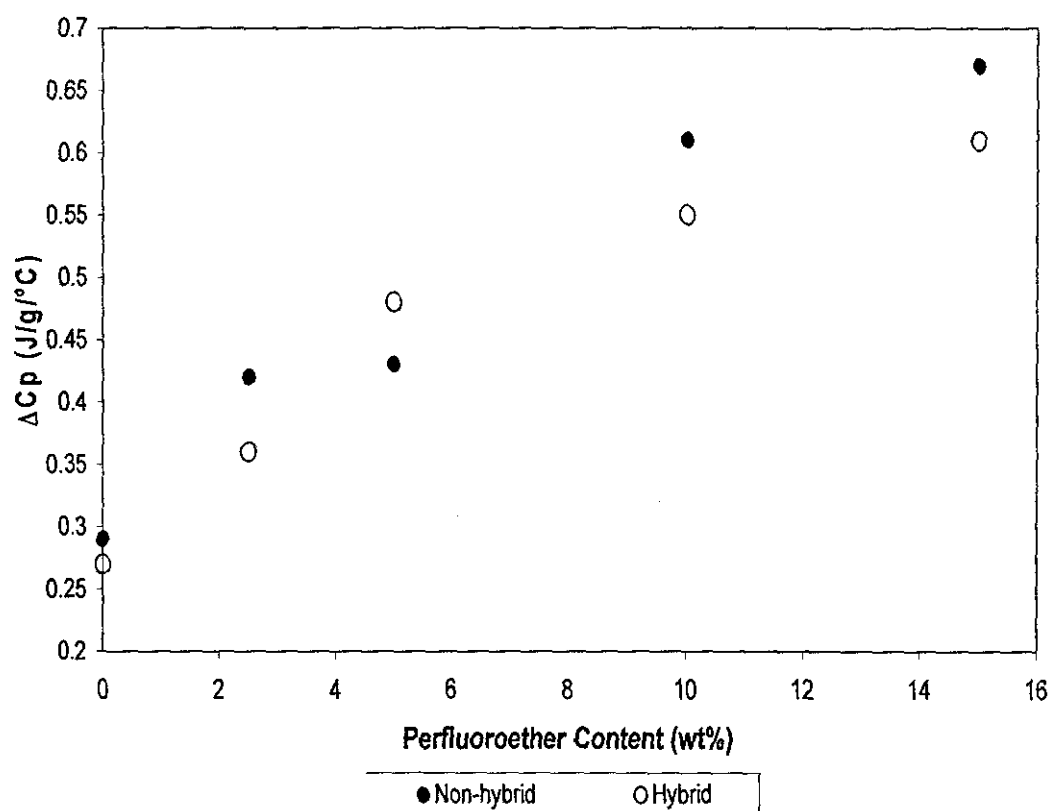


Figure 5.1: Derivative specific heat capacities (peak 1) of fully imidised polyimide and polyimide-silica hybrid films at various concentrations of perfluoroether modification.

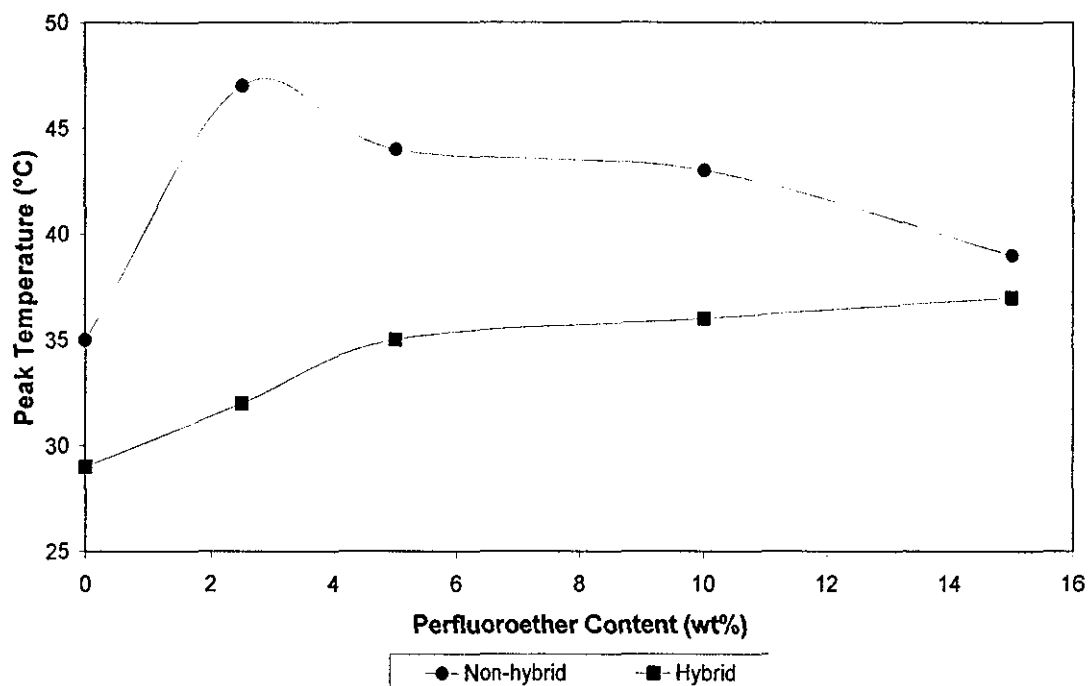


Figure 5.2: Peak temperatures (peak 1) of fully imidised polyimide and polyimide-silica hybrid films at various concentrations of perfluoroether modification.

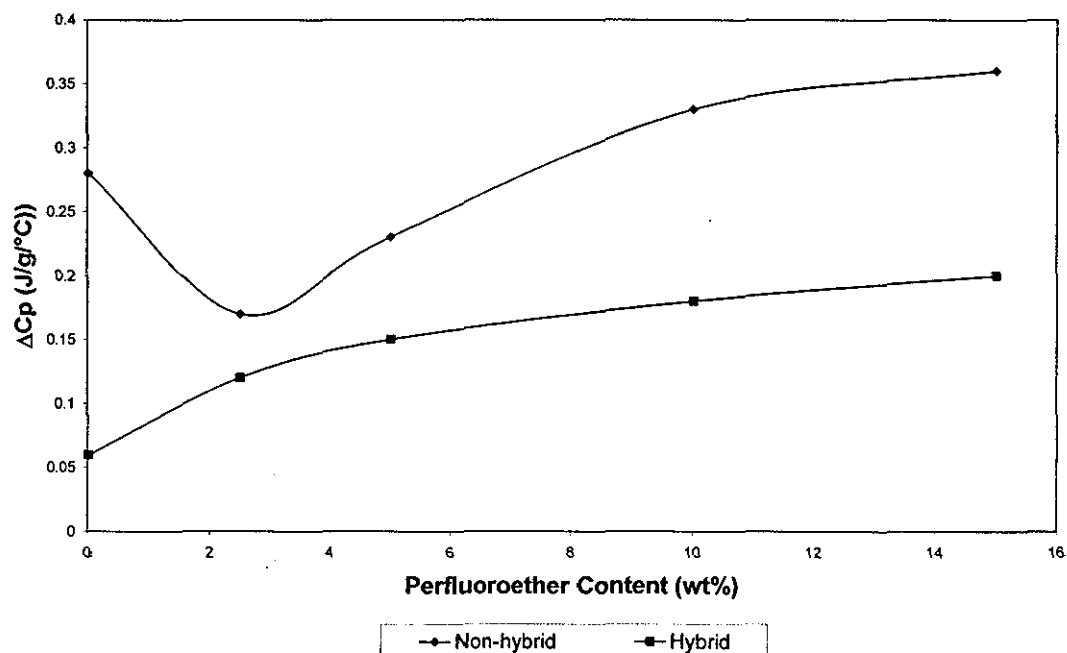


Figure 5.3: Derivative specific heat capacities (peak 3) of fully imidised polyimide and polyimide-silica hybrid films at various concentrations of perfluoroether modification.

progressive miscibilisation effect of the modifier is almost linear with increasing level of modification.

The effect of perfluoroether modification on the peak temperature is shown in figure 5.4. The plasticisation of the modifier is obvious in both the hybrids and the non-hybrids.

The observations on the second peak are not amenable for discussion. This is because it is not significantly affected by both the hybridisation and the perfluoroether modification processes.

5.5 Thermogravimetric Weight-Loss Characteristics of Polyimide Composites

Method I

The thermogravimetric result of the control composite (see figure 4.71) has clearly shown that this method of fabricating the composites using the unmodified polyamic acid would result in a high concentration of solvent remaining in the composite (i.e. 23 wt%) after moulding. This effect may be attributed to a number of reasons:

- (a) The major solvent is NMP. This is a high boiling point solvent and has been illustrated earlier in the discussion to have a very affinity to polyamic acid / polyimide. This property, therefore, prevent the solvent from being removed from an unmodified polyimide system easily through evaporation.
- (b) The presence of the carbon fibre constitutes a physical barrier for solvent diffusion and evaporation and hence suppressed the rate of solvent volatisation.
- (c) The fabrication time during winding and impregnation is too short. This did not allow sufficient time for solvent evaporation before moulding.

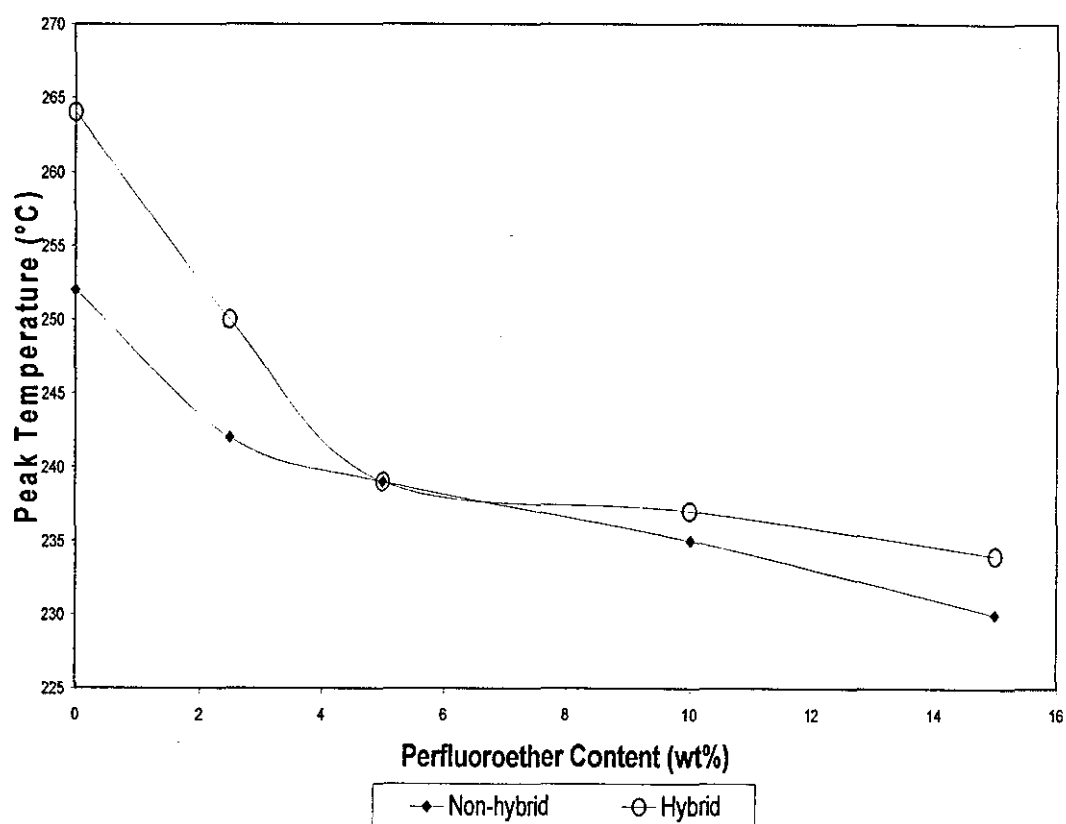


Figure 5.4: Peak temperatures (peak 3) of fully imised polyimide and polyimide-silica hybrid films at various concentrations of perfluoroether modification.

- (d) The use of a closed (leaky) moulding technique highly reduced the surface area available for the solvent to escape during moulding.

The effect of using perfluoroether modifier and silica hybridisation in enhancing the rate of solvent removal has been illustrated in figure 4.75 and has been discussed in depth earlier. As both method of modifications were very efficient in enhancing the removal of solvent, and there was only a finite quantity of solvent in the composite, by having the combination of both of the modification methods did not resulted in an additive effect in term of solvent removal.

The resin contents of the four samples evaluated thermogravimetrically were shown in figures 5.5. It is clear that both hybridisation and perfluoroether modification have an effect in increasing the resin content of the composites. This is believed to be due to the increased viscosity in both cases and hence resulting in lesser "squeeze out" of the resins during moulding. The perfluoroether modifier has a higher viscosity than the polyamic acid in solution and hence an increase in viscosity with modification is easy to understand. In the case of the hybrids, the increase in viscosity is a result of progressive condensation reaction of the hydrolysed alkoxysilane. An additive effect can be observed when both methods of modifications were used in combination (sample 10% AS (hybridised) in figure 5.5).

Method II

The thermogravimetric results of the various composites produced using method II are shown in figures 5.6 and 5.7, which correspond to their resin and solvent content, respectively.

First, it is clear from figure 5.6, the resin contents of all the composites were substantially higher than those produced using method I. The explanation is relatively simple. The winding and resin impregnation process was carried out with intervals of drying time. This allowed the resin solution to dry and for viscosity to built-up.

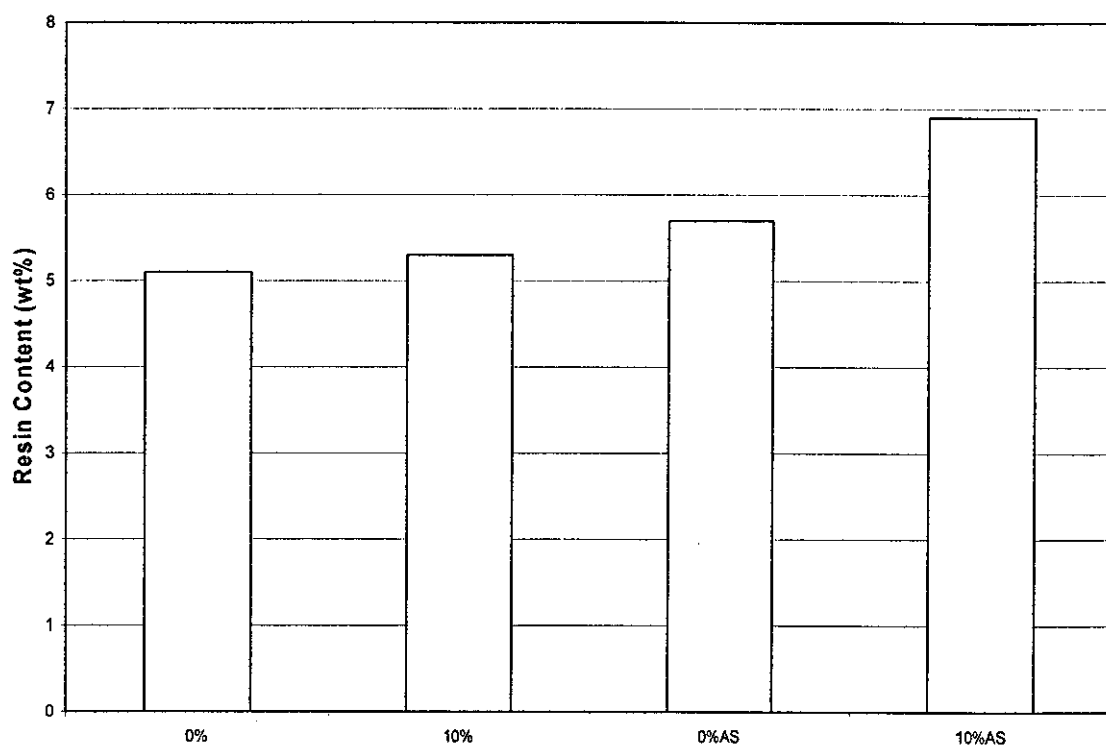


Figure 5.5: Resin content of composites produced using method I. Results were obtained from thermogravimetric analysis of the composites evaluated. AS = hybridised.

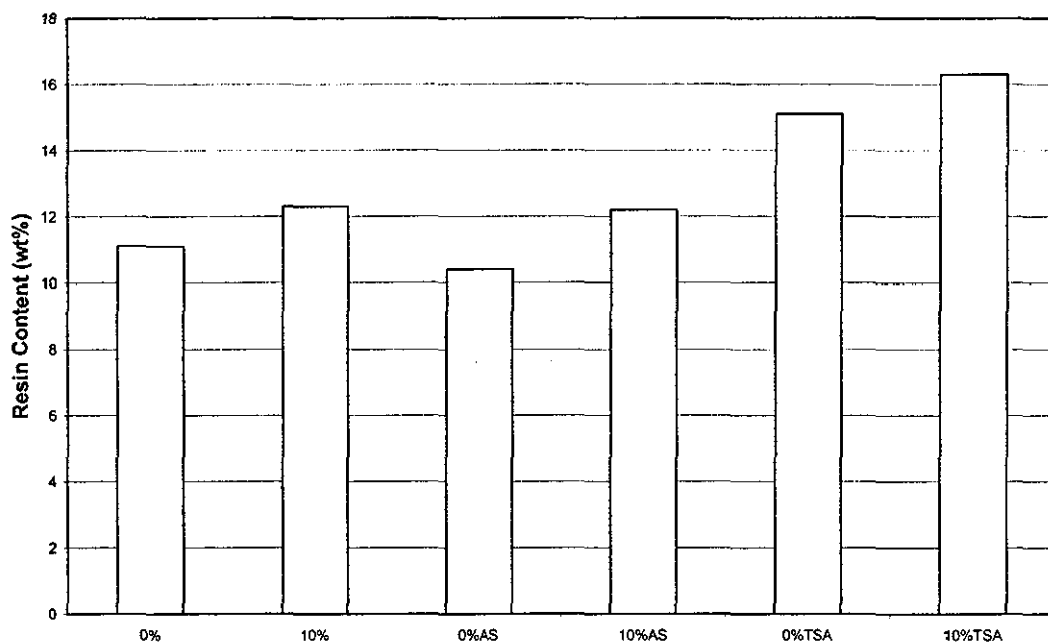


Figure 5.6: Resin content of composites produced using method II. Results were obtained from thermogravimetric analysis of the composites evaluated. AS = hybridised. TSA = p-toluene sulphonic acid.

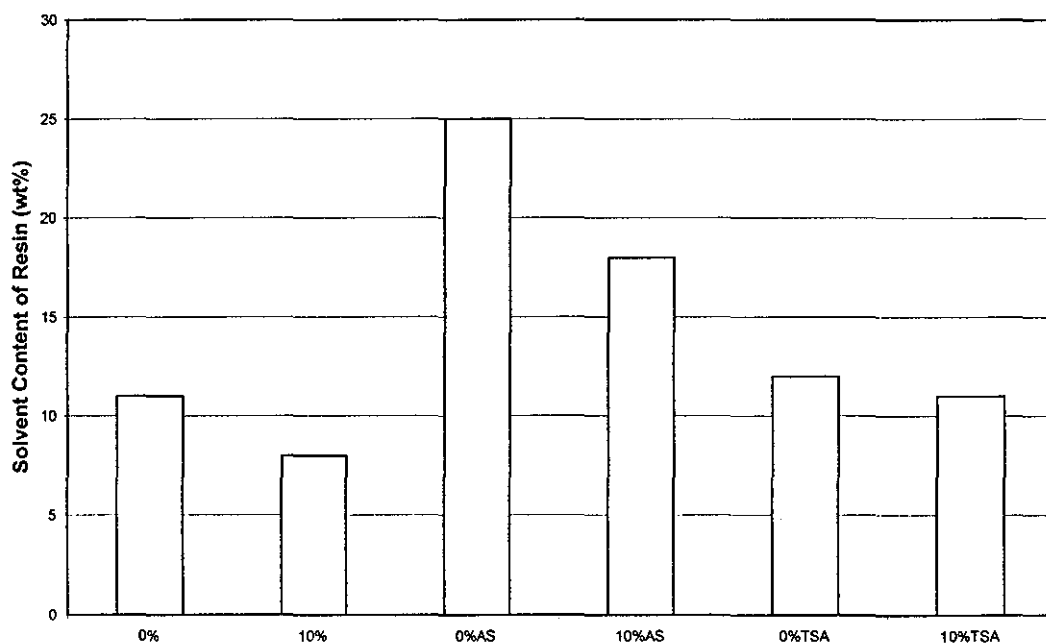


Figure 5.7: Solvent content of composites produced using method II. Results were obtained from thermogravimetric analysis of the composites evaluated. AS = hybridised. TSA = p-toluene sulphonic acid.

Consequently, more resin can be impregnated and less “squeeze out” occurred during moulding, leading to higher resin content.

Consistent to the observation in method I, perfluoroether modification resulted in further increase in resin content. However, in the case of hybrids that were produced using hydrochloric acid prehydrolysed alkoxysilane, a slight reduction in resin content was found (see samples 0% AS and 10% AS in figure 5.6), which was different to the trend shown in method I. Although perfluoroether modification did result in increased resin content in the hybrid (compare samples 0%AS and 10% AS in figure 5.6), the increment was not additive.

By studying the solvent content results shown in figure 5.7, some explanation may be offered to the discrepancies highlighted above, i.e. between the hybrids of method I and II. In the non-hybrid samples (0% and 10% of perfluoroether modification), the solvent contents were found to be considerably lower than those produced using method I, which reflect the effectiveness of the drying intervals associated with method II. In case of the hybrid samples (0% AS and 10% AS), the observations were very different. These samples had extremely high solvent contents and are thought to be the main reason for the lower than expected solid contents, which is the “dried” quantity after solvent removal in the thermogravimetric analyser.

The high solvent contents of the hybrids may be attributed to the premature gelation of the inorganic oxide phase. A rigid porous structure was formed during the impregnation stage which was thought to provide a “temporary storage” for solvent. In addition, the compression moulding step that was carried out subsequently may also became less effective in solvent removal as a result of the rigid phase, i.e. the solvent was not subjected to adequate compressive stress intrinsically for its efficient expulsion from the composites. These “stored” solvents were thought to be chiefly free and not “bound”, which can be evident by the gradual weight-loss trend observed before the first weight-loss step.

From figures 5.6 and 5.7, it is clear that the hybrid composites prepared using TSA have significantly less solvent in them than those prepared using HCl. In addition,

considerably higher resin contents are also observed. In fact, they have the highest resin contents of all composites discussed so far.

Previous study in IPTME has demonstrated that the use of TSA for hydrolytic catalysis of the alkoxysilane would result in a significant retardation of its condensation reaction following hydrolysis. Due to this reason, all the TSA composites did not suffer from premature gelation before moulding. Consequently, it is not difficult to understand that these composites have very high resin content, taking into account the combined effects of the drying intervals and the enhanced solvent removal efficiency from the evolving silica phase.

Method III

The thermogravimetric results of the various composites produced using method III are shown in figures 5.8 and 5.9, which correspond to their resin and solvent content, respectively.

Both the hybrids and non-hybrids result trends in term of solid contents were very similar to those of method II, except that they were even more pronounced, i.e. even higher resin contents, due to the prolonged drying procedures.

In term of solvent contents, lower values were observed in comparison to method II, which is understandable, taking into account the prolonged drying during fabrication. The solvent level is especially low in the non-hybridised composite with perfluoroether modification (see sample 10%). This sample has only 3 wt% of solvent with respect to its resin content, which reflect an enormous improvement from the initial control composite in method I with 23 wt% of solvent.

5.6 Thermomechanical and Mechanical Properties of Composites

It is important to note at this point that in the DMTA experiments, all the samples were tested in the transverse direction of the carbon fibre. Hence, small deviations in the thermomechanical and adhesion properties of the resin to the continuous fibre will result in an enormous “amplification” of the resulting trend.

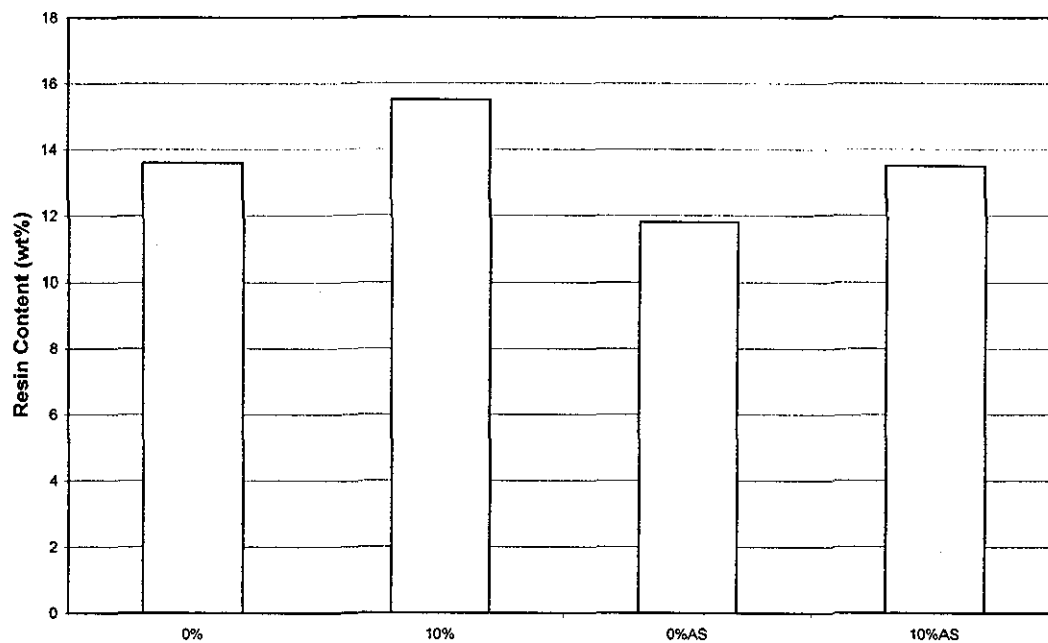


Figure 5.8: Resin content of composites produced using method III. Results were obtained from thermogravimetric analysis of the composites evaluated. AS = hybridised.

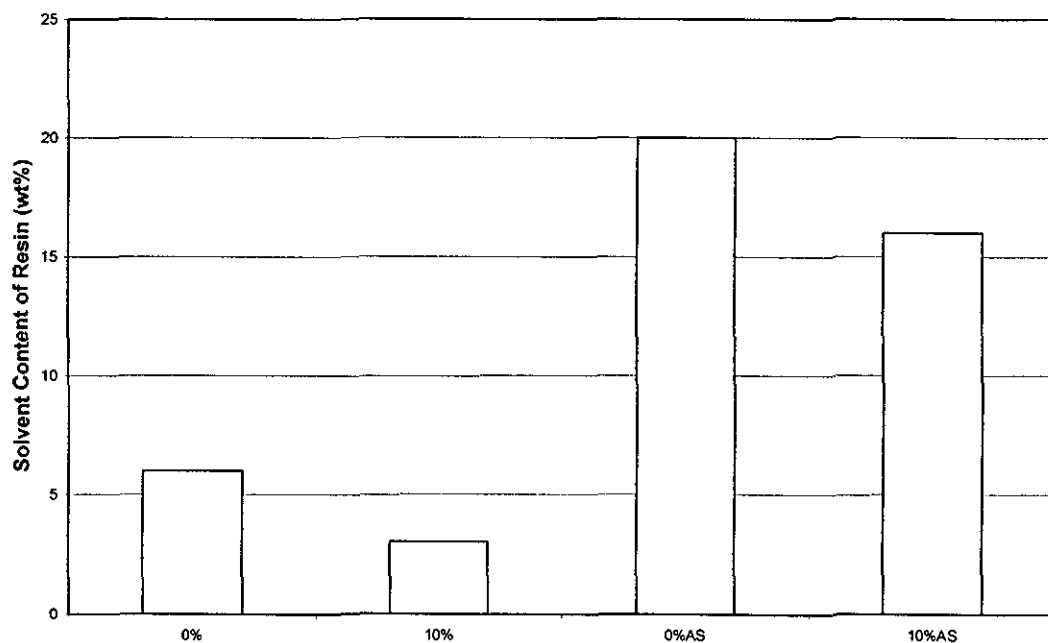


Figure 5.9: Solvent content of composites produced using method III. Results were obtained from thermogravimetric analysis of the composites evaluated. AS = hybridised.

On the other hand, the mechanical testing of the samples was evaluated along the fibre direction. In this case, the reinforcing characteristics of the composites as a whole were reflected in the results.

Method I – Non-hybridised Composites

As can be observed in the DMTA results of composites produced using method I relatively unpredictable trends were observed in the non-hybridised samples (see figures 4.90 and 4.91). These fluctuations may be attributed to the extremely low resin contents (approximately 5 wt% based on TGA results). At low perfluoroether modification levels (2.5 wt% and 5 wt%), the solvent contents may have dipped suddenly, causing the resin to lose its ability to wet the composite effectively. This deficiency was reflected explicitly due to the transverse orientation of the samples. At higher modification level (10%), the resin content and viscosity of the impregnating resin may started to build-up slightly, causing the dynamic mechanical properties of this composite to improve.

The improvement in mechanical properties of the non-hybridised composites with increasing perfluoroether content (flexural and interlaminar) may be attributed to the reduction of solvent, which is well known traditionally to have a serious detrimental effect on these properties.

Method I – Hybridised Composites

The scatter in the DMTA results was not observed in the hybrid samples (see figures 4.95 and 4.96). Instead, a progressive increase in damping characteristics was observed with increasing perfluoroether content. The enhanced damping capacity of the composite clearly reflected the rubbery nature of the perfluoroether phase.

On the other hand, the mechanical properties were shown to degenerate significantly with increasing perfluoroether content. This may be explained from the point of view that in the presence of the silica phase, solvent has been removed significantly and hence the plasticisation effect of the perfluoroether modifier became the dominant factor (see figures 4.97 and 4.99).

Method II – Non-hybridised Composites

Composites of method II have noticeably higher resin contents than those of method I. Unsurprisingly, a clear and well defined trend can be observed in the DMTA results (see figures 4.100 and 4.101). This observation therefore, further supported the deduction earlier that the scatter in method I composites was a result of very low resin content.

The effect of enhanced damping can be observed with the increasing perfluoroether content. More interestingly, this effect occurred in combination with an increasing glass transition temperature. By considering the fact that solvent was removed more efficiently by the modifier, the results of the glass transition were not unexpected.

The plasticisation of the perfluoroether modifier clearly is observed in all the mechanical properties evaluations in figures 4.102 to 4.103.

Method II - Hybridised Composites (HCl)

It has been hypothesized earlier that this group of composites suffered from premature gelation of the silica phase. The DMTA results of these composites clearly supported the hypothesis. The huge peaks shown in the $\tan \delta$ results are associated with the melting of NMP, which has a melting point around -24°C . The reduction of this peak with the addition of perfluoroether modifier is in agreement with the previous discussion stating its removal by the presence of the modifier (see figure 4.106).

It is believed in this study that the gelation of the silica phase prevented the matrix to become fully compacted during moulding. The curing resin was unable to experience adequate compressive stress and heat intrinsically in the presence of the rigid silica phase. However, the addition of the perfluoroether modifier increased the compliance of the resin and allowed the flow of the matrix resin to occur more readily. The progressive increase in storage modulus of the DMTA results with increasing perfluoroether content clearly supported this hypothesis (see figure 4.105). The

improvement in mechanical properties with increasing perfluoroether content can also be observed in figures 4.107 to 4.109.

Method II – Hybridised Composites (TSA)

The use of TSA for the hydrolytic catalysis of the alkoxysilane should allow the prevention of premature gelation. This is because condensation of hydrolysed alkoxysilane is known to retard substantially in the presence of TSA at room temperature [194].

The above prediction can be supported by the DMTA results. The melting peak of NMP was not present in the $\tan \delta$ result. The extremely high storage modulus of the unmodified composite also clearly illustrated that the sample was allowed to imidise and hybridise fully during moulding.

Method III – Non-hybridised Composites

From the DMTA mechanical properties results, it is clear that the plasticization of the perfluoroether modifier was considerably more pronounced than that observed in method II. This is a clear illustration that the resin content of composites has become too high with the extensive drying procedures.

Method III – Hybridised Composites

In the case of hybrid, the effect of pre-mature gelation of silica was observed to be less pronounced than method II. The smaller melting peak of NMP can be explained from the fact that more time was allowed for drying and hence more NMP was removed. In addition, the gelation of silica would have reached a more advanced stage. Therefore, this brittle silica phase may become more prone to “crushing” during moulding and hence has a lesser effect in preventing resin flow during moulding.

5.7 Scanning Electron Microscopy of the Composites

The effects of composites fabrication methods, perfluoroether modification and silica hybridisation discussed in detail above can also be appreciated to a certain extent by examining their various SEM micrographs.

The cross-sections of the composites produced using method I are shown in figures 4.130 to 4.133. The resin content of the control (figures 4.130) can be observed to be very low, i.e. all the fibres are packed very closely to each other. Both perfluoroether modification (see figure 4.131) and silica hybridisation (see figure 4.132) that were carried out in isolation did not seem to show to improve the resin content level to a significant degree. However, when perfluoroether and silica were present in combination, some increase in resin content can be observed (see figures 4.133).

The SEM micrographs of the composites produced using method II and method III are shown in figures 4.134 to 4.141. In these instances, the effects of prolonged drying time and perfluoroether modification in increasing resin content can be appreciated more substantially. Method III composites can be seen to have fibres less closely packed than method II composites. Perfluoroether modification enhances this effect of increasing resin content ever further.

The effect of premature gelation of silica is illustrated using method III hybrid composites (see figures 4.138 to 4.141). The porosity of the matrices can be seen to decrease noticeably with increasing level of perfluoroether modification.

6 CONCLUSIONS

The conclusions drawn in relation to the various aspects of this work can be summarised below:

- Hydroxyl-terminated perfluoroether oligomer was found to be immiscible with polyamic acid.
- Telechelic modification to produce acid functionality can be achieved using chlorendic anhydride. Miscibility was found to be achievable by preheating the acid functionalised perfluoroether with polyamic acid at elevated temperatures of 60° C and 80 °C.
- Epoxy functionalisation as a consecutive telechelic modification step was found to enhance the miscibility of the oligomer even further with polyamic acid, especially in the form of dried films.
- Epoxy functionalised perfluoroether was found to significantly enhance the removal of solvent during the curing of the polyamic acid to form polyimide.
- The resin content of carbon fibre composites may be increased by introducing intervals of drying time during the lay-up stage. In the case of composites containing perfluoroether modifier, the resin contents were increased further. In the case of hybrids (HCl type), the prolonged lay-up procedures were found to be undesirable as they resulted in premature gelation of the silica which was severely detrimental to the performance of the composites produced. This difficulty may be resolved to a large extent by using TSA for the hydrolytic catalysis of the alkoxysilane and to a smaller extent by perfluoroether modification.
- DMTA results of composites result show that perfluoroether modification would result in an increase in damping capacity and glass transition at the same time.

7 RECOMMENDATION FOR FURTHER WORKS

In view of the results and conclusions derived from the present work, the followings are recommended for further work:

1. The effects of perfluoroether modification on the overall toughness of the composites produced were not studied. Toughness enhancement is traditionally studied using fracture mechanics. However, this method of assessment is well known to be unreliable with composites. As such, the development of a more reliable technique should be considered.
2. The effects of varying the silica content of the hybrids produced should be studied.
3. The present study involved the modification of polyimide-silica hybrids with perfluoroether oligomer. This resulted in a heterophase material where the silica domains were present predominantly in the polyimide matrix. To this end, it would be interesting to explore the possibility of modifying polyimide with perfluoroether-silica hybrids, where the silica domains are contained predominantly in the perfluoroether phase.

8 REFERENCES

1. J.A. Brydson, *Plastics Materials*, Butterworth Heinemann, (1995)
2. A.A. Collyer, *Rubber Toughened Engineering Plastics*, Chapman and Hall, (1994)
3. D.A. Scola, J.H. Vontel, *Polym. Compos.*, 9, 443, (1988)
4. W. Volksen, *Adv. Polym. Sci.*, 117, 113, (1994)
5. R. Juran, *Modern Plastics Encyclopedia*, McGraw-Hill, (1989)
6. V. Wigotski, *Plastics Engineering*, 259, (1988)
7. D.C. Clagett, *Encyclopedia of Polymer Science and Engineering*, Wiley, 6, 94, (1986)
8. M. Bakker, *Kirk-Other Encyclopedia of Chemical Technology*, Wiley, 9, 118, (1980)
9. L.A. Utracki, *Soc. Plast. Eng.*, 33, 1339, (1987)
10. G.D. Cooper, G.F. Lee, A. Katchman, C.P. Shank, *Mater. Technol.*, 13, (1981)
11. C.B. Bucknall, *Toughened Plastics*, Applied Science, (1977)
12. M.E. Soderquist, R.P. Dion, *Encyclopedia of Polymer Science and Engineering*, Wiley, 16, (1989)
13. S.Y. Hobbs, M.E.J. Dekkers, V.H. Watkins, *Polymer*, 29, 1598, (1988)
14. S.Y. Hobbs, M.E.J. Dekkers, V.H. Watkins, *J. Mater. Sci.*, 24, 2025, (1989)
15. S.Y. Hobbs, M.E.J. Dekkers, V.H. Watkins, *J. Mater. Sci.*, 23, 1219, (1988)
16. D.R. Paul, J.W. Barlow, H. Keskkula, *Encyclopedia of Polymer Science and Engineering*, Wiley, 12, 339, (1988)
17. S. Wu, *Polymer*, 26, 1855, (1985)
18. S. Wu, *Polym. Eng. Sci.*, 27, 335 (1987)
19. S. Wu, *J. Appl. Polym. Sci.*, 35, 549, (1988)
20. R.J.M. Borggreve, R.J. Gaymans, *Polymer*, 30, 63, (1989)
21. R.J.M. Borggreve, R.J. Gaymans, J. Schuijjer, *Polymer*, 30, 71, (1989)
22. R.J.M. Borggreve, R.J. Gaymans, A.R. Luttmer, *Macromol. Symp.*, 16, 195, (1988)
23. A.J. Oshinski, H. Keskkula, D.R. Paul, *Polymer*, 33, 268, (1992)
24. A.J. Oostenbrink, L.J. Molenaar, R.J. Gaymans, *Polyamide-Rubber Blends*, (1990)

25. E.A. Flexman, D.D Huang, H.L. Snyder, Polym. Prepr., 29, 189, (1988)
26. E.A. Flexman, US Patent 4804716, (1989)
27. S.Y. Hobbs, M.E.J Dekkers, V.H. Watkins, Proc. 2nd Topical Conf. Engineering Tech., AIChE, (1989)
28. N. Shibuya, Y. Sobajima, H.Sano, US Patent 4743651, (1988)
29. B.N. Epstein, US Patent 4174358, (1979)
30. O. Olabisi, L.M. Robeson, M.T. Shaw, Polymer-Polymer Miscibility, Academic Press, (1979)
31. E.H. Mertz, G.C. Claver, M. Baer, J. Polym. Sci., 22, 325, (1956)
32. S. Kunz-Douglas, P.W.R. Beaumont, M.F. Ashby, J. Mater. Sci., 15, 1109, (1980)
33. C.B. Bucknall, Adv. Polym. Sci., 27, 121, (1978)
34. C.B. Bucknall, R.R. Smith, Polym., 6, 437, (1965)
35. C.B. Bucknall, Appl. Sci., 6, 428, (1977)
36. A.M. Donald, E.J. Kramer, Philos. Mag. A, 8, 43, 857, (1981)
37. P. Beahan, M. Bevis, D. Hull, J. Mater. Sci., 8, 162, (1974)
38. E.J. Kramer, In Polym. Compatibility and Incompatibility Principles and Practices, K. Solc, Symp. Series, Hardwood Academic Publishers, 22, 251, (1982)
39. H.R. Brown, J. Polym. Sci., Polym. Phys., 17, 1431, (1979)
40. J.D. Moore, Polym., 12, 478, (1971)
41. S. Newman, S. Strella, J. Appl. Polym. Sci., 9, 2297, (1965)
42. A.J. Kinloch, S.J. Shaw, D.L. Hunston, Polym., 24, 1355, (1983)
43. R.A. Pearson, A.F. Yee, Polym. Mater. Sci. Eng., 49, 316, (1983)
44. A. Lazzeri, C.B. Bucknall, J. Mater. Sci., 28, 6799, (1993)
45. C.B. Bucknall, A. Karpodinis, X.C. Zhang, J. Mater. Sci., 29, 3377, (1994)
46. A. Lazzeri, C.B. Bucknall, Polym., 36, 2895, (1995)
47. L. Mascia, F. Zitouni, C. Tonelli, J. Appl. Sci., 51, 905, (1994)
48. L. Mascia, F. Zitouni, C. Tonelli, Polym. Eng. Sci., 35, 1069, (1995)
49. E. Martuscelli, P. Musto, G. Ragosta, F. Riva, L. Mascia, J. Mater. Sci., 25, 3719, (2000)
50. P. Musto, E. Martuscelli, G. Ragosta, L. Mascia, Polym., 41, 565, (2000)
51. A. Kioul, L.Mascia, J. Non-Crys. Solids, 175,169 (1994)
52. L. Mascia, A. Kioul, Polym., 36, 3649, (1995)

53. L. Mascia, T. Tang, *Polym.*, 39, 3045, (1998)
54. J.M. Verbicky, *Enc. Polym. Eng. Sci.*, Mark, Bikales, Overberger, Menges, Wiley, 1, 364, (1988)
55. S.R. Sandler, W. Karo, *Polym. Syntheses*, Academic Press, 1, 256, (1992)
56. L.W. Frost, I. Kesse, *J. Appl. Polym. Sci.*, 8, 1039, (1964)
57. J.A. Kreuz, *J. Polym. Sci., Polym. Chem.*, 28, 3787, (1990)
58. C.C. Walker, *J. Polym. Sci., Polym. Chem.*, 26, 1649, (1988)
59. W. Volksen, P.M. Kotts, *Polyimides: Synthesis, Characterisation and Applications*, K.L. Mittal, Plenum, 163, (1984)
60. D.E. Kranbuehl, J. Takeuchi, D. Gibbs, G. Tsahakis, *Stabilisation and Degradation of Polymers*, *Adv. in Chem. Series*, D.L. Allara, W.L. Hawkins, ACS, 169, 198, (1978)
61. P.R. Young, R.E. Escott, *Polyimides*, D. Wilson, H.D Stenzenberger, P.M Hergenrother, Blackie, 129, (1990)
62. T. Miwa, S. Numata, *Polym.*, 30, 893, (1989)
63. C.E. Sroog, A.L. Endrey, S.V. Abramo, C.E. Berr, W.M. Edwards, K.L. Olivier, *J. Polym. Sci.*, A3, 1372, (1965)
64. R.J.W. Reynolds, J.D. Seddon, *J. Polym. Sci.*, C23, 45, (1968)
65. R.A. Dine-Hart, W.W. Wright, *J. Appl. Sci.*, 11, 609, (1967)
66. F.W. Harris, *Polyimides*, D. Wilson, H.D. Stenzenberger, P.M Hergenrother, Blackie, 1, (1990)
67. P.R. Young, J.R. Davis, A.C. Chang, J.N. Richardson, *J. Polym. Sci., Polym. Chem.*, 28, 3107, (1990)
68. S. Numata, K. Fujisaki, N. Kinjo, *Polyimides: Synthesis, Characterisation and Applications*, K.L. Mittal, Plenum, 259, (1984)
69. M.I. Isapovetskii, L.A. Lauis, M.I. Bessonov, M.M. Koton, *Dokl. Akad. Nauk. USSR*, 240, 732, (1978)
70. L.A. Laius, *Polyimides: Synthesis and Characterisation*, K.L. Mittal, Plenum, 295, (1984)
71. P.R. Young, A.C. Chang, *SAMPE Prepr.*, 30, 889, (1985)
72. V.V. Korshak, S.V. Vinogradova, Ya.S. Vygodskii, Z.V. Gerashchenko, *Polym. Sci. USSR*, 13, 1341, (1971)
73. V.V. Korshak, Ye. D. Molodtsova, L.A. Pankratova, S.A. Pavlova, G.I. Timofeyeva, *Dokl. Akad. Nauk. USSR (Eng. trans.)*, 208, 65, (1973)

74. S.V. Vinogradova, V.V. Korshak, Ya. Vyogodskii, *Polym. Sci. USSR*, 8, 888, (1966)
75. S.V. Vinogradova, Ya. Vyogodskii, V.V. Korshak, N.A. Churochkina, D.R. Tur, V.G. Danilov, *Polym. Sci. USSR*, 13, 1695, (1971)
76. W.J. Farrissey, P.S. Andrews, *US Pat. 3, 787, 367* (1964), *US Pat. 3, 870, 677* (1975)
77. F.W. Harris, L.H. Lanier, *Structure-Solubility Relationships in Polymers*, F.W. Harris, R.B. Seymour, 183, (1977)
78. J. Bateman, D.A. Gordon, *US Pat. 3, 856, 752*, (1974)
79. I.M. Salin, J.C. Seferis, *J. Appl. Polym. Sci.*, 47, 847, (1993)
80. D.W. van Krevelen, C. van Herden, F.J. Huntijens, *Fuel*, 30, 253, (1951)
81. J.D. Nam, J.C. Seferis, *J. Polym. Sci., Polym. Phys.*, 29, 601, (1991)
82. J.D. Nam, J.C. Seferis, *J. Polym. Sci., Polym. Phys.*, 30, 455, (1992)
83. J.H. Flynn, B. Dickens, *Thermochim. Acta*, 15, 1, (1976)
84. H.E. Kissinger, *Anal. Chem.*, 29, 1702, (1957)
85. J.H. Flynn, L.A. Wall, *J. Polym. Sci., Polym. Lett.*, 4, 323, (1966)
86. H.H. Horowitz, G. Metzger, *Anal. Chem.*, 1464, (1963)
87. A.W. Coates, J.P. Redfern, *Nature*, 201, 68, (1964)
88. B. Dickens, *J. Polym. Sci., Polym. Chem.*, 20, 1065, (1982)
89. C.D. Doyle, *J. Appl. Polym. Sci.*, 5, 285, (1961)
90. J. Zsako, *J. Thermal. Anal.*, 5, 239, (1973)
91. L.A. Laius, M.I. Bessonov, Ye.V. Kallistova, N.A. Adrovva, F.S. Florinskii, *Polym. Sci. USSR*, A9, 2470, (1957)
92. J.A. Kreuz, A.I. Endrey, F.P. Gay, C.E. Sroog, *J. Polym. Sci.*, A14, 2607, (1966)
93. M.I. Tsapovetsky, *Polyimide: Synthesis and Characterisation and Applications*, K.L. Mittal, Plenum, 295, (1984)
94. S. Numata, K. Fujisaki, N. Kinjo, *Polyimides*, K.L. Mittal, 1, 259, (1984)
95. M.I. Bessonov, M.M. Koton, V.V. Kudryutsev, L.A. Laius, *Polyimides: Thermally Stable Polymers*, Consultants Bureau, (1987)
96. C. Feger, *Polym. Eng. Sci.*, 29, 5, 347, (1989)
97. M.J. Brekner, C. Feger, *J. Polym. Sci., Polym. Chem.*, 25, 2479, (1987)
98. C. Johnson, S.L. Wunder, *J. Polym. Sci., Polym. Phys.*, 31, 677, (1993)
99. M.J. Brekner, C. Feger, *J. Polym. Sci., Polym. Chem.*, 25, 2005, (1987)

100. J.R. Ojeda, J. Mobley, D.C. Martin, *J. Polym. Sci., Polym. Phys.*, 32, 559, (1995)
101. C. Johnson, S.L. Wunder, *J. Polym. Sci.*, B31, 677, (1993)
102. T.J. Hsu, Z. Liu, *J. Appl. Polym. Sci.*, 46, 1821, (1992)
103. R. Ginsberg, J.R. Susko, *Polyimides: Synthesis, Characterisation and Applications*, K.L. Mittal, Plenum, 235, (1984)
104. C. Feger, *Polym. Eng. and Sci.* 29, 347, (1989)
105. M. Fryd, *Polyimides: Synthesis, Characterisation and Applications*, K.L. Mittal, Plenum, 295, (1984)
106. M. Kochi, S. Isoda, R. Yokota, I. Mita, H. Kambe, *Polyimides: Synthesis, Characterisation and Applications*, K.L. Mittal, Plenum, 650, (1984)
107. T.S. St. Clair, J.F. Dezern, C.I. Croall, ANTEC '93, SPE, Brookfield Connecticut, 650, (1993)
108. R.A. Dine Hart, W.W. Wright, *J. Polym. Br.*, 3, 163, (1971)
109. M. Pottiger, J.C. Coburn, J.R. Edman, *J. Polym. Sci., Polym. Phys.*, 32, 825, (1994)
110. J. Jou, P. Huang, H. Chen, C. Liao, *Polym.*, 33, 967, (1992)
111. M.T. Pottiger, J.C. Coburn, ANTEC '93, SPE, Brookfield Connecticut, 1925, (1993)
112. S. Numata, N. Kinjo, *Polym. Eng. Sci.*, 28, 906, (1988)
113. P.M. Hergenrother, N.T. Wakelyn, S.J. Havens, *J. Polym. Sci.*, 25, 1093, (1987)
114. M. Fryd, *Polyimides*, K.L. Mittal, 1, 377, (1984)
115. V.L. Bell, B.L. Stump, H. Gager, *J. Polym. Sci., Polym. Chem.*, 14, 2275, (1976)
116. M.K. Gerber, J.R. Pratt, T.L. St. Clair, *Proceedings of the 3rd Int. Conf. on Polyimides*, 101, (1988)
117. A.K. St. Clair, T.L. St. Clair, *Polyimides: Synthesis, Characterisation and Applications*, K.L. Mittal, Plenum, 977, (1984)
118. A.K. St. Clair, T.L. St. Clair, *SAMPE Q.*, 13, 20, (1981)
119. R.O. Johnson, H.S. Burlhis, *J. Polym. Sci., Polym. Symp.*, 70, 129, (1983)
120. I.W. Serfaty, *Polyimides: Synthesis, Characterisation and Application*. K.L. Mittal, Plenum, 149, (1984)

121. D.S. Gollob, J.F. Mandell, F.J. McGarry, Toughening of Thermosetting Polyimides. Massachusetts Institute of Technology Research Report, R-1, (1979)
122. I.K. Varma, G.M. Fohlen, J.A. Parker, D.S. Varma, Polyimides: Synthesis, Characterisation and Applications K.L. Mittal, Plenum, 683, (1984)
123. G. Maglio, R. Palumbo, V.M. Vitagliano, Polym., 30, 1175, (1989)
124. S. Maugal, T.I. St. Clair, Proc. 29th Natl SAMPE Symp., 437, (1984)
125. A.J. Kinloch, S.J. Shaw, D.A. Tod, Rubber-Modified Thermoset Resins, C.K. Riew, J.K. Gillham, Am. Chem. Society, 101, (1984)
126. S.J. Shaw, A.J Kinloch, Int. J. Adhes., 5, 123,(1985)
127. S.J. Shaw, Recent Advances in Polyimides Science and Technology, M.R. Gupta, W.D. Weber, Society of Plastics Engineers, (1987)
128. C.L. Segal, H.D. Stenzenberger, M. Herzorg, W. Romer, S. Pierce, M.S. Canning, Proc. 17th Natl. SAMPE Technical Conf., 147, (1985)
129. H.D. Stenzenberger, W. Romer, M. Herzog, S. Pierce, M. Canning, K. Fear, Proc. 31st Int. SAMPE Symp., 920, (1986)
130. S.J. Shaw, Rubber Toughened Engineering Plastics, A.A. Collyer, Chapman and Hall, (1994)
131. A.K. St. Clair, T.L. St. Clair, Int. J. Adhes., 2, 249, (1981)
132. S. Takeda, H. Kakiuchi, J. Appl. Polym. Sci., 35, 1351, (1988)
133. S. Takeda, H. Akiyama, H. Kakiuchi, J. Appl. Polym. Sci., 35, 1341, (1988)
134. H.D. Stenzenberger, P. Konig, M. Herzog, W. Romer, S. Pierce, K. Fear, M.S. Canning, Proc. 19th Int. SAMPE Technical Conf., 372, (1987)
135. D.A. Tod, S.J. Shaw, J. Polym. Br., 20, 397, (1988)
136. A.K. St. Clair, T.L. St. Clair, Proc. 12th Natl. SAMPE Technical Conf., 729, (1980)
137. S.A. Ezzell, A.K. St. Clair, J.A. Hinkley, Polym., 28, 1779, (1987)
138. R.J. Spontak, M.C. Williams, J. Appl. Polym. Sci, 38,1607, (1989)
139. C.A. Arnold, J.D. Summers, Y.P. Chen, R.H. Bott, D. Chen, J.E. McGrath, Polym., 30, 986, (1989)
140. C.J. Brinker, G.W. Scherer, Sol-Gel Science: The Physics and Chemistry of Sol-Gel Processing, Academic Press, (1990)
141. C.J. Brinker, G.W. Scherer, J. Non-Crystalline Solids, 70, 301, (1985)

142. L.C. Klein, G.J Garvey, Better Ceramics Through Chemistry, Mat. Res. Soc. Symp. Proc., C.J. Brinker, D.E. Clark, D.R. Ulrich, Elsevier, 33, (1984)
143. J.D. Mackenzie, J. Non-Crystalline Solids, 48, 1, (1982)
144. R.K. Iler, The Chemistry of Silica, Wiley Interscience, (1979)
145. M.F. Bechtold, R.D. Vest, L. Plambeck Jr, J. Am. Chem. Soc., 90, 4590, (1968)
146. B. Yoldas, Design of New Materials, Proceedings of the 4th Annual Industry-University Co-op. Chem. Progr., March 24, (1986), College Station, TX, D.L. Cocke, A. Clearfield, 13, (1987)
147. L.C. Klein, Thin Film Processes, J.L Voccen, W. Kern, Academic Press, 2, 501, (1991)
148. E.P. Plueddemann, Silanes and other Coupling Agents, K.L. Mittal, VSP, 3, (1992)
149. G. Tesoro, Y. Wu, Silanes and other Coupling Agents, K.L. Mittal, VSP, 215, (1992)
150. P.G. Pape, E.P. Plueddemann, Silanes and other Coupling Agents, K.L. Mittal, VSP, 105, (1992)
151. H.G. Linde, J. Polym. Sci., Polym. Chem., 20, 1031, (1982)
152. E.P. Plueddeman, Silane and Coupling Agents, Plenum, 3, (1982)
153. E.P. Plueddeman, Silane and Coupling Agents, Plenum, 2, (1982)
154. G. Philipp, H. Schmidt, J. Non-Crystalline Solids, 63, 283, (1984)
155. H.K. Schmidt, Better Ceramics Through Chemistry IV, Mat. Res. Soc. Symp. Proc., MRS, 180, 961, (1990)
156. R. Aelion, A. Loebel, F. Eirich, J. Am. Chem. Soc., 72, 5075, (1950)
157. K. D. Keefer, Better Ceramics Through Chemistry, Mat. Res. Soc. Symp. Proc., C.J. Brinker, D.E. Clark, D.R. Ulrich, Elsevier, 32, 15, (1984)
158. K.D. Keefer, Silicon-Based Polym. Sci., A Comprehensive Approach, J.M. Ziegler, F.W.G. Fearon, Advances in Chem. Series, Am. Chem. Soc., 224, 227, (1990)
159. J. Cihlár, Colloids and Surfaces, Phys. Eng. Asp., 70, 239, (1993)
160. J.C. Pouxviel, J.P. Boilot, Better Ceramics Through Chemistry III, Mat. Res. Soc. Symp. Proc., C.J. Brinker, D.E. Clark, D.R. Ulrich, MRS, 121, 37, (1988)
161. R.A. Assink, B.D. Kay, Polym. Preprints, 32, 506, (1991)
162. C.J. Brinker, K.D. Keefer, D.W. Schaefer, C.S. Ashley, J. Non-Crystalline Solids, 48, 47, (1982)

163. J. Sanchez, A. McCormick in Chem. Proc. of Adv. Mater., L.L. Hench, J.K. Wests, Wiley, 43, (1992)
164. H. Schmidt, H. Scholze, A. Keizer, J. Non-Crystalline Solids, 63, 1, (1984)
165. S. Sakka, H. Kozuka, S. Sim, Ultrastructure Proc. of Adv. Cer., J.D. Mckenzie, D.R. Ulrich, Wiley, 159, (1988)
166. I. Hasegawa, S. Sakka, J. Non-Crystalline Solids, 100, 201, (1988)
167. B.E. Yoldas, J. Non-Crystalline Solids, 83, 375, (1986)
168. J.E. McGrath, J.P. Pullockarren, J.S. Riffle, S. Kilic, C.S. Elsbernd, Ultrastruct. Proc. Adv. Cer., J.D. Mckenzie, D.R. Ulrich, Wiley, 55, (1988)
169. I. Atraki, T.W. Zerda, J. Jonas, J. Non-Crystalline Solids, 81, 381, (1986)
170. A.H. Boonstra, J.M.E. Baken, J. Non-Crystalline Solids, 122, 171, (1980)
171. A.H. Boonstra, T.N.M. Bernards, J.J.T. Smits, J. Non-Crystalline Solids, 109, 141, (1989)
172. G. Orcel, L.L. Hench, I. Artaki, J. Jones, T.W. Zerda, J. Non-Crystalline Solids, 105, 223, (1988)
173. N. Viart, J.L. Rehspringer, J. Non-Crystalline Solids, 195, 223, (1996)
174. E.J.A. Pope, J.D. Mackenzie, J. Non-Crystalline Solids, 87, 185 (1996)
175. E. Giannelis, Materials Chemistry, L.V. Interrante, L.A. Casper, A.B. Ellis , Adv. in Chem. Series, 144, 259, (1995)
176. E.J.A. Pope, J.D. Mackenzie, Mater. Res. Soc. Symp. Proc., 73, 809, (1986)
177. B. Abramoff, L.C. Klein, Ultrastructure Processing of Advanced Materials, D.R. Ulrich, D.R. Uhlmann, John Wiley, 401, (1992)
178. C.J.T. Landry, B.K. Coltrain, B.K. Brady, Polym., 33, 1486, (1992)
179. B.M. Novak, M.Ellsworth, T.I Wallow, C. Davies, Polym. Prep., 31, 698, (1990)
180. K. Yano, A. Usuki, A. Okada, T. Kurauchi, O.Kamigaito, Polym. Prep., 32, 65, (1991)
181. M. Nandi, J.A. Conklin, L. Salvati Jr., A. Sen, Chem. of Mater., 3, 201, (1991)
182. A. Morikawa, Y. Iyoku, M. Kakimoto, Y. Imai, Polym., 24, 107, (1992)
183. A. Morikawa, Y. Iyoku, M. Kakimoto, Y. Imai, J. Mater. Chem., 2, 679, (1992)
184. A. Morikawa, H. Yamaguchi, M. Kakimoto, Y. Imai, Chem. of Mater., 6, 913, (1994)
185. S. Wang, Z. Ahmad, J.E. Mark, Chem. of Mater., 6, 943, (1994)
186. L. Mascia, T. Tang, J. Mater. Chem., 8, 2417, (1998)

187. L. Mascia, T. Tang, J. Sol-Gel Sci. Tech., 13, 405, (1998)
188. L. Mascia, Z. Zhang, S.J. Shaw, Compos., 27A, 1211, (1996)
189. L. Mascia, A. Kioul, Polym., 36, 3649, (1995)
190. L. Mascia, C. Xenopoulos, S.J. Shaw, Mater. Sci. and Eng., C6, 99, (1998)
191. A. Kioul, L. Mascia, J. Non-Crystalline Solids, 175, 169, (1994)
192. V. Arcella, M. Albano, M. Apostolo, I. Wlassics, R. Ferro, New Peroxide Curable Perfluoroether for High Temperature Applications, Solvay Solexis, Internal Circulation, (1997)
193. R.J Weston, 4th Int. Conf., High Performance Engineering Polymers, 4, (1990)
194. L. Matejka, K. Dusek, J. Plestil, J. Kriz, F. Lednicky, Polymer, 40, 171, (1998)

